frontiers | Research Topics

# Ecophysiological traits-based community assembly and maintenance of ecosystem functioning in tropical rainforests

**Edited by**
Hui Zhang, Robert John, Xiang Liu and Suping Zhou

**Published in**
Frontiers in Plant Science

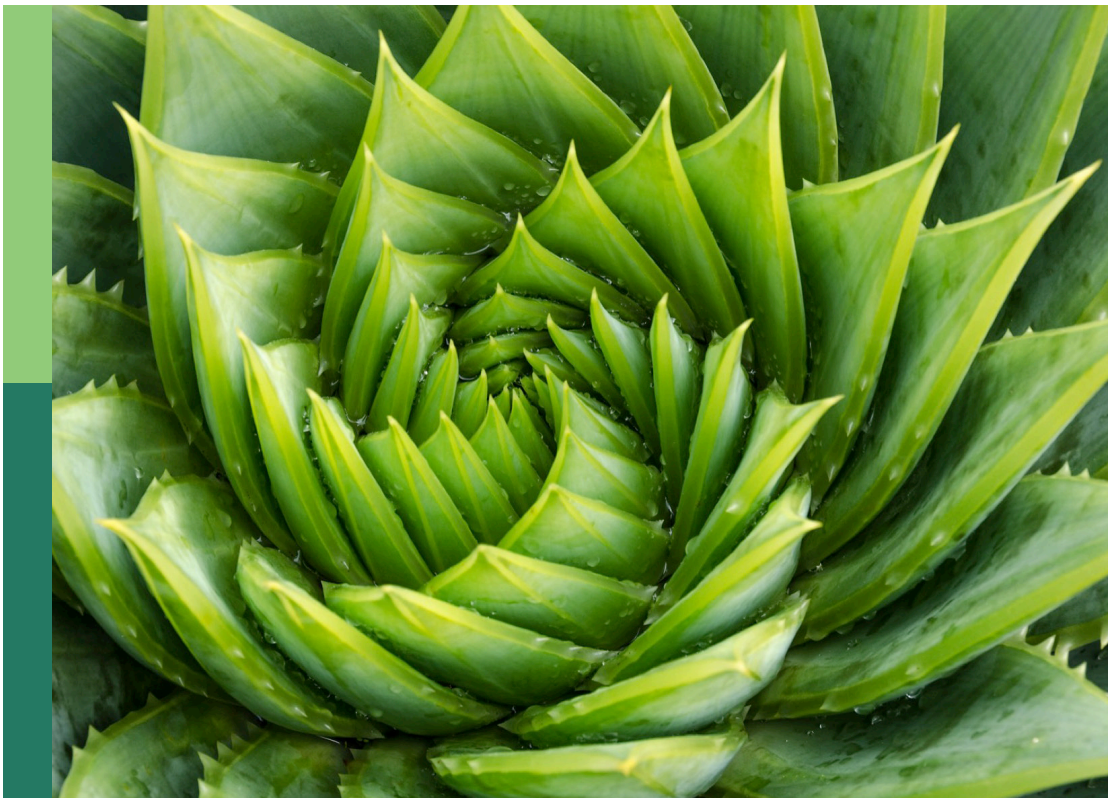

ISSN 1664-8714
ISBN 978-2-8325-7394-5
DOI 10.3389/978-2-8325-7394-5

**Generative AI statement**
Any alternative text (Alt text) provided alongside figures in the articles in this ebook has been generated by Frontiers with the support of artificial intelligence and reasonable efforts have been made to ensure accuracy, including review by the authors wherever possible. If you identify any issues, please contact us.

## About Frontiers

Frontiers is more than just an open access publisher of scholarly articles: it is a pioneering approach to the world of academia, radically improving the way scholarly research is managed. The grand vision of Frontiers is a world where all people have an equal opportunity to seek, share and generate knowledge. Frontiers provides immediate and permanent online open access to all its publications, but this alone is not enough to realize our grand goals.

## Frontiers journal series

The Frontiers journal series is a multi-tier and interdisciplinary set of open-access, online journals, promising a paradigm shift from the current review, selection and dissemination processes in academic publishing. All Frontiers journals are driven by researchers for researchers; therefore, they constitute a service to the scholarly community. At the same time, the *Frontiers journal series* operates on a revolutionary invention, the tiered publishing system, initially addressing specific communities of scholars, and gradually climbing up to broader public understanding, thus serving the interests of the lay society, too.

## Dedication to quality

Each Frontiers article is a landmark of the highest quality, thanks to genuinely collaborative interactions between authors and review editors, who include some of the world's best academicians. Research must be certified by peers before entering a stream of knowledge that may eventually reach the public - and shape society; therefore, Frontiers only applies the most rigorous and unbiased reviews. Frontiers revolutionizes research publishing by freely delivering the most outstanding research, evaluated with no bias from both the academic and social point of view. By applying the most advanced information technologies, Frontiers is catapulting scholarly publishing into a new generation.

## What are Frontiers Research Topics?

Frontiers Research Topics are very popular trademarks of the *Frontiers journals series*: they are collections of at least ten articles, all centered on a particular subject. With their unique mix of varied contributions from Original Research to Review Articles, Frontiers Research Topics unify the most influential researchers, the latest key findings and historical advances in a hot research area.

Find out more on how to host your own Frontiers Research Topic or contribute to one as an author by contacting the Frontiers editorial office: frontiersin.org/about/contact

# Ecophysiological traits-based community assembly and maintenance of ecosystem functioning in tropical rainforests

**Topic editors**

Hui Zhang — Hainan University, China

Robert John — Indian Institute of Science Education and Research Kolkata, India

Xiang Liu — Lanzhou University, China

Suping Zhou — Tennessee State University, United States

**Citation**

Zhang, H., John, R., Liu, X., Zhou, S., eds. (2026). *Ecophysiological traits-based community assembly and maintenance of ecosystem functioning in tropical rainforests*. Lausanne: Frontiers Media SA. doi: 10.3389/978-2-8325-7394-5

# Table of contents

frontiers | Frontiers in Plant Science

TYPE Original Research
PUBLISHED 14 August 2024
DOI 10.3389/fpls.2024.1456740



OPEN ACCESS

EDITED BY
Xiang Liu,
Lanzhou University, China

REVIEWED BY
Xinwei Guo,
Chinese Academy of Tropical Agricultural Sciences, China
Zhongyu Sun,
Guangzhou Institute of Geography, China

*CORRESPONDENCE
Hui Zhang
13925183735@139.com
Huai Yang
Yanghuai2008@163.com
Cui Chen
421656231@qq.com

RECEIVED 29 June 2024
ACCEPTED 24 July 2024
PUBLISHED 14 August 2024

CITATION
Xu C, Zhang H, Yang H, Chen C and Wang C (2024) A quick and effective trait-based protocol for selecting appropriate native plant species for the reforestation of degraded tropical mines.
*Front. Plant Sci.* 15:1456740.
doi: 10.3389/fpls.2024.1456740



# A quick and effective trait-based protocol for selecting appropriate native plant species for the reforestation of degraded tropical mines

Changbin Xu[1], Hui Zhang[2]*, Huai Yang[3]*, Cui Chen[4]* and Chen Wang[5]

[1]College of International Tourism and Public Administration, Hainan University, Haikou, China, [2]Hainan Institute of National Park, Haikou, China, [3]Institute of Tropical Bamboo, Rattan & Flower, Sanya Research Base, International Center for Bamboo and Rattan, Sanya, China, [4]School of Geography and Tourism, Huanggang Normal University, Huanggang, Hubei, China, [5]Department of Agricultural and Environmental Sciences, Tennessee State University, Nashville, TN, United States

**Introduction:** A critical issue in tropical forests is that anthropogenic deforestation (i.e., mining) degrades the integrity of its ecosystem. Reforestation with appropriate native plant species helps to alleviate these detrimental impacts. A protocol to select appropriate plant species for this purpose currently lacks efficacy and timeliness.

**Methods:** We provided a trait-based protocol to quickly and effectively select native plant species for mining reforestation. A 0.2-km$^2$ area of Baopoling (BPL) at Hainan Island, China, was used as a study site, which has been severely degraded by 20 years of limestone mining for cement production. First, we identified the tree species in nearby undisturbed tropical forests, followed by evaluating the similarities in functional traits of the most dominant one (target species) and 60 local candidate native plant species (candidate species) whose saplings can be purchased from a local market.

**Results and discussion:** This dataset was used in our trait-based protocol, and only within 1 month, we successfully selected eight plant species which are very similar to target species from the 60 candidate species. We also quantified whether the eight selected plant species were indeed suitable for sustained reforestation by testing their effects on landscape and also their survival rate and recruitment ability after using them to perform reforestation in BPL from 2016 to 2023. Finally, these eight plant species are indeed suitable for reforestation due to their huge influences on a significant shift from originally degraded landscape (comprising only barren rocks) to a forest landscape totally and also their high survival rate (90%–97%) and ability for natural recruitment after 7 years' reforestation in BPL. Thus, we anticipate that this protocol would be integral to species selection during reforestation of tropical mining areas.

KEYWORDS

**deforestation, human disturbances, trait-based plant species selection protocol, tropical forest ecosystem, reforestation, Hainan Island**

# Introduction

Disproportionate human disturbances (e.g., ore mining and agricultural use) potentially lead to an extensive deforestation of tropical forests (Laurance et al., 2014). This degradation manifests into global biodiversity loss, increases carbon emissions, and water loss (Aleman et al., 2018; Mitchard, 2018; Symes et al., 2018; Taubert et al., 2018). Industrial concessions for logging and plantations (e.g., for fiber, and oil palm) may explain the high ratios of forest loss compared with their gain in the tropics. However, mining is increasingly identified as an important driver of deforestation (Butsic et al., 2015; González-González et al., 2021). Yet, mining is rarely listed as a major cause of forest loss in the global or regional assessments (Abood et al., 2015). As a result, the true extent and impacts of mining may be significantly underestimated (Sonter et al., 2017; Siqueira-Gay and Sánchez, 2021).

There is little doubt, however, that mining is a rapidly growing, highly destructive industrial activity, and a significant contributor to forest loss and land degradation (Ahmed et al., 2021). The rapid removal of vegetation and soils and the overburden of rock substrates that remain after mining make the vegetation recovery difficult (Macdonald et al., 2015). Restoration of mined-out lands to forests is therefore a major goal of land management (Lamb et al., 2005). In practice, reforestation has been recognized as an effective method to restore mined areas (Ahirwal et al., 2017) and derive biodiversity and ecosystem service benefits (Hua et al., 2022).

Reforestation and forest protection are commonly used to alleviate the detrimental impacts of deforestation (Griscom et al., 2017; Taubert et al., 2018). An important challenge in a successful reforestation exercise is the identification of appropriate native tree species (Brown and Amacher, 1999; Fry et al., 2013; Jones, 2013). A trial-and-error method is usually employed to select the best-fitting tree species from candidate native tree species for reforestation. This requires expert knowledge of historical tree species composition, habitat requirements, and trailing (Packard and Mutel, 1997). Moreover, selected tree species may only be applicable for reforestation in specific ecosystems (Laughlin and Laughlin, 2013). Therefore, a method is needed that can quickly and effectively select several appropriate tree species.

The trait-based species selection framework focuses on quickly and effectively choosing native candidate species for ecological restoration (Laughlin, 2014; Wang et al., 2020). This framework assumes that plant functional traits, including morphological, physiological, and phenological traits, reflect a plant's life history. Plant species that thrive in a given habitat should therefore possess similar functional traits, to similarly respond to abiotic environmental influences (Funk et al., 2008; Laughlin, 2014). Based on this assumption, tree species with functional traits similar to those thriving in the target ecosystem (e.g., dominant species) should be suitable for reforestation. Indeed, Wang et al. (2020) found that candidate species selected by using the criteria of similarity of functional traits could effectively reforest a degraded island ecosystem. Yet, a study that applies this trait-based species selection method to mining reforestation is still lacking. Moreover, a general quantitative protocol for using such trait-based species selection framework to guide mining restoration is also still needed (Wang et al., 2020). As a result, here we expect to use such a trait-based plant species selection framework to develop a general protocol for quickly and effectively choosing appropriate tree species for mining reforestation. This protocol required the following: a measurement of dominant plant species' functional traits from nearby undisturbed forests; an identification of candidate species; and the use of the trait-based plant species selection software platform provided in Wang et al. (2020) to designate an appropriate reforestation plan. To assess the efficacy of our protocol, we quantified whether selected plant species could successfully reforest a 0.2-km$^2$ study site in Baopoling (BPL), Hainan island, China. A 20-year limestone extraction for cement production had rendered BPL as barren and unforgiving, with no vegetation. Since the selected tree species has colonized and survived in this area, our protocol may have wide applicability in identifying a larger pool of candidate species for reforestation of degraded tropical forest ecosystems across the world.

# Materials and methods

## Study sites

Our study site was located in Baopoling (BPL), on a limestone mountain in Sanya City, Hainan, China (109°51′01"E, 18°31′99"N). It has a tropical monsoon oceanic climate with a mean annual temperature of 28°C. The average annual precipitation on Hainan Island is 1,500 mm, and most (approximately 91%) of the precipitation occurs from June to October (Zhang et al., 2023). Typical vegetation in BPL is composed of tropical monsoon broad-leaf forest. One part (0.2-km$^2$ area) of BPL was extensively degraded and lacks vegetation (Zhang et al., 2024). The other parts of BPL remain undisturbed and possess a rich tropical rainforest (Figure 1).

## Determining target and candidate tree species

Our protocol requires an identification of target species (nearby native species which are proven appropriate for a degraded ecosystem) as a baseline from which the selection of candidate tree species could be made. If restoration is initiated from bare soil conditions, data measured from dominant plant species in a nearby or similar habitat could be used as a proxy (Ostertag et al., 2015). We therefore selected the most dominant tree species (*Bridelia tomentosa*) in the nearby undisturbed tropical monsoon forests in BPL as our target species. Since our study site lacked any vegetation, restoring this area is comparable with an early forest succession. Fast-growing tree species usually dominate an early succession (Lohbeck et al., 2014). As a result, we selected all the fast-growing candidate native tree species that could be purchased from a local nursery in Sanya City. Finally, we have found 60 candidate tree species (Table 1).

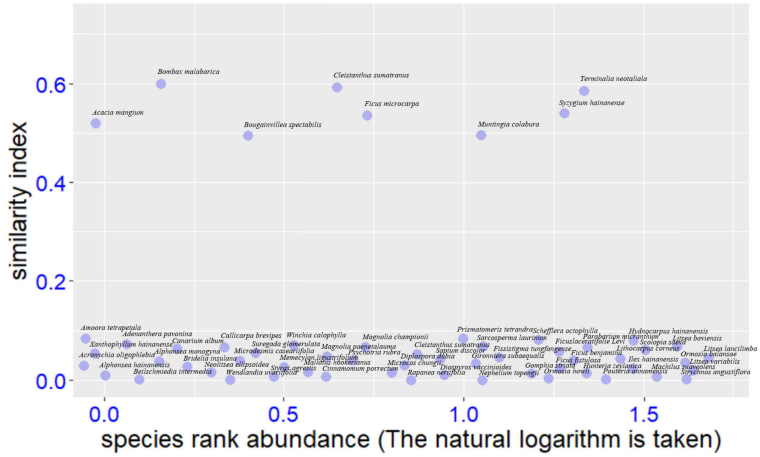


FIGURE 1
Results of selection of target species, *Bridelia tomentosa*, and 60 candidate native tree species, with similarity index >0.5 indicating appropriate for restoration.

## Evaluation of functional trait

It has been found that various types of traits need to be evaluated for selecting an appropriate species for reforestation (Wang et al., 2021). BPL's notable dry season favor drought-tolerant plants. In February of 2016, at the peak of the dry season, we evaluated functional traits that are highly related to growth rate and drought stress tolerance. These traits included the following: upper epidermic thickness (μm); palisade tissue (μm); spongy tissue (μm); lower epidermic thickness (μm); stomatal density (numbers $mm^{-2}$); transpiration rate (mol $m^{-2}$ $s^{-1}$); maximum photosynthesis rate (mol $m^{-2}$ $s^{-1}$); stomatal conductance (mmol $m^{-2}$ $s^{-1}$); leaf water conductance (mmol $m^{-2}$ $s^{-1}$ $MPa^{-1}$); specific leaf area ($g/cm^2$); leaf dry matter content (%); and leaf turgor loss point (MPa). Measurements were conducted on the target species (*Bridelia tomentosa*) and 60 candidate plant species. There were 20 fully expanded, healthy, and sun-exposed leaves collected from five mature trees of each target and candidate species, all of which possessed a diameter at breast height (DBH) value comparable with the mean DBH values of respective (target and candidate) species. Traits were measured following the methods described in Hua et al. (2017) and Zhang et al. (2018). The detailed procedures for measuring these functional traits are described in the Supplementary Materials. All measured traits for target and candidate plant species were further inputted into our following tree species selection software platform to check the similarity between target and candidate plant species.

## Tree species selection software platform

In a previous work, a trait-based plant species selection software platform was developed, which could identify plant species that possess functional traits that are similar to a target plant species from an available candidate pool (Wang et al., 2020). The software platform uses the maximum entropy model developed by Shipley et al. (2006) to calculate the similarity index, which determines whether candidate species are suitable for reforestation. A high similarity index (i.e., >0.5) indicates greater similarity between a candidate and target plant species and thus the candidate species is fit for restoration (Wang et al., 2020). In contrast, a low similarity index (e.g., 0.1–0.2) indicates that the candidate species is not suitable for reforestation (Wang et al., 2020). For further details on our software platform, please see Wang et al. (2020); the Home page of the platform is shown in Supplementary Figure 1.

## Survival rates, mean height, and diameter at breast height

Monoculture plantation of fast-growing species can accelerate forest recovery (Lugo, 1997). We monocultured seedlings for all selected tree species in eight reconstructed soil layers in BPL by the end of 2016 (Zhang et al., 2023). There was at least a 3-m interval between any two planted stems. For detailed descriptions of our plantation, please see Zhang et al. (2024). The initial height and DBH for saplings of all selected tree species ranged 1 m–2 m and 1 cm–2 cm, respectively. The planting density was kept at 50–80 stems per hectare. If these selected tree species are really appropriate, they should not only have a high survival rate (Wang et al., 2020) but also can recruit naturally, without requiring manual management (Holl et al., 2017). In addition, the original landscape should also have a big alteration after using selected tree species to perform reforestation. As a result, we recorded their survival rates from 2016 to 2023 as.

10.3389/fpls.2024.1456740

TABLE 1 Species list for the 60 fast-growing candidate native tree species that could be purchased from a local nursery in Sanya City.

| Species | Family | Genus |
|---|---|---|
| *Acacia mangium* | Leguminosae | acacia |
| *Acronychia oligophlebia* | Rutaceae | Acronychia |
| *Adenanthera pavonina* | Leguminosae | Adenanthera |
| *Alphonsea hainanensis* | Annonaceae | Alphonsea |
| *Alphonsea monogyna* | Annonaceae | Alphonsea |
| *Amoora tetrapetala* | Meliaceae | Amoora |
| *Beilschmiedia intermedia* | Lauraceae | Beilschmiedia |
| *Bombax malabarica* | Malvaceae | Bombax |
| *Bougainvillea spectabilis* | Nyctaginaceae | Bougainvillea |
| *Bridelia insulana* | Phyllanthaceae | Bridelia |
| *Callicarpa brevipes* | Lamiaceae | Callicarpa |
| *Canarium album* | Burseraceae | Canarium |
| *Cinnamomum porrectum* | Lauraceae | Cinnamomum |
| *Cleistanthus sumatranus* | Phyllanthaceae | Cleistanthus |
| *Cleistanthus sumatranus* | Phyllanthaceae | Cleistanthus |
| *Diospyros vaccinioides* | Ebenaceae | Diospyros |
| *Diplospora dubia* | Rubiaceae | Diplospora |
| *Ficus benjamina* | Moraceae | Ficus |
| *Ficus fistulosa* | Moraceae | Ficus |
| *Ficus microcarpa* | Moraceae | Ficus |
| *Ficuslaceratifolie Levl* | Moraceae | Ficus |
| *Fissistigma tungfangense* | Annonaceae | Fissistigma |
| *Gironniera subaequalis* | Cannabaceae | Gironniera |
| *Gomphia striata* | Ochnaceae | Campylospermum |
| *Hunteria zeylanica* | Apocynaceae | Hunteria |
| *Hydnocarpus hainanensis* | Achariaceae | Hydnocarpus |
| *Ilex hainanensis* | Aquifoliaceae | llex |
| *Lithocarpus corneus* | Fagaceae | Lithocarpus |
| *Litsea baviensis* | Lauraceae | Litsea |
| *Litsea lancilimba* | Lauraceae | Litsea |
| *Litsea variabilis* | Lauraceae | Litsea |
| *Machilus suaveolens* | Lauraceae | Machilus |
| *Magnolia championii* | Magnoliaceae | Magnolia |
| *Magnolia paenetalauma* | Magnoliaceae | Magnolia |
| *Mallotus hookerianus* | Euphorbiaceae | Mallotus |
| *Memecylon ligustrifolium* | Melastomataceae | Memecylon |
| *Microcos chungii* | Malvaceae | Microcos |
| *Microdesmis casearifolia* | Pandaceae | Microdesmis |
| *Muntingia colabura* | Muntingiaceae | Muntingia |
| *Neolitsea ellipsoidea* | Lauraceae | Neolitsea |
| *Nephelium topengii* | Sapindaceae | Nephelium |
| *Ormosia balansae* | Fabaceae | Ormosia |
| *Ormosia howii* | Fabaceae | Ormosia |
| *Parabarium micranthum* | Apocynaceae | Parabarium |
| *Pouteria annamensis* | Sapotaceae | Pouteria |
| *Prismatomeris tetrandra* | Rubiaceae | Prismatomeris |
| *Psychotria rubra* | Rubiaceae | Psychotria |
| *Rapanea neriifolia* | Primulaceae | Rapanea |
| *Sapium discolor* | Euphorbiaceae | Sapium |
| *Sarcosperma laurinum* | Sapotaceae | Sarcosperma |
| *Schefflera octophylla* | Araliaceae | Schefflera |
| *Scolopia saeva* | Salicaceae | Scolopia |
| *Strychnos angustiflora* | Loganiaceae | Strychnos |
| *Styrax agrestis* | Styracaceae | Styrax |
| *Suregada glomerulata* | Euphorbiaceae | Suregada |
| *Syzygium hainanense* | Myrtaceae | Syzygium |
| *Terminalia neotaliala* | Combretaceae | Terminalia |
| *Wendlandia uvariifolia* | Rubiaceae | Wendlandia |
| *Winchia calophylla* | Apocynaceae | Winchia |
| *Xanthophyllum hainanense* | Polygalaceae | Xanthophyllum |

$$\text{survival rate} = \frac{\text{Remaining seedings}}{\text{Original seedings}} \times 100\,\%$$

We also measured the height and DBH for all individuals for all selected tree species in 2023 to find out whether they can naturally recruit. In addition, we compared the landscape change between before reforestation and after reforestation by comparing the differences in remote sensing image.

## Results

Final screening results which are based on using the functional traits to compare the similarity index between target species and candidate species are shown in Figure 2. Eight native tree species (*Acacia mangium*, *Bombax malabarica*, *Bougainvillea spectabilis*, *Cleistanthus sumatranus*, *Ficus microcarpa*, *Muntingia calabura*, *Syzygium hainanense*, and *Terminalia neotaliala*) showed very suitable for restoration, as they were very similar to the target species, *Bridelia tomentosa*, which is clearly witnessed by the similarity index for the eight species all being more than 0.5 (Figure 1). In contrast, the similarity index for the rest of the 52


FIGURE 2
The landscape for extremely degraded and undisturbed tropical monsoon forests in Baopoling (BPL) before reforestation and after reforestation.

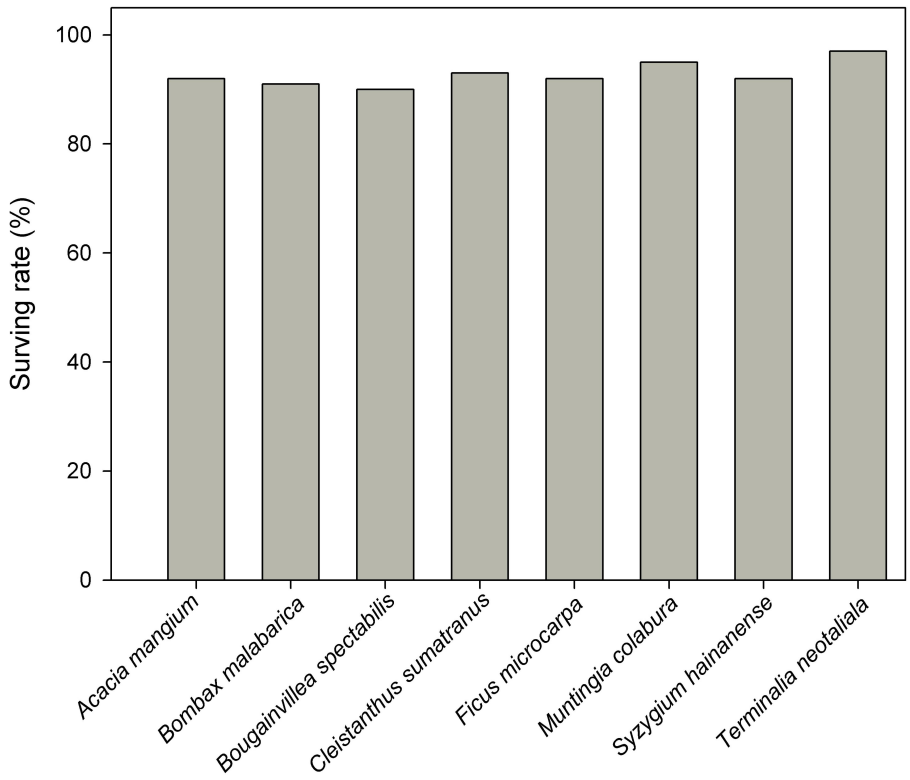


FIGURE 3
The survival rate of eight selected tree species. Acacia mangium, Bombax malabarica, Bougainvillea spectabilis, Cleistanthus sumatranus, Ficus microcarpa, Muntingia calabura, Syzygium hainanense, and Terminalia neotaliala were used for reforestation in 2016 in BPL. Survival rates were recorded in 2023.

candidate native species were from 0.1 to 0.2 (Figure 1), indicating they are not appropriate for reforestation.

After 7 years of the planting of the saplings of these eight tree species was performed, we found that the originally degraded landscape (comprising only barren rocks) has transformed into a forest landscape (Figure 2). Moreover, the survival rates of all the selected tree species were very high (90%–97%, Figure 3). Additionally, all the eight species could naturally recruit, which was inferred by comparing large height and DBH of the planted trees (30 m height, 30 cm DBH), compared with very small height and DBH (1 m and 1 cm, respectively) of the new trees (Figure 4). The large height and DBH would have been achieved by trees initially planted in 2016, whereas trees with the very small height and DBH should have been naturally recruited.

## Discussion

The standard for judging whether selected tress species are suitable for restoration in degraded ecosystem include the following aspects: 1) the original landscape has fully changed after deploying selected tree species to perform restoration (Lei et al., 2016); 2) selected tree species could adapt well to the severe environment in the degraded ecosystem, thereby having a high survival rate (Wang et al., 2020); 3) the selected tree species could recruit naturally, without requiring manual management (Holl et al., 2017). In this study, it was obvious that the originally barren land had transformed into a forest landscape after the selected tree species were deployed for restoration (Figure 2). Moreover, all the selected tree species had very high survival rates (Figure 3). In addition, all selected tree species could recruit naturally, which was indicated by presence of new trees with very small DBH and height (Figure 4). Furthermore, there was no need for a manual management of the reforested area since 2021. All of these results clearly indicate that the tree species selected by our protocol are suitable for reforestation in the target ecosystem.

Traditional trial-and-error-based methods have been widely used to select candidate species for ecosystem restoration, but these usually take at least one to three years to select one to five appropriate plant species (Giardina et al., 2007; Funk et al., 2008; Hall et al., 2011; Kanowski, 2014). Trait-based frameworks have been widely applied across tropical forest communities to understand variations in assemblage during a succession and at different spatial scales (Garnier et al., 2004; McGill et al., 2006; Shipley et al., 2006; Kraft et al., 2008; Zhu et al., 2013; Zhang et al., 2018). While these have established a theoretical basis for ecological restoration in degraded tropical forests, more thorough field research is needed to prove that these frameworks can be successfully applied to restore extremely degraded tropical forest ecosystems. Based on these theoretical basis, here we have provided a trait-based selection protocol that can be used to identify appropriate tree species for reforestation in degraded tropical

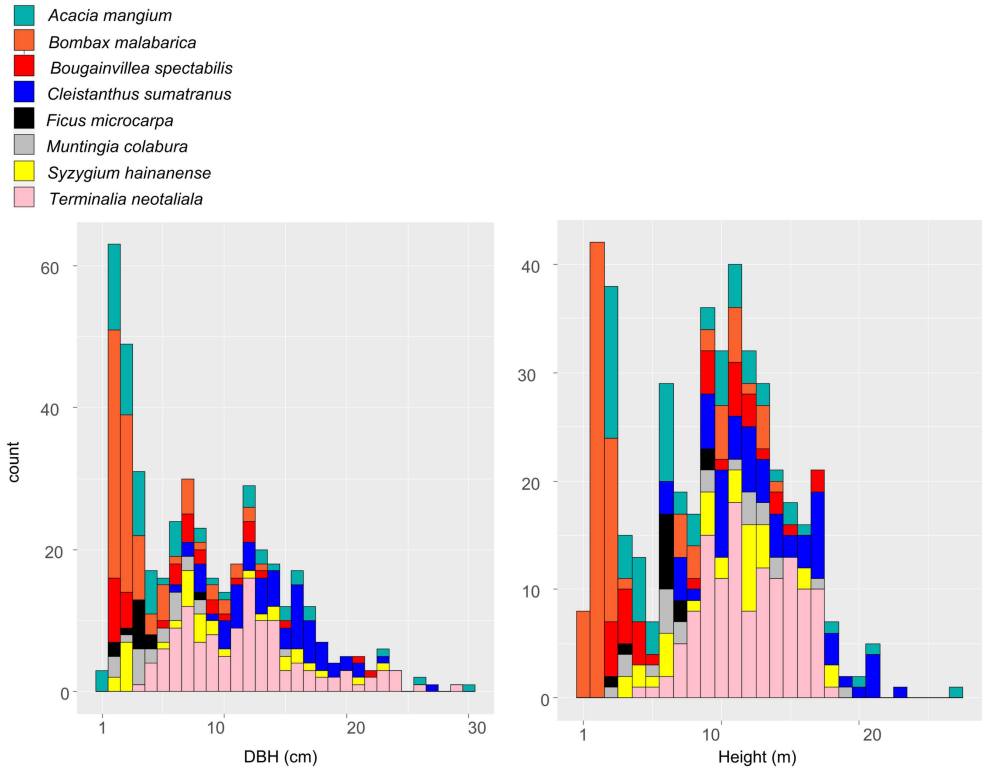


FIGURE 4
The differences in height (m) and diameter at breast height (DBH, cm) among eight selected tree species (*Acacia mangium*, *Bombax malabarica*, *Bougainvillea spectabilis*, *Cleistanthus sumatranus*, *Ficus microcarpa*, *Muntingia calabura*, *Syzygium hainanense*, and *Terminalia neotaliala*) in BPL after reforestation. Measurements were recorded in 2023.

forests. Indeed, our protocol required only 1 month to measure functional traits. Using our trait-based protocol, we successfully selected eight tree species from 60 candidates which are proven very appropriate for quickly restoring the degraded tropical mining. Our protocol is therefore effective in the selection of appropriate tree species for reforestation in degraded tropical mining.

It should be noted that a successful forest restoration must follow the ecological successional theory so that the degraded forest could recover to the originally undisturbed conditions (Funk et al., 2008). Fast-growing tree species usually dominate early forest succession (Lohbeck et al., 2014), whereas late successional slow-growing tree species gradually replace these early-successional species (Grime, 2006; Mason et al., 2012). Our current reforestation work only simulates early forest succession. Future studies are needed where we would use these eight selected tree species (*Bombax malabarica* and *Cleistanthus sumatranus*) in conjunction with our tree species selection software platform to select late successional tree species, which possess different sets of functional traits. Then, we mix-planted saplings of all selected late-successional tree species in the understory of these eight species, which may gradually make late-successional tree species to replace these eight species. This may facilitate to finally recover to originally late-successional tropical rainforest.

## Conclusions

Our native plant species selection protocol and the software program could help to identify appropriate tree species for reforestation in degraded tropical mining. The efficacy and the speed with which our methodology works are important for the timeliness of ecosystem restoration in highly degraded and vulnerable areas.

## Data availability statement

The raw data supporting the conclusions of this article will be made available by the authors, without undue reservation.

## Author contributions

CX: Conceptualization, Data curation, Formal analysis, Methodology, Validation, Writing – original draft, Writing – review & editing. HY: Conceptualization, Investigation, Methodology, Supervision, Writing – original draft, Writing – review & editing. CC: Conceptualization, Data curation, Investigation, Methodology, Validation, Writing – original draft, Writing – review & editing. HZ: Conceptualization, Data curation, Investigation, Methodology, Project administration, Software, Validation, Writing – original draft, Writing – review & editing. CW: Formal Analysis, Methodology, Validation, Writing – original draft, Writing – review & editing.

## Funding

The author(s) declare financial support was received for the research, authorship, and/or publication of this article. This work was funded by the National Natural Science Foundation of China (U22A20449), the Hainan Provincial Natural Science Foundation of China (422CXTD508), the specific research fund of the Innovation Platform for Academicians of Hainan Province, the Hainan Province Science and Technology Special Fund (ZDYF2022SHFZ320), and Hainan Institute of National Park.

## Conflict of interest

The authors declare that the research was conducted in the absence of any commercial or financial relationships that could be construed as a potential conflict of interest.

## Publisher's note



## Supplementary material

The Supplementary Material for this article can be found online at: https://www.frontiersin.org/articles/10.3389/fpls.2024.1456740/full#supplementary-material

## References

Abood, S. A., Lee, J. S. H., Burivalova, Z., Garcia-Ulloa, J., and Koh, L. P. (2015). Relative contributions of the logging, fiber, oil palm, and mining industries to forest loss in Indonesia. *Conserv. Lett.* 8, 58–67. doi: 10.1111/conl.12103

Ahirwal, J., Subodh., K. M., and Ashok, K. S. (2017). Changes in ecosystem carbon pool and soil CO2 flux following post-mine reclamation in dry tropical environment, India. *Sci. Total. Environ.* 583, 153–162. doi: 10.1016/j.scitotenv.2017.01.043

Ahmed, AI, Bryant, RG, and Edwards, DP (2021). Where are mines located in sub Saharan Africa and how have they expanded overtime? *Land Degrad Dev.* 32, 112–122. doi: 10.1002/ldr.3706

Aleman, J. C., Jarzyna, M. A., and Staver, A. C. (2018). Forest extent and deforestation in tropical Africa since 1900. *Nat. Ecol. Evol.* 2, 26–33. doi: 10.1038/s41559-017-0406-1

Brown, R. W., and Amacher, M. C. (1999). Selecting plant species for ecological restoration: a perspective for land managers. Pages 1–16 in Holzworth, L.K., and Brown, R.W. compilers. *Revegetation with Native Species: Proceedings, 1997 Society for Ecological Restoration annual meeting, Ft. Lauderdale, Florida, 12–15 November 1997. Proc. RMRS-P-8*. U.S. Department of Agriculture, Forest Service, Rocky Mountain Research Station, Ogden, Utah.

Butsic, V. A., Baumann, M., Shortland, A., Walker, S., and Kuemmerle, K. (2015). Conservation and conflict in the Democratic Republic of Congo: The impacts of warfare, mining, and protected areas on deforestation. *Bio. Conserv.* 3, 266–273. doi: 10.1016/j.biocon.2015.06.037

Fry, E. L., Power, S. A., and Manning, P. (2013). Trait-based classification and manipulation of plant functional groups for biodiversity–ecosystem function experiments. *J. Veg. Sci.* 25, 248–261. doi: 10.1111/jvs.12068

Funk, J. L., Cleland, E. E., Suding, K. N., and Zavaleta, E. S. (2008). Restoration through reassembly: plant traits and invasion resistance. *Trends Ecol. Evol.* 23, 695–703. doi: 10.1016/j.tree.2008.07.013

Garnier, E., Cortez, J., Billès, G., Navas, M. L., Roumet, C., Debussche, M., et al. (2004). Plant functional markers capture ecosystem properties during secondary succession. *Ecology* 85, 2630–2637. doi: 10.1890/03-0799

Giardina, C. P., Litton, C. M., Thaxton, J. M., Cordell, S., Hadway, L. J., Sandquist, D. R., et al. (2007). Science driven restoration: A candle in a demon haunted world—Response to cabin. *Restor. Ecol.* 15, 171–176. doi: 10.1111/j.1526-100X.2007.00227.x

González-González, A., Clerici, N., and Quesada, B. (2021). Growing mining contribution to Colombian deforestation. *Environ. Res. Lett.* 16, 064046. doi: 10.1088/1748-9326/abfcf8

Grime, J. P. (2006). Trait convergence and trait divergence in herbaceous plant communities: mechanisms and consequences. *J. Veg. Sci.* 17, 255–260. doi: 10.1111/j.1654-1103.2006.tb02444.x

Griscom, B. W., Adams, J., Ellis, P. W., Houghton, R. A., Lomax, G., Miteva, D. A., et al. (2017). Natural climate solutions. *P. Natl. Acad. Sci. U.S.A.* 114, 11645–11650. doi: 10.1073/pnas.1710465114

Hall, J. S., Ashton, M. S., Garen, E. J., and Jose, S. (2011). The ecology and ecosystem services of native trees: Implications for reforestation and land restoration in Mesoamerica. *For. Ecol. Manage.* 261, 1553–1557. doi: 10.1016/j.foreco.2010.12.011

Holl, K. D., Reid, J. L., Chaves-Fallas, J. M., Federico OviedoBrenes, F. O., and Zahawi, R. A. (2017). Local tropical forest restoration strategies affect tree recruitment more strongly than does landscape forest cover. *J. Appl. Ecol.* 54, 1091–1099. doi: 10.1111/1365-2664.12814

Hua, L., Chen, Y., Zhang, H., Fu, P., and Fan, Z. (2017). Stronger cooling effects of transpiration and morphology of the plants from a hot dry habitat than from a hot wet habitat. *Funct. Ecol.* 31, 2202–2211. doi: 10.1111/1365-2435.12923

Hua, F. Y., Bruijnzeel, L. A., Meli, P., Martin, P. A., and Zhang, J. (2022). The biodiversity and ecosystem service contributions and trade-offs of forest restoration approaches. *Science* 376, 839–844. doi: 10.1126/science.abl4649

Jones, T. A. (2013). Ecologically appropriate plant materials for restoration applications. *BioScience* 63, 211–219. doi: 10.1525/bio.2013.63.3.9

Kanowski, J. (2014). Restoration ecology: the new frontier 2nd edition, edited by J. Van andel and J. Aronson, blackwell publishing, oxford. *Ecol. Manage. Restor.* 15, 1–7. doi: 10.1111/emr.12078

Kraft, N. J., Valencia, R., and Ackerly, D. D. (2008). Functional traits and niche-based tree community assembly in an Amazonian forest. *Science* 322, 580–582. doi: 10.1126/science.1160662

Lamb, D., Epskine, P.D., and Parrotta, J. (2005). Restoration of degraded tropical forest landscapes. *Science* 310, 1628–1632. doi: 10.1126/science.1111773

Laughlin, D. C. (2014). Applying trait-based models to achieve functional targets for theory-driven ecological restoration. *Ecol. Lett.* 17, 771–784. doi: 10.1111/ele.12288

Laughlin, D. C., and Laughlin, D. E. (2013). Advances in modelling trait-based plant community assembly. *Trends Plant Sci.* 18, 584–593. doi: 10.1016/j.tplants.2013.04.012

Laurance, W. F., Sayer, J., and Cassman, K. G. (2014). Agricultural expansion and its impacts on tropical nature. *Trends Ecol. Evol.* 29, 107–116. doi: 10.1016/j.tree.2013.12.001

Lei, K., Pan, H., and Lin, C. (2016). A landscape approach towards ecological restoration and sustainable development of mining areas. *Ecol. Engineer.* 13, 13–19. doi: 10.1016/j.ecoleng.2016.01.080

Lohbeck, M., Poorter, L., Martínez-Ramos, M., Rodriguez-Velázquez, J., Breugel, M., Bongers, F., et al. (2014). Changing drivers of species dominance during tropical forest succession. *Funct. Ecol.* 28, 1052–1058. doi: 10.1111/1365-2435.12240

Lugo, A. E. (1997). The apparent paradox of reestablishing species richness on degraded lands with tree monocultures. *For. Ecol. Manage.* 99, 9–19. doi: 10.1016/S0378-1127(97)00191-6

Macdonald, S. E., Landhäusser, S. M., Skousen, J., Franklin, J., Frouz, J., Hall, S., et al (2015). Forest restoration following surface mining disturbance: challenges and solutions. *New For.* 46, 703–732. doi: 10.1007/s11056-015-9506-4

Mason, N. W., Richardson, S. J., Peltzer, D. A., de Bello, F., Wardle, D. A., Allen, R. B., et al. (2012). Changes in coexistence mechanisms along a long-term soil chronosequence revealed by functional trait diversity. *J. Ecol.* 100, 678–689. doi: 10.1111/j.1365-2745.2012.01965.x

McGill, B. J., Enquist, B. J., Weiher, E., and Westoby, M. (2006). Rebuilding community ecology from functional traits. *Trends Ecol. Evol.* 21, 178–185. doi: 10.1016/j.tree.2006.02.002

Mitchard, E. T. A. (2018). The tropical forest carbon cycle and climate change. *Nature* 559, 527–534. doi: 10.1038/s41586-018-0300-2

Ostertag, R., Warman, L., Cordell, S., and Vitousek, P. M. (2015). Using plant functional traits to restore Hawaiian rainforest. *J. Appl. Ecol.* 52, 805–809. doi: 10.1111/1365-2664.12413

Packard, S., and Mutel, C. F. (1997). *The tallgrass restoration handbook: for prairies, savannas, and woodlands* (Washington, DC: Island Press).

Shipley, B., Vile, D., and Garnier, É. (2006). From plant traits to plant communities: a statistical mechanistic approach to biodiversity. *Science* 314, 812–814. doi: 10.1126/science.1131344

Siqueira-Gay, J., and Sánchez, L. E. (2021). The outbreak of illegal gold mining in the Brazilian Amazon boosts deforestation. *Reg Environ Change* 21, 28. doi: 10.1007/s10113-021-01761-7

Sonter, L. J., Herrera, D., Barrett, D. J. , Galford, G. L., Moran, C. J., and Soares-Filho, B. S. (2017). Mining drives extensive deforestation in the Brazilian Amazon. *Nat Commun.* 8, 1013. doi: 10.1038/s41467-017-00557-w

Symes, W. S., Edwards, D. P., Miettinen, J., Rheindt, F. E., and Carrasco, L. R. (2018). Combined impacts of deforestation and wildlife trade on tropical biodiversity are severely underestimated. *Nat. Commun.* 9, 4052. doi: 10.1038/s41467-018-06579-2

Taubert, F., Fischer, R., Groeneveld, J., Lehmann, S., Müller, M. S., Rödig, E., et al. (2018). Global patterns of tropical forest fragmentation. *Nature* 554, 519–522. doi: 10.1038/nature25508

Wang, C., Liu, H., Zhu, L., Ren, H., Yan, J., Li, Z., et al. (2021). Which traits are necessary to quickly select suitable plant species for ecological restoration? *Ecol. Solu. Evi.* 2, e12102. doi: 10.1002/2688-8319.12102

Wang, C., Zhang, H., Liu, H., Jian, S., Yan, J., Liu, N., et al. (2020). Application of a trait-based species screening framework for vegetation restoration in a tropical coral island of China. *Funct. Ecol.* 6, 1193–1204. doi: 10.1111/1365-2435.13553

Zhang, H., H. Chen, J. Y., Lian, J., Robert, R., Li, H., Liu, W. H., et al. (2018). Using functional trait diversity patterns to disentangle the scale-dependent ecological processes in a subtropical forest. *Funct. Ecol.* 32, 1379–1389. doi: 10.1111/1365-2435.13079

Zhang, H., He, M. F., Shree, P. P., Liu, L., and Zhou, S. R. (2023). Soil fungal community is more sensitive than bacterial to mining and reforestation in a tropical rainforest. *Land. Degrad. Dev.* 12, 22–27. doi: 10.1002/ldr.4734

Zhang, H., Li, Y. S., Xu, Y. K., and Robert, J. (2024). The recovery of soil N-cycling and P-cycling following reforestation in a degraded tropical limestone mine. *J. Clean. Prod.* 2, 141580. doi: 10.1016/j.jclepro.2024.141580

Zhu, S. D., Song, J. J., Li, R. H., and Ye, Q. (2013). Plant hydraulics and photosynthesis of 34 woody species from different successional stages of subtropical forests. *Plant Cell Environ.* 36, 879–891. doi: 10.1111/pce.12024

frontiers | Frontiers in Plant Science

TYPE Original Research
PUBLISHED 04 September 2024
DOI 10.3389/fpls.2024.1442807



OPEN ACCESS

EDITED BY
Xiang Liu,
Lanzhou University, China

REVIEWED BY
Hongwei Wang,
Henan Agricultural University, China
Wen-Bin Yu,
Chinese Academy of Sciences (CAS), China

*CORRESPONDENCE
Liang Tang
tangliang@hainanu.edu.cn
Li Yan
yanli@mail.cgs.gov.cn
Yong-bo Liu
liuyb@craes.org.cn

†These authors have contributed equally to this work

RECEIVED 03 June 2024
ACCEPTED 09 August 2024
PUBLISHED 04 September 2024

CITATION
Tang L, Long J-q, Wang H-y, Rao C-k, Long W-x, Yan L and Liu Y-b (2024) Conservation genomic study of *Hopea hainanensis* (Dipterocarpaceae), an endangered tree with extremely small populations on Hainan Island, China. *Front. Plant Sci.* 15:1442807. doi: 10.3389/fpls.2024.1442807



# Conservation genomic study of *Hopea hainanensis* (Dipterocarpaceae), an endangered tree with extremely small populations on Hainan Island, China

Liang Tang [1,2*†], Jun-qiao Long [3†], Hai-ying Wang [2], Chao-kang Rao [2], Wen-xing Long [4], Li Yan [3*] and Yong-bo Liu [5*]

[1]International Joint Center for Terrestrial Biodiversity around the South China Sea of Hainan Province, Hainan University, Haikou, China, [2]School of Ecology, Hainan University, Haikou, China, [3]Haikou Marine Geological Survey Center, China Geological Survey, Haikou, China, [4]School of Tropical Agriculture and Forestry, Hainan University, Haikou, China, [5]State Environmental Protection Key Laboratory of Regional Eco-Process and Function Assessment, Chinese Research Academy of Environmental Sciences, Beijing, China

**Introduction:** *Hopea hainanensis* Merrill & Chun is considered a keystone and indicator species in the tropical lowland rainforests of Hainan Island. Owing to its high-quality timber, *H. hainanensis* has been heavily exploited, leading to its classification as a first-class national protected plant in China and a plant species with extremely small populations (PSESPs).

**Methods:** This study analyzed genome-wide single nucleotide polymorphisms obtained through restriction site-associated DNA sequencing from 78 adult trees across 10 *H. hainanensis* populations on Hainan Island.

**Results and discussion:** The nucleotide diversity of the sampled populations ranged from 0.00096 to 0.00138, which is lower than that observed in several other PSESPs and endangered tree species. Bayesian unsupervised clustering, principal component analysis, and neighbor-joining tree reconstruction identified three to five genetic clusters in *H. hainanensis*, most of which were geographically widespread and shared by multiple populations. Demographic history analysis based on pooled samples indicated that the decline in the *H. hainanensis* population began approximately 20,000 years ago, starting from an ancestral population size of approximately 10,000 individuals. The reduction in population size accelerated approximately 4,000 years ago and has continued to the present, resulting in a severely reduced population on Hainan Island. Intensified genetic drift in small and isolated *H. hainanensis* populations may contribute to moderate differentiation between some of them, as revealed by pairwise $F_{st}$. In conclusion, our conservation genomic

study confirms a severe population decline and an extremely low level of nucleotide variation in *H. hainanensis* on Hainan Island. These findings provide critical insights for the sustainable management and genetic restoration of *H. hainanensis* on Hainan Island.

KEYWORDS

*Hopea hainanensis* Merrill & Chun, conservation genomics, plant species with extremely small populations, population decline, reduced-representation genome sequencing

## 1 Introduction

Tropical rainforests play crucial roles in local economies and ecosystem services (Corlett and Primack, 2011). They produce a variety of biomass materials, sustain extremely high biodiversity, and are key in carbon sequestration, temperature regulation, watershed services, and climate change mitigation (Montagnini and Jordan, 2005; Corlett and Primack, 2011). Asian tropical rainforests flourish in the Malay Peninsula, Sumatra, Borneo, Java, New Guinea, and wetter region of the Philippine Islands, extending north through the Indochina Peninsula to the southern parts of Yunnan, Guangxi, Guangdong, and Taiwan Provinces, as well as Hainan Island in China (Hu and Li, 1992). A single family, the Dipterocarpaceae, dominates the lowland rainforests in Asia, with the species diversity, richness, and cross-sectional area at breast height being most prominent in these forests (Ghazoul, 2016). Trees of the Dipterocarpaceae are primarily large canopy trees, accounting for more than 50% of all canopy species, with many exceeding 50 m in height. No other tropical forests have such a high proportion of dominant species in a single family (Ghazoul, 2016). Research on the phylogeny, divergence time, historical biogeography, and population genetics of Dipterocarpaceae will facilitate a better understanding of the assembly, evolution, and adaptation of Asian tropical rainforest communities (Ashton, 1988; Ghazoul, 2016).

Hainan Island is located on the northern edge of tropical Asia, where the climate is heavily influenced by the Asian monsoon. The temperature and precipitation on Hainan Island are markedly different from those in Southeast Asia near the equator (Hu and Li, 1992; Zhu, 1993). The species diversity and abundance of dipterocarps on Hainan Island are much less prominent than those in Southeast Asia (Hu and Li, 1992). In fact, there are only three species of Dipterocarpaceae on the island: *Vatica mangachapoi* Blanco, *Hopea hainanensis* Merrill & Chun, and *H. reticulata* Tardieu (Li et al., 2007; Xing et al., 2012). *V. mangachapoi* is the dominant species and is widely distributed in the lowland rainforests of Hainan Island (Hu and Li, 1992; Li et al., 2006). However, *H. reticulata* is confined to the Ganza Ridge, and its fruits are wingless, falling directly to the ground after maturity (Hu et al., 2020). *H. hainanensis*, a species with an extremely small population, is rare in the lowland rainforests. Two sepals in the flower of this species continue to grow and develop into wing-like lobes in the fruits, aiding in seed dispersal (Li et al., 2007). It is worth noting that *H. hainanensis* serves as an indicator of the development of tropical rainforests on Hainan Island and has the highest importance value in the lowland rainforest communities (Hu, 1983). Additionally, the timber from *H. hainanensis* is highly valued in Hainan due to its high density, hardness, and corrosion resistance (Xie and Huang, 1990). As a result, *H. hainanensis* has been excessively logged, and mature trees are now very rare, with fewer than 250 remaining (Information system of Chinese Rare and Endangered Plants: http://www.iplant.cn/bhzw/info/985). In addition to Hainan Island, the occurrence of this species has been recorded in a few locations in Vietnam (Li et al., 2007). Owing to the extremely small size of its natural populations and its ecological significance in the tropical forests of Hainan Island, *H. hainanensis* has been listed as a national first-class protected plant in China (Yang et al., 2016; Lu et al., 2020).

Plant species with extremely small populations (PSESPs) refer to endangered plants that are at risk of extinction without protection because their wild population sizes are smaller than the minimum viable population size (Ren et al., 2012; Ma et al., 2013; Zang et al., 2016). In the past 10 years, increasing attention has been paid to exploring the possible causes of population declines and the sustainable management of PSESPs. Yao et al. (2021) suggested that reduced fertility and consequent difficulty in regeneration, loss of genetic diversity and compromised adaptation potential in small populations, human disturbance, natural disasters, and global climate change contribute to the occurrence of PSESPs. Zang et al. (2016) proposed a scheme for the maintenance and restoration of PSESPs, which includes *in situ* conservation and habitat restoration, *ex situ* conservation, seedling propagation and field planting, and genetic evaluation of germplasm resources.

The proposal of PSESPs and efforts to protect them have facilitated the rescue of critically endangered plant species in China (Sun et al., 2019). Conservation genetic studies have been carried out for some PSESPs in Yunnan Province, China. Using a combined strategy of *de novo* genome sequencing and whole-genome resequencing, the nucleotide diversity and demographic history of two PSESPs, *Rhododendron griersonianum* and *Acer yangbiense*, were assessed (Ma et al., 2021, 2022). Research on another PSESP, *H. hainanensis*, has mainly focused on its population ecology, seed germination, and seedling growth (Wen et al., 2002; Zhang et al., 2019; Lu et al., 2020). Previous

studies have found that adult *H. hainanensis* trees can bear a large number of fruits that easily germinate and form a large number of seedlings after falling to the forest ground. However, few of these seedlings grow into saplings or young trees, indicating a severe recruitment constraint in the natural populations of *H. hainanensis* on Hainan Island (Lu et al., 2020; Luo et al., 2023). The shady environment under the canopy and fierce competition between the seedlings result in the death of almost all the seedlings. The development of the seedings is also affected by other habitat factors, such as slope, soil moisture and nutrients, and distance from mother trees (Pei et al., 2015; Lu et al., 2020). These studies have provided valuable insights into the *in situ* conservation and restoration of *H. hainanensis*.

Knowledge of the level and pattern of genetic variation in endangered species can be used to infer the causes of population declines, define conservation units, identify populations needing urgent protection, and design sampling schemes for *ex situ* conservation (Chen et al., 2002; DeSalle and Amato, 2004; Benestan et al., 2016; Li et al., 2020). By genotyping 12 polymorphic microsatellite markers, Wang et al. (2020) assessed the genetic variation patterns of *H. hainanensis* on Hainan Island. It was found that there is a lack of low-frequency alleles in the wild population of *H. hainanensis*, suggesting a potential recent bottleneck in this species. However, details of its demographical history, such as the timing and intensity of the bottleneck, have not been fully determined. It remains unclear whether the bottleneck was induced by paleoclimate changes or human disturbance or both. Additionally, there are inherent limitations in the application of microsatellite markers in population genetic analyses (Schlotterer, 2004; Putman and Carbone, 2014). Fortunately, genome-wide single nucleotide polymorphisms (SNPs) can be detected and genotyped using next-generation sequencing in a high-throughput and cost-effective manner (Davey et al., 2011). For non-model species without reference genomes, restriction site-associated DNA sequencing (RADseq) has been routinely performed to discover a large number of SNPs, enabling ecological, evolutionary, and conservation genetics studies (Davey and Blaxter, 2010; Andrews et al., 2016; Parchman et al., 2018).

In the present study, genome-wide SNPs were genotyped for *H. hainanensis* using RADseq, and conservation genomic research was conducted to shed light on the sustainable management of this dipterocarp species on the northern edge of the Asian tropics. The aims of this study were to determine the following: (1) the level of nucleotide diversity in *H. hainanensis* on Hainan Island—is it higher or lower compared with other endangered trees? (2) The geographic distribution of genetic variation—how is the nucleotide variation in this species structured on the island? (3) The demographic history of *H. hainanensis* and possible causes of its population decline.

# 2 Materials and methods

## 2.1 Population sampling

We collected 10 populations of *H. hainanensis* on Hainan Island, including most of the known locations of this species. Among them, nine populations were sampled from the Hainan Tropical Rainforest National Park, and one was collected from Baolong Forest Farm in Sanya City. Detailed information on population codes, sample sizes, and geographic locations (latitude and longitude) is listed in Table 1. Leaf samples were collected from adult trees with a diameter at breast height greater than 0.1 m. All sampled trees were separated by a distance of at least 10 m. Young disease-free leaves were collected and dried with silica gel immediately. After completely drying, the leaves were stored in a –nore refrigerator for later use.

## 2.2 Restriction site-associated DNA sequencing and data analyses

Total genomic DNA was extracted from the silica gel-dried leaves using a Qiagen plant genome extraction kit (Qiagen, Shanghai, China). The concentration and quality of the DNA were determined using a Qubit 3.0 Fluorometer. After appropriate

TABLE 1 Geographic origin, population size, and nucleotide diversity of *Hopea hainanensis* on Hainan Island.

| Population code | Sample size | Collection locality | Geographic coordinates | $H_o$ | $H_e$ | $F_{is}$ | π |
|---|---|---|---|---|---|---|---|
| FJ | 9 | Fanjia natural reserve | 19.2722°N, 109.6150°E | 0.09910 | 0.20210 | 0.30837 | 0.00129 |
| LM | 8 | Limu Mountain | 19.1909°N, 109.7417°E | 0.23612 | 0.22192 | 0.01669 | 0.00110 |
| BW | 8 | Bawang Mountain | 19.0982°N, 109.1313°E | 0.15116 | 0.19720 | 0.14599 | 0.00125 |
| QW | 7 | Qiwang Mountain | 18.9388°N, 109.4468°E | 0.26692 | 0.22875 | -0.01922 | 0.00101 |
| JX | 8 | Jiaxi natural reserve | 18.8429°N, 109.1662°E | 0.24881 | 0.22565 | -0.00205 | 0.00112 |
| JF | 8 | Jianfeng Mountain | 18.7422°N, 108.9902°E | 0.16262 | 0.23548 | 0.22844 | 0.00134 |
| KF | 7 | Kafa Mountain | 18.6988°N, 109.3303°E | 0.21524 | 0.19869 | 0.02133 | 0.00096 |
| MR | 7 | Maorui forestry station | 18.6724°N, 109.4116°E | 0.10925 | 0.22807 | 0.34535 | 0.00138 |
| DL | 8 | Diaoluo Mountain | 18.6961°N, 109.8839°E | 0.13987 | 0.18339 | 0.13718 | 0.00107 |
| BL | 8 | Baolong forestry station | 18.4855°N, 109.4385°E | 0.22960 | 0.23223 | 0.06851 | 0.00114 |
| Total | 78 | | | 0.20414 | 0.25982 | 0.26431 | 0.00119 |

$H_o$, observed heterozygosity; $H_e$, expected heterozygosity; $F_{is}$, inbreeding coefficient; πo nucleotide diversity.

dilution, genomic DNA was double digested with EcoRI and MseI. The digested fragments were cleaned and subsequently quantified using agarose gel electrophoresis, then ligated to EcoRI and MseI adapters containing sample specific barcodes. After ligation, individually barcoded samples were size-selected (350-sel bp) using agarose gel (Omega kit) and purified. The resulting fragments were further amplified by PCR to the desired concentration and sequenced on the HiSeq X Ten platform (Illumina) with PE 150 mode.

Raw reads generated by RADseq were analyzed using the Stacks version 2 package (Rochette et al., 2019). The script '*process_radtags.pl*' was executed to demultiplex the raw sequencing reads and remove low quality data. Then, the '*denovo_map.pl*' program was run to assemble loci and call SNPs without a reference genome using the demultiplexed reads. The number of mismatches allowed between the two alleles of an individual was controlled by the parameter *M*, and its optimal value was determined according to the method suggested by Rochette and Catchen (2017). SNPs were filtered using the '*populations*' program in Stacks 2. The filters included the following: 1) at least 50% of the studied populations and at least 60% of the individuals in each population must be present to process a locus; 2) the minimum minor allele frequency at a locus is 0.05; and 3) only one random SNP per locus is retained for the analyses of population structure and historical demography. A variant call format (VCF) file and an input file for STRUCTURE version 2.3.4 (Pritchard et al., 2000) were also generated by '*populations*' and used for subsequent data analysis.

## 2.3 Population genetic data analyses

Nucleotide diversity (ive observed and expected heterozygosity ($H_o$ and $H_e$), inbreeding coefficient ($F_{is}$), and genetic differentiation between populations ($F_{st}$) were estimated by the '*populations*' program in the Stacks 2 package. An individual-based *p*-distance matrix was calculated using the software VCF2Dis (https://github.com/BGI-shenzhen/VCF2Dis), then a neighbor-joining (NJ) tree was reconstructed using the '*fneighbor*' program and the bootstrapping consensus tree was inferred by the '*fconsense*' program (Rice et al., 2000). Population structure was analyzed using the model-based clustering method implemented in the software STRUCTURE version 2.3.4 (Pritchard et al., 2000). The number of populations (*K*) varied from 1 to 12, and for each value of *K*, 10 independent replicates were run with 100,000 burn-in iterations followed by 1,000,000 Markov chain Monte Carlo simulations. A mixed model with correlated allele frequencies was used (Falush et al., 2003). STRUCTURE Harvester was used to determine the most likely number of populations (*K*) following the procedure described by Evanno et al. (2005), and a graphical representation of the clustering analysis was generated by the web-based software StructureSelector (Li and Liu, 2018). Principal component analysis was performed using the GCTA package with default settings, and the first and second principal components were selected for plotting (Yang et al., 2011).

To assess whether populations followed a pattern of isolation by distance, we plotted the pairwise genetic differentiation between populations, estimated by Wrightte $F_{st}$, against the geographical distance using the Mantel test (Mantel, 1967) as implemented in Arlequin 3.5 (Excoffier and Lischer, 2010). The significance of the test was determined by 9,999 random permutations. An analysis of molecular variance (AMOVA), implemented in Arlequin 3.5, was conducted to detect population genetic differentiation at inter-population and intra-population levels. The significance of the *F*-statistics was determined by 9,999 random permutations.

A folded SNP frequency spectrum (SFS) was generated by the Python script *easySFS* (https://github.com/isaacovercast/easySFS). To utilize SNPs with partially missing data, the "down projection method" implemented in *easySFS* was used to determine the optimal projection value for the input data. The demographic history of *H. hainanensis* on Hainan Island was inferred based on the folded SFS using the software Stairway Plot 2, a model-free method that does not require whole-genome sequencing data or a reference genome (Liu and Fu, 2015; 2020). A mutation rate was required to convert time into the unit of years. Based on node times and the nucleotide sequences reported in Heckenhauer et al. (2017), the averaged mutation rate of the genus *Hopea* was estimated to be 2.13e−9 at per site per year. Field records indicate that *H. hainanensis* begins to bloom at approximately 30 years old. Therefore, the generation time of this species was set to 20, 30, and 40 years per generation to account for the potential variation in the timing of first flowering. The 10 sampled populations were pooled for Stairway Plot 2 analysis.

# 3 Results

## 3.1 Nucleotide diversity of *H. hainanensis* on Hainan Island

After the removal of low-quality reads, 247,235,540 clean reads remained, with an average of 3,169,686 reads per sample. The numbers of reads and nucleotides for each individual are listed in Supplementary Table S1. The filtered sequencing data have been deposited in the National Center for Biotechnology Information (NCBI) Sequence Read Archive (SRA) under accession number PRJNA1083891. The best fit value of the assembly parameter *M* was determined to be 3, following the method proposed by Rochette and Catchen (2017). Using this value of *M*, 6,017 loci were kept after filtering, of which 3,411 were found to contain 7,804 SNPs. The filtered SNPs were saved in a VCF format file for subsequent data analysis. The observed and expected heterozygosity, inbreeding coefficient, and nucleotide diversity were calculated using the '*populations*' program. The observed heterozygosity ranged from 0.09910 (FJ) to 0.26692 (QW), and the expected heterozygosity ranged from 0.19720 (BW) to 0.23548 (JF). The observed heterozygosity of the FJ and MR populations was approximately half of the expected heterozygosity. The inbreeding coefficients of these two populations were relatively high, indicating significant inbreeding levels. The observed heterozygosity was much higher than the expected heterozygosity in the JX and QW populations, and the inbreeding coefficients of these two populations were negative, indicating that they are likely outbreeding. The nucleotide diversity of the *H. hainanensis* populations ranged from 0.00096 to 0.00138, with the KF population having the

lowest genetic diversity and the MR, JF, FJ, and BW populations having a relatively higher genetic diversity (Table 1).

## 3.2 Population structure and genetic differentiation among populations

In model-based STRUCTURE analysis, the maximum value of Ln(*K*) was achieved when $K = 5$. Following the method developed by Evanno et al. (2005), $K = 5$ was found to best fit the data, indicating five distinct genetic clusters within the *H. hainanensis* populations on Hainan Island (Figure 1). There was no apparent geographic structure among the five genetic clusters (Figure 2). The genetic clusters colored in red and blue were geographically widespread and found in most of the sampled populations. The other three were more population specific, detected in 1 to 4 populations. The BW and DL populations were dominated by one genetic cluster, whereas the rest had at least two clusters. Only a few individuals showed mixed membership in the STRUCTURE analysis. Based on the first two principal components (PC1 and PC2), the *H. hainanensis* samples collected from Hainan Island were classified into three discrete genetic groups, each containing individuals from multiple populations (Figure 3). Except for the BW, DL, and FK populations, individuals sampled from the same population were assigned to at least two different genetic groups (Figure 3). The NJ tree reconstructed using the SNP data showed a similar pattern of individual clusters to that identified in the STRUCTURE analysis (Supplementary Figure S1).

A pairwise comparison of genetic differentiation showed that Wrighten $F_{st}$ ranged from 0.0321, between the BL and QW populations, to 0.1814, between the BW and DL populations, with a mean of 0.0975, indicating low to moderate differentiation among *H. hainanensis* populations (Table 2). The *F*-statistics, calculated by AMOVA, was 0.1367, suggesting that the overall differentiation is moderate (Supplementary Table S2). When intra- and inter-population levels were considered in AMOVA, 86.33% of the total molecular variation was found to be partitioned within populations. Isolation-by-distance, i.e., a significant linear correlation between genetic divergence and geographic distance, could not be detected by Mantel's test (Supplementary Figure S2).

## 3.3 Historical demography

The results of stairway plot analysis indicated that the population of *H. hainanensis* on Hainan Island began to shrink approximately 20,000 years ago from an initial population size of approximately 10,000 individuals (Figure 4). The decline of the *H.*

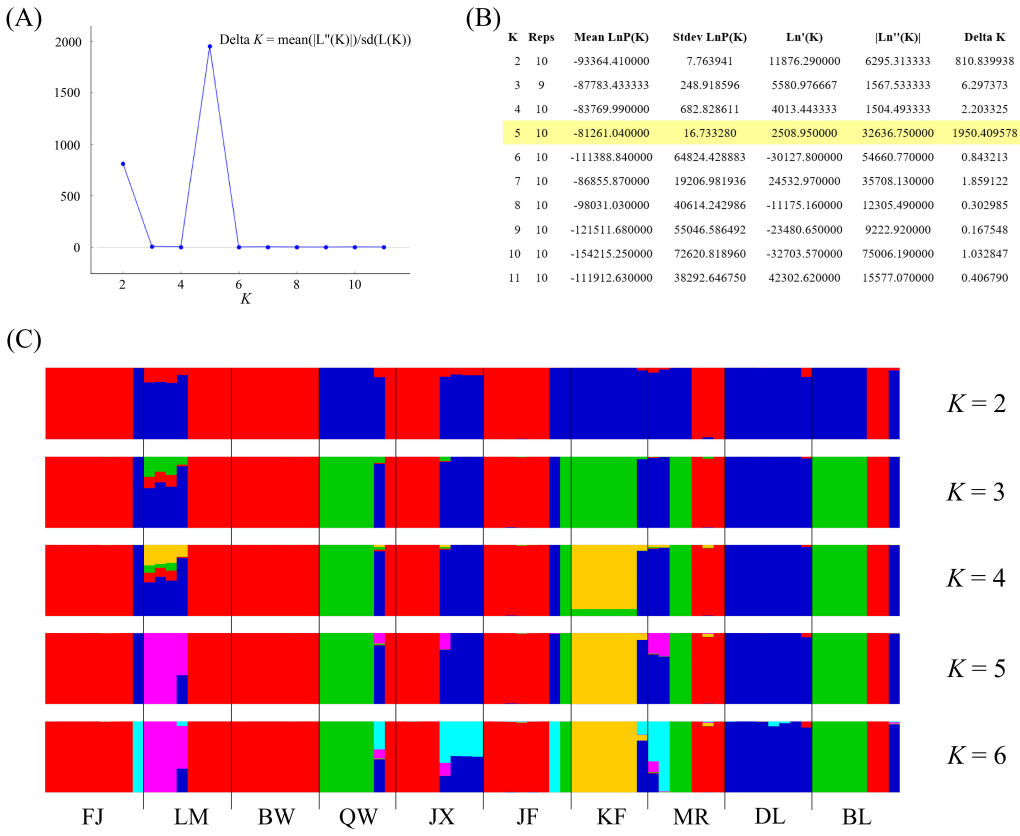


| K | Reps | Mean LnP(K) | Stdev LnP(K) | Ln'(K) | \|Ln''(K)\| | Delta K |
|---|---|---|---|---|---|---|
| 2 | 10 | -93364.410000 | 7.763941 | 11876.290000 | 6295.313333 | 810.839938 |
| 3 | 9 | -87783.433333 | 248.918596 | 5580.976667 | 1567.533333 | 6.297373 |
| 4 | 10 | -83769.990000 | 682.828611 | 4013.443333 | 1504.493333 | 2.203325 |
| 5 | 10 | -81261.040000 | 16.733280 | 2508.950000 | 32636.750000 | 1950.409578 |
| 6 | 10 | -111388.840000 | 64824.428883 | -30127.800000 | 54660.770000 | 0.843213 |
| 7 | 10 | -86855.870000 | 19206.981936 | 24532.970000 | 35708.130000 | 1.859122 |
| 8 | 10 | -98031.030000 | 40614.242986 | -11175.160000 | 12305.490000 | 0.302985 |
| 9 | 10 | -121511.680000 | 55046.586492 | -23480.650000 | 9222.920000 | 0.167548 |
| 10 | 10 | -154215.250000 | 72620.818960 | -32703.570000 | 75006.190000 | 1.032847 |
| 11 | 10 | -111912.630000 | 38292.646750 | 42302.620000 | 15577.070000 | 0.406790 |

FIGURE 1
Results of the STRUCTURE analysis. **(A)** The number of clusters *K* was inferred to be 5 using the Δ*K* method proposed by Evanno et al. (2005). **(B)** Log probabilities and Δ*K* values for K from 2 to 11. **(C)** The results of individual assignment at five different *K* (from 2 to 6). Each vertical bar represents an individual, and the proportion of the colors corresponds to the posterior probability of assignment to one of *K* genetic clusters.

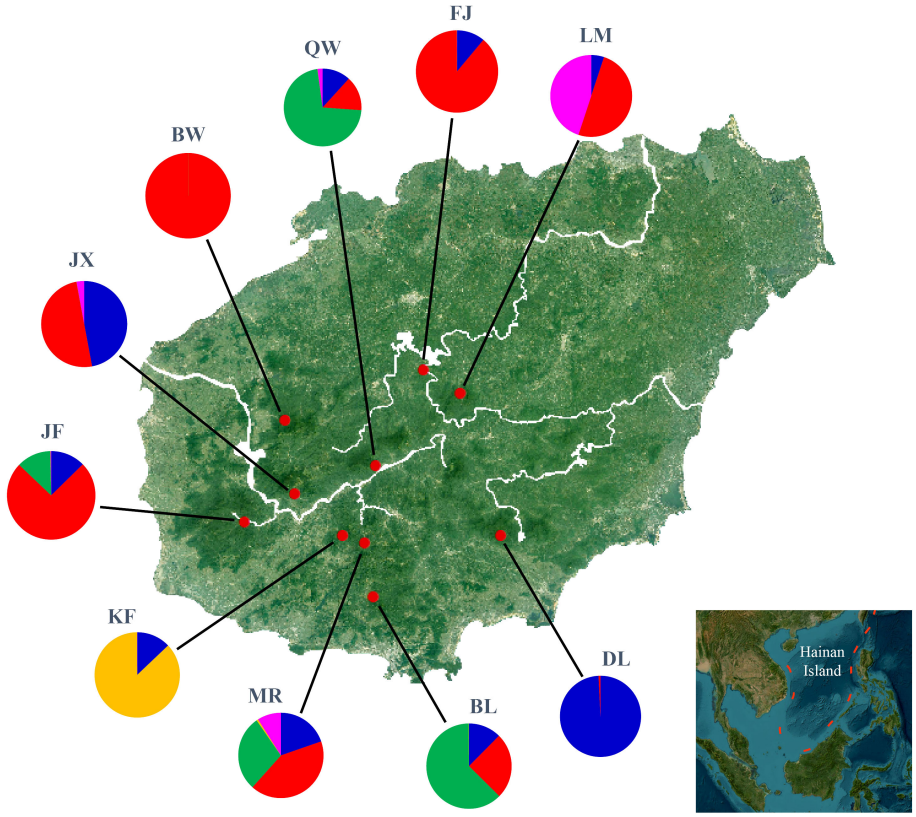


FIGURE 2
Geographic location of *Hopea hainanensis* populations sampled in this study (red dots). Pie charts illustrate the proportion of each of the five genetic clusters identified by STRUCTURE analyses for each population.

*hainanensis* population accelerated approximately 4,000 years ago and continued to the present, resulting in a small remaining population. Variations in generation time only slightly influenced the onset of population decline and size of the ancestral population before the decrease (Supplementary Figure S3).

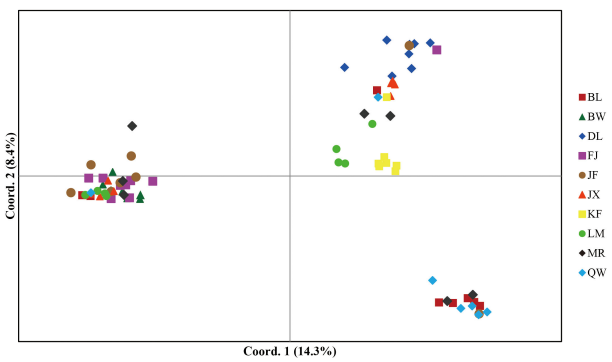


FIGURE 3
Principal component analysis (PCA) of individual samples from the *H. hainanensis* populations. The amount of variance explained by each component is indicated on PC1 and PC2 axes. Distinct colors and shapes represent individuals of different geographic origins.

# 4 Discussion

## 4.1 Low genetic diversity of *H. hainanensis* due to a severe population decline

Genetic diversities are commonly assessed for endangered dipterocarps and those that are predominant in Asian rainforest communities. Moderate to high levels of genetic variation within populations and weak differentiation among populations have been reported in some studies, e.g., Tito de Morais et al. (2015); Ghazoul (2016); Utomo et al. (2018), and Ng et al. (2019). Using 12 simple sequence repeat markers, Wang et al. (2020) found that heterozygosity, the number of alleles, and the proportions of low-frequency alleles in the endangered *H. hainanensis* were significantly lower than the non-endangered *H. dryobalanoides* of the same genus. As low-frequency alleles are more susceptible to loss than common alleles during population bottlenecks (Luikart et al., 1998), Wang et al. (2020) proposed that *H. hainanensis* on Hainan Island might have recently undergone such an event. This likely resulted in the loss of low-frequency alleles and a significant reduction in genetic diversity.

In this study, using RADseq, the nucleotide diversity ($\pi$) of *H. hainanensis* was shown to range from $0.96 \times 10^{-3}$ to $1.38 \times 10^{-3}$, with an average of $1.17 \times 10^{-3}$ (Table 1). The genetic variation of *H. reticulata*, another species of the genus *Hopea* in Hainan Island, has

TABLE 2 Pairwise comparison of the genetic differentiation between populations measured by $F_{st}$.

| | BL | BW | DL | FJ | JF | JX | KF | LM | MR | QW |
|---|---|---|---|---|---|---|---|---|---|---|
| BL | | 0.106426 | 0.128166 | 0.106411 | 0.066407 | 0.075980 | 0.113281 | 0.080823 | 0.061390 | 0.032097 |
| BW | | | 0.181353 | 0.057191 | 0.062590 | 0.083326 | 0.163143 | 0.078393 | 0.095148 | 0.127676 |
| DL | | | | 0.172434 | 0.129984 | 0.113467 | 0.151688 | 0.137713 | 0.120300 | 0.133270 |
| FJ | | | | | 0.052953 | 0.069807 | 0.159265 | 0.073314 | 0.081180 | 0.119384 |
| JF | | | | | | 0.053057 | 0.118488 | 0.059931 | 0.063274 | 0.074939 |
| JX | | | | | | | 0.115707 | 0.062044 | 0.059894 | 0.078807 |
| KF | | | | | | | | 0.122776 | 0.127102 | 0.111446 |
| LM | | | | | | | | | 0.067560 | 0.086638 |
| MR | | | | | | | | | | 0.053428 |

been studied recently using RADseq, yielding an average nucleotide diversity of $0.91 \times 10^{-3}$, slightly lower than that of *H. hainanensis* (Tang et al., 2024). The limited geographic distribution and severe population decline have been suggested as reasons for the low genetic variation observed in *H. reticulata*. However, the nucleotide diversity of *H. hainanensis* is significantly lower than several other PSESPs. For example, *Acer yangbiense*, a PSESP native to northwest Yunnan, showed a nucleotide diversity ranging from $2.54 \times 10^{-3}$ to $3.41 \times 10^{-3}$ based on whole-genome resequencing of 105 individuals from 10 populations (Ma et al., 2022). Only 31 individuals from the two wild populations of *R. griersonianum*, another PSESP in Yunnan, yielded an average $\pi$ of $1.94 \times 10^{-3}$, based on whole-genome resequencing (Ma et al., 2021). Furthermore, first-class protected wild plants, such as *Ginkgo biloba* ($i = 2.19 \times 10^{-3}$–$2.41 \times 10^{-3}$, Zhao et al., 2019), *Thuja sutchuenensis* ($u = 2.19 \times 10^{-3}$, Qin et al., 2021), and *Cathaya argyrophylla* ($\pi = 2.10 \times 10^{-3}$, Wang and Ge, 2006), also exhibit higher nucleotide diversities than *H. hainanensis*. Population genetic theory suggests that effective population size is positively related to the amount of genetic variation maintained in a population (Charlesworth, 2009; Ellegren and Galtier, 2016). A reduction in population size and demographic bottlenecks have been generally observed in endangered species. For instance, there have been at least two bottleneck events in *A. yangbiense* (Ma et al., 2022) and three significant bottlenecks in *R. griersonianum* (Ma et al., 2021) and *G. biloba* (Zhao et al., 2019). As with *H. reticulata*, a significant decline in the *H. hainanensis* population on Hainan Island over the last 20,000 years has been demonstrated. In conclusion, both the small effective population size and low genetic diversity in *H. hainanensis* are attributable to a severe population contraction in this species.

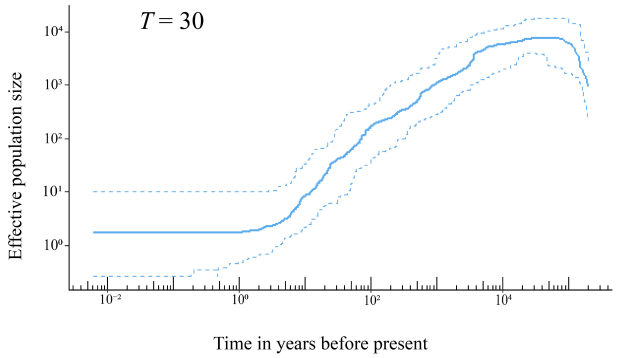


FIGURE 4
The demographic history of *H. hainanensis* inferred using stairway plot 2 with pooled individuals from the sampled populations. Thirty years was employed as the generation time of this species based on field observation. The solid line represents the estimation of the effective population size, with the two dotted lines delineating the 95% confidence interval of the estimation.

The shrinking of the *H. hainanensis* population on Hainan Island may have been induced by rising sea levels following the Last Glacial Maximum (LGM) [$26.5–19 \times 10^3$ years ago (Clark et al., 2009)]. During the LGM, the landmass of Sundaland expanded due to lower sea levels, and environmental conditions were indicated to be suitable for Dipterocarpaceae (Raes et al., 2014). The rainforests of Sundaland covered a substantially larger area than they do at present (Cannon et al., 2009). Following the end of the LGM, the low-altitude areas of Sundaland gradually submerged into the sea due to rising sea levels. Approximately 38.5% of the lowland rainforests in Sundaland disappeared compared with the LGM period (Cannon et al., 2009). Hainan Island, once on the edge of the landmass in the north South China Sea, was eventually separated from the mainland, with its land area reduced because of the rising sea levels after the LGM (Xiong et al., 2020). Stairway plot analysis indicated that the decline in the *H. hainanensis* population began approximately $20 \times 10^3$ years ago, aligning well with the timing of the end of the LGM (Figure 4). Consequently, the rising sea levels after the LGM likely led to the contraction of the *H. hainanensis* population on Hainan Island.

Deforestation and excessive logging have also contributed to the reduction in the *H. hainanensis* population. Trees from the Dipterocarpaceae family are a well-known resource for timber production. Ly et al. (2018) estimated that approximately 50% to 70% of the *H. hainanensis* population has been cut down over the past 300 years. The high-quality wood produced from this species is suitable for building boats, bridges, and houses and making furniture. It is likely that *H. hainanensis* has been logged since human activity commenced on Hainan Island, approximately 7,000 to 3,000 years ago (Pan, 1999). Moreover, deforestation accelerated greatly in the 20th century, with approximately 80 to 95% of the primary forest

being destroyed or converted into rubber or eucalyptus plantations on the Island (Zhou et al., 2005; Lin et al., 2017). The stairway plot showed an accelerated reduction in the *H. hainanensis* population over the past 100 years, in line with the intensified deforestation and logging during the 20th century on Hainan Island. This indicates that human disturbance is a significant factor exacerbating the decline in the *H. hainanensis* population.

It is worth noting that Chen et al. (2022) also assessed the genetic diversity and population structure of *H. hainanensis* on Hainan Island using RADseq. Nonetheless, there are several important differences between Chen et al. (2022) and the current study. First, we sampled 78 individuals from 10 populations, whereas Chen et al. (2022) collected 47 samples from 7 populations. Four populations—FJ, KF, BL, and MR—included in the current study were not represented in Chen et al. (2022). Notably, the KF population was characterized by a population-specific genetic cluster (Figure 2), and the MR population had the highest level of nucleotide diversity among the 10 sampled populations (Table 1). Extensive geographic sampling lays the foundation for a comprehensive understanding of the pattern of genetic variation in *H. hainanensis*. Differences in population sampling may contribute to the differences in genetic structure inferred by the two studies. In our STRUCTURE analysis, the best *k* was 5, whereas Chen et al. (2022) identified it as 2. Knowledge of the number and geographic distribution of genetic clusters is essential for accurately recognizing populations that require priority in conservation. Underestimation of genetic clusters may cause a loss of variation due to the misidentification of populations that need conservation. Finally, by performing stairway plot analysis, we demonstrated a severe and persistent decline in the *H. hainanensis* population on Hainan Island (Figure 4) and discussed potential reasons for the population size contraction. However, historical demography was not addressed in Chen et al. (2022). In conclusion, based on broader geographic population sampling, we studied the genetic diversity, population structure, and demographic history of *H. hainanensis* on Hainan Island, which could shed new light on the pattern of genetic variation and demographic history of *H. hainanensis* on this Island.

## 4.2 Genetic differentiation among *H. hainanensis* populations

Before the rise in sea levels and human colonization, *H. hainanensis* likely had a wider distribution on Hainan Island than it does today. Populations of *H. hainanensis* were probably connected through gene flows mediated by seed and pollen dispersal. Typically, the dispersal distance of seeds from the Dipterocarpaceae family is usually within 100 m (Suzuki and Ashton, 1996; Smith et al., 2015). Seeds may be carried by storms and transferred as much as several hundred meters from their parent trees (Ghazoul, 2016). Dipterocarps with winged fruits could realize longer distance of seed dispersal through autorotation when falling than those with wingless fruits (Seidler and Plotkin, 2006). Pollen-mediated gene flow for species in this family has been estimated to extend from tens to more than three hundreds of meters (Widiyatno et al., 2017). Notably, long-distance pollen flows have been reported in *Neobalanocarpus heimii*, *Dipterocarpus tempheses*, and several *Shorea* species (Konuma et al., 2000; Kenta et al., 2004; Widiyatno et al., 2017). Using paternity analysis, the average distance of pollen flow in *N. heimii* was estimated to be 191 m, with several pollination events exceeding 400 m (Konuma et al., 2000). Owing to the potential for the long-distance dispersal of pollen and seeds, weak differentiation among populations with continuous distribution is commonly observed in dipterocarps (Lee et al., 2000; Lim et al., 2002; Ohtani et al., 2021; Mishra et al., 2023). Consequently, we might expect a low level of differentiation among Hainan Island's *H. hainanensis* populations because of gene flows among them prior to habitat fragmentation and population contraction.

With rising sea levels and increased logging activities, the populations of *H. hainanensis* on Hainan Island became gradually fragmented and diminished in both size and distribution area. According to population genetic theory, small and isolated *H. hainanensis* populations should increasingly diverge from each other due to intensified genetic drift (Hartl and Clark, 2007). Consistent with theoretical expectations, moderate levels of differentiation between some geographically distant populations of *H. hainanensis* were detected (Table 2). The genetic clusters identified in this species are generally widely distributed in the lowland rainforests of Hainan Island, suggesting potential gene flow among populations. This could explain the lack of detectable geographic structure in SNP variations within this species (Supplementary Figure S2). After population fragmentation and contraction, different populations probably retained different alleles due to random genetic drift, driving divergence among them (Figure 2). In conclusion, the increased differentiation between *H. hainanensis* populations is likely the result of genetic drift in small and isolated populations, as well as interrupted gene flow caused by habitat fragmentation and population contraction.

## 4.3 Conservation implication

Genetic diversity is crucial for a species to adapt to changing environments and ensure long-term survival. The genetic diversity of *H. hainanensis*, assessed using genome-wide SNP variation, is significantly lower than several other studied endangered species and species with extremely small populations. The key to conserving *H. hainanensis* lies in expanding its population size and restoring its genetic diversity. Populations such as JF and MR, which exhibit the highest levels of nucleotide diversity, and JF, MR, QW, and BL, which harbor diverse genetic clusters, should be prioritized for conservation efforts. These populations could be served as a provenance to cultivate saplings and young trees utilized in the restoration of *H. hainanensis* populations. Assisting the growth of seedlings into the sapling stage is an effective method for promoting population growth. Implementing the above recommendation in conservation activities would prevent a further loss of genetic diversity in this species, gradually restore wild populations, and thereby enhance the integrity and ecological services of the lowland rainforest ecosystem on Hainan Island.

## Data availability statement

The datasets generated during the current study are available inthe National Center for Biotechnology Information (NCBI) SequenceRead Archive (SRA) under accession number PRJNA1083891, https://www.ncbi.nlm.nih.gov/sra/PRJNA1083891.

## Author contributions

LT: Conceptualization, Formal analysis, Funding acquisition, Investigation, Methodology, Project administration, Resources, Software, Visualization, Writing – original draft, Writing – review & editing. J-qL: Investigation, Writing – original draft. H-yW: Investigation, Writing – original draft. C-kR: Investigation, Writing – original draft. W-xL: Conceptualization, Investigation, Resources, Writing – review & editing. LY: Funding acquisition, Writing – review & editing. Y-bL: Conceptualization, Funding acquisition, Investigation, Project administration, Writing – review & editing.

## Funding

The author(s) declare financial support was received for the research, authorship, and/or publication of this article. This work was supported by the National Nature Science Foundation of China (32060236), the Hainan Institute of National Park, HINP, KY-24ZK02, and grants from Hainan Province Science and technology Special Fund (ZDYF2023RDYL01), and grants from Geological Survey Project of China Geological Survey (Grant No.DD20220992).

## Conflict of interest

The authors declare that the research was conducted in the absence of any commercial or financial relationships that could be construed as a potential conflict of interest.

## Publisher's note

All claims expressed in this article are solely those of the authors and do not necessarily represent those of their affiliated organizations, or those of the publisher, the editors and the reviewers. Any product that may be evaluated in this article, or claim that may be made by its manufacturer, is not guaranteed or endorsed by the publisher.

## Supplementary material

The Supplementary Material for this article can be found online at: https://www.frontiersin.org/articles/10.3389/fpls.2024.1442807/full#supplementary-material.

## References

Andrews, K. R., Good, J. M., Miller, M. R., Luikart, G., and Hohenlohe, P. A. (2016). Harnessing the power of RADseq for ecological and evolutionary genomics. *Nat. Rev. Genet.* 17, 81–92. doi: 10.1038/nrg.2015.28

Ashton, P. S. (1988). Dipterocarp biology as a window to the understanding of tropical forest structure. *Annu. Rev. Ecol. Evol. Syst.* 19, 347–370. doi: 10.1146/annurev.es.19.110188.002023

Benestan, L. M., Ferchaud, A. L., Hohenlohe, P. A., Garner, B. A., Naylor, G. J. P., Baums, I. B., et al. (2016). Conservation genomics of natural and managed populations: building a conceptual and practical framework. *Mol. Ecol.* 25, 2967–2977. doi: 10.1111/mec.13647

Cannon, C. H., Morley, R. J., and Bush, A. B. G. (2009). The current refugial rainforests of Sundaland are unrepresentative of their biogeographic past and highly vulnerable to disturbance. *Proc. Natl. Acad. Sci. U. S. A.* 106, 11188–11193. doi: 10.1073/pnas.0809865106

Charlesworth, B. (2009). Effective population size and patterns of molecular evolution and variation. *Nat. Rev. Genet.* 10, 195–205. doi: 10.1038/nrg2526

Chen, X. Y., Lu, H. P., Shen, L., and Li, Y. Y. (2002). Identifying populations for priority conservation of important species. *Biodiv. Sci.* 10, 332–338. doi: 10.3321/j.issn:1005-0094.2002.03.013

Chen, Y., Zhang, H. L., Zhang, L., Nizamani, M. M., Zhou, T., et al (2002). Genetic diversity assessment of Hopea hainanensis in Hainan Island. *Front. Plant Sci.* 13, 1075102. doi: 10.3389/fpls.2022.1075102

Clark, P. U., Dyke, A. S., Shakun, J. D., Carlson, A. E., Clark, J., Wohlfarth, B., et al. (2009). The last glacial maximum. *Science* 325, 710–714. doi: 10.1126/science.1172873

Corlett, R. T., and Primack, R. B. (2011). *Tropical rain forests: an ecological and biogeographical comparison* (Chichester: Wiley-Blackwell).

Davey, J. W., and Blaxter, M. L. (2010). RADSeq: next-generation population genetics. *Brief. Funct. Genomics* 9, 416–423. doi: 10.1093/bfgp/elq031

Davey, J. W., Hohenlohe, P. A., Etter, P. D., Boone, J. Q., Catchen, J. M., and Blaxter, M. L. (2011). Genome-wide genetic marker discovery and genotyping using next-generation sequencing. *Nat. Rev. Genet.* 12, 499–510. doi: 10.1038/nrg3012

DeSalle, R., and Amato, G. (2004). The expansion of conservation genetics. *Nat. Rev. Genet.* 5, 702–712. doi: 10.1038/nrg1425

Ellegren, H., and Galtier, N. (2016). Determinants of genetic diversity. *Nat. Rev. Genet.* 17, 422–433. doi: 10.1038/nrg.2016.58

Evanno, G., Regnaut, S., and Goudet, J. (2005). Detecting the number of clusters of individuals using the software STRUCTURE: a simulation study. *Mol. Ecol.* 14, 2611–2620. doi: 10.1111/j.1365-294X.2005.02553.x

Excoffier, L., and Lischer, H. E. L. (2010). Arlequin suite ver 3.5: a new series of programs to perform population genetics analyses under Linux and Windows. *Mol. Ecol. Resour.* 10, 564–567. doi: 10.1111/j.1755-0998.2010.02847.x

Falush, D., Stephens, M., and Pritchard, J. K. (2003). Inference of population structure using multilocus genotype data: Linked loci and correlated allele frequencies. *Genetics* 164, 1567–1587. doi: 10.1093/genetics/164.4.1567

Ghazoul, J. (2016). *Dipterocarp biology, ecology, and conservation* (New York: Oxford University Press).

Hartl, D. L., and Clark, A. G. (2007). *Principles of population genetics* (Sunderland: Sinar Associates, Inc. Publishers).

Heckenhauer, J., Samuel, R., Ashton, P. S., Turner, B., Barfuss, M. H. J., Jang, T. S., et al. (2017). Phylogenetic analyses of plastid DNA suggest a different interpretation of morphological evolution than those used as the basis for previous classifications of Dipterocarpaceae (Malvales). *Bot. J. Linn. Soc* 185, 1–26. doi: 10.1093/botlinnean/box044

Hu, X., Xu, R. J., Shu, Q., Guo, W., Zhang, J., Shang, Z. A., et al. (2020). Population structure and dynamics of *Hopea reticulata*, a plant endemic to Ganshiling, Hainan Island. *Chin. J. Trop. Crops* 41, 1939–1945. doi: 10.3969/j.issn.1000-2561.2020.09.030

Hu, Y. J. (1983). The phytocoenological features and types of Dipterocarp forest in Hainan Island. *Ecol. Sci.* 2, 16–24.

Hu, Y. J., and Li, Y. X. (1992). *Tropical rain forest of Hainan Island* (Guangzhou: Guangdong Higher Education Press).

Kenta, T., Isagi, Y., Nakagawa, M., Yamashita, M., and Nakashizuka, T. (2004). Variation in pollen dispersal between years with different pollination conditions in a tropical emergent tree. *Mol. Ecol.* 13, 3575–3584. doi: 10.1111/j.1365-294X.2004.02345.x

Konuma, A., Tsumura, Y., Lee, C. T., Lee, S. L., and Okuda, T. (2000). Estimation of gene flow in the tropical-rainforest tree *Neobalanocarpus heimii* (Dipterocarpaceae),

inferred from paternity analysis. *Mol. Ecol.* 9, 1843–1852. doi: 10.1046/j.1365-294x.2000.01081.x

Lee, S. L., Wickneswari, R., Mahani, M. C., and Zakri, A. H. (2000). Genetic diversity of a tropical tree species, *Shorea leprosula* Miq. (Dipterocarpaceae), in Malaysia: Implications for conservation of genetic resources and tree improvement. *Biotropica* 32, 213–224. doi: 10.1111/j.1744-7429.2000.tb00464.x

Li, X. W., Li, J., and Ashton, P. S. (2007). "Dipterocarpaceae," in *Flora of China*, vol. 13 . Eds. Z. Y. Wu, P. H. Raven and D. Y. Hong (Science Press and St. Louis: Missouri Botanical Garden Press, Beijing).

Li, Y. D., Fang, H., Luo, W., Chen, H. Q., and Jiang, Z. L. (2006). The resource and community characteristics of *Vatica mangachapoi* forest in Jianfengling National Nature Reserve, Hainan Island. *Scientia Silvae Sinicae* 42, 1–6. doi: 10.11707/j.1001-7488.20060101

Li, Y. L., and Liu, J. X. (2018). STRUCTURESELECTOR: A web-based software to select and visualize the optimal number of clusters using multiple methods. *Mol. Ecol. Resour.* 18, 176–177. doi: 10.1111/1755-0998.12719

Li, Y. Y., Liu, C. N., Wang, R., Luo, S. X., Nong, S. Q., Wang, J. W., et al. (2020). Applications of molecular markers in conserving endangered species. *Biodiv. Sci.* 28, 367–375. doi: 10.17520/biods.2019414

Lim, L. S., Wickneswari, R., Lee, S. L., and Latiff, A. (2002). Genetic variation of *Dryobalanops aromatica* Gaertn. F. (Dipterocarpaceae) in Peninsular Malaysia using microsatellite DNA markers. *For. Genet.* 9, 127–138.

Lin, S. L., Jiang, Y. Z., He, J. K., Ma, G. Z., Xu, Y., and Jiang, H. S. (2017). Changes in the spatial and temporal pattern of natural forest cover on Hainan Island from the 1950s to the 2010s: implications for natural forest conservation and management. *Peer J.* 5, e3320. doi: 10.7717/peerj.3320

Liu, X. M., and Fu, Y. X. (2015). Exploring population size changes using SNP frequency spectra. *Nat. Genet.* 47, 555–559. doi: 10.1038/ng.3254

Liu, X. M., and Fu, Y. X. (2020). Stairway Plot 2: demographic history inference with folded SNP frequency spectra. *Genome Biol.* 21, 280. doi: 10.1186/s13059-020-02196-9

Lu, X. H., Zang, R. G., Ding, Y., Huang, J. H., and Xu, Y. (2020). Habitat characteristics and its effects on seedling abundance of *Hopea hainanensis*, a Wild Plant with Extremely Small Populations. *Biodiv. Sci.* 28, 289–295. doi: 10.17520/biods.2019143

Luikart, G., Allendorf, F. W., Cornuet, J. M., and Sherwin, W. B. (1998). Distortion of allele frequency distributions provides a test for recent population bottlenecks. *J. Hered.* 89, 238–247. doi: 10.1093/jhered/89.3.238

Luo, W., Xu, H., Li, Y. P., Xie, C. P., Lu, C. Y., Liang, C. S., et al. (2023). Population structure and quantitative dynamics of a wild Plant with Extremely Small Populations *Hopea hainanensis*. *For. Res.* 36, 169–177. doi: 10.12403/j.1001-1498.20220510

Ly, V., Nanthavong, K., Pooma, R., Hoang, V. S., Khou, E., and Newman, M. F. (2018).Hopea hainanensis. In: *The IUCN red list of threatened species 2018* (Accessed May 20, 2018).

Ma, H., Liu, Y. B., Liu, D. T., Sun, W. B., Liu, X. F., Wan, Y. M., et al. (2021). Chromosome-level genome assembly and population genetic analysis of a critically endangered rhododendron provide insights into its conservation. *Plant J.* 107, 1533–1545. doi: 10.1111/tpj.15399

Ma, Y. P., Chen, G., Grumbine, R. E., Dao, Z. L., Sun, W. B., and Guo, H. J. (2013). Conserving plant species with extremely small populations (PSESP) in China. *Biodivers. Conserv.* 22, 803–809. doi: 10.1007/s10531-013-0434-3

Ma, Y. P., Liu, D. T., Wariss, H. M., Zhang, R. G., Tao, L. D., Milne, R. I., et al. (2022). Demographic history and identification of threats revealed by population genomic analysis provide insights into conservation for an endangered maple. *Mol. Ecol.* 31, 767–779. doi: 10.1111/mec.16289

Mantel, N. (1967). The detection of disease clustering and a generalized regression approach. *Cancer Res.* 27, 209–220.

Mishra, G., Meena, R. K., Kant, R., Pandey, S., Ginwal, H. S., and Bhandari, M. S. (2023). Genome-wide characterization leading to simple sequence repeat (SSR) markers development in *Shorea robusta*. *Funct. Integr. Genomics* 23, 51. doi: 10.1007/s10142-023-00975-8

Montagnini, F., and Jordan, C. F. (2005). *Tropical forest ecology: the basis for conservation and management* (Heidelberg: Springer Berlin).

Ng, C. H., Lee, S. L., Tnah, L. H., Ng, K. K. S., Lee, C. T., Diway, B., et al. (2019). Genetic diversity and demographic history of an upper hill dipterocarp (*Shorea platyclados*): implications for conservation. *J. Hered.* 110, 844–856. doi: 10.1093/jhered/esz052

Ohtani, M., Tani, N., Ueno, S., Uchiyama, K., Kondo, T., Lee, S. L., et al. (2021). Genetic structure of an important widely distributed tropical forest tree, *Shorea parvifolia*, in Southeast Asia. *Tree Genet. Genomes* 17, 44. doi: 10.1007/s11295-021-01525-8

Pan, Z. J. (1999). "History," in *Encyclopedia of hainan*. Ed. K. Li (Encyclopedia of China Publishing House, Beijing).

Parchman, T. L., Jahner, J. P., Uckele, K. A., Galland, L. M., and Eckert, A. J. (2018). RADseq approaches and applications for forest tree genetics. *Tree Genet. Genomes* 14, 39. doi: 10.1007/s11295-018-1251-3

Pei, X. J., Zhou, X. F., Liu, N., Hong, X. J., Zhou, Z. L., and Cheng, K. W. (2015). Relationship between distribution of *Hopea hainanensis* seedings and its seed tree. *J. Hebei Agric. Univ.* 38, 46–51. doi: 10.13320/j.cnki.jauh.2015.0058

Pritchard, J. K., Stephens, M., and Donnelly, P. (2000). Inference of population structure using multilocus genotype data. *Genetics* 155, 945–959. doi: 10.1093/genetics/155.2.945

Putman, A. I., and Carbone, I. (2014). Challenges in analysis and interpretation of microsatellite data for population genetic studies. *Ecol. Evol.* 4, 4399–4428. doi: 10.1002/ece3.1305

Qin, A. L., Ding, Y. M., Jian, Z. J., Ma, F. Q., Worth, J. R. P., Pei, S. X., et al. (2021). Low genetic diversity and population differentiation in *Thuja sutchuenensis* Franch., an extremely endangered rediscovered conifer species in southwestern China. *Glob. Ecol. Conserv.* 25, e01430. doi: 10.1016/j.gecco.2020.e01430

Raes, N., Cannon, C. H., Hijmans, R. J., Piessens, T., Saw, L. G., van Welzen, P. C., et al. (2014). Historical distribution of Sundaland's Dipterocarp rainforests at Quaternary glacial maxima. *Proc. Natl. Acad. Sci. U.S.A.* 111, 16790–16795. doi: 10.1073/pnas.1403053111

Ren, H., Zhang, Q. M., Lu, H. F., Liu, H. X., Guo, Q. F., Wang, J., et al. (2012). Wild Plant Species with Extremely Small Populations require conservation and reintroduction in China. *Ambio* 41, 913–917. doi: 10.1007/s13280-012-0284-3

Rice, P., Longden, I., and Bleasby, A. (2000). EMBOSS: the european molecular biology open software suite. *Trends Genet.* 16, 276–277. doi: 10.1016/s0168-9525(00)02024-2

Rochette, N. C., and Catchen, J. M. (2017). Deriving genotypes from RAD-seq short-read data using Stacks. *Nat. Protoc.* 12, 2640–2659. doi: 10.1038/nprot.2017.123

Rochette, N. C., Rivera-Colon, A. G., and Catchen, J. M. (2019). Stacks 2: Analytical methods for paired-end sequencing improve RADseq-based population genomics. *Mol. Ecol.* 28, 4737–4754. doi: 10.1111/mec.15253

Schlotterer, C. (2004). The evolution of molecular markers - just a matter of fashion? *Nat. Rev. Genet.* 5, 63–69. doi: 10.1038/nrg1249

Seidler, T. G., and Plotkin, J. B. (2006). Seed dispersal and spatial pattern in tropical trees. *PloS Biol.* 4, e344. doi: 10.1371/journal.pbio.0040344

Smith, J. R., Bagchi, R., Ellens, J., Kettle, C. J., Burslem, D. F. R. P., Maycock, C. R., et al. (2015). Predicting dispersal of auto-gyrating fruit in tropical trees: a case study from the Dipterocarpaceae. *Ecol. Evol.* 5, 1794–1801. doi: 10.1002/ece3.1469

Sun, W. B., Ma, Y. P., and Blackmore, S. (2019). How a new conservation action concept has accelerated plant conservation in China. *Trends Plant Sci.* 24, 4–6. doi: 10.1016/j.tplants.2018.10.009

Suzuki, E., and Ashton, P. S. (1996). Sepal and nut size ratio of fruits of Asian Dipterocarpaceae and its implications for dispersal. *J. Trop. Ecol.* 12, 853–870. doi: 10.1017/S0266467400010129

Tang, L., Duan, J. Y., Cai, Y., Wang, W. N., and Liu, Y. B. (2024). Low genetic diversity and small effective population size in the endangered *Hopea reticulata* (Dipterocarpaceae) on Hainan Island, China. *Glob. Ecol. Conserv.* 50, e02846. doi: 10.1016/j.gecco.2024.e02846

Tito de Morais, C., Ghazoul, J., Maycock, C. R., Bagchi, R., Burslem, D., Khoo, E., et al. (2015). Understanding local patterns of genetic diversity in dipterocarps using a multi-site, multi-species approach: Implications for forest management and restoration. *For. Ecol. Manage.* 356, 153–165. doi: 10.1016/j.foreco.2015.07.023

Utomo, S., Uchiyama, K., Ueno, S., Matsumoto, A., Widiyatno,, Indrioko, S., et al. (2018). Effects of Pleistocene climate change on genetic structure and diversity of *Shorea macrophylla* in Kalimantan rainforest. *Tree Genet. Genomes* 14, 16. doi: 10.1007/s11295-018-1261-1

Wang, C., Ma, X., Ren, M. X., and Tang, L. (2020). Genetic diversity and population structure in the endangered tree *Hopea hainanensis* (Dipterocarpaceae) on Hainan Island, China. *PloS One* 15, e0241452. doi: 10.1371/journal.pone.0241452

Wang, H. W., and Ge, S. (2006). Phylogeography of the endangered *Cathaya argyrophylla* (Pinaceae) inferred from sequence variation of mitochondrial and nuclear DNA. *Mol. Ecol.* 15, 4109–4122. doi: 10.1111/j.1365-294X.2006.03086.x

Wen, B., Lan, Q. Y., and He, H. Y. (2002). Effects of illumination, temperature and soil miosture content on seed germination of *Hopea hainanensis*. *J. Trop. Subtrop. Bot.* 10, 258–262. doi: 10.3969/j.issn.1005-3395.2002.3.012

Widiyatno,, Indrioko, S., Na'iem, M., Purnomo, S., Hosaka, T., Uchiyama, K., et al. (2017). Effects of logging rotation in a lowland dipterocarp forest on mating system and gene flow in *Shorea parvifolia*. *Tree Genet. Genomes* 13, 13. doi: 10.1007/s11295-017-1167-3

Xie, G. G., and Huang, S. M. (1990). Dipterocarpaceae, precious timber tree species in Hainan Island. *Trop. Geography.* 10, 217–222. doi: 10.13284/j.cnki.rdd1.002078

Xing, F. W., Zhou, J. S., Wang, F. G., Zeng, Q. W., Yi, Q. F., and Liu, D. M. (2012). *Inventory of plant species diversity of hainan* (Wuhan: Huazhong University of Science & Technology Press).

Xiong, P., Harff, J., Xie, X. N., Zhang, W. Y., Chen, H. J., Tao, J., et al. (2020). Modeling paleogeographic scenarios of the last glacial cycle as a base for source-to-sink studies: An example from the northwestern shelf of the South China Sea. *J. Asian Earth Sci.* 203, 104542. doi: 10.1016/j.jseaes.2020.104542

Yang, J., Lee, S. H., Goddard, M. E., and Visscher, P. M. (2011). GCTA: A Tool for genome-wide complex trait analysis. *Am. J. Hum. Genet.* 88, 76–82. doi: 10.1016/j.ajhg.2010.11.011

Yang, X. B., Chen, Y. K., Li, D. H., and Mo, Y. N. (2016). *Study on illustrations and distribution characteristics of rare protected plants in Hainan* (Beijing: Science Press).

Yao, Z., Guo, J., Jin, C. Z., and Liu, Y. B. (2021). Endangered mechanisms for the first-class protected Wild Plants with Extremely Small Populations in China. *Biodiv. Sci.* 29, 394–408. doi: 10.17520/biods.2020316

Zang, R. G., Dong, M., Li, J. Q., Chen, X. Y., Zeng, S. J., Jiang, M. X., et al. (2016). Conservation and restoration for typical critically endangered wild plants with extremely small population. *Acta Ecol. Sin.* 36, 1–6. doi: 10.5846/stxb201610082011

Zhang, L., Yang, X. B., Nong, S. Q., Li, D. H., Li, Y. L., and Song, J. Y. (2019). Comparative study on population development characteristics of *Hopea hainanensis* base in two different protection modes. *Acta Ecol. Sin.* 39, 3740–3748. doi: 10.5846/stxb201811012359

Zhao, Y. P., Fan, G. Y., Yin, P. P., Sun, S., Li, N., Hong, X. N., et al. (2019). Resequencing 545 ginkgo genomes across the world reveals the evolutionary history of the living fossil. *Nat. Commun.* 10, 4201. doi: 10.1038/s41467-019-12133-5

Zhou, J., Wei, F., Li, M., Zhang, J. F., Wang, D. L., and Pan, R. L. (2005). Hainan black-crested gibbon is headed for extinction. *Int. J. Primatol.* 26, 453–465. doi: 10.1007/s10764-005-2933-x

Zhu, H. (1993). Floristic plant geography on the dipterocarp forest of Xishuangbanna. *Acta Botanica Yunnanica* 15, 233–252. Available at: http://ir.kib.ac.cn:8080/handle/151853/9523.

frontiers | Frontiers in Plant Science

TYPE Original Research
PUBLISHED 24 September 2024
DOI 10.3389/fpls.2024.1478094



OPEN ACCESS

EDITED BY
Hui Zhang,
Hainan University, China

REVIEWED BY
Jianfeng Liu,
Chinese Academy of Forestry, China
Shengkui Cao,
Qinghai Normal University, China

*CORRESPONDENCE
Shuxuan Yin
yinsx1218@163.com

RECEIVED 09 August 2024
ACCEPTED 09 September 2024
PUBLISHED 24 September 2024

CITATION
Yin S (2024) Carbon, nitrogen and phosphorus contents and their ecological stoichiometric characteristics in leaf litter from the Jianfengling Tropical Montane Rainforest.
*Front. Plant Sci.* 15:1478094.
doi: 10.3389/fpls.2024.1478094



# Carbon, nitrogen and phosphorus contents and their ecological stoichiometric characteristics in leaf litter from the Jianfengling Tropical Montane Rainforest

Shuxuan Yin*

Department of Environmental Science, Inner Mongolia University, Hohhot, China

Investigating carbon (C), nitrogen (N) and phosphorus (P) contents and ecological stoichiometric characteristics in leaf litter from tropical rainforests is crucial for elucidating nutrient cycling and energy flow in forest ecosystems. In this study, a 60-ha tropical montane rainforest dynamic monitoring plot in Jianfengling, was selected as the research site and 60 subplots were selected for detailed study. Leaf litter was collected monthly throughout 2016, branches of similar height were placed atthe four corners of each sample square to support a nylon cloth (1 m× 1 m) with 1 mm apertures. The collected plant leaves were sorted,placed into envelopes, labelled, and transported to the laboratory and samples from various plant species were identified, resulting in a total of 107 samples collected and analyzed. For the 31 dominant species, the leaf litter had C, N and P contents of 312.71 ± 28.42, 4.95 ± 0.46 and 0.40 ± 0.03 g/kg, respectively. The C:N, C:P and N:P ratios were 63.61 ± 7.50, 790.91 ± 82.30 and 12.49 ± 1.00, respectively, indicating moderate variability. The C, N and P contents exhibited greater variability among the plant groups, indicating significant heterogeneity among the samples. In contrast, the data from the subplots exhibited less variability, highlighting significant homogeneity. Overall, the mean carbon, nitrogen and phosphorus contents in the leaf litter from tropical montane rainforests were lower than those observed at national and global scales. The N:P ratios in leaf litter below 14 indicated that nitrogen limited litter decomposition in Jianfengling. However, no significant correlations were observed between the C, N and P contents and their stoichiometric ratios in leaf litter and those in soil. The above results provide important reference data and scientific basis for the nutrient cycling and energy flow processes, and in the future, we can explore the limiting role and mechanism of nitrogen in the decomposition process of leaf litter.

KEYWORDS

**leaf litter, organic carbon, total nitrogen, total phosphorus, stoichiometry**

# 1 Introduction

Ecological stoichiometry, a popular field of ecological research in recent years, focuses on the balance between various interacting chemical elements in ecosystems (Elser et al., 2000; Peguero et al., 2023). Plants require over 30 elements for growth, with carbon (C), nitrogen (N) and phosphorus (P) being crucial for constructing plant structures and supporting metabolic processes. Carbon, the most dominant element in plants, comprises about 50% of their dry weight. Additionally, carbon is vital for producing sugars necessary for plant growth, reproduction, and structural development (Friedlingstein et al., 2020; Cook-Patton et al., 2020). Nitrogen is crucial for synthesizing all enzymes and chlorophyll in plants and plays a key role in the primary production of organic compounds. Phosphorus is vital for controlling ribosome synthesis in plants and is a key component of RNA, DNA and ATP. Moreover, phosphorus significantly influences information transfer, energy storage, and cellular architecture in plants (Farrer and Goldberg, 2009; Du et al., 2020; Sardans et al., 2012). To analyze organisms as integrated systems and connect research across different areas, ecologists have proposed linking the molecular structure of genes to various levels of ecosystem organization and dynamics. This approach forms the basis of ecological stoichiometry, which provides new insights into leaf-litterfall-soil nutrient cycling and regulation and is a key indicator for maintaining and preserving forest communities. Elser et al. (2000) indicated that the stoichiometry of C, N and P in organisms is closely associated with their growth. Furthermore, autotrophic organisms exhibit variable C:N:P ratios both within and among species. These ratios in plant leaves influence plant growth, nutrient cycling, and primary production (Falcell and Pickett, 1991; Tie et al., 2023). Therefore, investigating the carbon, nitrogen and phosphorus contents in plants and their stoichiometric characteristics is crucial for elucidating their dynamic role in regional biogeochemical cycles.

Litterfall consists of all organic matter produced by the above-ground parts of plants and deposited onto the surface, including components such as leaf litter, propagules and twigs (Tian et al., 2024). Litter serves as a crucial link between plants and soil and plays a key role in nutrient cycling and energy flow within forest ecosystems (Njoroge et al., 2022; Zhang et al., 2023a; Li et al., 2023). Notably, leaf litter decomposes rapidly and has been extensively investigated by scholars. Yuan et al. (2024) quantified global patterns of C, N and P contents in litter and its returns. The study identified climate and soil as the main factors influencing litter ecological stoichiometry. Additionally, C, N and P contents in leaf litter were influenced by mycorrhizal associations, taxonomic divisions and/or life forms. He et al. (2024) investigated the dynamics of decomposition and elemental release from both single and mixed types of litter, their non-additive effects on soil C:N:P ratios and the potential factors regulating these non-overlapping effects. The results revealed that mixing different types of leaves promoted mass loss and elemental release, while single types of leaf litter exhibited greater residual mass. The effects of decomposing mixed leaf litter on residual mass, elemental release and soil C:N:P stoichiometry varied based on the litterfall type and showed non-additive effects. This indicates that carbon, nitrogen and phosphorus contents in plant leaves and their stoichiometric characteristics are crucial indicators of soil nutrients. Plant functional traits can respond to changes in the living environment and have an impact on ecosystem processes and functions. Functional traits reflect various aspects of a species' use of natural resources such as light energy and soil nutrients, as well as its life history. At the small scale, elevation and relief are the two most critical topographic factors affecting plant functional traits in tropical broadleaf evergreen forests, while soil water content and total nitrogen content are the most important soil factors affecting plant functional traits in subtropical broadleaf evergreen forests (Ke et al., 2014). Therefore, extensive research on these issues is needed in the tropical regions.

Jianfengling is a unique tropical montane rainforest and semi-deciduous monsoon rainforest located in the western part of Hainan Island (Jun-pei and Qi-han, 1988). Numerous studies have investigated the structure and diversity of vegetation communities and the physicochemical properties of soils in this region. However, few studies have examined the eco-chemometrics of carbon, nitrogen and phosphorus in the leaf litter from tropical montane rainforests in Jianfengling. The Jianfengling tropical montane rainforest, a transitional ecosystem between tropical and subtropical rainforests, is a key site for investigating both types of rainforests globally (Jing-Yun et al., 2004). Therefore, analyzing the stoichiometric characteristics of carbon, nitrogen and phosphorus in the leaf litter from the Jianfengling tropical rainforest is crucial for improving and supporting existing forest data. In this study, a 60-ha dynamic monitoring plot in the Jianfengling tropical montane rainforest was selected as the research site. Litterfall was collected monthly throughout 2016, and the species of the leaf litter were identified. The carbon, nitrogen and phosphorus contents in various leaf litter types were analyzed to investigate the C, N and P contents and the C:N, C:P and N:P ratios in dominant plant species and different subplots of the tropical montane rainforest in Jianfengling. To thoroughly elucidate the stoichiometric characteristics of the 'leaf-litterfall-soil' system, we analyzed data on the relationships between leaf litter properties and soil physical and chemical properties across 60 subplots. Based on the phylogenetic signals of carbon, nitrogen, phosphorus and stoichiometric characteristics and ecological traits of the litter leaf in the tropical montane rainforest region of the Jianfengling, we explored which stoichiometric characteristics are the main limiting factors affecting forest function and ecosystem material cycling, with a deeper discussion on whether there are any correlation between litter decomposition and soil nutrients, and explored potential correlations of plant functional traits by observing the developmental signals of ecological traits.

# 2 Materials and methods

## 2.1 Study area

Hainan Jianfengling National Nature Reserve is positioned at the boundary of Ledong County and Dongfang City in the southwestern part of Hainan Island (18°20′–18°57′N, 108°41′–

109°12′E). This nature reserve is one of the few tropical forest ecosystems in China, covering a total area of about 640 $km^2$ (Xu et al., 2015). Additionally, the reserve exhibits a tropical island monsoon climate, characterized by indistinguishable seasons and high levels of precipitation (Xu et al., 2015). The highest peak in the reserve rises over 1,400 m above sea level, while the lowest elevation is about 200 m. Owing to its significant altitude difference and complex topography, the reserve serves as a vast gene pool, containing over 2,800 vascular plants and more than 300 tree species. The reserve includes nearly all vegetation types found in tropical regions. Among these vegetation types, tropical montane rainforest has the highest distribution area in the Jianfengling forest (Zhongmin et al., 1998). The Jianfengling 60-ha forest biodiversity dynamic monitoring plot (1000 m east-west, 600 m north-south), known as the 'Jianfengling large plot', is located in the primary forest of one of the five sub-areas within the Jianfengling tropical mountain rainforest forest region. This plot, established from 2009 to 2012, adheres to the standards set by the Tropical Forest Research Centre of the Smithsonian Tropical Research Institute in the United States (Xu et al., 2015).

## 2.2 Sample collection and analysis

In the 60-ha (1000 m × 600 m) dynamic monitoring plots in Jianfengling, 60 subplots were selected for detailed study (Liu et al., 2021). To collect leaf litter, branches of similar height were placed at the four corners of each sample square to support a nylon cloth (1 m × 1 m) with 1 mm apertures. The collected plant leaves were sorted, placed into envelopes, labelled, and transported to the laboratory. In the lab, the leaves were dried at 65 ° for 24 h in an oven. After drying, the plant leaves were weighed, identified by experts, and classified into a total of 107 leaf litter species. Leaf litter of the same species was then aggregated for analysis. According to Xu et al. (2015) study on species composition and dominance in the Jianfengling region, this study analyzed the carbon, nitrogen and phosphorus contents from 31 dominant species in this region and their stoichiometric characteristics, as well as the phylogenetic signals of ecological traits.

## 2.3 Analytical test methods and data processing

Microsoft Office Excel 2021 software was used to calculate and organize each sample data. IBM SPSS Statistics 27 software was used to analyze and process the data for determining the stoichiometric characteristics of carbon, nitrogen, phosphorus and other elements in the leaf litter samples. Soil physicochemical property data were obtained from Liu et al. (2021). The stoichiometric characteristics of leaf litter, including the C:N, C:P and N:P ratios and soil physicochemical properties across 60 sample plots in the Jianfengling area, were analyzed. Correlation analyses were performed using Corrplot to explore potential correlations between leaf litter decomposition and soil physicochemical properties. Statistical significance was set at a p-value of <0.05. Additionally, the carbon, nitrogen and phosphorus contents of leaf litter from 31 dominant plant species and 60 subplots were statistically analyzed using boxplots. This analysis examined the correlation between the dominant plant species and the sample plots and observed the degree of data dispersion. A smaller p-value indicated a stronger significant difference. Hierarchical Clustering Analysis (HCA) was used to group the 60 subplots into microhabitats based on altitude, convexity, and slope, in order to analyze the phylogenetic signals of ecological characteristics across all studied species. In this dendrogram, each leaf node represents a sample or data point, and the inner nodes represent the clustering results. The branch length of the dendrogram indicates the similarity and distance between samples or data points, with shorter branch lengths indicating higher similarity.

# 3 Results and analysis

## 3.1 C, N and P contents and stoichiometric ratios across 60 subplots

Table 1 presents the statistical results for C, N, P contents and C:N, C:P and N:P ratios in leaf litter from the tropical montane rainforest in Jianfengling. The C, N and P contents in the leaf litter moderately varied from 242.29 to 378.27, 4.01 to 6.14 and 0.29 to 0.48 g/kg, respectively. The corresponding C:N, C:P and N:P ratios ranged from 45.82 to 80.21, 613.06 to 1012.75 and 10.49 to 15.44, respectively. The leaf litter in tropical montane rainforests exhibited mean C, N and P contents of 312.71 ± 28.42, 4.95 ± 0.46 and 0.40 ± 0.03 g/kg, respectively. The mean C: N, C: P and N: P ratios were 63.61 ± 7.50, 790.91 ± 82.30 and 12.49 ± 1.00, respectively.

## 3.2 C, N and P contents in leaf litter across different plant species and subplots

The organic carbon, total nitrogen and total phosphorus (TP) contents and different species in leaf litter from 31 dominant plant species in the sample area were summarized and analyzed (Table 2). The organic carbon content in leaf litter ranged from 191.57 to 494.20 g/kg, with an average of 323.43 ± 87.67 g/kg and a coefficient of variation (CV) of 27.11%. *Cryptocarya chinensis* exhibited the highest average organic carbon content at 473.68 ± 13.63 g/kg and a

TABLE 1 Statistical results of C, N and P contents and C: N, C: P and N: P ratios (n = 60).

| | Min | Max | Mean | SD | SEM | CV % |
|---|---|---|---|---|---|---|
| TOC g/kg | 242.29 | 378.27 | 312.71 | 28.42 | 3.64 | 9.09 |
| TN g/kg | 4.01 | 6.14 | 4.95 | 0.46 | 0.06 | 9.35 |
| TP g/kg | 0.29 | 0.48 | 0.40 | 0.03 | 0.00 | 8.29 |
| C: N | 45.82 | 80.21 | 63.61 | 7.50 | 0.96 | 11.79 |
| C: P | 613.06 | 1012.75 | 790.91 | 82.30 | 10.54 | 10.41 |
| N: P | 10.49 | 15.44 | 12.49 | 1.00 | 0.13 | 8.01 |

TABLE 2 Carbon, nitrogen, and phosphorus content of different plant dominant species and sun or shade-loving species as well as nitrogen-fixing (NF) and non-nitrogen-fixing (NNF) types (n=31).

| Dominant species | C (g/kg) | N (g/kg) | P (g/kg) | Species | Types |
|---|---|---|---|---|---|
| Altingia obovata | 394.51± 3.88 | 8.35± 0.87 | 0.86± 0.20 | shade | NNF |
| Beilschmiedia | 415.64± 14.52 | 10.53± 0.29 | 0.44± 0.04 | | |
| Beilschmiedia brevipaniculata | 294.35± 20.95 | 2.91± 0.61 | 0.29± 0.05 | sun | NF |
| Beilschmiedia glauca | 432.88± 10.00 | 13.75± 0.96 | 0.30± 0.03 | sun | NF |
| Beilschmiedia tungfangensis | 325.28± 23.15 | 3.65± 0.77 | 0.39± 0.07 | sun | NF |
| Canarium album | 365.38± 7.29 | 10.97± 0.23 | 0.66± 0.11 | sun | NNF |
| Fagaceae | 360.61± 105.26 | 5.45± 2.93 | 0.27± 0.08 | | |
| Castanopsis | 429.82± 16.87 | 13.8± 0.27 | 0.58± 0.10 | | |
| Castanopsis carlesii | 432.95± 34.08 | 6.80± 4.63 | 0.35± 0.14 | shade | NF |
| Castanopsis concinna | 449.78± 32.01 | 7.70± 1.62 | 0.44± 0.08 | sun | NF |
| Castanopsis hystrix | 335.24± 23.86 | 8.48± 1.79 | 0.38± 0.07 | shade | NF |
| Castanopsis jianfenglingensis | 448.28± 31.74 | 7.32± 2.22 | 0.41± 0.05 | shade | NF |
| Castanopsis tonkinensis | 291.1± 20.72 | 6.31± 1.33 | 0.43± 0.08 | shade | NF |
| Cyclobalanopsis patelliformis | 440.27± 0.56 | 12.21± 0.14 | 0.86± 0.20 | sun | NNF |
| Lithocarpus amygdalifolius | 456.39± 10.4 | 12.41± 0.91 | 0.15± 0.02 | shade | NNF |
| Lithocarpus fenzelianus | 435.31± 32.68 | 10.37± 0.54 | 0.21± 0.05 | shade | NNF |
| Gironniera subaequalis | 397.56± 14.49 | 17.23± 0.73 | 0.38± 0.01 | sun | NNF |
| Ilex goshiensis | 356.63± 45.34 | 8.26± 7.67 | 0.34± 0.03 | | |
| Lauraceae | 395.65± 13.00 | 10.58± 0.38 | 0.37± 0.14 | | |
| Cinnamomum validinerve | 402.31± 22.65 | 4.93± 0.56 | 0.41± 0.02 | shade | NNF |
| Cryptocarya chinensis | 473.68± 22.32 | 13.39± 0.62 | 0.24± 0.07 | shade | NNF |
| Cryptocarya metcalfiana | 326.78± 23.26 | 5.34± 1.12 | 0.41± 0.08 | shade | NNF |
| Neolitsea phanerophlebia | 191.57± 13.63 | 3.32± 0.70 | 0.28± 0.05 | shade | NNF |
| Litsea baviensis | 294.53± 20.96 | 5.83± 1.23 | 0.74± 0.14 | sun | NNF |
| Alseodaphne hainanensis | 400.04± 4.76 | 10.54± 0.10 | 0.52± 0.09 | sun | NNF |
| Livistona saribus | 399.69± 4.53 | 8.37± 1.46 | 1.01± 0.29 | sun | NNF |
| Madhuca hainanensis | 383.12± 4.52 | 2.33± 0.54 | 0.30± 0.00 | sun | NF |
| Prismatomeris tetrandra | 319.3± 74.74 | 8.51± 7.75 | 0.45± 0.01 | sun | NNF |
| Wendlandia uvariifolia | 297.92± 135.76 | 6.78± 6.34 | 0.51± 0.12 | shade | NNF |
| Winchia calophylla | 407.93± 1.01 | 12.07± 0.20 | 0.17± 0.01 | sun | NNF |
| Xanthophyllum hainanense | 408.9± 10.74 | 14.34± 2.31 | 0.63± 0.10 | sun | NNF |

lower CV of 2.88%. However, *Neolitsea phanerophlebia* had the lowest average organic carbon content at 191.57 ± 17.99 g/kg, with a higher CV of 14.10%.

The total nitrogen content in lead litter ranged from 1.94 to 17.71 g/kg, with an average of 4.82 ± 1.76 g/kg and a CV of 36.45%. *Gironniera subaequalis* exhibited the highest total nitrogen content at 17.23 ± 0.42 g/kg, with a CV of 4.23%. In contrast, *Madhuca hainanensis* had the lowest average organic carbon content at 2.33 ± 0.38 g/kg, with a CV of 23.28%.

The TP content in leaf litter ranged from 0.14 to 1.34 g/kg, with a mean of 0.42 ± 0.10 g/kg and a CV of 23.62%. *Livistona saribus* exhibited the highest mean TP content at 1.01 ± 0.17 g/kg, with a CV of 28.56%. Conversely, *Lithocarpus amygdalifolius* had the lowest mean TP content at 0.15 ± 0.01 g/kg, with a CV of 10.24%.

The sun-loving and shade-loving plant species leaf litter had C, N and P contents of 326.18 ± 90.34, 5.25 ± 1.98 and 0.45 ± 0.12 g/kg and 322.62 ± 105.16, 4.79 ± 1.61 and 0.39 ± 0.07 g/kg. There was no significant difference between the two fractions as the p-value >0.05.

The p-value of organic carbon between the nitrogen-fixing and non-nitrogen-fixing types was 0.02, which exists a significant difference. Their C, N and P contents of 393.07 ± 62.21, 5.45 ± 1.99 and 0.42 ± 0.07 g/kg and 288.25 ± 90.89, 4.82 ± 1.71 and 0.43 ± 0.42 g/kg.

Based on altitude, convexity, and slope, the 60 sample plots were divided into three categories (Figure 1): numbered 5013-3514, 1901-2405, and 1823-4206, respectively; Plot 1 had an altitude of 966.46 - 1010.54, a convexity of -0.58 - 4.67, and a slope of 16.64 - 45.58; Sample plot 2 elevation is 870.47 - 909.52, convexity is -4.00 - 3.88, slope is 5.61 - 30.01; Sample plot 3 elevation is 917.35 - 961.58, convexity is -5.33 - 7.19, slope is 14.66 - 31.56.

Four different types of plants, sun or shade-loving species as well as NF and NNF types were selected from the subplots (Table 3). The effect of phylogenetic signals of ecological characteristics and altitude, convexity, and slope on plant functional trait was analyzed by examining the ratio of dry weight to total dry weight of leaf litter in the three fractions. *Beilschmiedia brevipaniculata* and *Castanopsis carlesii* are sun-loving and NF and shade-loving and NF types, respectively, and their leaf litter content decreased and then increased with altitude; *Gironniera subaequalis* is the sun-loving and NNF type, and its leaf litter content gradually decreased with increasing altitude; *Altingia obovate* is a shade-loving and NNF type, and its leaf litter content decreased significantly with altitude. In addition, *Gironniera subaequalis* and *Altingia obovate* decreased in leaf litter content as the slope steepened. And the relationship between them and convexity is not obvious.

No significant differences in C, N and P contents were observed across 60 subplots and 31 dominated plant species (Figure 2). Additionally, the C, N and P contents in the plant taxa exhibited higher variability and more outliers, indicating significant heterogeneity in the samples. In contrast, the data from the subplots exhibited less variability, indicating distinct homogeneity.

## 3.3 Correlations between leaf litter and soil C, N and P contents and their stoichiometric ratios

Significant positive correlations were observed between carbon and nitrogen (Figure 3), carbon and phosphorus (Figure 4) and nitrogen and phosphorus (Figure 5) contents in the leaf litter.

Figure 6 shows the correlation analyses for the stoichiometric characteristics of leaf litter and the relationships between C:N, C:P and N:P ratios and soil physicochemical properties in the 60-ha tropical montane rainforest dynamics monitoring plot within Jianfengling. A significant positive correlation was found between the C content in leaf litter and the C:N and C:P ratios. However, no significant correlation was observed between the P and N contents and the C:N, C:P and N:P ratios. Moreover, the mean C content exhibited a significant positive correlation with both C:N and C:P ratios in leaf litter. The mean N content featured a significant negative correlation with C:N and C:P ratios but exhibited a significant positive correlation with the N:P ratio in leaf litter. Conversely, the mean P content had a significant negative correlation with C:P and N:P ratios in leaf litter. Additionally, both the mean C and N contents in leaf litter were significantly positively correlated with the mean P content. However, no significant correlations were observed between C, N, P contents, their stoichiometric ratios in leaf litter and those in the soil. The mean N content in leaf litter exhibited a significant negative correlation with soil aromatic-C and carboxyl-C and a significant positive correlation with soil potassium content. Furthermore, the leaf P content had significant negative correlations with soil light fraction organic carbon (LFOC), aromatic-C, carboxyl-C and TP.

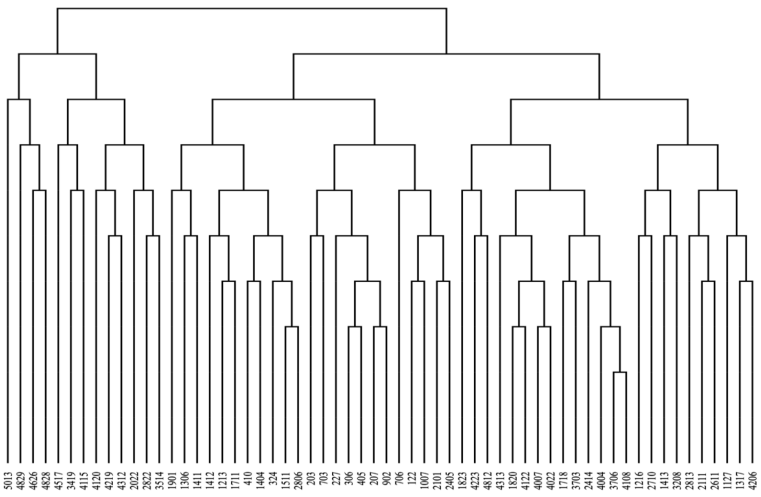


FIGURE 1
Microhabitat classification of 60 subplots based on altitude, convexity, and slope.

TABLE 3 The ratio of dry weight to total dry weight of leaf litter for the four representative plants in the three fractions.

| Representative plant | Plot 1 | Plot 2 | Plot 3 | Species | Types |
|---|---|---|---|---|---|
| Beilschmiedia brevipaniculata % | 4.54 | 3.04 | 0.86 | sun | NF |
| Castanopsis carlesii % | 3.51 | 4.12 | 2.56 | shade | NF |
| Gironniera subaequalis % | 3.57 | 11.76 | 5.78 | sun | NNF |
| Altingia obovate % | 3.27 | 11.91 | 3.45 | shade | NNF |

## 4 Discussion

The C, N P contents and their stoichiometric ratios in the leaf litter from the Jianfengling tropical rainforest in Hainan exhibited moderate variability. The C content of leaf litter observed in this study (242.29–378.28 g/kg) (Table 1) is lower than the global range reported by Wang et al. (2011) (370.10–568.00 g/kg) and significantly lower than the values for eastern China reported by Ren and Yu (2011) (374.10–646.50 g/kg, with a mean value of 480.1 g/kg) Carbon in leaves is mainly stored in chloroplasts. The lower carbon content observed in the leaf litter from the Jianfengling rainforest may result from microbial decomposition, which breaks down organic matter and releases nutrients. The N and P contents of leaf litter in this study (geometric means of 4.95 and 0.40 g/kg, respectively) (Table 1) are lower than the national averages for 753 plant leaves (geometric means of 18.6 g/kg and 1.21 g/kg, respectively) (Han et al., 2005). Additionally, these values are significantly lower than the global averages for N and P contents (geometric means of 17.66 and 1.42 g/kg, respectively) (Elser et al., 2000; Reich and Oleksyn, 2004). This difference may be attributed to the intense plant competition for limited resources in the Jianfengling region and the inherently low nutrient levels, such as nitrogen and phosphorus, in tropical soils (Peguero et al., 2023). Furthermore, the Jianfengling region in Hainan, located in the tropics, exhibits high temperatures and frequent rainfalls throughout the year (Wardle et al., 2004a). The higher temperatures and precipitation may contribute to the leaching of more mobile N (Hui et al., 2005), which may not be effectively absorbed by plants, resulting in lower N content in the plant leaves. The low P content in plant leaves may be due to insufficient P release from the leaf litter (Wu et al., 2023; Xing et al., 2023). Additionally, the low P content may be attributed to the lower soil P content in the study area compared with other global regions (Zhang et al., 2005).

The N:P ratio of leaf litter in this study (11.06) (Table 1) is lower than the average value of 14.4 reported for 753 plant leaves in China but higher than the global average of 11.0 (Dynarski et al., 2023; Tian et al., 2024). The amount and rate of litter decomposition significantly affect forest productivity and nutrient cycling efficiency within ecosystems. Plant biodiversity, at both species and genotype levels, plays a crucial role in litter decomposition and nutrient cycling in forest ecosystems (Njoroge et al., 2022). The observed negative correlation between leaf litter N:P values and decomposition rate (Chapin et al., 2002) suggests that the Jianfengling area in Hainan exhibits a faster litterfall decomposition rate than other regions in China. This could be attributed to higher temperatures and humid climate in the area and increased microbial activity and metabolism of decomposers

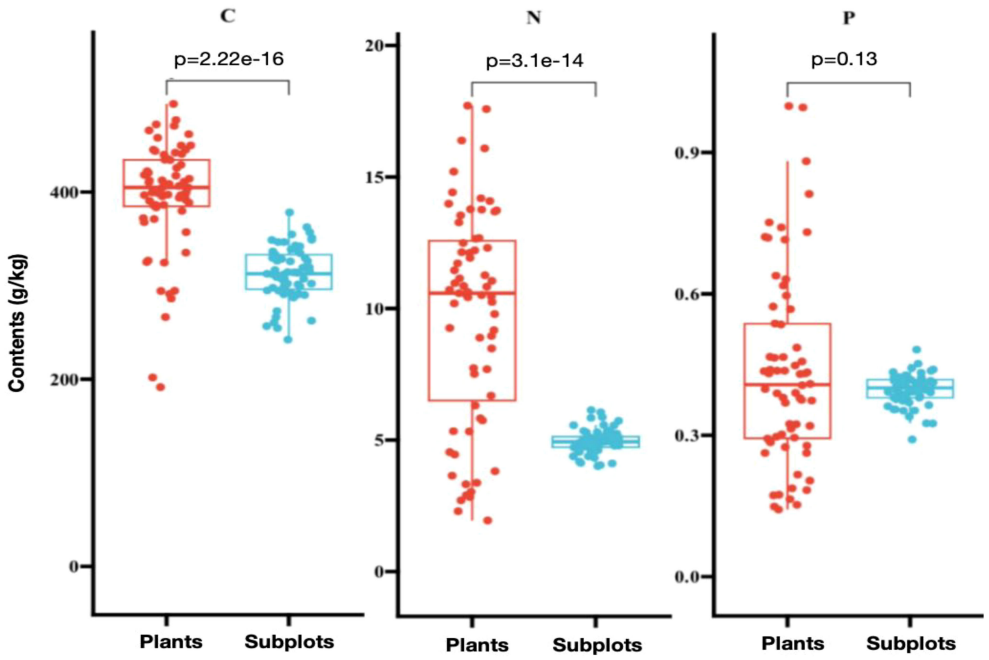


FIGURE 2
Correlations between carbon, nitrogen and phosphorus components across 60 subplots and 31 dominated plant species. The values at the top of the graph indicate the *p*-values for the correlations between plant species and sample plots.

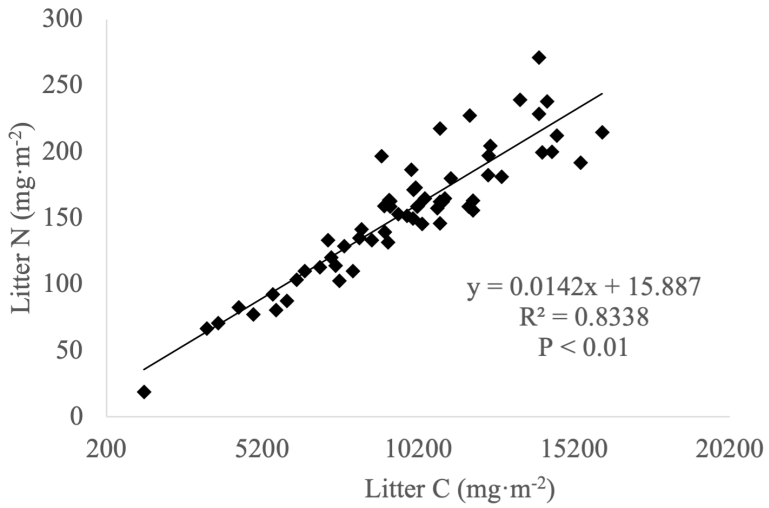


FIGURE 3
Relationship between carbon and nitrogen contents in leaf litter.

(Zhang et al., 2023b). At leaf litter N:P ratios higher than 14 and P content below 0.22 g/kg, litterfall decomposition is significantly limited by P. Conversely, at N:P ratios below 14, litterfall decomposition is mainly limited by N (Wang et al., 2018), suggesting that litterfall decomposition in the Jianfengling region is mainly limited by N. However, other studies have indicated that the productivity of tropical subtropical forests at low latitudes is often limited by P (Reich and Oleksyn, 2004; Wardle et al., 2004a; Yan et al., 2008). Bui and Henderson (2013) analyzed the ecological stoichiometry of carbon, nitrogen and phosphorus across different vegetation types in Australia. The results revealed that the N:P ratio was significantly limited by nitrogen in temperate regions and by phosphorus in tropical regions. But due to the high soil P content in Hainan Province, which exceeds the national average but remains below the global average (Zhang et al., 2005; Sardans et al., 2021), this is attributed to the lower leaf litter N:P ratios in the study region compared with the national average but higher than the global average and the predominance of N limitation in litterfall decomposition. This study supplements the previous research on leaf litter data and provides a complete dataset from the 60-ha tropical montane rainforest dynamic monitoring plot in Jianfengling. This confirms the unique chemometric characteristics of the Jianfengling rainforest in Hainan. Future research should explore the effects of factors such as dominant species, seasonal variations, and slope exposure to light on ecological stoichiometry.

No significant correlations are observed between the C, N and P contents and their stoichiometric characteristics of leaf litter and those in the soil (Figure 6). This suggests that the C, N and P stoichiometric characteristics of leaf litter in Jianfengling have minimal influence on soil physicochemical properties (Zhang et al., 2023a). These findings are consistent with those of

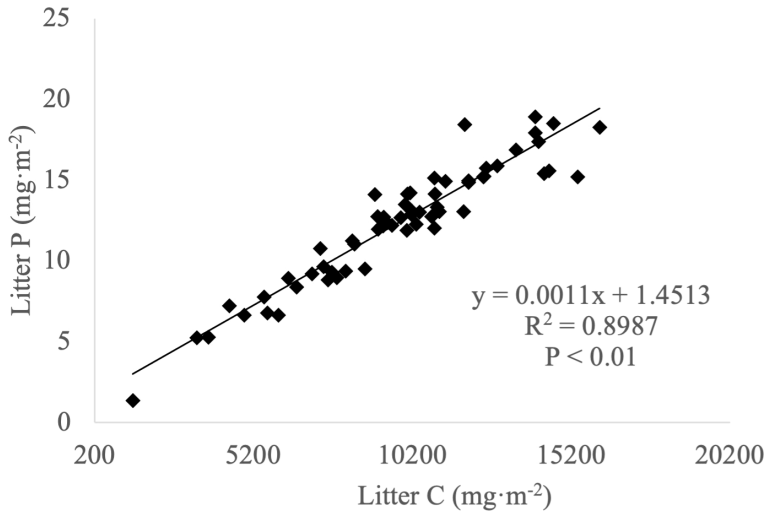


FIGURE 4
Correlation between carbon and phosphorus contents in leaf litter.

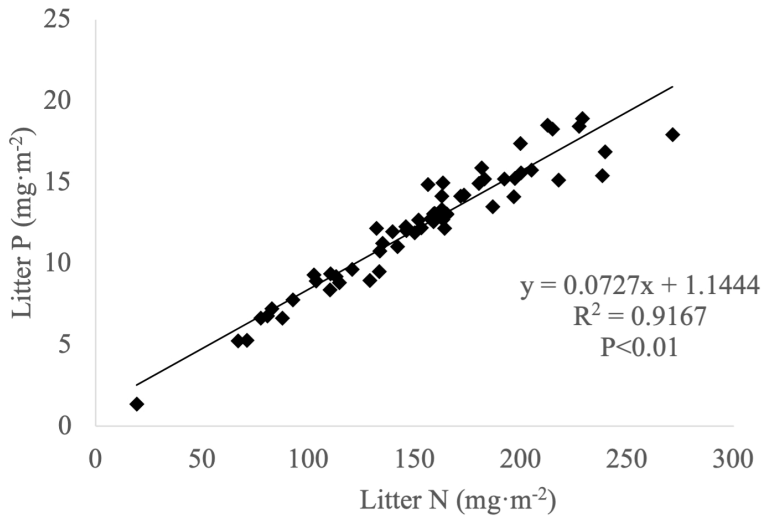


FIGURE 5
Correlation between nitrogen and phosphorus contents in leaf litter.

Song et al. (2024), who reported that the amount of annual litter does not significantly affect soil organic carbon (SOC) contents. Most studies have indicated that leaf litter cover increases soil organic carbon content, with over 50% of the primary net productivity being returned to the soil through litterfall. This process is the main pathway for recycling plant nutrients into the soil (Wardle et al., 2004b; Hobbie, 2015; Guo et al., 2021; Liu et al., 2022; Yuan et al., 2024). The lack of significant correlations among soil C, N and P stoichiometry may be attributed to non-additive changes resulting from litterfall decomposition (He et al., 2024; Song et al., 2024). In our study, the ley connection between soil and plant leaves involves N and P traits. This observation supports the growth rate hypothesis, which suggests that fast-growing plants require N- and P-rich resources to meet their high demands for RNA and protein synthesis (Sistla and Schimel, 2012), consistent with findings from large-scale global studies

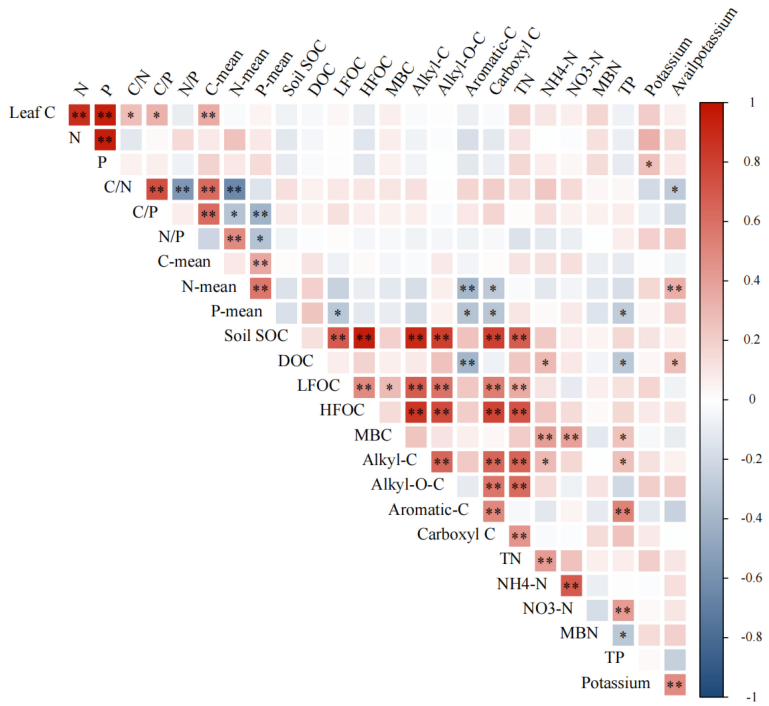


FIGURE 6
Correlation analysis of leaf litter C, N and P contents and their ratios with soil physicochemical properties. Note: * denotes significance at the 0.05 level (two-sided) and ** indicates significance at the 0.01 level (two-sided).

(Reich and Oleksyn, 2004). However, this study does not extensively address nutrient efficiency and cycling in plants within the Jianfengling region and serves as a preliminary basis for more detailed future research.

According to Table 3, we can see the changes in the leaf litter content of the four species with altitude. *Beilschmiedia brevipaniculata* and *Castanopsis carlesii* decreased and then increased with altitude, *Gironniera subaequalis* and *Altingia obovate* decreased significantly with increasing altitude. The differences among the four species were mainly due to their different ecological requirements. Nitrogen-fixing plants decreased and then increased with increasing altitude, while non-nitrogen-fixing plants decreased significantly with increasing altitude. As the altitude increases, both light intensity and maximum temperature show a decreasing trend (Xu et al., 2020), and sun-loving plants will have a decrease in leaf litter content when the altitude increases, however, *Beilschmiedia brevipaniculata* shows a decreasing and then an increasing trend, and the leaf litter content of the shade-loving plants likewise appears to be decreasing and decreasing and then increasing, which suggests that light and temperature are not decisive factors for their distribution. It seems that nitrogen-fixing plants are more adaptable to changes in altitude and are able to acclimatize to different environments, while non-nitrogen-fixing plants are more sensitive to changes in altitude, resulting in a greater reduction in the amount of leaf litter. Meanwhile the decrease in leaf litter content of *Gironniera subaequalis* and *Altingia obovate* at increasing slopes may be due to erosion and deposition caused by higher slopes, which would result in loss of leaf litter. The relationship between the four plants and convexity was not significant, which may be due to the fact that convexity was not a major factor in the leaf litter content of these plants. Other factors such as climate and soil type may be more important in influencing the leaf litter content of these plants. There was a significant difference in organic carbon content between nitrogen-fixing and non-nitrogen-fixing types of plants, with nitrogen-fixing types having a significantly higher organic carbon content than non-nitrogen-fixing types because of their ability to fix nitrogen, which in turn improves the nutrient level and growth rate of the plants, leading to an increase in organic carbon content (Guo et al., 2023). It indicates that nitrogen limitation plays a decisive factor in this region, influencing plant functional traits which is consistent with the mentioned process of leaf litter decomposition which is mainly limited by nitrogen.

## 5 Conclusion and outlook

This study utilizes sample plots and samples collected from the Jianfengling area in Hainan to investigate the stoichiometric characteristics of C, N and P in the 'leaf-litterfall-soil' system and the effects of ecological traits phylogenetic signals on plant functional traits. The findings indicate that the levels of C, N and P in leaf litter are lower in Jianfengling than those observed at both the national and global scales. Moreover, no differences in leaf litter carbon, nitrogen and phosphorus contents are observed among the subplots and dominant plant species. However, the C, N and P contents across different plant groups exhibit greater variability, indicating significant heterogeneity in the samples. In contrast, the data from the subplots feature less variability, indicating significant homogeneity.

Furthermore, significant positive correlations are observed between C and N, C and P, and N and P in leaf litter. The mean contents of C and N are significantly positively correlated with mean P contents. Additionally, mean C values are significantly positively correlated with both C:N and C:P ratios. Conversely, mean P contents are significantly negatively correlated with C:P and N:P ratios. Mean N values exhibit a significant negative correlation with C:N and N:P but feature a significant positive correlation with N:P in leaves. Overall, litter decomposition is mainly limited by elemental N, as indicated by N:P values below 14 in the leaf litter. There were significant phylogenetic signals for three functional traits, namely nitrogen content, altitude and slope, in the Jianfengling 60-ha forest biodiversity dynamic monitoring plot. Light and temperature are not decisive factors affecting plants distribution. Only 31 dominant species or genera were analyzed in this study, and the number of samples may not be sufficient to represent the whole ecosystem; further only the whole year of 2016 was monitored, without considering the long-term trends and spatial variations. In the future, we will continue to monitor the leaf litter in the tropical montane rainforests of the Jianfengling to understand the long-term trends and patterns of change, and to explore the role and mechanism of nitrogen limitation in the decomposition process of leaf litter.

## Data availability statement

The raw data supporting the conclusions of this article will be made available by the author, without undue reservation.

## Author contributions

SY: Writing – original draft, Writing – review & editing.

## Funding

The author declares that no financial support was received for the research, authorship, and/or publication of this article.

## Conflict of interest

The author declares that the research was conducted in the absence of any commercial or financial relationships that could be construed as a potential conflict of interest.

## Publisher's note

# References


Bui, E. N., and Henderson, B. L. (2013). C:N:P stoichiometry in Australian soils with respect to vegetation and environmental factors. *Plant and Soil* 373(1–2), 553–568. doi: 10.1007/s11104-013-1823-9

Chapin, F. S. III, Matson, P. A., and Mooney, H. A. (2002). *Principles of terrestrial ecosystem ecology* (New York: Springer-Verlag).

Cook-Patton, S. C., Leavitt, S. M., Gibbs, D., Harris, N. L., Lister, K., Anderson-Teixeira, K. J., et al. (2020). Mapping carbon accumulation potential from global natural forest regrowth. *Nature* 585, 545–550. doi: 10.1038/s41586-020-2686-x

Du, E., Terrer, C., Pellegrini, A. F. A., Ahlström, A., Van Lissa, C. J., Zhao, X., et al. (2020). Global patterns of terrestrial nitrogen and phosphorus limitation. *Nat. Geosci.* 13, 221–226. doi: 10.1038/s41561-019-0530-4

Dynarski, K. A., Soper, F. M., Reed, S. C., Wieder, W. R., and Cleveland, C. C. (2023). Patterns and controls of leaf nutrient stoichiometry and flexibility across United States forests. *Ecology* 104, e3909.

Elser, J. J., Fagan, W. F., Denno, R. F., Dobberfuhl, D. R., Folarin, A., Huberty, A., et al. (2000). Nutritional constraints in terrestrial and freshwater food webs. *Nature* 408, 578–580. doi: 10.1038/35046058

Falcell, J. M., and Pickett, S. T. A. (1991). Plant litter: its dynamics and effects on plant communitystructure. *Botanical Rev.* 57, 1–32.

Farrer, E. C., and Goldberg, D. E. (2009). Litter drives ecosystem and plant community changes in cattail invasion[J]. *Ecological Applications* 19, 398–412.

Friedlingstein, P., O'Sullivan, M., Jones, M. W., Andrew, R. M., Hauck, J., Olsen, A., et al. (2020). Global carbon budget 2020. *Earth System Sci. Data* 12, 3269–3340. doi: 10.5194/essd-12-3269-2020

Guo, K., Yang, J., Yu, N., Luo, L., and Wang, E. (2023). Biological nitrogen fixation in cereal crops: Progress, strategies, and perspectives. *Plant Commun.* 4, 100499. doi: 10.1016/j.xplc.2022.100499

Guo, L., Deng, M., Yang, S., Liu, W., Wang, X., Wang, J., et al. (2021). The coordination between leaf and fine root litter decomposition and the difference in their controlling factors. *Global Ecol. Biogeography* 30, 2286–2296. doi: 10.1111/geb.v30.11

Han, W., Fang, J., Guo, D., and Zhang, Y. (2005). Leaf nitrogen and phosphorus stoichiometry across 753 terrestrial plant species in China. *New Phytol.* 168, 377–385. doi: 10.1111/j.1469-8137.2005.01530.x

He, P., Deng, X., Liu, J., Li, M., and Cheng, F. (2024). Non-additive responses of litter decomposition, litter chemical traits, and soil C:N:P stoichiometry to mixing with Eucalyptus in plantation environments. *Plant Soil* 499, 457–472. doi: 10.1007/s11104-023-06470-0

Hobbie, S. E. (2015). Plant species effects on nutrient cycling: Revisiting litter feedbacks. *Trends Ecol. Evol.* 30, 357–363. doi: 10.1016/j.tree.2015.03.015

Hui, W., Quanjiu, W., and Min-an, S. (2005). Characteristics of nitrogen leaching from sloping land on loess plateau under rainfall conditions. *J. Soil Water Conserv.* 19, 61–64.

Jing-Yun, F. A. N. G., Yi-De, L. I., Biao, Z. H. U., Guo-Hua, L. I. U., and Guang-Yi, Z. H. O. U. (2004). Community structures and species richness in the montane rain forest of Jianfengling, Hainan Island, China. *Biodiversity Sci.* 12, 29–43. doi: 10.17520/biods.2004005

Jun-pei, Lu, and Qi-han, L. (1988). Litter-fall in tropical forest at Jianfengling mountains, Hainan Island. *Chin. J. Plant Ecol.* 12, 104–112.

Ke, C., Mide, R., Jianzhong, Y., Xiaojuan, L., Xiangcheng, M., and Jianhua, C. (2014). The phylogenetic signal of functional traits and their effects on community structure in an evergreen broad-leaved forest: The phylogenetic signal of functional traits and their effects on community structure in an evergreen broad-leaved forest. *Biodiversity Sci.* 21, 564–571. doi: 10.3724/SP.J.1003.2013.08068

Li, S., Xu, Z., Yu, Z., Fu, Y., Su, X., Zou, B., et al. (2023). Litter decomposition and nutrient release are faster under secondary forests than under Chinese fir plantations with forest development. *Sci. Rep.* 13, 16805. doi: 10.1038/s41598-023-44042-5

Liu, W., Jiang, Y., Yang, Q., Yang, H., Li, Y., Li, Z., et al. (2021). Spatial distribution and stability mechanisms of soil organic carbon in a tropical montane rainforest. *Ecol. Indic.* 129, 107965. doi: 10.1016/j.ecolind.2021.107965

Liu, M., Wen, J. H., Chen, Y. M., Xu, W. J., Wang, Q., and Ma, Z. L. (2022). Warming increases soil carbon input in a Sibiraea angustata -dominated alpine shrub ecosystem. *J. Plant Ecol.* 15, 335–346. doi: 10.1093/jpe/rtab101

Njoroge, D. M., Chen, S., Zuo, J., Dossa, G. G. O., and Cornelissen, J. H. C. (2022). Soil fauna accelerate litter mixture decomposition globally, especially in dry environments. *J. Ecol.* 110, 659–672. doi: 10.1111/1365-2745.13829

Peguero, G., Coello, F., Sardans, J., Asensio, D., Grau, O., Llusià, J., et al. (2023). Nutrient-based species selection is a prevalent driver of community assembly and functional trait space in tropical forests. *J. Ecol.* 111, 1218–1230. doi: 10.1111/1365-2745.14089

Reich, P. B., and Oleksyn, J. (2004). Global patterns of plant leaf N and P in relation to temperature and latitude. *Proc. Natl. Acad. Sci. United States America* 101, 11001–11006.

Ren, S.-J., and Yu, G.-R. (2011). Statistical characteristics of leaf carbon, nitrogen and phosphorus stoichiometry of 102 dominant species in forest ecosystems of a north-south sample zone in eastern China[J]. *J. Appl. Ecol.* 23(3):581-586. doi: 10.3724/SP.J.1258.2011.00119

Sardans, J., Janssens, I. A., Ciais, P., Obersteiner, M., and Peñuelas, J. (2021). Recent advances and future research in ecological stoichiometry. *Perspect. Plant Ecology Evol. Systematics* 50, 125611. doi: 10.1016/j.ppees.2021.125611

Sardans, J., Rivas-Ubach, A., and Peñuelas, J. (2012). The elemental stoichiometry of aquatic and terrestrial ecosystems and its relationships with organismic lifestyle and ecosystem structure and function: a review and perspectives. *Biogeochemistry* 111, 1–39. doi: 10.1007/s10533-011-9640-9

Sistla, S. A., and Schimel, J. P. (2012). Stoichiometric flexibility as a regulator of carbon and nutrient cycling in terrestrial ecosystems under change. *New Phytol.* 196, 68–78. doi: 10.1111/j.1469-8137.2012.04234.x

Song, Z., Zuo, X., Zhao, X., Qiao, J., Ya, H., Li, X., et al. (2024). Plant functional traits mediate the response magnitude of plant-litter-soil microbial C: N: P stoichiometry to nitrogen addition in a desert steppe. *Sci. Total Environ.* 915, 169915. doi: 10.1016/j.scitotenv.2024.169915

Tian, D., Yan, Z., Schmid, B., Kattge, J., Fang, J., and Stocker, B. D. (2024). Environmental versus phylogenetic controls on leaf nitrogen and phosphorous concentrations in vascular plants. *Nat. Commun.* 15, 5346. doi: 10.1038/s41467-024-49665-4

Tie, L., Wei, S., Peñuelas, J., Sardans, J., Liu, X., Zhou, S., et al. (2023). N and P combined addition accelerates the release of litter C, N, and most metal nutrients in a N-rich subtropical forest. *Sci. Total Environ.* 881, 163491. doi: 10.1016/j.scitotenv.2023.163491

Wang, N., Fu, F., Wang, B., and Wang, R. (2018). Carbon, nitrogen and phosphorus stoichiometry in Pinus tabulaeformis forest ecosystems in warm temperate Shanxi Province, north China. *J. Forestry Res.* 29, 1665–1673. doi: 10.1007/s11676-017-0571-8

WANG, J. Y., WANG, S. Q., LI, R. L., YAN, J. H., and SHA, L. Q. (2011). C: N: P stoichiometric characteristics of four forest types' dominant tree species in China. *Chin. J. Plant Ecol.* 35, 587.

Wardle, D. A., Bardgett, R. D., Klironomos, J. N., Setälä, H., Van Der Putten, W. H., and Wall, D. H. (2004b). Ecological linkages between aboveground and belowground biota. *Science* 304, 1629–1633. doi: 10.1126/science.1094875

Wardle, D. A., Walker, L. R., and Bardgett, R. D. (2004a). Ecosystem properties and forest decline in contrasting long-term chronosequences. *Science* 305, 509–513. doi: 10.1126/science.1098778

Wu, T., Long, C., Xiong, L., Li, J., and Liu, Q. (2023). Relationship between plant leaf functional traits and soil factors at different succession stages in karst forest of Maolan. 43 (03), 463–472.

Xing, G., Wang, X., Jiang, Y., Yang, H., Mai, S., Xu, W., et al. (2023). Variations and influencing factors of soil organic carbon during the tropical forest succession from plantation to secondary and old–growth forest. *Front. Ecol. Evol.* 10, 1104369. doi: 10.3389/fevo.2022.1104369

XU, S., HE, X., YANG, P., BAI, T., FAN, H., YI, K., et al. (2020). Effect of climatic factors on the banana growth and its fruit quality at different altitudes. *J. OF YUNNAN Agric. Univ. (Natural Science)* 35, 102–107. doi: 10.12101/j.issn.1004-390X(n).201805051

Xu, H., Li, Y., Lin, M., Wu, J., Luo, T., Zhou, Z., et al. (2015). Community characteristics of a 60 ha dynamics plot in the tropical montane rain forest in Jianfengling, Hainan Island. *Biodiversity Sci.* 23, 192–201. doi: 10.17520/biods.2014157

Yan, E. R., Wang, X. H., and Zhou, W. (2008). N:P stoichiometry in secondary succession in evergreen broad-leaved forest, Tiantong, East China. *J. Plant Ecol.* 32, 13–22.

Yuan, J., Wu, F., Peng, C., Peñuelas, J., Vallicrosa, H., Sardans, J., et al. (2024). Global spectra of plant litter carbon, nitrogen and phosphorus concentrations and returning amounts. *J. Ecol.* 112, 717–729. doi: 10.1111/1365-2745.14250

Zhang, J., Li, X., Chen, M., Huang, L., Li, M., Zhang, X., et al. (2023b). Response of plant, litter, and soil C:N:P stoichiometry to growth stages in Quercus secondary forests on the Loess Plateau, China. *J. Forestry Res.* 34, 595–607. doi: 10.1007/s11676-022-01512-2

Zhang, L., Liu, J., Yin, R., Xu, Z., You, C., Li, H., et al. (2023a). Soil fauna accelerated litter C and N release by improving litter quality across an elevational gradient. *Ecol. Processes* 12, 47. doi: 10.1186/s13717-023-00459-4

Zhang, C., Tian, H., Liu, J., Wang, S., Liu, M., Pan, S., et al. (2005). Pools and distributions of soil phosphorus in China. *Global Biogeochemical Cycles* 19, 347–354. doi: 10.1029/2004GB002296

Zhongmin, Wu, Yide, Li, Qingbo, Z., Guangyi, Z., Bufeng, C., Zhihu, Du, et al. (1998). Carbon pool of tropical mountain rain forests in Jianfengling and effect of clear-cutting on it. *Chin. J. Appl. Ecol.* 9, 341–344.

frontiers | Frontiers in Plant Science

TYPE Original Research
PUBLISHED 17 October 2024
DOI 10.3389/fpls.2024.1488163



OPEN ACCESS

EDITED BY
Xiang Liu,
Lanzhou University, China

REVIEWED BY
Xiaoshuang Sun,
Shandong University of Technology, China
Liu Gao,
Yunnan Agricultural University, China

*CORRESPONDENCE
Hui Zhang
13925183735@139.com
Huai Yang
Yanghuai2008@163.com

RECEIVED 29 August 2024
ACCEPTED 30 September 2024
PUBLISHED 17 October 2024

CITATION
Yang Q, Zhang Z, Zhang H, Yang H, Pandey S and John R (2024) The contributions of rainfall and fog to leaf water of tree and epiphyte communities in a tropical cloud forest. *Front. Plant Sci.* 15:1488163. doi: 10.3389/fpls.2024.1488163



# The contributions of rainfall and fog to leaf water of tree and epiphyte communities in a tropical cloud forest

Qingqing Yang[1,2,3], Zijing Zhang[4], Hui Zhang[5*], Huai Yang[6*], Shree Pandey[4] and Robert John[4]

[1]School of Ecology, Hainan University, Haikou, China, [2]Hainan Academy of Forestry (Hainan Academy of Mangrove), Haikou, China, [3]Key Laboratory of Tropical Forestry Resources Monitoring and Application of Hainan Province, Haikou, China, [4]Key Laboratory of Genetics and Germplasm Innovation of Tropical Special Rainforest Trees and Ornamental Plants (Hainan University), Ministry of Education, School of Tropical Agriculture and Forestry, Hainan University, Haikou, China, [5]Hainan Institute of National Park, Haikou, China, [6]Institute of Tropical Bamboo, Rattan & Flower, Sanya Research Base, International Center for Bamboo and Rattan, Sanya, China

**Introduction:** Tropical cloud forest ecosystems are expected to face reduced water inputs due to climatic changes.

**Methods:** Here, we study the ecophysiological responses of trees and epiphytes within in an Asian cloud forest to investigate the contributions of rainfall, fog, and soil to leaf water in 60 tree and 30 vascular epiphyte species. We measured multiple functional traits, and $\delta^2H$, and $\delta^{18}O$ isotope ratios for leaf water, soil water, rainfall, and fog in the wettest (July) and driest (February) months. Using a Bayesian stable isotope mixing model, we quantified the relative contributions of soil water, fog, and rainfall to leaf water.

**Results and discussion:** Rainfall contributes almost all the leaf water of the epiphytes in July, whereas fog is the major source in February. Epiphytes cannot tap xylem water from host trees, and hence depended on fog water when rainfall was low. Most of leaf water was absorbed from soil water in July, while fog was an important source for leaf water in February despite the soil moisture content value was high. In February, lower temperatures, along with reduced photosynthesis and transpiration rates, likely contributed to decreased soil water uptake, while maintaining higher soil moisture levels despite the limited rainfall. These contrasting contributions of different water sources to leaf water under low and high rainfall and for different plant groups outline the community-level ecophysiological responses to changes in rainfall. While direct measurements of water flux, particularly in roots and stems, are needed, our results provide valuable insights on tropical cloud forest hydrology under scenarios of decreased fog immersion due to climatic changes.

KEYWORDS

**hydraulic response, leaf water supply, isotope, photosynthesis rate, transpiration rate**

# 1 Introduction

Tropical cloud forests, despite occupying only 1.4% of the world's tropical forest area (Scatena et al., 2011), there is disproportionately high diversity and endemism for plant and animal species (Bruijnzeel et al., 2010; Karger et al., 2021). They occur in mountains where cloud or fog immersion of the forest canopy is a frequent phenomenon, and where plants benefit from the foliar uptake of 'occult' precipitation (i.e., mist, cloud water, fog, fine drizzle and wind-driven rain), at least during the dry season (Bruijnzeel et al., 2010). Due to their distinct climatic and hydrological, tropical cloud forests are widely regarded as sensitive to climatic change response. This was evident in the dramatic declines and extinctions of amphibian species in the cloud forests of Central America in the 1990s due to warming-induced drought stress, which drew global attention to the vulnerability of these ecosystems to biodiversity loss (Pounds et al., 1999; Alan Pounds et al., 2006; Fisher and Garner, 2020). Model projections (Still et al., 1999; Helmer et al., 2019) and empirical evidence (Ray et al., 2006; Nair et al., 2008; Diaz et al., 2011; Krishnaswamy et al., 2014; Los et al., 2021) support the hypothesis of 'lifting cloud base' and drying in tropical montane environments in response to climate warming, with projected negative impacts on hydrology due to reduced cloud immersion (Hildebrandt and Eltahir, 2007; Hu and Riveros-Iregui, 2016; Los et al., 2021). Despite the existing knowledge, the variability observed in cloud forest types and the documented ecohydrological patterns (Hu and Riveros-Iregui, 2016) highlight the necessity for further studies encompassing diverse ecosystems and major taxonomic groups, particularly in cloud forest sites with seasonal rainfall patterns and potential drought stress.

Tropical cloud forests exhibit a remarkable diversity and structural complexity in their vegetation and ecohydrological attributes, yet research efforts have not been evenly distributed across all cloud forests. Climatic stressors are already changing the ecohydrological conditions of cloud forests, with negative impacts on regional watersheds and fresh-water supply, particularly in sites that face seasonal water stress (Hildebrandt and Eltahir, 2007; Los et al., 2019). Rising temperatures in tropical montane regions can alter the spatial-temporal dynamics of fog occurrence and reduce cloud water interception by vegetation, resulting in loss of moisture inputs (Hu and Riveros-Iregui, 2016; Los et al., 2019; Li et al., 2022). Combined with other factors such as strong climatic variation and shallow soils, the impact of reduced cloud water interception on tree populations (Werner, 1988; Aiba and Kitayama, 2002; Anchukaitis and Evans, 2010) will depend on plant hydraulic responses to water availability (Anderegg et al., 2012; Berry et al., 2015; Choat et al., 2018). Besides, the importance of 'occult' precipitation in alleviating any decline in soil water availability due to decreasing rainfall or seasonal drought stress needs to be quantified across cloud forest sites.

The first step in understanding the importance of 'occult' precipitation in tropical cloud forests is to examine fog-induced specific hydraulic responses of plant species. Previous studies have only been explored within subsets of species (Burgess and Dawson, 2004; Johnson and Smith, 2008; Ritter et al., 2009; Eller et al., 2013, 2016; Gotsch et al., 2014, 2018; Binks et al., 2019; Cavallaro et al., 2020), thereby constraining our comprehension of community-level responses. As a phenomenon, foliar uptake of fog water has been reported widely, but the relative contribution of fog uptake to leaf water may vary considerably within and among individuals and species (Burgess and Dawson, 2004; Limm et al., 2009; Goldsmith et al., 2013). Foliar fog water uptake may also depend on rainfall distribution, fog duration, and plant life-form (e.g., trees vs. epiphytes) (Oliveira et al., 2014; Gotsch et al., 2014; 2015; Wu et al., 2018; Berry et al., 2015, 2019; Binks et al., 2019). An effective assessment of community-level hydraulic responses to changes in fog incidence would require a wide coverage of the species and life forms in cloud forests (Suding et al., 2008; Laughlin, 2014).

In this study, we quantify the contributions of rain, fog, and soil waters to vegetation in an old-growth tropical cloud forest in Hainan Island, southern China. The tropical cloud forests in Hainan Island are stunted ('elfin' forests) and experience highly seasonal rainfall (Long et al., 2011b). The basic fog induced plant hydraulic responses are unknown and we cannot yet assess the impact of climatic changes on cloud forest vegetation in this region. We argue that quantifying community-level responses (such as possible differences in photosynthesis, transpiration, and soil- and foliar/fog water uptake) between seasons (dry winter vs. wet summer) and life-forms (e.g., trees vs. epiphytes) are the key to understanding how this tropical cloud forest plant community copes with seasonal or temporal changes in water availability. Therefore, we evaluated community-wide ecophysiological responses of the trees and epiphytes to changes in water availability by examining the following: (i) leaf isotope ratios ($\delta^2H$, $\delta^{18}O$ and $\delta^{13}C$) and several key functional traits (transpiration rate, leaf turgor loss point, leaf hydraulic capacitance and photosynthesis rate) for 60 tree species and 30 vascular epiphyte species in the wettest and driest months; (ii) the isotope ratios ($\delta^2H$ and $\delta^{18}O$) in soil water, rain, and fog water in the wettest and driest months; (iii) species abundances of 60 tree species and 30 vascular epiphyte species in 21 plots of 400 $m^2$ each, and (iv) soil water content in the peak months of the wet and dry seasons.

Our study design, and the selection of ecophysiological measurements are based on hypothesized plant responses to seasonal changes in precipitation. Fog, along with fine drizzle (wind-driven rain), increases water inputs to the ecosystem (Bruijnzeel et al., 2011; Giambelluca and Gerold, 2011; Binks et al., 2019). However, it may also exert an influence on water movement within plants by diminishing solar radiation and temperature, which subsequently impedes photosynthesis, transpiration, and soil water absorption by roots (Goldsmith et al., 2013; Weathers et al., 2020). This might explain in part why cloud forests maintain high soil water content (Goldsmith et al., 2013; Muñoz-Villers and McDonnell, 2013; Dawson and Goldsmith, 2018; Gerlein-Safdi et al., 2018), even during the dry season (Bruijnzeel and Veneklaas, 1998). Nevertheless, a predicted 2°C warming may elevate the cloud-base heights by 250 m (predictions for 2052 by IPCC 5th assessment reports) with differential impact on plant growth forms (trees, grasses, epiphytes) (Nadkarni and Solano, 2002; Zotz and Bader et al., 2009; Wu et al., 2018; Liu et al., 2005), and result in a significant loss of tropical cloud forest cover in some sites (Los et al., 2019; de Meyer et al., 2022).

We tracked hydrological inputs through leaf isotope ratios ($\delta^2H$ and $\delta^{18}O$), which when analyzed with a Bayesian stable isotope mixing model, can trace the relative contribution of rainfall, soil, and fog to leaf water in both trees and epiphytes (Wu et al., 2018; Wang et al., 2019). We then used several ecophysiological traits including leaf-level photosynthesis and transpiration rates, leaf carbon isotopic composition ($\delta^{13}C$) as an indicator of long-term intrinsic water use efficiency (Cernusak et al., 2013; Ellsworth and Cousins, 2016; Acosta-Rangel et al., 2018), leaf turgor loss point (TLP) (Bartlett et al., 2012; Werner, 1988; Jarvis and Mulligan, 2011), and leaf hydraulic capacitance (Brodribb and Holbrook, 2003), all of which capture critical plant hydraulic responses. We therefore investigated (1) whether there is differential contribution to leaf water between species, life forms, and seasons from the three possible sources of leaf water - soil, rainfall, and fog; (2) whether community-level ecophysiological responses vary between the wettest and driest months and between life forms; and (3) how these ecophysiological responses help to maintain the hydraulic safety of vegetation and the ecohydrology of this cloud forest plant community.

# 2 Materials and methods

## 2.1 Study site

The study was conducted in a tropical montane evergreen dwarf cloud forest ('elfin' forest; tropical cloud forest) at Bawangling Area of Hainan Tropical Rainforest National Park (109°05′-109°25′E, 18°50′-19°05′N), located in Hainan Island, southern China (Long et al., 2011b). This region belongs to the tropical monsoon climate area with a mean annual rainfall of ~2500 mm, and a distinct wet season from May to October, which accounts for about 80% of the annual rainfall. In 2017, a local meteorological station was established near our experimental site and observations during the 2018 show that the mean monthly rainfall during the wet season was 306 mm, with July emerging as the wettest month with a rainfall of 375 mm (Supplementary Figure S1). The lowest rainfall (58 mm) and frequency (5 days) of rain were observed for February. The dry season (monthly rainfall<100 mm), spanning a period of five months from November to March, is characterized by monthly average rainfall below 78 mm (see also Long et al., 2011b). April was relatively wetter with 138 mm of rain, after which the wet season begins in May. Based on these meteorological data, effective monthly rainfall (monthly rainfall – monthly potential evapotranspiration) was +235.7 mm for July and -16.7 mm for February, indicating only a slight rainfall deficit in the driest month.

The reserve is predominantly comprised of old-growth tropical cloud forest, on a substrate of lateritic soil developed primarily from sandstone bedrocks (Cheng et al., 2020). These forests typically occur as mountaintop islands over 1250 m above sea level, where terrain slope range from 3° to 65° (Long et al., 2011a). The sites typically have very shallow (30-70 cm) soil, high spatial extent (40%) of exposed rock, and very short tree root length (less than 30 cm) (Long et al., 2011c; Yang et al., 2021). The dominant plant species include *Distylium racemosum, Syzygium buxifolium, Xanthophyllum hainanense, Camellia sinensis* var. *assamica and Cyclobalanopsis championii*. The average tree height in these forests is rather low at 4.8 ± 2.8 m, but as is typical of cloud forests, average tree density is high at 9633 stems $ha^{-1}$ (Long et al., 2011b). A total of 89 tree species have been recorded in 41 plots of 100 $m^2$ each (Long et al., 2011a).

## 2.2 Field sampling

We carried out field sampling and measurements in the months of February and July of 2019, primarily to quantify the contributions of various water sources to leaf water in tree and epiphyte species in the wettest and driest months of the year (Supplementary Figure S1). The sampling was carried out in 21 vegetation plots, each of size 20 × 20 $m^2$, which we had established in previous work (Long et al., 2011b). These plots are located within a narrow elevation range of 1313 m to 1395 m above mean sea level (Long et al., 2011b; Supplementary Figure S2 and Supplementary Table S1). The plots are separated from each other by about 100 m and do not show significant spatial autocorrelation in species abundances or soil properties (Long et al., 2015). The total area of the tropical cloud forest in the reserve is just about 3 hectares, and the 21 plots are scattered as widely as possible across this mountaintop patch (Supplementary Figure S2).

In this study, we recorded all freestanding trees with a diameter of ≥ 1 cm at breast height (DBH) within each plot and identified them to species. The relatively low tree height in this cloud forest allowed us to accurately measure species abundance (total number of individuals) for all epiphyte species on the host trees in the 21 plots. We followed the method proposed by Sanford (1968) to record the species abundances for all vascular epiphytes in the plots. The specific details are given in Supplementary Data Sheet - Text S1 in the Supplementary Material.

To measure the contribution of different water sources to leaf water in the wettest and driest month of the year, we measured hydrogen and oxygen isotope ratios ($\delta^2H$ and $\delta^{18}O$) in leaf water (for tree and epiphyte communities), rain water, soil water, and fog drip water, for both of these seasons. We also measured soil water content using standard gravimetric analysis. For isotope measurements of leaf water, we sampled 20 mature, healthy, sun-exposed canopy leaves from three to five individuals of each tree and epiphyte species present in the 21 plots. Due to the evaporative enrichment of the heavier isotope in leaves, stem xylem water isotope ratios may provide a better integrated signal of plant water (Zhao et al., 2016). However, given the challenges associated with sampling stem water, particularly for epiphytes, we focus our study on leaf water. Many epiphyte species in our tropical cloud forest are orchids with pseudobulb stems, so extracting their stem xylem water would have been difficult (Wang et al., 2019). We note that evaporative enrichment is lower in cloud forests because leaf wetting, fog, and high atmospheric humidity reduce transpiration rates (Alvarado-Barrientos et al., 2014). Finally, leaf water analysis may be a relatively non-intrusive method for quantifying the sources of plant water (Benettin et al., 2021).

We also collected water samples of fog drip and rainfall within each plot purely to measure isotope ratios (and not to quantify fog precipitation). We followed Liu et al. (2005) for fog drip collection,

wherein a simple self-made fog drip collector made of plastic film was used to intercept and collect the fog droplets formed upon contact (Supplementary Figure S3C). Specifically, fog drip in each plot was collected by hanging a clean plastic film between the two trees, with clear exposure on the windward side (Supplementary Figures S3B, C). We set this from 19:00 to 21:00 h when heavy fog had set in and when there was no rain. The intercepted smaller fog droplets condense and gradually coalesce to form large water droplets, which are collected in a storage tank at the lower end of the plastic film. Finally, each condensed water sample was saved in a 20 ml tube. We collected fog drip water, soil water, and rain water separately. Rainfall samples were collected under the trees using a 20 ml tube at the beginning of a rainfall event. All the collected plant, soil, fog, and rainfall samples were stored in liquid nitrogen containers before measuring isotope ratios ($\delta^2H$, and $\delta^{18}O$). Due to the shallow soils and short tree root length, we sampled soils at 0-20 cm depth, collecting three samples (20 g each) in each plot, using a 5 cm diameter soil auger, in both the months. We collected soil water on a day when there was no rain. Before performing the isotope analysis, we needed to extract leaf water and soil water from all the samples, which we did using a fully automatic vacuum condensation extraction system (LI-2100, LICA United Technology Limited, Beijing, China). The extraction rate of water from the samples was assessed to be more than 98% on the basis of gravimetric analysis.

For plant trait measurements, undertaken in February and July, we severed a small branch from each tree being sampled and measured a set of plant traits including maximum photosynthesis rate ($A_{area}$; μmol $cm^{-2}$ $s^{-1}$), transpiration rate (mol $m^{-2}$ $s^{-1}$), stomatal density (number of stomata $mm^{-2}$ of leaf area), stomatal conductance (mmol $m^{-2}$ $s^{-1}$), leaf turgor loss point (TLP; MPa), and leaf $\delta^{13}C$ for tree and vascular epiphyte communities. To minimize intraspecific variation in trait measurements, we selected only individuals with DBH near the species mean value. We also ensured that leaves were collected from the same individuals for each species in both the wettest and driest months.

For the dry season measurements, we carried out the sampling and field measurements from February 5 to 10, 2019, during which period rainfall occurred only on February 10. We matched these measurements for the wettest month and started sampling on 5$^{th}$ July and completed the field work by the 10$^{th}$ of July. Although it rained almost every day in the month of July, we had only night rains from July 5 to 6, 2019. Thus, we collected soil water samples and leaf samples (for measuring leaf isotope) in the mornings of July 5 and 6 for the wet season. We collected fog drip from 19:00 to 21:00 h on the nights of July 8 and February 8 and rainfall samples on July 10 and February 10. This study design enabled us to quantify 1) the hydraulic responses of the tree and epiphyte communities in the wettest and driest parts of the year; and 2) the relative contributions of rainfall, fog, and soil water to the water use strategies of tree and epiphyte communities in wettest and driest conditions.

## 2.3 Isotope ($\delta^2H$, $\delta^{18}O$, and $\delta^{13}C$) measurements

We measured $\delta^{13}C$ using the conventional Pee Dee Belemnite standard (Farquhar et al., 1989). Then, we sampled 0.5-1.5 ml of leaf water, soil water, fog and rainfall, to measure $\delta^{18}O$ and $\delta^2H$. The isotopic compositions were analyzed using a liquid water isotope analyzer (Model DLT-100, Los Gatos Research, USA) that employs cavity enhanced absorption spectroscopy. The precision of the isotope analyzer was typically better than ± 1.2‰ for $\delta^2H$ and ± 0.3‰ for $\delta^{18}O$. To account for the possible presence of organic contaminants in cryogenically extracted water samples from plant tissues, the stable isotopic ratios of leaf water measured by the LGR system were corrected as described in previous studies (Schultz et al., 2011; Wu et al., 2016), and the specific details are given in Supplementary Data Sheet - Text S2 in the Supplementary Material.

## 2.4 Meteorological variables and soil water measurements

In 2017, an automatic weather station (YT-QXC4, Shandong, China) was installed in a central location, near the 21 sampling plots (also in forested area) and situated at an elevation of 1245 m a.s.l. (Supplementary Figure S2). This installation enabled the continuous monitoring and collection of data - rainfall frequency (number of rainy days in a month), and monthly mean values for rainfall, total solar radiation, air temperature, humidity and wind speed. We also surveyed fog duration or timing from 6:00 to 23:00 h in July and February by observing for fog on each day. Specifically, nocturnal fog was observed by setting up a light in the plot. We used about 20 g soil for each of the 21 soil samples to measure gravimetric soil water (g/kg). All soil samples were oven-dried for 24 h at 105 °C for these measurements.

## 2.5 Maximum photosynthesis rate, transpiration rate and stomatal conductance, stomatal density, leaf hydraulic capacitance and leaf turgor loss point measurements

We used the Li-6800 portable photosynthesis system (Li-Cor, Lincoln, Nebraska, USA) to measure maximum photosynthesis rate, transpiration rate and stomatal conductance between 9:00 AM and 11:00 AM on sunny days. Five canopy leaf-bearing branches at similar heights (~20 mm in diameter) were harvested, and then photosynthetic measurements were taken within 1 h (Wyka et al., 2012). Based on preliminary trials, we set the photosynthetic photon flux at 1200 μmol $m^{-2}$ $s^{-1}$ to ensure all the species were measured for light-saturated photosynthetic rates (Zhang et al., 2018). We set chamber $CO_2$ and air temperature as 400 μmol $mol^{-1}$ and 28 °C, respectively. Before collecting the data, we first exposed the leaves to the above conditions for about 5 minutes to allow photosynthetic parameters to stabilize. We sampled five to six fully expanded and sun-exposed leaves from three to five mature individuals to measure maximum photosynthesis rate, transpiration rate and stomatal conductance, whose values are referred to as leaf area units.

Stomatal density was measured using the protocol in Carins Murphy et al. (2012). We first collect leaf surface film and then use

an optical microscope (LEICA DM3000 LED) and Image J software to calculate stomatal density in the leaf cuticles (2 per leaf and 5 fields of view per cuticle).

Leaf turgor loss point was determined from leaf pressure-volume (P-V) curve (Sack et al., 2003) for each species in both seasons. For the measurement of P-V curve, we selected healthy leafy branches (or entire plants for several small epiphyte species) from five individuals in the early morning (05:00 and 07:00 h). The samples were packed in black plastic bags with the cut ends maintained underwater, and were immediately sent to the laboratory (within 1 h). The sampled leaves were water saturated because leaf water potential was higher than -0.3 MPa, and did not show a decrease during transportation. For each measured leaf, we determined saturated leaf mass and subsequently conducted a bench-drying procedure (dehydration on a lab bench at 25°C) to obtain a range of leaf water potentials. During leaf desiccation, we periodically measured leaf mass and leaf water potential ($K_{leaf}$) by using a precision scale (0.0001g) and a pressure chamber (PMS, Corvallis, OR, USA), respectively. Finally, the dry leaf mass was determined after drying in an oven at 70°C for about 72 h. We calculated relative water content (RWC) and then constructed P-V curve by plotting leaf RWC against $K_{leaf}$. Leaf P-V curves of the measured species showed distinct two-phase linear equation, and leaf water potential at turgor loss point (TLP) was estimated from the point of intersection of the two lines (Brodribb and Holbrook, 2003; Wang et al., 2021).

Leaf hydraulic capacitance (C) was determined from the slope of P-V curve for each species, with the help of following equation (Brodribb and Holbrook, 2003).

$$C = \delta RWC/\delta\Psi_l \times (DW/LA) \times (WW/DW)/M$$

Here, DW is leaf dry weight (g), LA is leaf area ($m^2$), WW is mass of leaf water at 100% RWC (g), and M is molar mass of water (g $mol^{-1}$). $\delta RWC/\delta\Psi_l$ could be attained from P-V curve.

## 2.6 Statistical analysis

Community weighted mean (CWM) of a functional trait is defined as the summation over all species in the community of the species mean trait values weighted by their respective relative abundances (Garnier et al., 2004). CWM is considered a good measure of ecosystem response to abiotic factors (Lavorel and Garnier, 2002; Suding et al., 2008; Laughlin, 2014). Therefore, for each of the 21 plots, community-level trait metrics or isotopes ($CWM_{jk}$) for the tree and epiphyte community were quantified for each trait or isotopes ($j$) in each plot ($k$) following Garnier et al. (2004) and Buzzard et al. (2016) and using the following formula:

$$CWM_{jk} = \sum x_{ik} t_{ik}$$

where $x_{ik}$ is the relative abundance of species $i$ in plot $k$ and $t_{ik}$ is the isotope or leaf functional trait value of species $i$ in plot $k$. In reality, $CWM_{jk}$ was calculated using function 'dbFD' in the *FD* package in R.

The Bayesian stable isotope mixing model (Parnell et al., 2013) is widely used for tracing the proportional contributions of various sources to a stable isotope mixture. It is based on isotopic mass conservation and that the isotopic mass for the mixture should contain the signature of the proportional contributions of the isotopic masses from all its potential sources (Wang et al., 2019). As long as the multiple isotope sources have clearly different isotope ratio signatures, one can reliably apportion the contributions from these sources to a mixture. The Bayesian approach can incorporate priors such as rooting depth and other attributes that affect the relative contribution of different sources. In the cloud forest ecosystem, leaf water in trees can originate from soil water, fog, and rainfall, whereas the epiphytes we studied can access water only from the air via rainfall and fog and cannot tap into the host tree xylem water. Thus, by using Bayesian stable isotope mixing model and the isotope ratios ($\delta^2H$ and $\delta^{18}O$) for leaf water, soil water, fog, and rainfall, we could trace the proportional contributions of soil water, rainfall, and fog to foliar/leaf water (Wu et al., 2018). This model was implemented using the 'siarmcmcdirichletv4' function in R (*siar* package), an algorithm which uses the distinctive $\delta^2H$ and $\delta^{18}O$ isotope ratios to quantify the relative contributions (%) of fog water, rainfall, and soil water to leaf water in tree and the epiphyte communities in the 21 plots for both the wettest and driest months.

We performed a series of comparisons to understand the differences in functional traits between life forms, differences in meteorological variables between seasons, and the impact of fog on plant physiology. We used a Wilcoxon Rank Sum test to compare differences in CWMs of maximum photosynthesis rate, transpiration rate and stomatal conductance and density for the tree and the epiphyte communities in the wettest and driest months. Further, we compared four meteorological variables (mean rainfall, total solar radiation, mean air temperature, and mean relative atmosphere humidity), and the soil water content between the two seasons. We also used Wilcoxon Rank Sum to compare the differences in CWMs of $\delta^{13}C$ and leaf turgor loss point (TLP) between tree and epiphyte communities during the wettest and driest months. The objective of this analysis was to examine whether the tropical cloud forest ecosystems can maintaining a sufficient water supply in the driest month. Additionally, we determined whether there were any significant differences in CWMs of $\delta^{13}C$ and leaf turgor loss point between the tree and epiphyte communities.

# 3 Results

## 3.1 Variations in four meteorological variables and soil water content in the wettest and driest months

In July, the mean daily rainfall, total solar radiation, and mean atmospheric temperature were recorded 12.11 mm, 22.23 MJ $m^{-2}$, and 25.46°C. Conversely, in February, these values decrease to 2.07 mm, 8.64 MJ $m^{-2}$, and 17.49°C (Figures 1A–C; Supplementary Figure S1). both July and February exhibited mean relative atmospheric humidity levels exceeding 90%, with July registering a slightly higher value of 98.63% compared to 91.53% in February. However, this discrepancy did not reach statistical significance (Figure 1D, $P>0.05$). Overall, soil water content was also not significantly different between July and February (Figure 1E, $P>0.05$). Rainfall occurred every day in July,

whereas there were just five days of light rain in February (Figure 1F). No discernible differences in fog occurrence were observed between July and February, as fog was consistently present during early morning hours (before 9:00 h) and night-time (after 19:00 h) daily in both months (Figure 1G). In other words, the driest month is marked by much lower rainfall, attenuated total solar radiation, and lower temperature, while some key attributes like fog frequency, air humidity, and soil water content were not significantly lower in this month compared to the values in the wettest (summer) month (Figure 1).

## 3.2 Species compositions of the tree and the epiphyte communities

We studied a total of 60 tree and 30 vascular epiphyte species belonging to a total of 38 families across the 21 plots (Supplementary Table S2). The common tree species (relative abundance >5%) include *Distylium racemosum, Psychotria rubra, Syzygium buxifolium, Ervatamia officinalis*, and *Symplocos poilanei*, and the dominant vascular epiphyte species were *Eria thao, Coelogyne fimbriata, Liparis delicatula*, and *Bulbophyllum retusiusculum* (Supplementary Table S2). Our sampled epiphyte community could be considered as totally dependent on atmospheric water (rain, fog, dew) for their leaf water, as all the epiphyte species in the 21 plots were anchored on the tree stems but could not tap into the tree xylem water (Supplementary Table S2).

## 3.3 Variations of $\delta^2H$ and $\delta^{18}O$ compositions in soil water, rainfall, and fog

As evident from the scatter plot in Figure 2, there were notable variations in the $\delta^2H$ and $\delta^{18}O$ isotopic values across various water sources (including soil water, rainfall, fog, and leaf water), between the tree and epiphyte communities, and between the months of July and February (Figure 2). Notably, the leaf water isotope values were different between seasons for both trees and epiphytes (Figure 2 and $p<0.001$, Wilcoxon signed-rank tests, Supplementary Table S3). An important exception being $\delta^2H$ and $\delta^{18}O$ values of leaf water for the tree community, which were similar to the values for soil water in the wettest month (Figure 2, $p>0.05$, Wilcoxon signed-rank tests, Supplementary Table S3). Another exception was for leaf $\delta^2H$ and $\delta^{18}O$ values for the epiphyte community, which were similar to the values for rainfall in July and fog in February (Figure 2, $p>0.05$, Wilcoxon signed-rank tests, Supplementary Table S3).

## 3.4 The relative contributions of soil water, rainfall, and fog to foliar water resources

Given the high and persistent rainfall in the wettest (summer) month, we found that soil water contributed nearly 100% of the leaf water for tree communities and rainfall contributed nearly all the leaf water for epiphyte communities (Figure 3A). The contribution of fog water to foliar water uptake was insignificant for the tree or the epiphyte community in the wettest summer month (Figures 3A, B). The contribution of soil water to leaf water declined to 46.4% for the tree community despite no decrease in soil water content in the dry/winter month. Fog contributed 52.3% of leaf water for the tree community in the driest/winter month (Figures 3A, B). Furthermore, the contribution of soil water to leaf water for the epiphyte community was extremely limited and infrequent (<2%; Figures 3A, B). Thus, in summer month, leaf water in trees appears to be entirely due to soil water uptake and leaf water in epiphytes was obtained from rainfall. In the peak dry/winter season, nearly all (99.2%) the leaf water of the epiphyte community was sourced from fog, while the tree community used both soil water and fog water uptake almost equally to maintain leaf water supply (Figure 3A).

We computed correlations of isotope ratios of rain and fog water to soil water in the wet (July/summer) and dry (February/winter) seasons. Isotope ratios of rain and soil water showed a highly significant correlation during the wet season ($R^2 = 0.61$, $P<0.005$; Figures 3C–F), when heavy rainfall occurs on a daily basis (Figure 1), whereas no significant correlation was observed during February ($R^2 = 0.21$, $p>0.05$; Figures 3C–F), when the rainfall was nearly 40 times lower (Figure 1). On the other hand, isotope ratios of fog and soil water were significantly correlated in the dry/winter season (February; $R^2 = 0.45$, $p<0.05$; Figures 3D–F). In comparison, there was no significant correlation between isotope ratios of fog water and soil water in the summer month (July; $p>0.05$; Figures 3D–F). In other words, rainfall is the main water input for the soil water during wet summer months, while fog contributes significantly to soil water in the dry winter season.

## 3.5 Variations in photosynthesis rate, transpiration rate, stomatal conductance, stomatal density, $\delta^{13}C$, leaf turgor loss point and leaf hydraulic capacitance for the tree and epiphyte communities in the wettest and driest months

We observed reduced photosynthesis and transpiration rates for both plant communities in the driest (winter) month compared to the wettest (summer) month: CWMs of photosynthesis rate in February (2.9 μmol $cm^{-2}$ $s^{-1}$ and 4.9 μmol $cm^{-2}$ $s^{-1}$ for the epiphytes and the trees, respectively) were approximately one-third to one-half of same values in July (8.2 μmol $cm^{-2}$ $s^{-1}$ and 10.7 μmol $cm^{-2}$ $s^{-1}$, for the epiphytes and the trees, respectively; $p<0.001$, Wilcoxon signed-rank tests, Figures 4A, B). Similarly, CWMs of transpiration rates for both the plant communities in February (0.001 and 0.002 mol $m^{-2}$ $s^{-1}$ for the epiphytes and trees, respectively) were about one-third of those in July (0.003 and 0.0067 mol $m^{-2}$ $s^{-1}$, respectively; $p<0.001$, Wilcoxon signed-rank tests, Figures 4C, D).

We also found a reduced stomatal density and stomatal conductance for both the plant communities in the driest (winter) month compared to the wettest (summer) month: CWMs of stomatal density for both the plant communities in February (62 stomata $mm^{-2}$ of leaf and 316 total stomata $mm^{-2}$ of leaf for the epiphytes and the trees, respectively) were about one-third to one-half of those in July (203 stomata $mm^{-2}$ of leaf and 676 stomata $mm^{-2}$ of leaf, for the

10.3389/fpls.2024.1488163

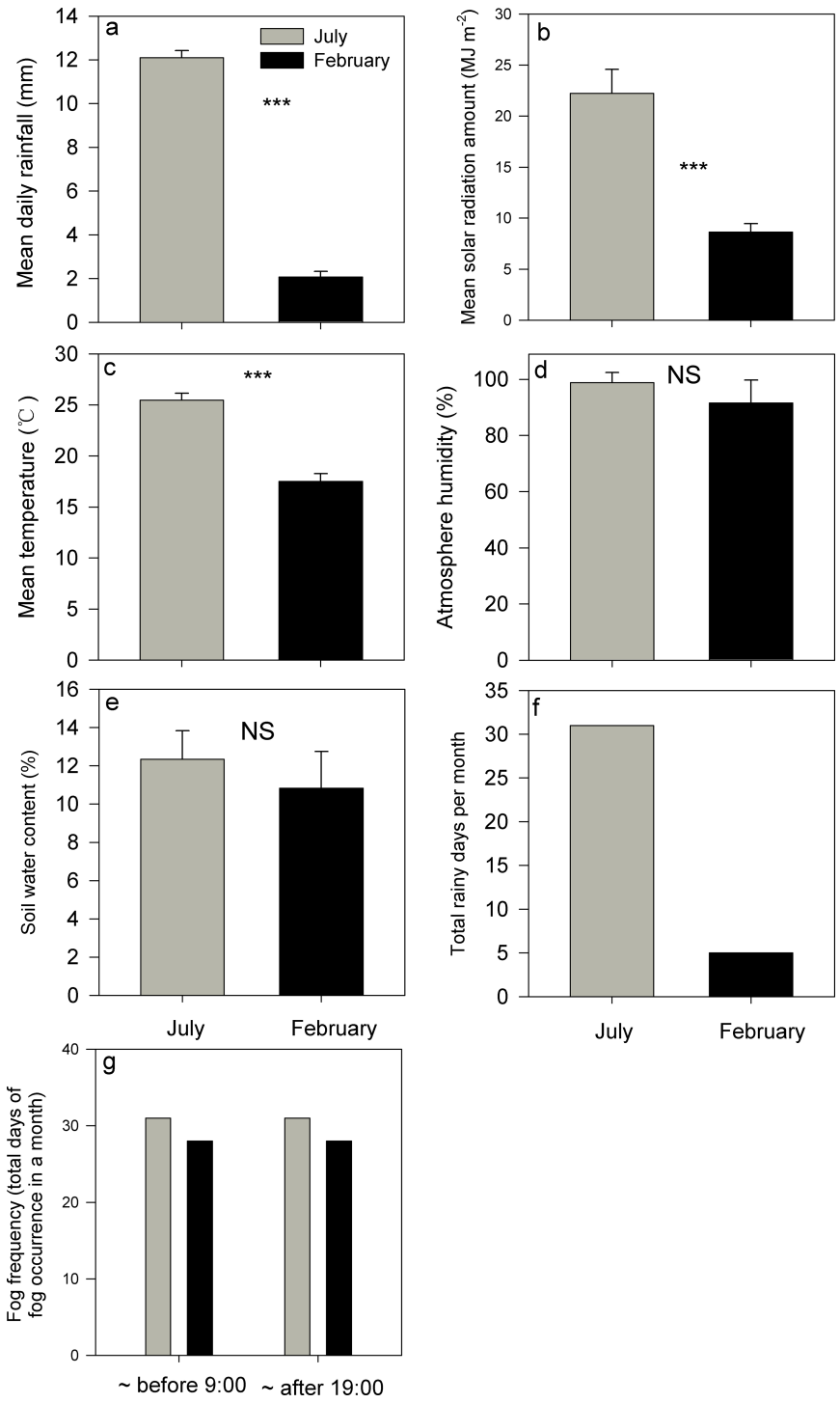


FIGURE 1
Evaluations of four below-canopy meteorological variables [**(A–D)**, mean daily rainfall, mean solar radiation amount, mean atmosphere temperature, and mean atmosphere humidity], **(E)**, soil water content, rainfall frequency [**(F)**, total rainfall days in a month] and fog frequency [**(G)**, the total days of fog occurrence in a month] in the July and February respectively. *** indicates significant differences at P<0.001, whereas NS indicates that the differences were not statistically significant (P>0.05) based on Wilcoxon signed-rank tests. Bars indicate the mean values; error bars denote standard errors.

epiphytes and the trees, respectively) (p<0.001, Wilcoxon signed-rank tests, Figures 4E, F). Similarly, CWMs of stomatal conductance in February (0.06 mmol $m^{-2}$ $s^{-1}$ and 0.1 mmol $m^{-2}$ $s^{-1}$ for the epiphytes and the trees, respectively) were approximately half of corresponding values in July (0.11 mmol $m^{-2}$ $s^{-1}$and 0.2 mmol $m^{-2}$ $s^{-1}$) for epiphytes and trees (p<0.001, Wilcoxon signed-rank tests, Figures 4G, H).

For the tree community, CWM values of $\delta^{13}C$ were -31.32 ‰ and -31.97 ‰ for July and February respectively, and CWMs for

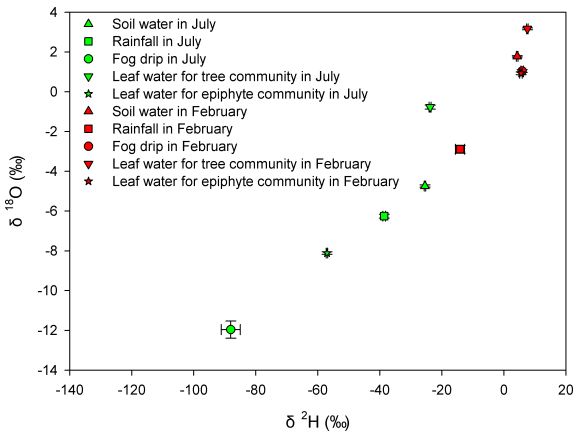


FIGURE 2
The dual isotope ($\delta^2H$ and $\delta^{18}O$) plot for soil water, rainfall, fog drip, and leaf water for tree and epiphyte communities in July and February respectively.

TLP were -1.07 MPa and -1.06 MPa for July and February, respectively. The CWM values for the tree community did not differ between July and February for $\delta^{13}C$ and TLP ($p>0.05$, Wilcoxon signed-rank tests, Figures 5A, B). In contrast, for the epiphyte community, the CWM values of $\delta^{13}C$ (-28.95 ‰ and -31.97 ‰ in July and February, respectively) and TLP (-1.06 MPa and -1.61 MPa in July and February, respectively) were all significantly more negative ($p<0.001$, Wilcoxon signed-rank tests, Figures 5A, B), in February compared to July (Figures 5A, B).

A significantly increased leaf hydraulic capacitance (C) was observed for both the plant communities in the driest (winter) month as compared to the wettest (summer) month: CWMs of C in February (4.77 mol $m^{-2}$ $MPa^{-1}$ and 4.19 mol $m^{-2}$ $MPa^{-1}$ for the epiphytes and the trees, respectively) were approximately 2.2-2.5 times the corresponding values in July (1.88 mol $m^{-2}$ $MPa^{-1}$ and 1.72 mol $m^{-2}$ $MPa^{-1}$, for the epiphytes and the trees, respectively; $p<0.001$, Wilcoxon signed-rank tests, Figure 5C).

# 4 Discussion

Our study quantifies the variation in the contribution of rain, fog, and soil waters to leaf water content in an old-growth tropical cloud forest ecosystem. The data presented herein illustrate the mechanism by which this tropical cloud forest plant community sustains an adequate water supply during contrasting periods, namely, the abundant rainfall of summer versus the scarcity of precipitation during winter. We infer that when there is heavy rainfall during a summer month (wet season), large quantities of this water are added to the soil. The trees take up the water from the soil using the standard hydrological process that depends on the well-known soil-plant-atmosphere continuum (SPAC) mechanism (Berry et al., 2019; Schreel and Steppe, 2020). Along with high recharge of soil water through precipitation, other climatic conditions of high temperature, high transpiration, ample solar radiation, enriched stomatal density, stomatal conductance and enhanced photosynthesis also favor this pathway of water movement during the summer. On the other hand, in a peak (dry) winter month, we see a significant downregulation of photosynthesis and transpiration, probably caused by low temperatures and reduced solar radiation/light availability, which could reduce (transpirational) water demand, and thus soil water uptake. Changes in climatic and physiological conditions, combined with factors such as leaf wetting, are known to favor foliar water uptake (FWU; Goldsmith et al., 2013; Eller et al., 2016; Oliveira et al., 2014; Schreel and Steppe, 2020). We hypothesize that during winter days, the water requirement of tissues at the top of the canopy would be greater than that in lower parts, especially in tall trees, and this could favor FWU to maintain leaf turgor. Low transpiration losses (reduced water needs for transpiration), combined with soil water uptake and foliar fog uptake could fulfil the leaf water requirements in the dry season.

## 4.1 The relative contributions of soil water, rainfall and fog to the tree community in the wettest and the driest months

Consistent with the previous observations (Scholl et al., 2011; Brinkmann et al., 2018; Schihada et al., 2018; Zhan et al., 2020), our results clearly show that soil water, rainfall, and fog have very different isotope ($\delta^2H$, and $\delta^{18}O$) concentrations with the changing intensity in rainfall between seasons. Therefore, the Bayesian stable isotope mixing model could apportion the relative contributions of fog, soil water, and rainfall to leaf water for tree and epiphyte communities. We found a clear contrast between the source of leaf water in July (wet summer) and February (peak of a dry winter season), with nearly all the leaf water in trees in the wettest summer month being taken up from soils. We also found that transpiration rates were significantly high in July (>3 times that in the winter month), and the soil water being continuously replenished by the daily rainfall (indeed, the isotope signals for soil water were highly related to those for rainfall). In this scenario, it is most likely that the trees rely on the SPAC pathway (instead of foliar uptake of rainfall). On the contrary, during dry winter weather, the temperatures are low, transpiration rates are much lower, and photosynthesis is also strongly reduced. In such scenario, we infer that soil water requirement (and thus its uptake) is reduced, and a FWU (of fog) could be facilitated by trees so that the leaf turgor remains maintained.

Pathways/strategies for FWU vary across different plant species (as reviewed extensively by Berry et al., 2019, and by Schreel and Steppe, 2020), and it is plausible that the net cumulative effect of FWU at the community/ecosystem levels are far reaching than initially thought, a hypothesis that our data indicates. Further research is warranted in this direction.

By examining our results in totality, we could infer that rain is a major contributor of soil water during summers and this water is taken up by the trees by adapting a traditional SPAC flow. But during dry winters, the trees might additionally adapt a strategy involving FWU of fog to replenish leaf water, while soil water uptake may still remain the primary source of transpired water. Further, there could be potentially confounded contributions of fog to soil water to some extent. It is possible that FWU might decouple

leaf-gas exchange from soil water availability (Schreel and Steppe, 2020), thus further complicating the quantification of the different sources to leaf water. It is also conceivable that trees might also tap deep underground water in the driest month, but some scholars have already reported that this tropical cloud forest has very shallow soil (less than 30 cm) and short root length (less than 30 cm) (Long et al., 2011c; Yang et al., 2021), therefore, this is very unlikely (Hildebrandt and Eltahir, 2007).

Surprisingly, we found that TLP and $\delta^{13}C$ do not differ between the peak wet and dry seasons even though TLP and $\delta^{13}C$ are good indicators of general water availability or water stress (Farrell et al., 2017; Acosta-Rangel et al., 2018). Also, these are highly associated

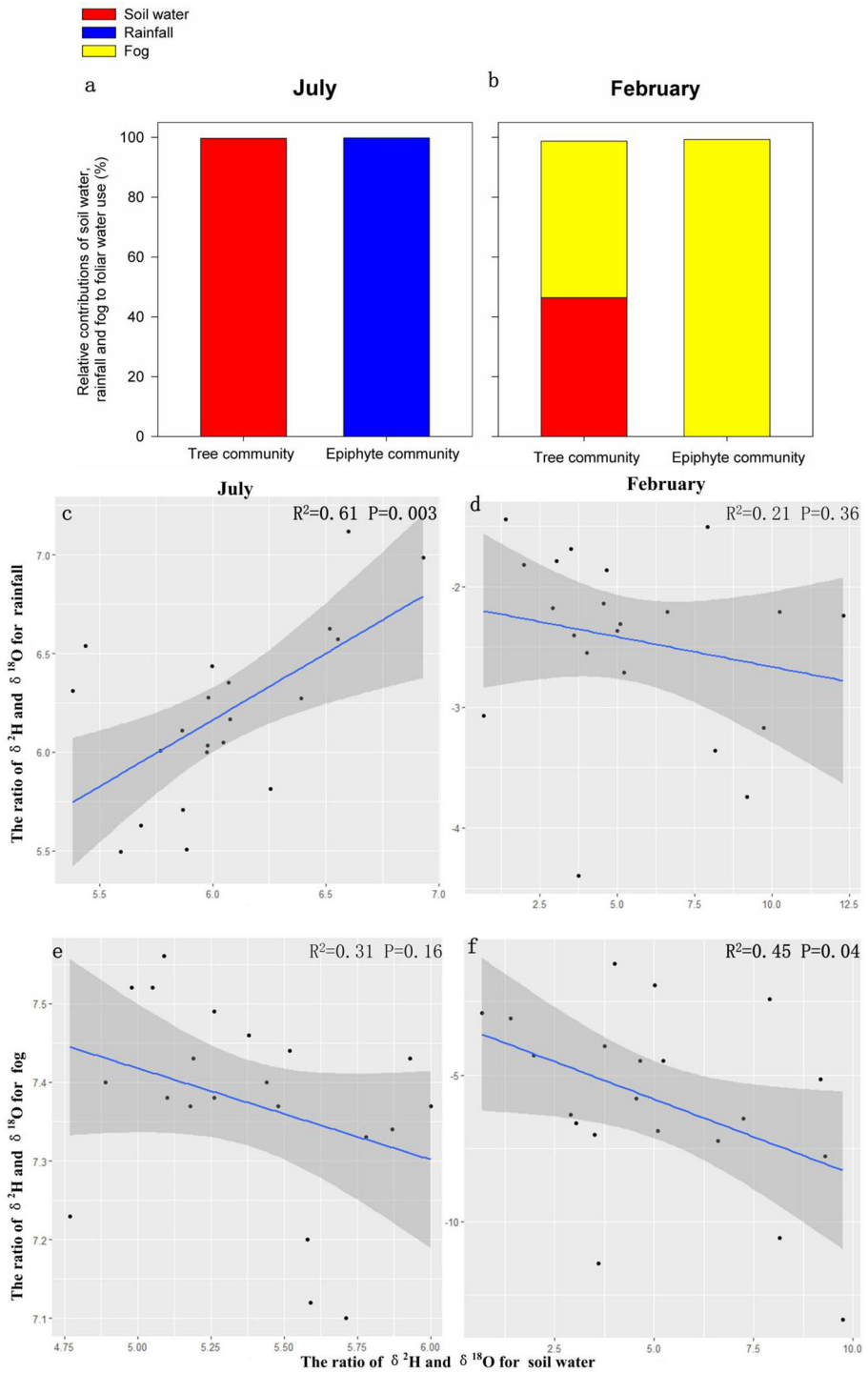


FIGURE 3
Relative contributions (%) of soil water, fog water, and rainfall towards foliar water resources for the tree and the epiphyte communities **(A, B)** and relationships among the ratio of $\delta^2H$ and $\delta^{18}O$ for soil water content, fog water and rainfall **(C)**. Contributions and correlations were assessed in July and February respectively **(D-F)**.

10.3389/fpls.2024.1488163

with photosynthesis rates, as they influence the ability of plants to maintain cell turgor under drought conditions and reflect long-term water-use efficiency (Nogueira et al., 2004; Bartlett et al., 2012). The stable TLP and $\delta^{13}C$ values for the tree community and comparable soil water content between July and February indicate adequate water availability to the trees in both seasons. Any difference in water availability between seasons may in part be compensated by differences in leaf hydraulic capacitance (Goldsmith et al., 2013). The observation that leaf hydraulic capacitance in the dry season was 2.5 times than in the wet season indicates modification of leaf traits for

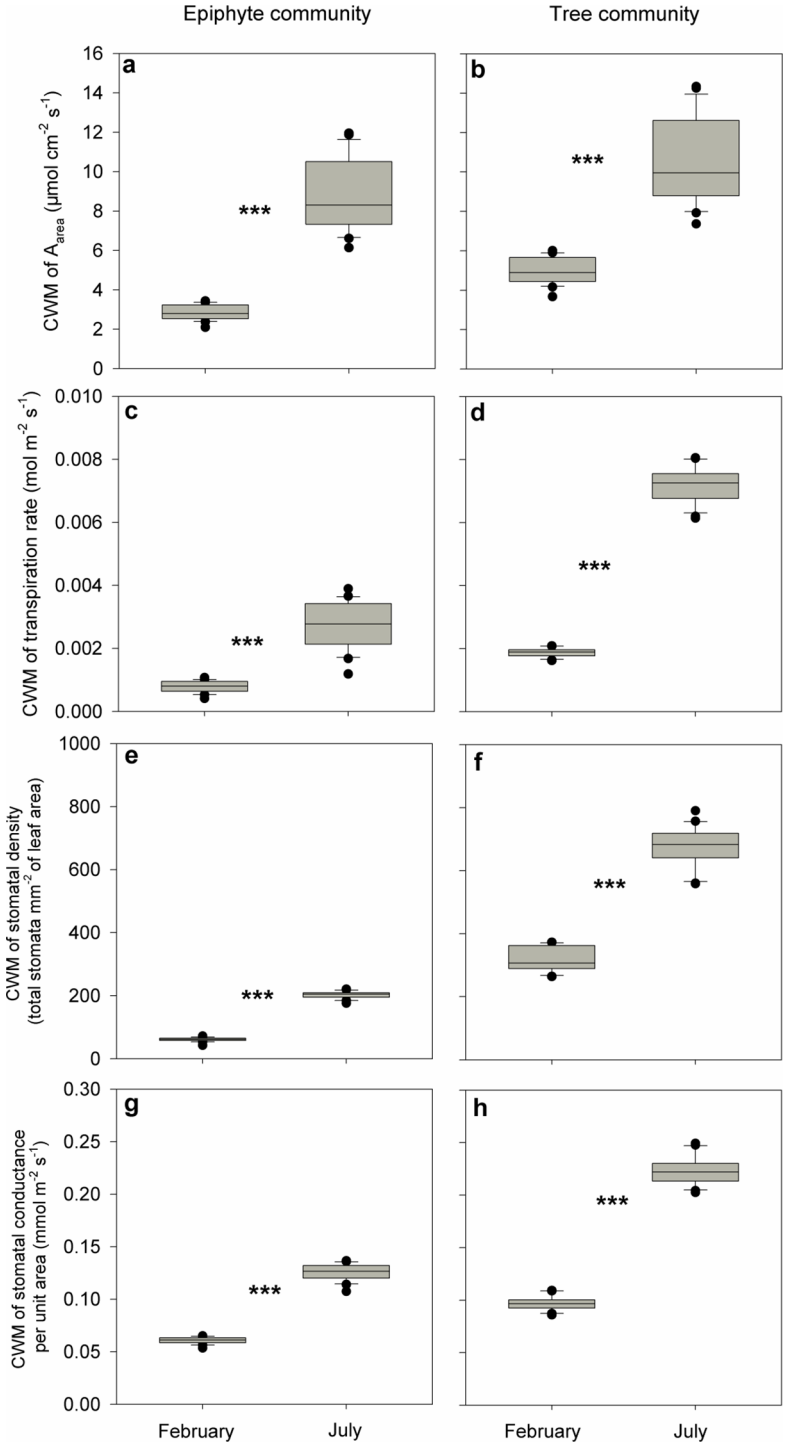


FIGURE 4
Differences in community-weighted mean values (CWM) of **(A, B)** maximum photosynthesis rate ($A_{area}$; μmol $cm^{-2}$ $s^{-1}$), **(C, D)** transpiration rate (mol $m^{-2}$ $s^{-1}$), **(E, F)** stomatal density (total stomata $mm^{-2}$ of leaf area), and **(G, H)** stomatal conductance (mmol $m^{-2}$ $s^{-1}$) and between July and February for all the tree and epiphyte species sampled. *** indicates significant differences at P<0.001 based on Wilcoxon signed-rank tests. Bars indicate the mean values and error bars denote standard errors.

better water retention in the dry season. All things considered, the low rainfall input in the driest month could have been compensated with increased leaf hydraulic capacitance, suppressed photosynthesis rate and transpiration, low temperature, high humidity, and possibly a fog input. These conditions appear sufficient to maintain adequate water availability for this cloud forest, at least for the tree and epiphyte communities (discussed below).

There remain some gaps in our understanding of water cycling for the tree community. We need further investigation to understand the mechanism of FWU for tree community in the dry season. We also need specific data on leaf temperature, leaf water potential, soil water potential, and sap flux measurements to understand the direction and flow rates of water movement. The effects of leaf phenology should also be considered in interpreting the effects of variation in solar radiation, temperature, and rainfall on this tropical cloud forest ecosystem. To assess fog inputs, we need data on fog intensity and duration, above-canopy observations of climatic variables, wind-driven rain and continuous soil water content measurements alongside sap-flow observations of transpiration (Holwerda et al., 2006; Schmid et al., 2011).

## 4.2 The relative contributions of rainfall, fog, and soil water to epiphyte community across the wettest and driest months

Given that the epiphyte community on Hainan Island derives its water fully relies on atmospheric sources, such as fog and rainfall, which could be directly absorbed by their leaves and roots, and could serve as leaf water resources in both the seasons (Gotsch et al., 2015, 2018; Wu et al., 2018). Although, fog and rainfall are equally frequent in July, rainfall can provide much higher water input than fog in the wet season. Moreover, photosynthesis rate and transpiration for epiphyte community are relatively high in July, which should favor root water absorption. In a peak dry winter period, fog still occurs every day, and the resultant leaf wetting should favor its uptake.

In February the epiphyte community has lower TLP than that in July. Further, the low temperature, and limited and infrequent rainfall in the driest month may cause epiphytes to lower their osmotic potential and to increase the uptake of fog water (Bartlett et al., 2014; Gotsch et al., 2015, 2018). Indeed, we observed that fog acted as a main source for leaf water for the epiphyte community in the driest month. We also found $\delta^{13}C$ in February was higher than that in July, indicating higher water use efficiency under lower water availability (Acosta-Rangel et al., 2018). However, water use efficiency could also be affected by the changes in the photosynthesis rates (Nogueira et al., 2004), and the suppressed photosynthetic rates in February could have counteracted the increase in water use efficiency to a certain extent.

## 4.3 Differences in community-level hydraulic responses between seasons and life-forms

Previous studies have documented reduced photosynthesis and transpiration rates during the arid winter season, but limited to a select few species (Burgess and Dawson, 2004; Goldsmith et al., 2013; Alvarado-Barrientos et al., 2014). We show that community level ecophysiological responses (such as reduced photosynthesis rate and transpiration, and fog utilization) vary with the quantity of rainfall and life-forms (trees *vs.* epiphytes). These findings therefore expand prior knowledge on the varied hydraulic responses as a function of water availability and life-forms from the species level (Oliveira et al., 2014; Gotsch et al., 2015; Wu et al., 2018; Berry et al., 2019) to the community level.

We also found that fog had different effects on tree and epiphyte communities. Given that the epiphytes here cannot tap into the host tree xylem water, foliar uptake of fog water could be critical to ensure leaf water supply for the epiphyte community when rainfall is critically low in the driest month. However, reduction in temperature and suppression of photosynthesis might result in lower leaf water use efficiency and higher leaf turgor loss point for the epiphyte community. Fog contributed to leaf water supply for tree community in the cold dry month, when rainfall was limited, and was therefore important for the tree community as well.

Detailed knowledge of the hydrological feedbacks of tropical forest ecosystems is only emerging (Staal et al., 2020), but there are

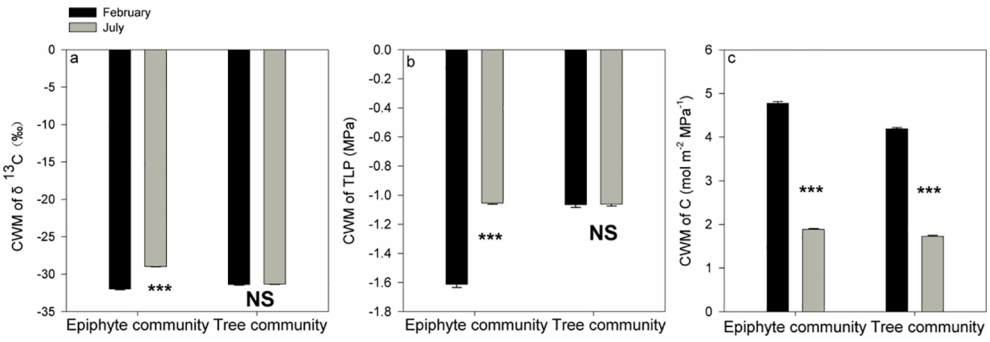


FIGURE 5
Differences in community-weighted mean values (CWM) of $\delta^{13}C$ **(A)**, the leaf turgor loss point [TLP, **(B)**], and leaf hydraulic capacitance **(C)** between July and February for all the tree and epiphyte species. *** indicates significant differences at P<0.001 and NS indicates that no significant differences were noticed (P>0.05) after Wilcoxon signed-rank tests were performed. Bars indicate the mean values; error bars denote standard errors.

predictions of dramatic losses (>50%) of tropical cloud forest cover due to climate warming and increase in cloud-base heights [predictions for 2052 by IPCC 5th assessment reports; as well as studies by (Los et al., 2019)]. Another independent simulation study predicts significant loss of tropical cloud forests in Mexico by 2080 if temperatures were to rise by >4°C and surrounding lowland forests were lost (Ponce-Reyes et al., 2012). We found that fog water made little contribution to tree and epiphyte communities in the wettest month, reasons of which need further investigations, which are out of scope of this report. However, in the peak of the dry season, fog appears to be important for water safety, hence the importance of maintaining cloud immersion for cloud forest persistence (Wu et al., 2018).

Forest ecosystems provide the most sustainable and highest quality freshwater (Vose, 2019) and soil water content appears to be the key determinant of freshwater supply from forest ecosystems (Neary et al., 2009). Sustaining this important ecohydrological process involves maintaining the structural and functional integrity of the cloud forest ecosystem and avoiding serious climatic changes (Zhan et al., 2020).

## 5 Conclusions

We conclude that both rainfall and aerial water such as fog, are important components of water budget safety for tree and epiphyte species in the cloud forests of Hainan Island. Further, reductions in solar radiation and atmospheric temperature, and a strong dry season results in two key ecosystem hydraulic responses: (i) reduced photosynthesis and transpiration, which might induce a large reduction in soil water uptake, and (ii) enhanced leaf hydraulic capacitance and foliar water uptake. These are the crucial factors that help tropical cloud forest plant species to operate within the hydraulic safety margins and maintain adequate water under seasonal changes in water supply. This ecohydrological relationship should be preserved in order to ensure freshwater supply across the wettest and driest months. The sensitivity of cloud-base heights to climate changes puts the cloud forest at great risk (Bruijnzeel et al., 2011; Sarmiento and Kooperman, 2019). Precise data on ecophysiological responses of tree and epiphyte species to changing climatic conditions are urgently needed to be incorporated in climate-vegetation models for tropical cloud forest.

## Data availability statement

The original contributions presented in the study are included in the article/Supplementary Material. Further inquiries can be directed to the corresponding authors.

## Author contributions

QY: Conceptualization, Formal analysis, Methodology, Writing – original draft, Writing – review & editing. ZZ: Writing – original draft. HZ: Writing – original draft, Writing – review & editing. HY: Writing – review & editing. SP: Writing – original draft. RJ: Writing – original draft.

## Funding

The author(s) declare financial support was received for the research, authorship, and/or publication of this article. This work was funded by the National Natural Science Foundation of China (U22A20449), the Hainan Provincial Natural Science Foundation of China (422CXTD508), the specific research fund of the Innovation Platform for Academicians of Hainan Province, Research project of Hainan academician innovation platform (YSPTZX202017), the Hainan Province Science and Technology Special Fund (ZDYF2022SHFZ320), and by a start-up funds from Lanzhou Universities.

## Conflict of interest

The authors declare that the research was conducted in the absence of any commercial or financial relationships that could be construed as a potential conflict of interest.

The handling editor XL declared a past co-authorship with the author HZ.

## Publisher's note



## Supplementary material

The Supplementary Material for this article can be found online at: https://www.frontiersin.org/articles/10.3389/fpls.2024.1488163/full#supplementary-material

## References

Acosta-Rangel, A., Ávila-Lovera, E., De Guzman, M. E., Torres, L., Haro, R., Arpaia, M. L., et al. (2018). Evaluation of leaf carbon isotopes and functional traits in avocado reveals water-use efficient cultivars. *Agric. Ecosyst. Environ.* 263, 60–66. doi: 10.1016/j.agee.2018.04.021

Aiba, S.-I., and Kitayama, K. (2002). Effects of the 1997-98 El Niño drought on rain forests of mount Kinabalu, Borneo. *J. Trop. Ecol.* 18, 215–230. Available at: http://www.jstor.org/stable/3068732.

Alan Pounds, J., Bustamante, M. R., Coloma, L. A., Consuegra, J. A., Fogden, M. P. L., Foster, P. N., et al. (2006). Widespread amphibian extinctions from epidemic disease driven by global warming. *Nature* 439, 161–167. doi: 10.1038/nature04246

Alvarado-Barrientos, M. S., Holwerda, F., Asbjornsen, H., Dawson, T. E., and Bruijnzeel, L. A. (2014). Suppression of transpiration due to cloud immersion in a seasonally dry Mexican weeping pine plantation. *Agric. For Meteorol.* 186, 12–25. doi: 10.1016/j.agrformet.2013.11.002

Anchukaitis, K. J., and Evans, M. N. (2010). Tropical cloud forest climate variability and the demise of the Monteverde golden toad. *PNAS* 107, 5036–5040. doi: 10.1073/pnas.0908572107

Anderegg, W. R. L., Berry, J. A., Smith, D. D., Sperry, J. S., Anderegg, L. D. L., and Field, C. B. (2012). The roles of hydraulic and carbon stress in a widespread climate-induced forest die-off. *PNAS* 109, 233–237. doi: 10.1073/pnas.1107891109

Bartlett, M. K., Scoffoni, C., and Sack, L. (2012). The determinants of leaf turgor loss point and prediction of drought tolerance of species and biomes: a global meta-analysis. *Ecol. Lett.* 15, 393–405. doi: 10.1111/j.1461-0248.2012.01751.x

Bartlett, M. K., Zhang, Y., Kreidler, N., Sun, S., Ardy, R., Cao, K., et al. (2014). Global analysis of plasticity in turgor loss point, a key drought tolerance trait. *Ecol. Lett.* 17, 1580–1590. doi: 10.1111/ele.12374

Benettin, P., Nehemy, M. F., Cernusak, L. A., Kahmen, A., and McDonnell, J. J. (2021). On the use of leaf water to determine plant water source: A proof of concept. *Hydrol Process.* 35, e14073. doi: 10.1002/hyp.14073

Berry, Z. C., Emery, N. C., Gotsch, S. G., and Goldsmith, G. R. (2019). Foliar water uptake: Processes, pathways, and integration into plant water budgets. *Plant Cell Environ.* 42, 410–423. doi: 10.1111/pce.13439

Berry, Z. C., Johnson, D. M., and Reinhardt, K. (2015). Vegetation-zonation patterns across a temperate mountain cloud forest ecotone are not explained by variation in hydraulic functioning or water relations. *Tree Physiol.* 35, 925–935. doi: 10.1093/treephys/tpv062

Binks, O., Mencuccini, M., Rowland, L., da Costa, A. C. L., de Carvalho, C. J. R., Bittencourt, P., et al. (2019). Foliar water uptake in Amazonian trees: Evidence and consequences. *Glob Chang Biol.* 25, 2678–2690. doi: 10.1111/gcb.14666

Brinkmann, N., Seeger, S., Weiler, M., Buchmann, N., Eugster, W., and Kahmen, A. (2018). Employing stable isotopes to determine the residence times of soil water and the temporal origin of water taken up by Fagus sylvatica and Picea abies in a temperate forest. *New Phytol.* 219, 1300–1313. doi: 10.1111/nph.15255

Brodribb, T. J., and Holbrook, N. M. (2003). Stomatal closure during leaf dehydration, correlation with other leaf physiological traits. *Plant Physiol.* 132, 2166–2173. doi: 10.1104/pp.103.023879

Bruijnzeel, L. A., Mulligan, M., and Scatena, F. N. (2011). Hydrometeorology of tropical montane cloud forests: emerging patterns. *Hydrol Process.* 25, 465–498. doi: 10.1002/hyp.7974

Bruijnzeel, L. A., Scatena, F. N., and Hamilton, L. S. (2010). *Tropical montane cloud forests: science for conservation and management* (Cambridge: Cambridge University Press).

Bruijnzeel, L. A., and Veneklaas, E. J. (1998). Climatic conditions and tropical montane forest productivity: the fog has not lifted yet. *Ecology* 79, 3–9. doi: 10.2307/176859

Burgess, S. S. O., and Dawson, T. E. (2004). The contribution of fog to the water relations of Sequoia sempervirens (D. Don): foliar uptake and prevention of dehydration. *Plant Cell Environ.* 27, 1023–1034. doi: 10.1111/j.1365-3040.2004.01207.x

Buzzard, V., Hulshof, C. M., Birt, T., Violle, C., and Enquist, B. J. (2016). Re-growing a tropical dry forest: functional plant trait composition and community assembly during succession. *Funct. Ecol.* 30, 1006–1013. doi: 10.1111/1365-2435.12579

Carins Murphy, M. R., Jordan, G. J., and Brodribb, T. J. (2012). Differential leaf expansion can enable hydraulic acclimation to sun and shade. *Plant Cell Environ.* 35, 1407–1418. doi: 10.1111/j.1365-3040.2012.02498.x

Cavallaro, A., Carbonell Silleta, L., Pereyra, D. A., Goldstein, G., Scholz, F. G., and Bucci, S. J. (2020). Foliar water uptake in arid ecosystems: seasonal variability and ecophysiological consequences. *Oecologia* 193, 337–348. doi: 10.1007/s00442-020-04673-1

Cernusak, L. A., Ubierna, N., Winter, K., Holtum, J. A. M., Marshall, J. D., and Farquhar, G. D. (2013). Environmental and physiological determinants of carbon isotope discrimination in terrestrial plants. *New Phytol.* 200, 950–965. doi: 10.1111/nph.12423

Cheng, Y., Zhang, H., Zang, R., Wang, X., Long, W., Wang, X., et al. (2020). The effects of soil phosphorus on aboveground biomass are mediated by functional diversity in a tropical cloud forest. *Plant Soil.* 449, 51–63. doi: 10.1007/s11104-020-04421-7

Choat, B., Brodribb, T. J., Brodersen, C. R., Duursma, R. A., López, R., and Medlyn, B. E. (2018). Triggers of tree mortality under drought. *Nature* 558, 531–539. doi: 10.1038/s41586-018-0240-x

Dawson, T. E., and Goldsmith, G. R. (2018). The value of wet leaves. *New Phytol.* 219, 1156–1169. doi: 10.1111/nph.15307

de Meyer, A. P. R. R., Ortega-Andrade, H. M., and Moulatlet, G. M. (2022). Assessing the conservation of eastern Ecuadorian cloud forests in climate change scenarios. *Perspect. Ecol. Conserv.* 20, 159–167. doi: 10.1016/j.pecon.2022.01.001

Diaz, H. F., Giambelluca, T. W., and Eischeid, J. K. (2011). Changes in the vertical profiles of mean temperature and humidity in the Hawaiian Islands. *Glob Planet Change.* 77, 21–25. doi: 10.1016/j.gloplacha.2011.02.007

Eller, C. B., Lima, A. L., and Oliveira, R. S. (2013). Foliar uptake of fog water and transport belowground alleviates drought effects in the cloud forest tree species, Drimys brasiliensis (Winteraceae). *New Phytol.* 199, 151–162. doi: 10.1111/nph.12248

Eller, C. B., Lima, A. L., and Oliveira, R. S. (2016). Cloud forest trees with higher foliar water uptake capacity and anisohydric behavior are more vulnerable to drought and climate change. *New Phytol.* 211, 489–501. doi: 10.1111/nph.13952

Ellsworth, P. Z., and Cousins, A. B. (2016). Carbon isotopes and water use efficiency in C4 plants. *Curr. Opin. Plant Biol.* 31, 155–161. doi: 10.1016/j.pbi.2016.04.006

Farquhar, G. D., Ehleringer, J. R., and Hubick, K. T. (1989). Carbon isotope discrimination and photosynthesis. *Annu. Rev. Plant Physiol. Plant Mol. Biol.* 40, 503–537. doi: 10.1146/annurev.pp.40.060189.002443

Farrell, C., Szota, C., and Arndt, S. K. (2017). Does the turgor loss point characterize drought response in dryland plants? *Plant Cell Environ.* 40, 1500–1511. doi: 10.1111/pce.12948

Fisher, M. C., and Garner, T. W. J. (2020). Chytrid fungi and global amphibian declines. *Nat. Rev. Microbiol.* 18, 332–343. doi: 10.1038/s41579-020-0335-x

Garnier, E., Cortez, J., Billès, G., Navas, M.-L., Roumet, C., Debussche, M., et al. (2004). Plant functional markers capture ecosystem properties during secondary succession. *Ecology* 85, 2630–2637. doi: 10.1890/03-0799

Gerlein-Safdi, C., Gauthier, P. P. G., and Caylor, K. K. (2018). Dew-induced transpiration suppression impacts the water and isotope balances of Colocasia leaves. *Oecologia* 187, 1041–1051. doi: 10.1007/s00442-018-4199-y

Giambelluca, T. W., and Gerold, G. (2011). "Hydrology and biogeochemistry of tropical montane cloud forests," in *Forest Hydrology and Biogeochemistry*. Eds. D. Levia, D. Carlyle-Moses and T. Tanaka (Ecological Studies, 216. Springer, Dordrecht). doi: 10.1007/978-94-007-1363-5_11

Goldsmith, G. R., Matzke, N. J., and Dawson, T. E. (2013). The incidence and implications of clouds for cloud forest plant water relations. *Eco. Lett.* 16, 307–314. doi: 10.1111/ele.12039

Gotsch, S. G., Asbjornsen, H., Holwerda, F., Goldsmith, G. R., Weintraub, A. E., and Dawson, T. E. (2014). Foggy days and dry nights determine crown-level water balance in a seasonal tropical montane cloud forest. *Plant Cell Environ.* 37, 261–272. doi: 10.1111/pce.12151

Gotsch, S. G., Dawson, T. E., and Dragulјić, D. (2018). Variation in the resilience of cloud forest vascular epiphytes to severe drought. *New Phytol.* 219, 900–913. doi: 10.1111/nph.14866

Gotsch, S. G., Nadkarni, N., Darby, A., Glunk, A., Dix, M., Davidson, K., et al. (2015). Life in the treetops: ecophysiological strategies of canopy epiphytes in a tropical montane cloud forest. *Ecol. Monogr.* 85, 393–412. doi: 10.1890/14-1076.1

Helmer, E. H., Gerson, E. A., Baggett, L. S., Bird, B. J., Ruzycki, T. S., and Voggesser, S. M. (2019). Neotropical cloud forests and páramo to contract and dry from declines in cloud immersion and frost. *PloS One* 14, e0213155. doi: 10.1371/journal.pone.0213155

Hildebrandt, A., and Eltahir, E. A. B. (2007). Ecohydrology of a seasonal cloud forest in Dhofar: 2. Role of clouds, soil type, and rooting depth in tree-grass competition. *Water Resour. Res.* 43, 19–26. doi: 10.1029/2006WR005262

Holwerda, F., Burkard, R., Eugster, W., Scatena, F. N., Meesters, A. G. C. A., and Bruijnzeel, L. A. (2006). Estimating fog deposition at a Puerto Rican elfin cloud forest site: comparison of the water budget and eddy covariance methods. *Hydrol Process.* 20, 2669–2692. doi: 10.1002/hyp.6065

Hu, J., and Riveros-Iregui, D. A. (2016). Life in the clouds: are tropical montane cloud forests responding to changes in climate? *Oecologia* 180, 1061–1073. doi: 10.1007/s00442-015-3533-x

Jarvis, A., and Mulligan, M. (2011). The climate of cloud forests. *Hydrol Process* 25, 327–343. doi: 10.1002/hyp.7847

Johnson, D. M., and Smith, W. K. (2008). Cloud immersion alters microclimate, photosynthesis and water relations in Rhododendron catawbiense and Abies fraseri seedlings in the southern Appalachian Mountains, USA. *Tree Physiol.* 28, 385–392. doi: 10.1093/treephys/28.3.385

Karger, D. N., Kessler, M., Lehnert, M., and Jetz, W. (2021). Limited protection and ongoing loss of tropical cloud forest biodiversity and ecosystems worldwide. *Nat. Ecol. Evol.* 5, 854–862. doi: 10.1038/s41559-021-01450-y

Krishnaswamy, J., John, R., and Joseph, S. (2014). Consistent response of vegetation dynamics to recent climate change in tropical mountain regions. *Glob Chang Biol.* 20, 203–215. doi: 10.1111/gcb.12362

Laughlin, D. C. (2014). Applying trait-based models to achieve functional targets for theory-driven ecological restoration. *Ecol. Lett.* 17, 771–784. doi: 10.1111/ele.12288

Lavorel, S., and Garnier, E. (2002). Predicting changes in community composition and ecosystem functioning from plant traits: revisiting the Holy Grail. *Funct. Ecol.* 16, 545–556. doi: 10.1046/j.1365-2435.2002.00664.x

Li, H.-J., Lo, M.-H., Juang, J.-Y., Wang, J., and Huang, C.-y. (2022). Assessment of spatiotemporal dynamics of diurnal fog occurrence in subtropical montane cloud forests. *Agric. For Meteorol.* 317, 108899. doi: 10.1016/j.agrformet.2022.108899

Limm, E. B., Simonin, K. A., Bothman, A. G., and Dawson, T. E. (2009). Foliar water uptake: a common water acquisition strategy for plants of the redwood forest. *Oecologia* 161, 449–459. doi: 10.1007/s00442-009-1400-3

Liu, W. J., Zhang, Y. P., Li, H. M., and Liu, Y. H. (2005). Fog drip and its relation to groundwater in the tropical seasonal rain forest of Xishuangbanna, Southwest China: a preliminary study. *Water Res.* 39, 787–794. doi: 10.1016/j.watres.2004.12.002

Long, W.-X., Ding, Y., Zang, R., Yang, M., and Chen, S.-W. (2011c). Environmental characteristics of tropical cloud forests in the rainy season in Bawangling National Nature Reserve on Hainan Island, South China. *Chin. J. Plant Ecol.* 35, 13–17. doi: 10.3724/SP.J.1258.2011.00137

Long, W., Schamp, B. S., Zang, R., Ding, Y., Huang, Y., and Xiang, Y. (2015). Community assembly in a tropical cloud forest related to specific leaf area and maximum species height. *J. Veg. Sci.* 26, 513–523. doi: 10.1111/jvs.12256

Long, W., Zang, R., and Ding, Y. (2011a). Air temperature and soil phosphorus availability correlate with trait differences between two types of tropical cloud forests. *Flora* 206, 896–903. doi: 10.1016/j.flora.2011.05.007

Long, W., Zang, R., Schamp, B. S., and Ding, Y. (2011b). Within- and among-species variation in specific leaf area drive community assembly in a tropical cloud forest. *Oecologia* 167, 1103–1113. doi: 10.1007/s00442-011-2050-9

Los, S. O., Street-Perrott, F. A., Loader, N. J., and Froyd, C. A. (2021). Detection of signals linked to climate change, land-cover change and climate oscillators in Tropical Montane Cloud Forests. *Remote Sens Environ.* 260, 112431. doi: 10.1016/j.rse.2021.112431

Los, S. O., Street-Perrott, F. A., Loader, N. J., Froyd, C. A., Cuní-Sanchez, A., and Marchant, R. A. (2019). Sensitivity of a tropical montane cloud forest to climate change, present, past and future: Mt. *Marsabit N. Kenya. Quat Sci. Rev.* 218, 34–48. doi: 10.1016/j.quascirev.2019.06.016

Muñoz-Villers, L. E., and McDonnell, J. J. (2013). Land use change effects on runoff generation in a humid tropical montane cloud forest region. *Hydrol Earth Syst. Sci.* 17, 3543–3560. doi: 10.5194/hess-17-3543-2013

Nadkarni, N. M., and Solano, R. (2002). Potential effects of climate change on canopy communities in a tropical cloud forest: an experimental approach. *Oecologia* 131, 580–586. doi: 10.1007/s00442-002-0899-3

Nair, U. S., Asefi, S., Welch, R. M., Ray, D. K., Lawton, R. O., Manoharan, V. S., et al. (2008). Biogeography of tropical montane cloud forests. Part II: mapping of orographic cloud immersion. *J. Appl. Meteorol Climatol.* 47, 2183–2197. doi: 10.1175/2007JAMC1819.1

Neary, D. G., Ice, G. G., and Jackson, C. R. (2009). Linkages between forest soils and water quality and quantity. *For. Ecol. Manage.* 258, 2269–2281. doi: 10.1016/j.foreco.2009.05.027

Nogueira, A., Martinez, C. A., Ferreira, L. L., and Prado, C. H. B. A. (2004). Photosynthesis and water use efficiency in twenty tropical tree species of differing succession status in a Brazilian reforestation. *Photosynthetica* 42, 351–356. doi: 10.1023/B:PHOT.0000046152.05364.77

Oliveira, R. S., Eller, C. B., Bittencourt, P. R. L., and Mulligan, M. (2014). The hydroclimatic and ecophysiological basis of cloud forest distributions under current and projected climates. *Ann. Bot.* 113, 909–920. doi: 10.1093/aob/mcu060

Parnell, A. C., Phillips, D. L., Bearhop, S., Semmens, B. X., Ward, E. J., Moore, J. W., et al. (2013). Bayesian stable isotope mixing models. *Environmetrics* 24, 387–399. doi: 10.1002/env.2221

Ponce-Reyes, R., Reynoso-Rosales, V.-H., Watson, J. E. M., VanDerWal, J., Fuller, R. A., Pressey, R. L., et al. (2012). Vulnerability of cloud forest reserves in Mexico to climate change. *Nat. Clim Change* 2, 448–452. doi: 10.1038/nclimate1453

Pounds, J. A., Fogden, M. P. L., and Campbell, J. H. (1999). Biological response to climate change on a tropical mountain. *Nature* 398, 611–615. doi: 10.1038/19297

Ray, D. K., Nair, U. S., Lawton, R. O., Welch, R. M., and Pielke, R. A. Sr. (2006). Impact of land use on Costa Rican tropical montane cloud forests: Sensitivity of orographic cloud formation to deforestation in the plains. *J. Geophys. Res. Atmos.* 111. doi: 10.1029/2005JD006096

Ritter, A., Regalado, C. M., and Aschan, G. (2009). Fog reduces transpiration in tree species of the Canarian relict heath-laurel cloud forest (Garajonay National Park, Spain). *Tree Physiol.* 29, 517–528. doi: 10.1093/treephys/tpn043

Sack, L., Cowan, P. D., Jaikumar, N., and Holbrook, N. M. (2003). The 'hydrology' of leaves: co-ordination of structure and function in temperate woody species. *Plant Cell Environ.* 26, 1343–1356. doi: 10.1046/j.0016-8025.2003.01058.x

Sanford, W. W. (1968). Distribution of epiphytic orchids in semi-deciduous tropical forest in southern Nigeria. *J. Ecol.* 56, 697–705. doi: 10.2307/2258101

Sarmiento, F. O., and Kooperman, G. J. (2019). A socio-hydrological perspective on recent and future precipitation changes over tropical montane cloud forests in the Andes. *Front. Earth Sci.* 7. doi: 10.3389/feart.2019.00324

Scatena, F. N., Bruijnzeel, L. A., Bubb, P., and Das, S. (2011). "Setting the stage," in *Tropical Montane Cloud Forests: Science for Conservation and Management*. Eds. F. N. Scatena, L. A. Bruijnzeel and L. S. Hamilton (London: Cambridge University Press), 38–63. doi: 10.1017/CBO9780511778384.003

Schihada, H., Vandenabeele, S., Zabel, U., Frank, M., Lohse, M. J., and Maiellaro, I. (2018). A universal bioluminescence resonance energy transfer sensor design enables high-sensitivity screening of GPCR activation dynamics. *Commun. Biol.* 1, 105. doi: 10.1038/s42003-018-0072-0

Schmid, S., Burkard, R., Frumau, K. F. A., Tobón, C., Bruijnzeel, L. A., Siegwolf, R., et al. (2011). Using eddy covariance and stable isotope mass balance techniques to estimate fog water contributions to a Costa Rican cloud forest during the dry season. *Hydrol Process.* 25, 429–437. doi: 10.1002/hyp.7739

Scholl, M., Eugster, W., and Burkard, R. (2011). Understanding the role of fog in forest hydrology: stable isotopes as tools for determining input and partitioning of cloud water in montane forests. *Hydrol Process.* 25, 353–366. doi: 10.1002/hyp.7762

Schreel, J. D. M., and Steppe, K. (2020). Foliar water uptake in trees: negligible or necessary? *Trends Plant Sci.* 25, 590–603. doi: 10.1016/j.tplants.2020.01.003

Schultz, N. M., Griffis, T. J., Lee, X., and Baker, J. M. (2011). Identification and correction of spectral contamination in $^{2}H/^{1}H$ and $^{18}O/^{16}O$ measured in leaf, stem, and soil water. *Rapid Commun. Mass Spectrom.* 25, 3360–3368. doi: 10.1002/rcm.5236

Staal, A., Fetzer, I., Wang-Erlandsson, L., Bosmans, J. H. C., Dekker, S. C., van Nes, E. H., et al. (2020). Hysteresis of tropical forests in the 21st century. *Nat. Commun.* 11, 4978. doi: 10.1038/s41467-020-18728-7

Still, C. J., Foster, P. N., and Schneider, S. H. (1999). Simulating the effects of climate change on tropical montane cloud forests. *Nature* 398, 608–610. doi: 10.1038/19293

Suding, K. N., Lavorel, S., Chapin, F. S., Cornelissen, J. H. C., Díaz, S., Garnier, E., et al. (2008). Scaling environmental change through the community level: a trait-based response-and-effect framework for plants. *Glob Chang Biol.* 14, 1125–1140. doi: 10.1111/j.1365-2486.2008.01557.x

Vose, J. M. (2019). Forest and water in the 21st century: A global perspective. *J. For.* 117, 80–85. doi: 10.1093/jofore/fvy054

Wang, J., Lu, N., and Fu, B. (2019). Inter-comparison of stable isotope mixing models for determining plant water source partitioning. *Sci. Total Environ.* 666, 685–693. doi: 10.1016/j.scitotenv.2019.02.262

Wang, Y.-Q., Ni, M.-Y., Zeng, W.-H., Huang, D.-L., Xiang, W., He, P.-C., et al. (2021). Co-ordination between leaf biomechanical resistance and hydraulic safety across 30 sub-tropical woody species. *Ann. Bot.* 128, 183–191. doi: 10.1093/aob/mcab055

Weathers, K. C., Ponette-González, A. G., and Dawson, T. E. (2020). Medium, vector, and connector: fog and the maintenance of ecosystems. *Ecosystems* 23, 217–229. doi: 10.1007/s10021-019-00388-4

Werner, W. L. (1988). Canopy dieback in the upper montane rain forests of Sri Lanka. *GeoJournal* 17, 245–248. doi: 10.1007/BF02432929

Wu, F., Qi, Y., Yu, H., Tian, S., Hou, Z., and Huang, F. (2016). Vanadium isotope measurement by MC-ICP-MS. *Chem. Geol.* 421, 17–25. doi: 10.1016/j.chemgeo.2015.11.027

Wu, Y., Song, L., Liu, W., Liu, W., Li, S., Fu, P., et al. (2018). Fog water is important in maintaining the water budgets of vascular epiphytes in an Asian tropical karst forests during the dry season. *Forests* 9, 260. doi: 10.3390/f9050260

Wyka, T. P., Oleksyn, J., Żytkowiak, R., Karolewski, P., Jagodziński, A. M., and Reich, P. B. (2012). Responses of leaf structure and photosynthetic properties to intra-canopy light gradients: a common garden test with four broadleaf deciduous angiosperm and seven evergreen conifer tree species. *Oecologia* 170, 11–24. doi: 10.1007/s00442-012-2279-y

Yang, Y., Xiao, C., Wu, X., Long, W., Feng, G., and Liu, G. (2021). Differing trade-off patterns of tree vegetative organs in a tropical cloud forest. *Front. Plant Sci.* 12. doi: 10.3389/fpls.2021.680379

Zhan, L., Chen, J., Zhang, C., Wang, T., Xin, P., and Li, L. (2020). Fog interception maintains a major waterfall landscape in southwest China revealed by isotopic signatures. *Water Resour. Res.* 56, e2019WR025628. doi: 10.1029/2019WR025628

Zhang, H., Chen, H. Y. H., Lian, J., John, R., Ronghua, L., Liu, H., et al. (2018). Using functional trait diversity patterns to disentangle the scale-dependent ecological processes in a subtropical forest. *Funct. Ecol.* 32, 1379–1389. doi: 10.1111/1365-2435.13079

Zhao, L., Wang, L., Cernusak, L. A., Liu, X., Xiao, H., Zhou, M., et al. (2016). Significant difference in hydrogen isotope composition between xylem and tissue water in *Populus euphratica*. *Plant Cell Environ.* 39, 1848–1857. doi: 10.1111/pce.12753

Zotz, G., and Bader, M. Y. (2009). "Epiphytic plants in a changing world-global: change effects on vascular and non-vascular epiphytes," in *Progress in Botany*. Eds. U. Lüttge, W. Beyschlag, B. Büdel and D. Francis (Berlin: Springer Berlin Heidelberg), 147–170. doi: 10.1007/978-3-540-68421-3_7

frontiers | Frontiers in Plant Science

TYPE Original Research
PUBLISHED 28 October 2024
DOI 10.3389/fpls.2024.1468816



OPEN ACCESS

EDITED BY
Xiang Liu,
Lanzhou University, China

REVIEWED BY
Yuping Hou,
Ludong University, China
Ming-Chao Liu,
Shenyang Agricultural University, China

*CORRESPONDENCE
Zhi-Cong Dai
daizhicong@163.com
Shan-Shan Qi
qishanshan1986120@163.com
Shafaqat Ali
shafaqataligill@yahoo.com
Dao-Lin Du
ddl@ujs.edu.cn

RECEIVED 22 July 2024
ACCEPTED 30 September 2024
PUBLISHED 28 October 2024

CITATION
Anas M, Khan IU, Alomrani SO, Nawaz M, Huang Z-Y, Alshehri MA, Al-Ghanim KA, Qi S-S, Li J, Dai Z-C, Ali S and Du D-L (2024) Evaluating *Sorghum bicolor* resistance to *Solidago canadensis* invasion under different nitrogen scenarios.
*Front. Plant Sci.* 15:1468816.
doi: 10.3389/fpls.2024.1468816



# Evaluating *Sorghum bicolor* resistance to *Solidago canadensis* invasion under different nitrogen scenarios

Muhammad Anas[1,2], Irfan Ullah Khan[2,3], Sarah Owdah Alomrani[4], Mohsin Nawaz[2], Zhi-Yun Huang[2], Mohammed Ali Alshehri[5], Khalid A. Al-Ghanim[6], Shan-Shan Qi[7]*, Jian Li[2], Zhi-Cong Dai[1,2,8]*, Shafaqat Ali[9,10]* and Dao-Lin Du[11]*

[1]School of Emergency Management, Jiangsu University, Zhenjiang, China, [2]Institute of Environment and Ecology, School of the Environment and Safety Engineering, Jiangsu University, Zhenjiang, China, [3]State Key Laboratory of Cotton Biology, Institute of Cotton Research, Chinese Academy of Agricultural Sciences, Anyang, China, [4]Department of Biology, College of Science and Arts, Najran University, Najran, Saudi Arabia, [5]Department of Biology, Faculty of Science, University of Tabuk, Tabuk, Saudi Arabia, [6]Department of Zoology, College of Science, King Saud University, Riyadh, Saudi Arabia, [7]School of Agricultural Engineering, Jiangsu University, Zhenjiang, China, [8]Jiangsu Collaborative Innovation Center of Technology and Material of Water Treatment, Suzhou University of Science and Technology, Suzhou, Jiangsu, China, [9]Department of Environmental Sciences, Government College University, Faisalabad, Pakistan, [10]Department of Biological Sciences and Technology, China Medical University, Taichung, Taiwan, [11]Jingjiang College, Jiangsu University, Zhenjiang, China

Ecosystem exposure to a biological invasion such as plant invasion could contribute to the extinction of native species and loss of productivity and ecosystem balance. *Solidago canadensis* (*S. canadensis*) is a highly invasive species that has formed monocultures in China, Europe, Asia, Australia, and New Zealand. It was designated as a notorious invasive species by the Chinese government. It has adversely affected the agroecosystem's ability to germinate various plant seeds, including wheat, lettuce, and pepper, which could lead to food insecurity. This study was conducted to control the invasive species *S. canadensis* by utilizing a competitive species, *Sorghum bicolor* (*S. bicolor*) as a cover plant. *Sorghum bicolor* exudes allelochemicals such as sorgoleone from its roots which suppress the photosystem II activity of nearby plants. The synthesis of sorgoleone depends on a supply of nitrogen. The present study involved the cultivation of *S. bicolor* alongside the invasive species *S. canadensis*, with three different invasion levels (high, medium, and low) and three different nitrogen forms (ammonical, nitrate, and combined ammonical and nitrate nitrogen) applied as a modified Hogland solution. *S. bicolor* expressed higher performance over the invasive species under ammonical and combined nitrogen forms under low and medium invasion levels. Furthermore, even at greater levels of invasion, *S. bicolor* was not suppressed by *S. canadensis*. However, the plant height and dry biomass of *S. bicolor* were significantly high across both nitrogen forms. Leaf area, $CO_2$ uptake, and photosystem II activity of *S. canadensis* were unable to sustain its growth under the low invasion condition. The plant biomass of *S. canadensis* was suppressed by up to 80% and the relative dominance index of *S. bicolor* was 5.22 over *S. canadensis*. There was a strong correlation between $CO_2$ uptake, leaf area, and plant biomass. Principal

component analysis showed that the first four components had a total variance of 96.89%, with principal component 1 (PC1) having the highest eigenvalue at 18.65. These promising findings suggested that *S. bicolor*, whose high intensity might be employed to control the invasion process for environmental safety, might be able to recover the barren ground that *S. canadensis* had invaded.

KEYWORDS

**ecosystem, *S. bicolor*, *S. canadensis*, nitrogen, invasion**

## 1 Introduction

Plant invasion is a major threat to biodiversity, ecosystem balance, and its management. The agroecosystem, which makes up over 40% of the world's land surface, is extremely vulnerable to invasion (Frost et al., 2019; Batish et al., 2022; Allen et al., 2022). *Solidago canadensis*, native to North America, is the most important and economically significant invasive species in the agroecosystems of Central and Western Europe, Asia, Australia, New Zealand, and China (Anastasiu and Negrean, 2005; Szabó et al., 2020; Qi et al., 2022; Tian et al., 2023). Strong propagation strategies, such as producing a large number of seeds and growing from rhizomes, allow it to dominate an invaded ecosystem (Gazoulis et al., 2022; Khan et al., 2023a). The invasion of *S. canadensis* has put several native species in danger of going extinct (Wang et al., 2021; Gazoulis et al., 2022). It has decreased agricultural productivity, biodiversity, and medicinal plants, and the Chinese government has declared it an exotic invasive species (Wang et al., 2017; Mitryasova and Koszelnic, 2021; Kato-Noguchi, 2023). Thus, sustainable and environmentally friendly management of ecosystems is crucial.

Potential native resources may be sustainable and eco-friendly ways to manage an invaded ecosystem. *Sorghum bicolor* is a strong domesticated plant that can re-sprout and vigorously grow and is mainly grown for its grain and fodder (Venkateswaran et al., 2019). It uptakes nutrients efficiently and grows in diversified soil types such as salt-affected, drought-prone, and water-logged soils (Calone et al., 2020; Chen et al., 2020; Zhang et al., 2023). Crop rotation, root exudates, and water extracts of *S. bicolor* have all been shown to be effective weed control measures in agroecosystems (Zucareli et al., 2019). Because of its effective nutrient intake, allelopathic nature, ability to cover soil, and rapid growth rate during the invasive species' vegetative growth cycle, it can inhibit *S. canadensis* (Werner et al., 1980; Afzal et al., 2023). It releases hydrophobic and hydrophilic allelochemicals. Sorgoleone is a unique hydrophobic allelochemical, a benzoquinone (2-hydroxy-5-methoxy-1,4-benzoquinone), that is secreted by root hairs, is present in the soil, and exhibits potent phytotoxicity towards a variety of nearby plants (Głąb et al., 2017; Besançon et al., 2020). It is produced throughout the growth period of *S. bicolor*. It inhibits several physiological functions, including the uptake of $CO_2$, the transport of electrons in mitochondria, the activity of p-hydroxyphenylpyruvate dioxygenase (HPPD) and $H^+$-ATPase in roots, and the uptake of water (Einhellig and Souza, 1992; Weidenhamer, 2005).

Plant-to-plant interaction is highly dependent on plant intensity. Many invasive species have been reported to exert high competition with native species and suppress them. For example, *Erodium cicutarium* invaded a granivore site and dominated all plots (Valone and Weyers, 2019). When invading species become more intense, they release more allelochemicals, which increases competition. *S. canadensis* suppresses *Lactuca sativa* and its suppression depends on the invasion intensity (Yu et al., 2022). Effective plant intensity of *S. bicolor* is important for successful competitiveness between invasive species and *S. bicolor*. It has not been tested against invasive species. However, it was studied to identify the effect of plant intensity on growth, forage, and grain yield and it was concluded that 88,888 plants $ha^{-1}$ was the best intensity to plant at in Ethiopia (Bayu et al., 2005). Yan et al. (2023) reported that a change in plant intensity from 83,000 to 166,000 plants $ha^{-1}$ increased yield by 188 kg $ha^{-1}$ per 10,000 plants.

The root and shoot growth of *S. bicolor* is highly responsive to the form of nitrogen (N). Plants uptake N either in nitrate or ammonical forms (Smil, 1999; Crawford and Glass, 1998). These two forms of N in the soil are interconnected with each other through the ammonification and nitrification processes (Anas et al., 2020). Plants show different adaptations for the uptake of ammonical and nitrate nitrogen forms (Fisher et al., 2010; Du et al., 2020; Zhao et al., 2023). The production of sorgoleone is prolonged by root growth, proton gradient, and H-ATPase under ammonical nitrogen (Di et al., 2018; Afzal et al., 2023). In previous studies, the relation of sorghum root exudates is dependent on the available N form. Afzal et al. (2020) reported that the application of the ammonical form of N improved the production of root exudates. Ammonical nitrogen is biologically nitrified, releasing $H^+$ ions and lowering the pH in the rhizosphere soil. Plasma membrane $H^+$-ATPase activity increases in the presence of $NH_4^+$ (Zeng et al., 2016). Zhao et al. (2023) reported that sorgoleone had a negative charge which was exuded in the rhizosphere due to the activity of plasma membrane $H^+$-ATPase. Sorgoleon production and $H^+$-ATPase activity increase under a rhizosphere ammonium concentration of ≤ 0.1 mM (Zeng et al., 2016).

The environment and human health are harmed by the previous ineffective and unsustainable methods of controlling *S. canadensis*, which included burning, eradication, and the use of herbicides (Narwal and Haouala, 2013; Mohd Ghazi et al., 2023). The purpose of this study was to determine the influence of *S. bicolor* on invasive species under different invasion gradients and different nitrogen conditions. We wanted to evaluate to what extent the changes induced by *S. bicolor* are systematic and predictable, and to what extent they are manageable under controlled conditions. In order to investigate how the changes would affect ecosystem services, the productivity of potentially degraded land restored by covering the invasive species and the performance of *S. bicolor w*ere assessed in an outdoor experiment. It was hypothesized that *S. bicolor* would (a) decrease the growth of invasive *S. canadensis* aboveground and belowground, (b) dominate the invasive plant species by changing their physiological properties, and (c) reduce the dominance of invasive *S. canadensis* compared with sorghum grown under different nitrogen conditions.

# 2 Materials and methods

## 2.1 Experimental site and plant culture

The study was carried out in an outdoor experiment in a greenhouse at the Institute of Environment and Ecology, School of Environmental Science and Safety Engineering, Jiangsu University, Zhenjiang, China from April to September 2023. There is an average of 1,500 mm of precipitation every year in that region, with July having the greatest average of 179 mm and December having the lowest average of 24 mm. The annual maximum and minimum temperatures were recorded as 27.4°C in July and 2.7°C in January (Shen et al., 2023). The riverside is more vulnerable to invasion and sand collected at this site was sieved (2 mm), washed, and sterilized to remove stones, weeds, seeds, and impurities. The pots were filled with 2.5 kg of sand from the Yangtze River, stabilized for 1 week, and wet with double distilled water prior to the transplantation of the seedlings.

The *S. canadensis* seedlings were raised to obtain healthy and similarly sized seedlings. To avoid seed dispersal of the invasive species, *S. canadensis*, seeds of *S. canadensis* were planted in petri plates for germination. The seedlings were then transplanted in plastic trays after 15 days of germination for 2 months to obtain similar two-to-three-leaf seedlings. *S. bicolor* seeds were disinfected with 75% ethanol for 30 s and 10% NaOCl for 10 min and washed thoroughly in double distilled water. Seed disinfection treatment was performed to ensure seed germination and seedlings without seed-born disease. *Sorghum bicolor* seedlings were raised in plastic trays from the disinfected seeds. According to Oswald et al. (2001), the 10-day-old healthy *S. bicolor* seedlings (two to three leaves) and two-to-three-leaf *S. canadensis* seedlings were transplanted into pre-described pots with a 23 cm diameter with plant densities of four *S. canadensis* plants (100% *S. canadensis*: P) per pot, three *S. canadensis* plants and one *S. bicolor* plant (75% *S. canadensis* (H) +25% *S. bicolor* (L) per pot, two *S. canadensis* plants and two *S. bicolor* plants (50% *S. canadensis* (M) + 50% *S. bicolor* (M) per pot, one *S. canadensis* plant and three *S. bicolor* plants (25% *S. canadensis* (L)+75% *S. bicolor* (H) per pot, and four *S. bicolor* plants (100% *S. bicolor*: P) per pot. Following the transplantation of the seedlings into the pots, the pots were kept moist with water for a week before the Hogland solutions were applied. After 1 week after the transplantation of the seedlings, 100 times diluted modified Hogland solutions (Supplementary Table S1) with two different forms of available N and their combinations, i.e., 100% $NO_3$, 100% $NH_4$, and 50% $NO_3$+50% $NH_4$ concentrations, as well as a control (0% N; CK), were applied at a rate of 100 ml/pot two to three times per week. In total, there were 120 pots with six repeats for each plant density and form of N (Supplementary Figure S1).

## 2.2 Plant height, diameter, and root growth traits

The plants in the experiment were harvested at the panicle initiation stage of *S. bicolor*. Before the plants were harvested, the height of five plants was randomly measured using a measuring tape, the number of green leaves was counted, and the plant diameter was measured using a digital Vernier caliber scale (DL91200). The aboveground and belowground parts of the plants were harvested. The dry weight of leaf blades, stems, and roots were noted using a digital weighing balance after the plant tissues were dried at 120°C until constant weight. Root length and root branches were measured according to Khan et al. (2023b). The roots were carefully removed from the pots and washed gently to remove sand media and the root length was measured with measuring tape and root branches were counted.

## 2.3 Gaseous exchange traits

The gas exchange parameters $CO_2$ uptake (Pn), transpiration rate (Tr), and stomatal conductance (gs) were measured with a Li-COR 6500 (Lincoln, NE, USA) on a full sunny day between 9:00 am and 11:30 am. The first fully expanded leaf from the top of the plant was selected from both the plant species and the conditions inside the chamber were 1000 μmol $m^{-2}s^{-1}$ photon flux density, 400 μmol $mol^{-1}$ carbon dioxide, and a 25°C temperature (Anas et al., 2021b). Water use efficiency (WUE) was measured as a ratio of $CO_2$ uptake and transpiration rate.

## 2.4 Chlorophyll fluorescence

The chlorophyll fluorescence of six different plant leaves was measured using a FluorPen (Photon Systems Instruments) for each treatment. Each leaf was clipped after a 20-min dark period. The clip was opened just before recording the electron transfer efficiency (Fm/Fo), potential photochemical activity (Fv/Fo) and maximum photochemical efficiency (Fv/Fm) readings (Davarzani et al., 2023).

## 2.5 Nitrogen content and leaf functions

Leaf N and greenness were measured according to Huang et al. (2022). Briefly, a portable handheld soil plant analysis development (SPAD) meter was used to measure leaf greenness and N content. Three distinct positions were used to assess the nitrogen content and leaf greenness of the first fully expanded leaf of six plants per treatment. Leaf area, perimeter, length, and width were measured using the YMJ-CH intelligent leaf area system (Topu Yunnong Technology, Zhejiang, China) (Cui et al., 2023).

## 2.6 Relative yield and relative dominance index

Relative yield and relative dominance index were measured by Equations 1, 2 respectively (Yau and Hamblin, 1994; Wang et al., 2020; Pan et al., 2023).

$$RY = Yi/(p \times Ymono) \quad (1)$$

where RY is relative yield, Yi is the yield of species 'i' in an interculture, Ymono is the yield of a pure stand, and p is the proportion of species 'i'.

$$RDI = Yi/Ytotal \quad (2)$$

where RDI is the relative dominance index, Yi is the yield of species 'i' in an interculture and Ytotal is the sum yield of all species in an interculture.

## 2.7 Statistical analysis

The mean value was calculated for plant height, diameter, root growth traits, gas exchange, chlorophyll fluorescence, nitrogen content, leaf functions, and relative yield and dominance index. The main effects and interactions for the computed mean values of the independent variables were examined using analysis of variance (ANOVA). The calculated mean values were also used as "Trait" values. For every treatment combination, these "Trait" values were converted to the natural log value as follows:

$$\ln R = \ln(\text{Trait}\_x/\text{Trait}\_y) \quad (3)$$

where Trait_$x$ is the trait value of species $x$ and Trait_$y$ is the trait value of species $y$. A negative lnR value shows that species $x$ is suppressed by the dominance of species $y$ (Meng et al., 2015; Huang et al., 2021; Guo et al., 2023).

The lnR values were calculated using Microsoft Excel 2010 and further analysis was performed in RStudio using the "stat" and "ggplot2" packages for ANOVA and the scatter plot, respectively. Pearson's correlation analysis shows a linear relationship among the variables and principal component analysis (PCA) visualizes the data to identify trends, patterns, or outliers. The "corrplot" and "fviz_pca" functions in R 4.3.2 were used to analyze the correlation and perform PCA, respectively, of the plant height, diameter, root growth traits, gas exchange, chlorophyll fluorescence, nitrogen contents, leaf functions, and relative yield and dominance index lnR values.

# 3 Results

## 3.1 Effect of invasion level of *S. canadensis* and nitrogen form on the phenotype and growth interaction of *S. bicolor*

Plant height, number of leaves, stem diameter, leaf greenness, and N content in the leaf were significantly influenced by the plant species and their interactions with invasion levels and available N forms (Table 1; Supplementary Table S2). However, the main effects of invasion level, nitrogen form, and interaction of invasion level with available N form were non-significant (Table 1; Supplementary Table S2).

The relative plant height of *S. canadensis* (-2.52 to -1.28) was significantly suppressed under the low invasion level of *S. bicolor* for all N forms in relation to the pure stand (Figure 1F). The growth of *S. canadensis* was higher under the low population of *S. bicolor* and the $NO_3^-$ N form compared to the medium and high populations of *S.*

TABLE 1 Plant height, leaves, diameter, florescence traits, and nitrogen uptake of *S. canadensis* and *S. bicolor* under varied invasion levels and available nitrogen forms for plant species (P), invasion level (I), and nitrogen form (F).

| SOV | Df | Plant height | Leaves | Diameter | Fm/Fo | Fv/Fo | Fv/Fm | Nitrogen uptake |
|---|---|---|---|---|---|---|---|---|
| **P** | 1 | 629.23** | 33.69** | 182.27** | 10.51** | 12.88** | 0.08** | 57.9** |
| **I** | 3 | 0ns | 0ns | 0ns | 0ns | 0ns | 0ns | 0ns |
| **F** | 3 | 0ns | 0ns | 0ns | 0ns | 0ns | 0ns | 0ns |
| **P*I** | 3 | 1.22** | 0.11** | 0.49** | 1.67** | 7.32** | 1.14** | 5.63** |
| **P*F** | 3 | 6.28** | 4.28** | 0.72** | 0.58** | 0.51** | 1.09** | 1.17** |
| **I*F** | 9 | 0ns | 0ns | 0ns | 0ns | 0ns | 0ns | 0ns |
| **P*I*F** | 9 | 0.15** | 0.12** | 0.07ns | 0.03** | 0.07** | 0.02** | 0.14** |
| **Residual** | 160 | 0.02 | 0.01 | 0.04 | 0 | 0.01 | 0.01 | 0.01 |

Mean square values of plant height, leaves, diameter, Fm/Fo, Fv/Fo, Fv/Fm, and nitrogen uptake; *, ** and ns represented the significance level at p<0.01, p<0.05, and non-significant (p>0.05) respectively. SOV, source of variations; Df, degree of freedom; Fm/Fo, electron transfer efficiency; Fv/Fo, potential photochemical activity; Fv/Fm, maximum photochemical efficiency.

10.3389/fpls.2024.1468816

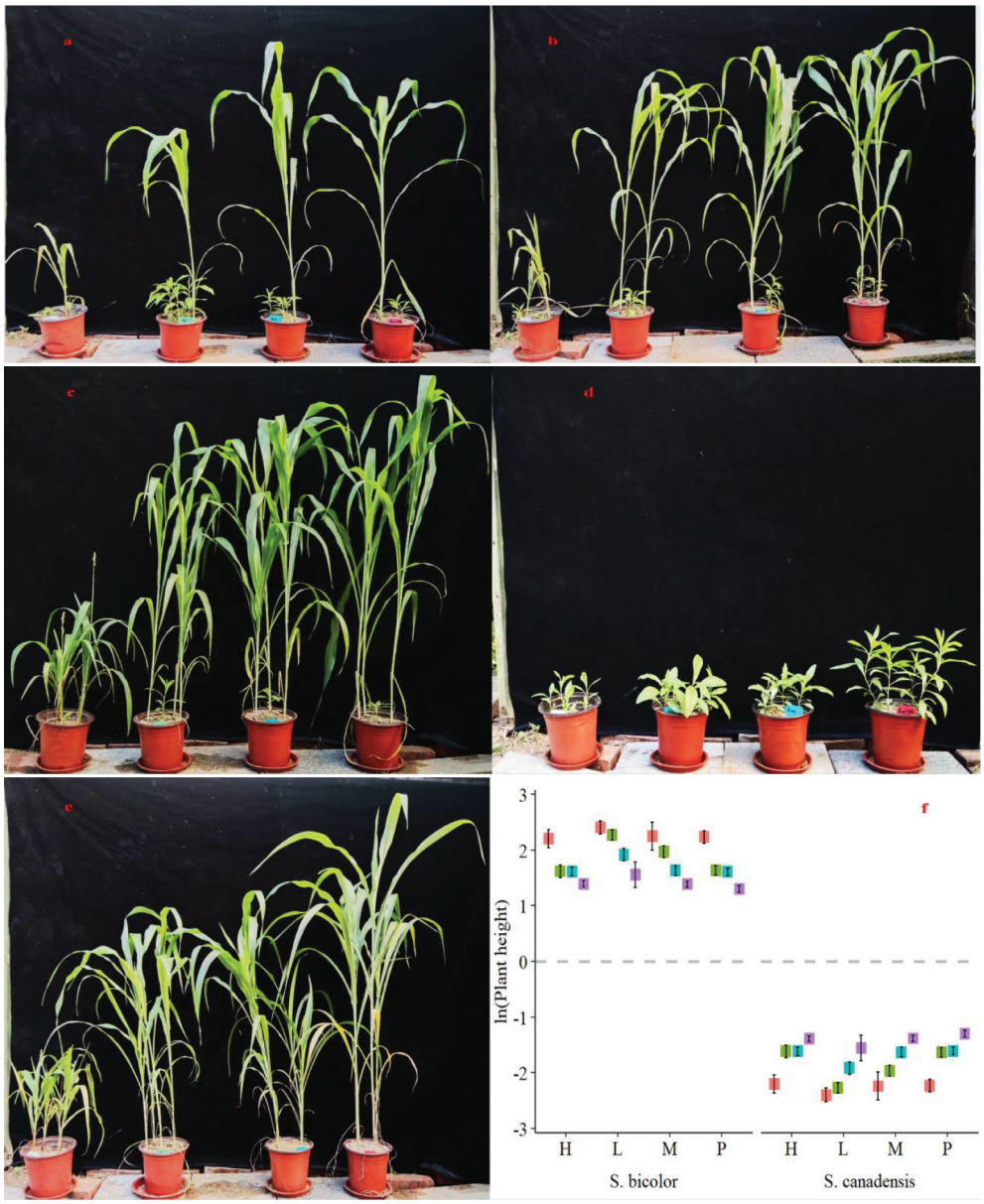


FIGURE 1
Phenotypic response of *S. canadensis* and *S. bicolor* under varied invasion levels and available nitrogen forms. **(A)** high invasion level; **(B)** medium invasion level; **(C)** low invasion level; **(D)** pure stand of invasive plant species (*S. canadensis*); **(E)** pure stand of domesticated plant (*S. bicolor*); **(F)** relative plant height of both plant species.

*bicolor* (Figures 1A–C). However, the highest competitive ability of *S. bicolor* was observed under the combined N form ($NH_4^+$+$NO_3^-$) and a low invasion level (Figure 1C). The pure stand of *S. canadensis* showed highest growth under nitrate nitrogen and *S. bicolor* showed under combined nitrogen form (Figures 1D, E). Maximum relative plant heights of 2.74 and -1.27 were observed for *S. bicolor* and *S. canadensis*, respectively. Furthermore, across the invasion levels, the height of *S. bicolor* (2.74) was higher under the low invasion level (Figure 1F). The respective mean plant heights of *S. bicolor* and *S. canadensis* varied from 61.8 to 15.9 cm and 12.36 to 0.98 cm, respectively (Supplementary Figure S2A).

The relative number of green leaves of *S. canadensis* was higher than *S. bicolor*. The highest relative number of leaves (0.88) of *S. canadensis* was observed against the low invasion level and the $NO_3^-$ N form (Figure 2A). The maximum number of green leaves per plant of *S. canadensis* was 16 under the pure culture. This was higher than the number of *S. bicolor* (Supplementary Figure S2B). The largest relative stem diameter of *S. canadensis* (-0.39) was noted under the high invasion levels, and the relative stem diameters of the two plant species differed significantly (Figure 2B). This was similar to plant height as it was higher under the low invasion levels (Supplementary Figure S2C). The leaf greenness (SPAD) values for *S. bicolor* were also higher (52.73) for the low invasion level and both nitrogen forms (Supplementary Figure S2D). The relative SPAD value (1.74 to -1.74) was generally influenced across the plant species but no significant difference was observed within a

10.3389/fpls.2024.1468816

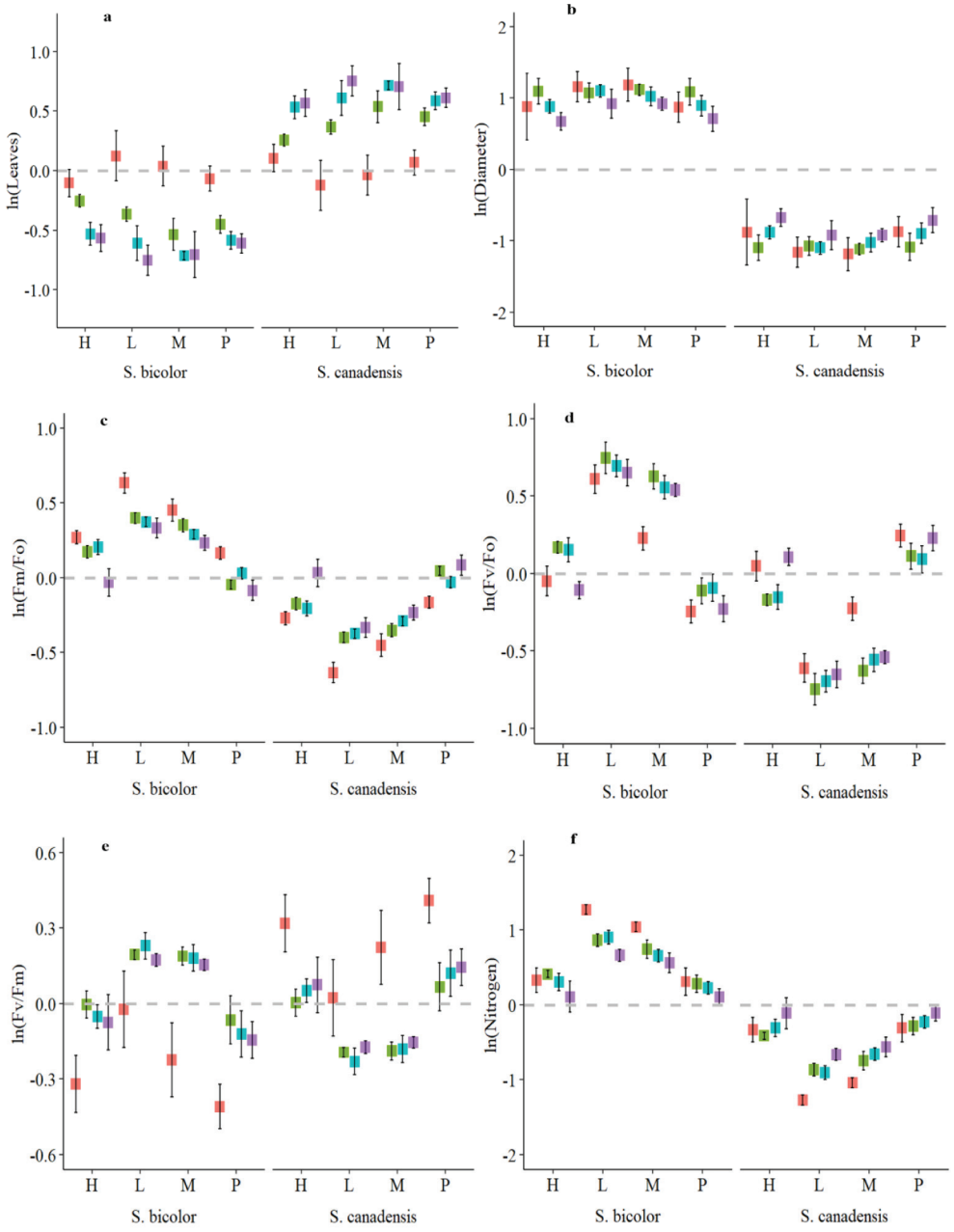


FIGURE 2
Relative number of leaves **(A)**, stem diameter **(B)**, chlorophyll fluorescence **(C–E)**, and leaf nitrogen **(F)** characteristics of *S. canadensis* and *S. bicolor* under varied invasion levels and available nitrogen forms. Red color, control; green color, ammonical N; blue color, both nitrogen forms; purple color, nitrate N; H, high invasion level; L, low invasion level; M, medium invasion level; P, no invasion.

single plant species under all invasion levels and available N forms (Supplementary Figure S6A).

For all invasion levels, *S. canadensis* had the largest relative plant leaf N content (0.28 to -0.80) under the nitrate N form; however, at low invasion levels, *S. canadensis* displayed lower relative leaf N content under both N forms (Figure 2F). The highest leaf nitrogen content was attained by *S. canadensis* (2.78 mg/g) in the pure culture under both nitrogen forms (Supplementary Figure S3A).

## 3.2 Physiological interaction of *S. bicolor* and *S. canadensis* under different invasion and nitrogen conditions

Chlorophyll fluorescence describes photosystem II functionality and Fv/Fm is the ratio of the variable and maximum fluorescence of a dark-adapted leaf. The relative Fv/Fm ratio ranged from 0.18 to -0.28 and from 0.42 to -.26 for low and medium invasion levels for

10.3389/fpls.2024.1468816

both plant species, respectively (Figures 2C–E). It was not significant within the species and was greatly impacted by the application of nitrogen, surpassing the control of both species (Supplementary Figures S2E, F).

The gaseous exchange parameters Pn, Tr, and gs were significantly different for the plant species, interactions of plant species with planting intensities, and N form (Table 2; Supplementary Table S2). The main effect of nitrogen and invasion and the interaction between these two variables were non-significant. However, the significance level of Tr and gs was less in the three-way interaction (Supplementary Table S2). Similarly, the fluorescence traits were significant for planting species, interaction of planting species with intensities, interaction of planting species with N forms, and their three-way interaction (Table 2; Table S2). However, these were unaffected by planting invasion levels and available N forms (Table 2, Supplementary Table S2).

*S. bicolor* had higher relative Pn (2.11) and Tr (1.47) levels compared to *S. canadensis* but gs (-3.35 to -5) was the opposite and Ci was not significant (Figure 3A; Supplementary Figure S6B). WUE was higher for nitrate N across the plant species and all planting intensities (Figure 3B). However, the pure stand for both species and the high invasion level had similar water use efficiency across all the N forms except the no N condition (Figure 3B). *S. bicolor* showed non-significant differences for gas exchange parameters under ammonical and combined available nitrogen forms (Supplementary Figures S3B–F).

## 3.3 Effect of invasion level of *S. canadensis* and nitrogen form on the leaf area and root growth of *S. bicolor*

Leaf area and its components were also affected only across the plant species and by its interactions with invasion levels and available N forms. (Table 1; Supplementary Table S2). The maximum relative leaf area for *S. bicolor* (3.55) was observed under the high invasion level and ammonical N form. *S. canadensis* had a maximum relative leaf area (-2.10) under high invasion levels and the nitrate N form (Figures 3C, D; Supplementary Figures S6E, F). Leaf parameters were influenced by plant species, invasion levels, and nitrogen forms, and the maximum leaf width for *S. bicolor* (26.2 mm) was observed under both nitrogen forms and low invasion levels (Supplementary Figure S4).

Root length and root spikes were significantly different for plant species and their interactions with invasion levels and available N forms. However, the largest relative root spikes (1.39) were observed for *S. canadensis* (Figures 3E, F). The species-specific root length varied from 64.18 to 4.32 cm for both and it was not statistically significant (Supplementary Figure S5A).

TABLE 2 Gaseous exchange, water use efficiency, leaf area, and leaf perimeter of *S. canadensis* and *S. bicolor* under varied invasion levels and available nitrogen forms for plant species (P), invasion level (I), and nitrogen form (F).

| SOV | Df | Pn | WUE | Leaf area | Leaf perimeter |
|---|---|---|---|---|---|
| **P** | 1 | 349.11** | 57.36** | 1451.12** | 851.09** |
| **I** | 3 | 0ns | 0ns | 0ns | 0ns |
| **F** | 3 | 0ns | 0ns | 0ns | 0ns |
| **P*I** | 3 | 8.06** | 1.35** | 11.31** | 4.32** |
| **P*F** | 3 | 2.3** | 2.22** | 1.09** | 0.11** |
| **I*F** | 9 | 0ns | 0ns | 0ns | 0ns |
| **P*I*F** | 9 | 0.06** | 0.04** | 0.21** | 0.08** |
| **Residual** | 160 | 0 | 0.01 | 0.03 | 0.02 |

Mean square values of Pn, WUE, leaf area, and leaf perimeter; *, ** and ns represented the significance level at p<0.01, p<0.05, and non-significant (p>0.05) respectively. SOV, source of variations; Df, degree of freedom; Pn, photosynthetic rate; WUE, water use efficiency.

## 3.4 Response of biomass and relative indices of *S. bicolor* under different invasion and nitrogen conditions

The root dry weight was significant against plant invasion levels, N forms, and their interaction (Table 3). The shoot/root weight was inversely correlated with the relative dry weight of the plant and, in comparison to ammonical N forms, it was comparable to the control and available N form under both low and high invasion levels (Figures 4A–C). The maximum relative plant biomass for *S. bicolor* (4.16) was observed under the high invasion level and ammonical N form and the lowest for *S. canadensis* (-4.16) was observed under the same conditions (Figure 4D). Shoot weight, root weight, and total plant dry biomass of *S. bicolor* were similar under the low and medium invasion conditions for the ammonical N form (Supplementary Figures S5C–F).

The relative yield and RDI for the plant species and their interactions with invasion level and available N forms, and three-way interactions were significantly different (Table 3). *S. bicolor* had a higher RDI (5.22) compared to *S. canadensis* even under high invasion levels, and the ammonical and combined N forms (Figure 4E). Similarly, *S. bicolor* had a higher relative yield (1.29) under the combined N form, and the relative yield of *S. canadensis* under the low medium and medium invasion levels was lower compared to *S. bicolor* (Figure 4F).

## 3.5 Relationship between response variables of *S. bicolor* and *S. canadensis* under different invasion and nitrogen conditions

Pearson's correlation coefficient determines the linear relationship between different datasets. A strong Pearson correlation coefficient was observed between Pn rate (0.98), plant height (0.98), and plant diameter (0.98; Figure 5). Plant dry biomass also showed a strong correlation with plant height (0.98), diameter (0.98), Pn rate (0.98), Tr rate (0.97), leaf area (0.99), and shoot weight (0.99). However, a weak correlation was observed between biomass and fluorescence parameters (0.67-0.82; Figure 5). The leaf N content had a strong correlation with RDI, SPAD, and relative yield, and negative correlations for gs and shoot-to-root ratio were observed against all the parameters (Figure 5).

10.3389/fpls.2024.1468816

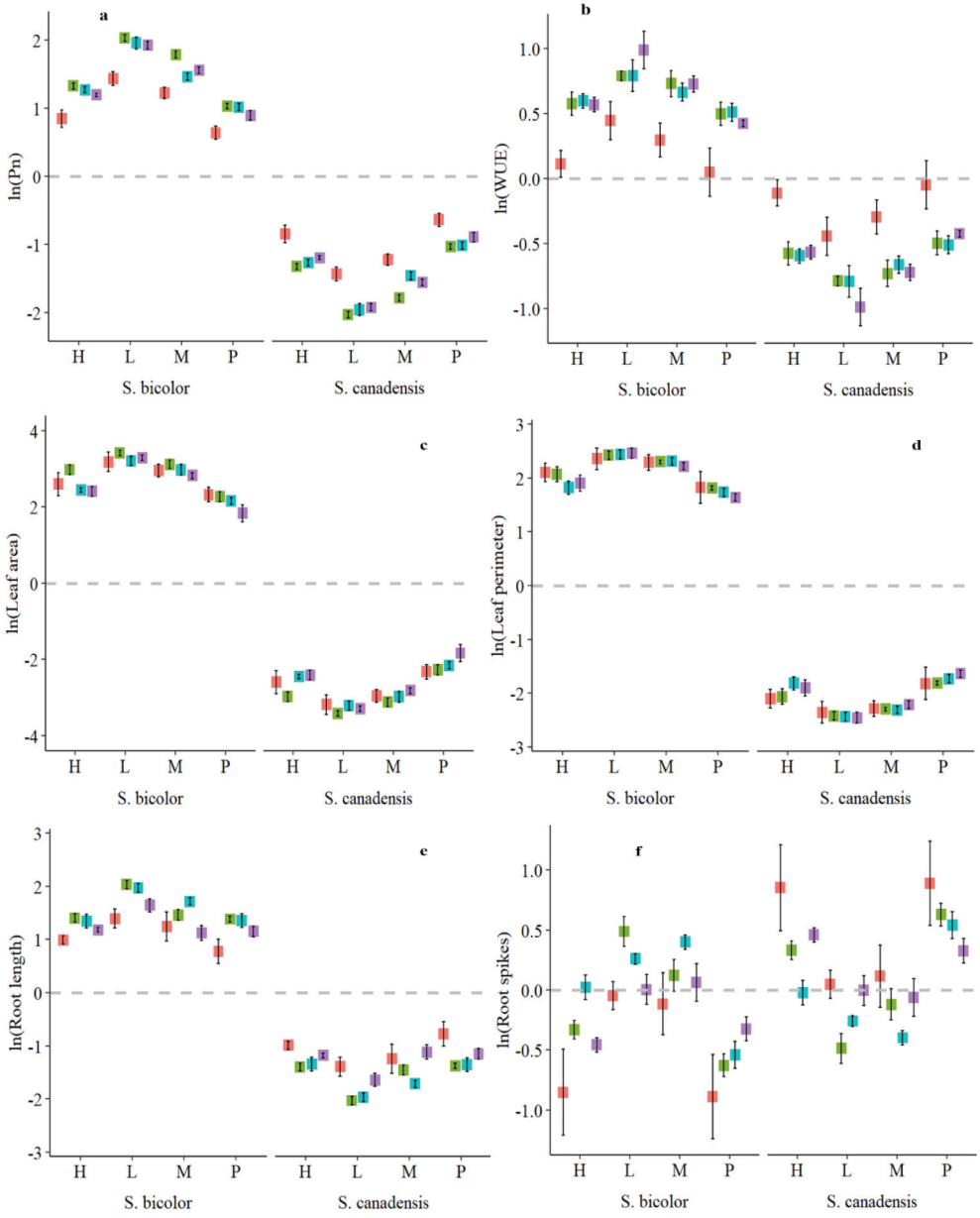


FIGURE 3
Relative photosynthetic rate **(A)**, water use efficiency **(B)**, leaf area **(C)**, leaf perimeter **(D)**, root dry weight **(E)**, and root spikes **(F)** of *S. canadensis* and *S. bicolor* under varied invasion levels and available nitrogen forms. Red color, control; green color, ammonical N; blue color, both nitrogen forms; purple color, nitrate N; H, high invasion level; L, low invasion level; M, medium invasion level; P, no invasion.

Principal component analysis separated three treatment factors from 23 components (Figure 6). Ellipse grouping showed two, four, and four groups for plant species, plant intensities, and available N forms, respectively (Figures 6A, C, E). The cumulative variance for PC1 to PC4 was distributed at 96.89%, and the eigenvalues of PC1, PC2, and PC3 were 18.65, 3.21, and 1.04, respectively (Figure 6B). The distribution of the cumulative variance of the top 10 components was displayed using a scree plot (Figure 6D). PC1 had the highest cumulative variance, at 77.7%, followed by PC2. The PCA plot showed the relationship of the most relevant principal components (Figure 6F). The components with less than a 90° angle were positively correlated with each other and the others were negatively correlated with each other. The PCA plot also showed the contribution of observations to PC1 and PC2 across all the treatment factors respectively (Figure 6F).

Except for the plant species, the main impacts of the treatment variables, invasion and N form, were not statistically significant. In the low to high invasion levels, *S. bicolor* exhibited a stronger dominance index over the invasive *S. canadensis* due to its higher plant height, leaf area, root length, and biomass values.

10.3389/fpls.2024.1468816

TABLE 3 Root length; root branches; dry biomass of roots, shoots, and total plant; shoot to root ratio; relative dominance index; and relative yield of *S. canadensis* and *S. bicolor* under varied invasion levels and available nitrogen forms for plant species (P), invasion levels (I), and nitrogen forms (F).

| SOV | Df | Root length | Root branches | Shoot weight | Root weight | Shoot/root | Total weight | RDI | RY |
|---|---|---|---|---|---|---|---|---|---|
| **P** | 1 | 367.69** | 6.03** | 1502.33** | 0.22ns | 392.27** | 1825.36** | 1138.27** | 33.63** |
| **I** | 3 | 0ns | 0ns | 0ns | 15.74** | 0ns | 0ns | 0ns | 0ns |
| **F** | 3 | 0ns | 0ns | 0ns | 12.39** | 0ns | 0ns | 0ns | 0ns |
| **P*I** | 3 | 3.39** | 7** | 8.21** | 0.22ns | 0.86** | 8.13** | 185.24** | 8.13** |
| **P*F** | 3 | 2.75** | 2.28** | 4.02** | 0.22ns | 4.49** | 3.98** | 2.17** | 0.78** |
| **I*F** | 9 | 0ns | 0ns | 0ns | 1.51** | 0ns | 0ns | 0ns | 0ns |
| **P*I*F** | 9 | 0.16** | 0.41** | 0.22** | 0.22ns | 1.06** | 0.19** | 0.38** | 0.19** |
| **Residual** | 160 | 0.02 | 0.03 | 0.02 | 0.26 | 0.06 | 0.01 | 0.01 | 0.01 |

Mean square values of relative root length, root branches, shoot weight, root weight, total weight, shoot/root, RDI, and RY; *, ** and ns represented the significance level at $p<0.01$, $p<0.05$, and non-significant ($p>0.05$) respectively. SOV, source of variations; Df, degree of freedom; RDI, relative dominance index; RY, relative yield.

Furthermore, the ammonical N form and the combined forms showed a positive relationship with the growth of *S. bicolor* which suggested that it was more responsive to the ammonical N form.

# 4 Discussion

## 4.1 Effect of *S. bicolor* on the growth of *S. canadensis*

*S. bicolor* suppressed the growth of invasive *S. canadensis* by obtaining more height and leaf area and covering the invasive species. Plant dry biomass is the ultimate indicator that describes the successful growth and development of a plant under the provided conditions. Our results showed that *S. bicolor* attained more biomass which supported our first hypothesis that *S. bicolor* would decrease the growth of invasive *S. canadensis* both above and belowground (Figure 4D). Allelopathy is an ecological phenomenon in which plants release secondary metabolites that suppress or promote nearby plants. *S. bicolor* is well-established for its allopathy (Farooq et al., 2013). Cheema and Khaliq (2000) reported that *S. bicolor* decreased weed dry biomass by up to 40% in a wheat field. The persistence of *S. bicolor* root exudates also decreased the growth of different weed species (Farooq et al., 2020; Roth et al., 2000). Plant dry biomass is also influenced by plant intensity, for example, the dry biomass of *S. bicolor* was higher in the low plant intensity treatments compared to the high plant intensity treatment but *S. canadensis* under a low intensity had lower plant dry biomass (Figure 4D). Furthermore, *S. bicolor* significantly suppressed *S. canadensis* in a combination of high and low *S. bicolor* and *S. canadensis* intensities. This supported our hypothesis that a higher intensity of *S. bicolor* suppresses the growth of *S. canadensis* by changing plant physiology. Similar results were reported by Guo et al. (2023) for *Oenothera biennis*, which could not compete with *Artemisia argyi* in a particular plant population. Previous studies reported that high intensity of *S. bicolor* reduced light interception by weeds (Contreras et al., 2022; Burnside, 1977; Gholami et al., 2013; Besançon et al., 2017a, b). This might be due to low $CO_2$ uptake by *S. canadensis* underneath. Similarly, the allelochemicals of *S. bicolor* overcame a weed population by decreasing the production of chlorophyll and the photosynthetic rate (Gonzalez et al., 1997; Jabran and Farooq, 2012; Farooq et al., 2020).

*S. bicolor* is a C4 plant that uptakes $CO_2$, water, and nitrogen more efficiently than the C3 *S. canadensis* plant (Zhao et al., 2005; Young and Long, 2000; Anten et al., 1995; Fay et al., 2006). Plant height and diameter have a direct relationship with the application of nitrogen (Anas et al., 2021b). The plant height of *S. bicolor* was also an indicator of its ability to overcome *S. canadensis*, because it covers *S. canadensis* underneath, captures more light and nutrients, and decreases the biomass of *S. canadensis* (Table 1; Liu et al., 2022; Ying et al., 2023). Plant diameter was significantly influenced by the planting intensity for both plant species under all N conditions. The results are in line with a previous study that found that a high-intensity plant population resulted in a thin plant stem compared to a low-intensity plant population (Anas et al., 2017).

The roots are responsible for the uptake of nutrients and water as well as interacting with soil bacteria. These secrete the secondary metabolites into the soil and have a direct relationship with the uptake process from the soil (Jiang et al., 2019). Plants produce more roots when grown together with other plants instead of alone and this phenomenon is known as self/non-self root discrimination (Hess and De Kroon, 2007). In this study, root length was found to be significantly different which may be due to the capacity to absorb more nutrients due to close contact with a greater volume of growing media (Table 3). Nutrient uptake is dependent on root length instead of root volume. Nutrients in the soil solution are taken up by roots either by mass flow or diffusion (Hodge, 2005). The use of photosynthates is defined by the shoots/roots (Anas et al., 2021a). Compared to *S. canadensis*, the shoots/roots of *S. bicolor* showed a substantial difference, indicating a superior usage of photosynthates (Figure 4C). These results were contrary to those of Ren et al. (2019) who found that *S. canadensis* had a greater shoot/root ratio and leaf area allocation with respect to non-invasive plant species. The reason might be that the growth of *S. canadensis* in the early stages was lower when compared to *S. bicolor* (Cox et al., 2018; Kelly et al., 2021). *S. bicolor* had more shoots/roots

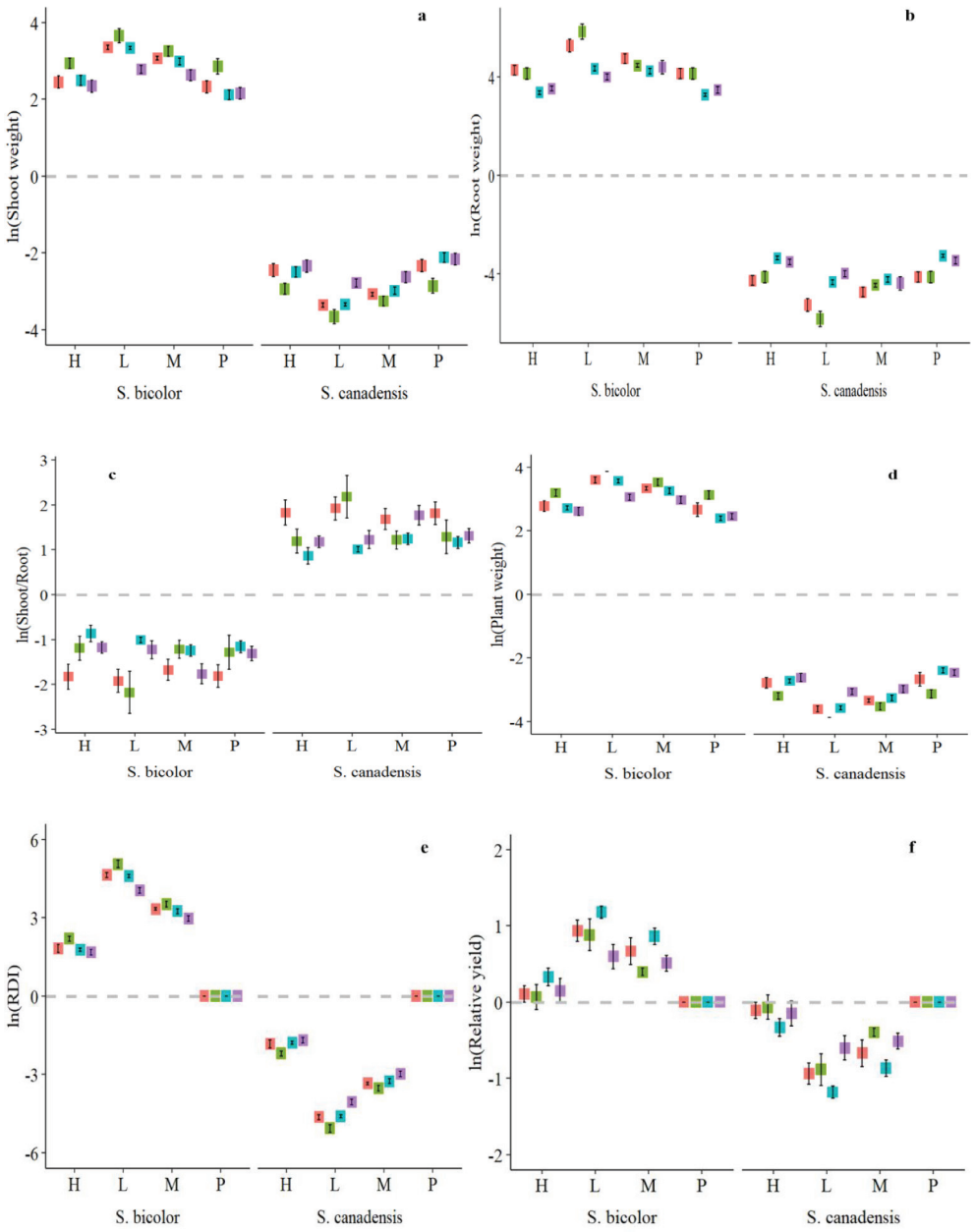


FIGURE 4
Relative shoot dry weight **(A)**, root dry weight **(B)**, plant dry weight **(C)**, shoot to root ratio **(D)**, relative yield **(E)**, and relative dominance index **(F)** of *S. canadensis* and *S. bicolor* under varied invasion levels and available nitrogen forms. Red color, control; green color, ammonical N; blue color, both nitrogen forms; purple color, nitrate N; H, high invasion level; L, low invasion level; M, medium invasion level; P, no invasion.

than *Zea mays* in an interculture with *Panicum millet* and *Zea mays* (Amanullah and Stewart, 2013). *S. bicolor* grew better in drought conditions than *Zea mays* (Danalatos et al., 2009).

## 4.2 Effect of available nitrogen forms on *S. bicolor* overcoming *S. canadensis*

Plant uptake N mainly in two available N forms, either nitrate ($NO_3^-$) or ammonium ($NH_4^+$), and they prefer a particular form according to their adaptation and environment (Sanchez-Zabala et al., 2015). It has been reported that *S. bicolor* prefers the $NH_4^+$ form of N and *S. canadensis* grew better under the $NO_3^-$ form (de Souza Miranda et al., 2016; Miranda et al., 2013; Afzal et al., 2020; Wang et al., 2023). Leaf N content was higher in *S. bicolor* under the combined N and ammonical forms but *S. canadensis* positively responded to the nitrate N form. These results were the same as previous studies that showed that *S. bicolor* is ammonical N-loving and *S. canadensis* is nitrate-loving. *S. bicolor* growth was higher under ammonical N compared to nitrate N due to a low accumulation of $H_2O_2$ and improved $K^+/Na^+$ homeostasis under saline conditions (de Oliveira et al., 2020). Further, Mrid et al. (2016) reported that the application of ammonical N

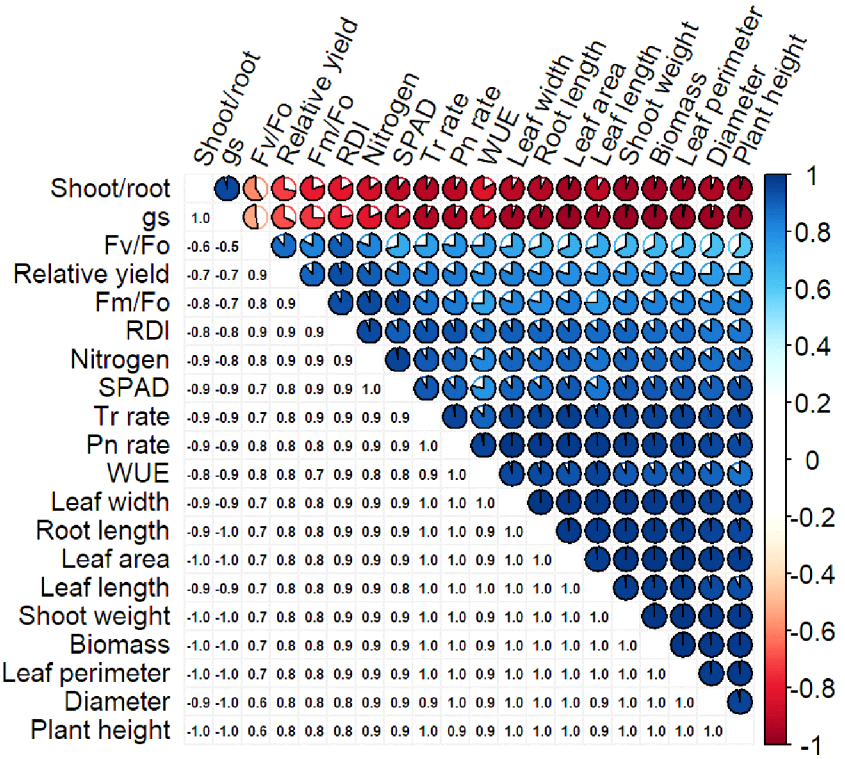


FIGURE 5
Correlation of different characteristics of *S. canadensis* and *S. bicolor* under varied invasion levels and available nitrogen forms.

enhanced the growth of *S. bicolor* by improving the activities of glutamine synthetase and aspartate aminotransferase. These enzymes are important parts of the nitrogen metabolic pathway for protein synthesis. However, root growth and exudation of *S. bicolor* increase when ammonical N is present, releasing $H^+$ into the rhizosphere and causing the pH to drop (Afzal et al., 2023; Di et al., 2018; Zhao et al., 2023). Root exudates of *S. bicolor* have the potential to retard the growth of nearby plants. The positive responses of *S. bicolor* under ammonical N for protein synthesis and root exudation might enhance its biomass and dominance over the invasive *S. canadensis*. However, another study showed that *S. canadensis* was flexible with regard to available N forms and it tended to take up dominant forms of available N (Guan et al., 2023). Although *S. canadensis* is independent of available N forms, in this study, it gained more biomass under the nitrate N form, similar to Wang et al. (2023) and Afzal et al. (2023). Guan et al. (2023) also used dry biomass as a reference to describe the uptake of a specific N form. Our result supported both arguments as *S. bicolor* acquired the ammonical N form either in the combined treatment or the ammonical form treatment and left less available N for *S. canadensis* due to its dominant growth (Figure 2F).

The leaf is the main plant organ that provides the surface for sunlight absorption through chlorophyll pigments and starts photosynthetic metabolism. A high leaf area is the key factor for growth, development, and biomass, and an early development of leaf area is key to gaining more biomass (Liu et al., 2020). The higher leaf area of *S. bicolor* at the early stage might be responsible for its dominance over *S. canadensis* (Figure 3C). In this study, we found that leaf greenness was significantly higher in *S. bicolor* under low plant intensity, but higher in *S. canadensis* in the pure stands and at the high invasion level (Supplementary Figure S6A). However, it was higher for *S. bicolor* under the combined and ammonical N forms, and *S. canadensis* had higher leaf greenness under the nitrate N form (Supplementary Figure S6A). Plants that adopt an N acquisition strategy for the ammonical N form have increased leaf chlorophyll content but excessive application of that form of N might cause chlorosis (Sarasketa et al., 2014; Sanchez-Zabala et al., 2015) because a higher amount of ammonical N degrades the chloroplasts by triggering the ABA signaling pathway (Li et al., 2012). Tomato leaves showed leaf chlorosis through bursting $H_2O_2$ under a medium supply of ammonical N (Liu and von Wirén, 2017).

Plants transform light energy into chemical energy through a process called photosynthesis that occurs in green leaves when they get sunshine. Based on Li et al. (2013), chloroplasts account for 20–30% of the weight of leaves and are the photosynthetic site. One pigment in chloroplasts that absorbs light energy and transforms it into biomass is called leaf chlorophyll (Du et al., 2017). The structural component of proteins, such as chloroplast, is the N. In a previous study, it was reported that the coexistence of N forms had the highest photosynthetic rate which is in line with our results (Figure 2F) and followed by nitrate and ammonical N forms (Li et al., 2013). However, nitrate N form was suppressive for photosynthetic rate in this study which might be due to the different carbon fixation pathways of *S. bicolor* (C4) and *S. canadensis* (C3), and C4 plants have higher photosynthetic rates (Smart et al., 2012; Wang et al., 2012; Nawaz et al., 2023).

10.3389/fpls.2024.1468816

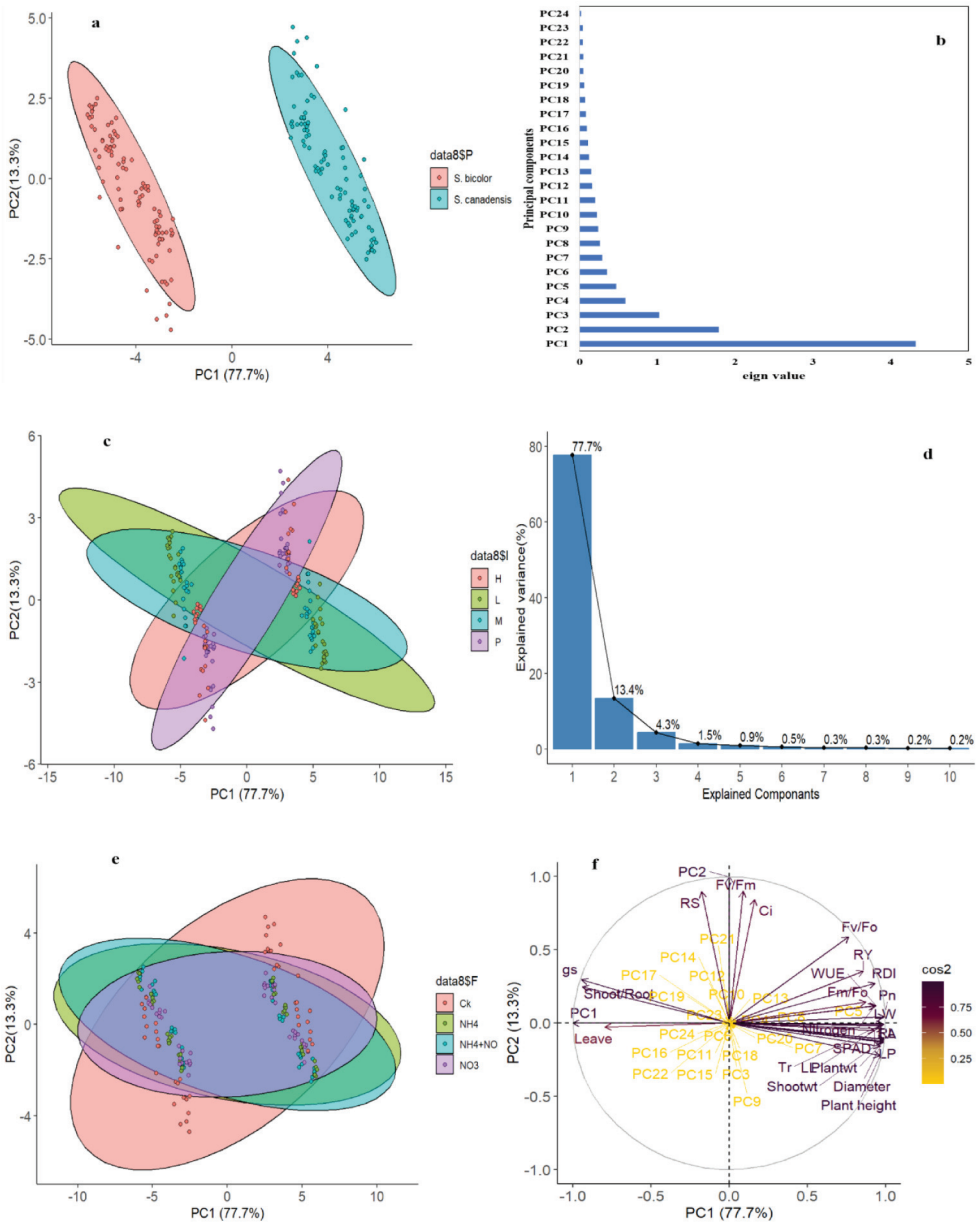


FIGURE 6
Principal component analysis of *S. canadensis* and *S. bicolor* under varied invasion levels and available nitrogen forms. Biplot of plant species **(A)**, eigenvalue for principal component **(B)**, biplot for invasion levels **(C)**, variance distribution **(D)**, biplot for available nitrogen forms **(E)**, and principal component plot **(F)**.

## 4.3 Dominance and suppressive effect of *S. bicolor* on *S. canadensis*

The relative yield of any plant species shows its position in an ecosystem because it has a direct relationship with successful growth (Leger and Rice, 2003). A change in the behavior of *S. canadensis* due to nearby other plant species describes the invasion level (Conti et al., 2018). The degree of invasion and the evolution of a native species in an invaded ecosystem can be described by an understanding of the adaption mechanism of the invading species (Ren et al., 2022). Relative yield in this study was significantly correlated with plant species, interactions with intensities, N forms, and their combined interaction (Table 3). Similarly, *S. bicolor* showed a higher relative yield under the combined N form and low planting intensity. *S. canadensis* did not attain a relative yield equivalent to *S. bicolor* in the intercultures and under all N forms (Figure 4F). Thus, choosing the correct plant species is crucial in light of planting intensities and available N sources; these findings are consistent with those of Ren et al. (2022). Agronomic yield is the sum of grains and total dry biomass of plants. It is also calculated on acreage for fodder crops or to calculate an economic return. In this case, ideal plant intensity per acre ensures successful crop growth. Recommended planting intensity utilizes all resources judicially and increases the cost-benefit ratio (Anas et al., 2017). The planting of *S. bicolor* plants in a medium to high intensity may be able to control invasive species according to our

testing of plant intensity against various invasion levels in this study. Similarly, de Witt (1960) reported that the yield is dependent on the area available in a mixed culture.

The entry of a non-native species into an ecosystem may change its functions and reshape it for successful invasion and be either partially or fully dominant. The relative dominance of *S. bicolor* based on the plant's dry biomass was higher than *S. canadensis* for the combined available N forms under low planting intensities (Figure 4E). It has been reported that *S. canadensis* may co-exist with non-invasive plant species without changing the species richness, diversity, and composition of the recipient ecosystem (Lai et al., 2015). Usually, invasive plant species change the diversity, species richness, and structure of an ecosystem after entry into that particular ecosystem (Powell et al., 2013; Florens et al., 2017). By developing robust physiological systems both above and below ground, native plant species have the potential to outcompete invasive species. Allelopathy is an ecological strategy used by plants to outcompete neighboring plants by releasing allelochemicals into the air, scattering them on the soil's surface, and secreting these chemicals from their roots (Farooq et al., 2013; Cheema and Khaliq, 2000; Shan et al., 2023). Plants with greater height and leaf area may cover the vegetation underneath which results in low light penetration and decreases the photosynthetic process (Angadi et al., 2022). Dense populations of plants hinder weed growth in an agroecosystem by stifling their ability to capture resources (Anas et al., 2017). Moreover, plant adaptations for available nitrogen forms may contribute to a native species' capacity to thrive successfully due to priority (Fisher et al., 2010; Zhao et al., 2023).

## 5 Conclusion

The competitiveness of the domesticated plant *S. bicolor* against the invasive species *S. canadensis* was first documented in this study. It was discovered that *S. bicolor* outcompeted *S. canadensis* because of its greater biomass yield, $CO_2$ uptake, leaf area, and plant height. Furthermore, the two plant species exhibited distinct behaviors in response to various N sources. *S. bicolor* performed better under the ammonical N form and combined N form (ammonical+nitrate), and the growth of *S. canadensis* was better under the nitrate N form. *S. canadensis* was suppressed by *S. bicolor* under all interculture combinations and the results were more pronounced at a higher plant intensity of *S. bicolor* under the ammonical N form.

## Data availability statement

The original contributions presented in the study are included in the article/Supplementary Material. Further inquiries can be directed to the corresponding authors.

## Author contributions

MA: Conceptualization, Methodology, Writing – original draft. IK: Methodology, Writing – review & editing. SOA: Software, Writing – review & editing. MN: Data curation, Software, Writing – review & editing. ZYH: Visualization, Writing – review & editing. MAA: Data curation, Validation, Writing – review & editing. KAG: Methodology, Writing – review & editing. SSQ: Supervision, Validation, Writing – review & editing. JL: Supervision, Validation, Writing – review & editing. ZCD: Funding acquisition, Project administration, Supervision, Writing – review & editing. DDL: Project administration, Validation, Writing – review & editing. SA: Writing – review & editing, Software, Conceptualization.

## Funding

The author(s) declare financial support was received for the research, authorship, and/or publication of this article. This work was supported by National Natural Science Foundation of China (32271587, 32171509, 32071521), Natural Science Foundation of Jiangsu (BK20211321), the Carbon Peak and Carbon Neutrality Technology Innovation Foundation of Jiangsu Province (BK20220030), and Jiangsu Funding Program for Excellent Postdoctoral Talent (2023ZB861). Part of the funding for this research was supported by the Priority Academic Program Development of Jiangsu Higher Education Institutions (PAPD) and the Special Scientific Research Project of the School of Emergency Management, Jiangsu University.

## Acknowledgments

The authors would like to acknowledge all the team members of the Institute of Environment and Ecology, School of the Environment and Safety Engineering, Jiangsu University, Zhenjiang 212013, China and the researchers at King Saud University in Riyadh, Saudi Arabia, who are sponsoring project number (RSP2024R48).

## Conflict of interest

The authors declare that the research was conducted in the absence of any commercial or financial relationships that could be construed as a potential conflict of interest.

## Publisher's note



## Supplementary material

The Supplementary Material for this article can be found online at: https://www.frontiersin.org/articles/10.3389/fpls.2024.1468816/full#supplementary-material

# References


Afzal, M. R., Naz, M., Ullah, R., and Du, D. (2023). Persistence of Root Exudates of *Sorghum bicolor* and *Solidago canadensis*: Impacts on Invasive and Native Species. *Plants* 13, 58. doi: 10.3390/plants13010058

Afzal, M. R., Zhang, M., Jin, H., Wang, G., Zhang, M., Ding, M., et al. (2020). Post-translational regulation of plasma membrane H+-ATPase is involved in the release of biological nitrification inhibitors from sorghum roots. *Plant Soil* 450, 357–372. doi: 10.1007/s11104-020-04511-6

Allen, W. J., Bufford, J. L., Barnes, A. D., Barratt, B. I., Deslippe, J. R., Dickie, I. A., et al. (2022). A network perspective for sustainable agroecosystems. *Trends Plant Sci.* 27, 769–780. doi: 10.1016/j.tplants.2022.04.002

Amanullah, A., and Stewart, B. A. (2013). Shoot: root differs in warm season C4-cereals when grown alone in pure and mixed stands under low and high water levels. *Pak. J. Bot.* 45, 83–90. Available at: http://www.pakbs.org/pjbot/PDFs/45(S1)/12.pdf (Accessed June 28, 2024)

Anas, M., Jabbar, A., Sarwar, M. A., Ullah, R., Abuzar, M. K., Ijaz, A., et al. (2017). Intercropping sunflower with mungbean for improved productivity and net economic return under irrigated conditions. *Pak. J. Agr. Res.* 30, 338–345. doi: 10.17582/journal.pjar/2017/30.4.338.345

Anas, M., Liao, F., Verma, K. K., Sarwar, M. A., Mahmood, A., Chen, Z.-L., et al. (2020). Fate of nitrogen in agriculture and environment: agronomic, eco-physiological and molecular approaches to improve nitrogen use efficiency. *Biol. Res.* 53, 1–20. doi: 10.1186/s40659-020-00312-4

Anas, M., Verma, K. K., Haq, I. U., Naeem, M., Li, Q., Liao, F., et al. (2021a). Characterization of exotic, native and wild-type genotypes of sugarcane (Saccharum spp. Hybrids) for internal nitrogen use efficiency under different nitrogen levels. *Sugar Tech* 23, 1258–1267. doi: 10.1007/s12355-021-01014-1

Anas, M., Verma, K. K., Riaz, M., Qiang, L., Liao, F., Liu, Y., et al. (2021b). Physio-morphological and biochemical mechanism of nitrogen use efficiency in sugarcane (Saccharum spp.) genotypes under different growth stages and nitrogen levels. *J. Plant Interact.* 16, 332–343. doi: 10.1080/17429145.2021.1933224

Anastasiu, P., and Negrean, G. (2005). Alien plants in Romania (I). Analele Stiintifice ale Universitatii "Al. I. Cuza" din Iasi Tomul LI, s. II a. *Biol. Veget.* 51, 87–96. Available at: http://cercetare.bio.uaic.ro/publicatii/anale_vegetala/issue/2005/13-2005.pdf.

Angadi, S. V., Umesh, M. R., Begna, S., and Gowda, P. (2022). Light interception, agronomic performance, and nutritive quality of annual forage legumes as affected by shade. *Field Crops Res.* 275, 108358. doi: 10.1016/j.fcr.2021.108358

Anten, N. P., Schieving, F., Medina, E., Werger, M. J. A., and Schuffelen, P. (1995). Optimal leaf area indices in C3 and C4 mono-and dicotyledonous species at low and high nitrogen availability. *Physiologia plantarum* 95, 541–550. doi: 10.1111/j.1399-3054.1995.tb05520.x

Batish, D. R., Jose, S., Kaur, S., and Chauhan, B. S. (2022). Reducing the susceptibility of agroecosystems to invasion through sustainable weed management. *Front. Agron.* 4. doi: 10.3389/fagro.2022.1086681

Bayu, W., Rethman, N. F. G., and Hammes, P. S. (2005). Growth and yield compensation in sorghum (*Sorghum bicolor* L. Moench) as a function of planting density and nitrogen fertilizer in semi-arid areas of northeastern Ethiopia. *South Afr. J. Plant Soil* 22, 76–83. doi: 10.1080/02571862.2005.10634685

Besançon, T. E., Dayan, F. E., Gannon, T. W., and Everman, W. J. (2020). Conservation and divergence in sorgoleone production of sorghum species. *J. Environ. Qual.* 49, 368–377. doi: 10.1002/jeq2.20038

Besançon, T., Heiniger, R., Weisz, R., and Everman, W. (2017a). Weed response to agronomic practices and herbicide strategies in grain sorghum. *Agron. J.* 109, 1642–1650. doi: 10.2134/agronj2016.06.0363

Besançon, T. E., Heiniger, R. W., Weisz, R., and Everman, W. J. (2017b). Grain sorghum and Palmer amaranth (*Amaranthus palmeri*) response to herbicide programs and agronomic practices. *Weed Tech.* 31, 781–792. doi: 10.1017/wet.2017.53

Burnside, O. C. (1977). Control of weeds in non-cultivated, narrow-row sorghum 1. *Agron. J.* 69, 851–854. doi: 10.2134/agronj1977.00021962006900050031x

Calone, R., Sanoubar, R., Lambertini, C., Speranza, M., Vittori Antisari, L., Vianello, G., et al. (2020). Salt tolerance and Na allocation in *Sorghum bicolor* under variable soil and water salinity. *Plants* 9, 561. doi: 10.3390/plants9050561

Cheema, Z. A., and Khaliq, A. (2000). Use of sorghum allelopathic properties to control weeds in irrigated wheat in a semi arid region of Punjab. *Agric. Eco. Env.* 79, 105–112. doi: 10.1016/S0167-8809(99)00140-1

Chen, X., Wu, Q., Gao, Y., Zhang, J., Wang, Y., Zhang, R., et al. (2020). The role of deep roots in sorghum yield production under drought conditions. *Agronomy* 10, 611. doi: 10.3390/agronomy10040611

Conti, L., Block, S., Parepa, M., Münkemüller, T., Thuiller, W., Acosta, A. T., et al. (2018). Functional trait differences and trait plasticity mediate biotic resistance to potential plant invaders. *J. Ecol.* 106, 1607–1620. doi: 10.1111/1365-2745.12928

Contreras, D., Leon, R. G., Post, A. R., and Everman, W. J. (2022). Critical period of grass weed control in ALS-tolerant grain sorghum (*Sorghum bicolor*) is affected by planting date and environment. *Front. Agron.* 4. doi: 10.3389/fagro.2022.1014801

Cox, S., Nabukalu, P., Paterson, A. H., Kong, W., and Nakasagga, S. (2018). Development of perennial grain sorghum. *Sustainability* 10, 172. doi: 10.3390/su10010172

Crawford, N. M., and Glass, A. D. (1998). Molecular and physiological aspects of nitrate uptake in plants. *Trends Plant Sci.* 3, 389–395. doi: 10.1016/S1360-1385(98)01311-9

Cui, M., Yang, B., Ren, G., Yu, H., Dai, Z., Li, J., et al. (2023). Effects of Warming, Phosphorous Deposition, and Both Treatments on the Growth and Physiology of Invasive *Solidago canadensis* and Native Artemisia argyi. *Plants* 12, 1370. doi: 10.3390/plants12061370

Danalatos, N., Archontoulis, S. V., and Tsiboukas, K. (2009). "Comparative analysis of sorghum vs corn growing under optimum and under water/nitrogen limited conditions in central Greece," in *17th European Biomass Conference and Exhibition*, Vol. 2. 538–544. Available at: https://www.researchgate.net/publication/235797946.

Davarzani, M., Aliniaeifard, S., Mehrjerdi, M. Z., Roozban, M. R., Saeedi, S. A., and Gruda, N. S. (2023). Optimizing supplemental light spectrum improves growth and yield of cut roses. *Sci. Rep.* 13, 21381. doi: 10.1038/s41598-023-48266-3

de Oliveira, F. D. B., de Souza Miranda, R., dos Santos Araújo, G., Coelho, D. G., Lobo, M. D. P., de Oliveira Paula-Marinho, S., et al. (2020). New insights into molecular targets of salt tolerance in sorghum leaves elicited by ammonium nutrition. *Plant Physiol. Biochem.* 154, 723–734. doi: 10.1016/j.plaphy.2020.06.051

de Souza Miranda, R., Gomes-Filho, E., Prisco, J. T., and Alvarez-Pizarro, J. C. (2016). Ammonium improves tolerance to salinity stress in Sorghum bicolor plants. *Plant Growth Regul.* 78, 121–131. doi: 10.1007/s10725-015-0079-1

de Witt, C. T. (1960). On competition. *Verslagen Van Landouskundige Onderzoekingen* 66, 1–82. Available at: https://edepot.wur.nl/187113.

Di, T., Afzal, M. R., Yoshihashi, T., Deshpande, S., Zhu, Y., and Subbarao, G. V. (2018). Further insights into underlying mechanisms for the release of biological nitrification inhibitors from sorghum roots. *Plant Soil.* 423, 99–110. doi: 10.1007/s11104-017-3505-5

Du, E., Dong, D., Zeng, X., Sun, Z., Jiang, X., and de Vries, W. (2017). Direct effect of acid rain on leaf chlorophyll content of terrestrial plants in China. *Sci. Total Environ.* 605, 764–769. doi: 10.1016/j.scitotenv.2017.06.044

Du, E., Terrer, C., Pellegrini, A. F., Ahlström, A., van Lissa, C. J., Zhao, X., et al. (2020). Global patterns of terrestrial nitrogen and phosphorus limitation. *Nat. Geosci.* 13, 221–226. doi: 10.1038/s41561-019-0530-4

Einhellig, F. A., and Souza, I. F. (1992). Phytotoxicity of sorgoleone found in grain sorghum root exudates. *J. Chem. Ecol. 18*, 1–11. doi: 10.1007/BF00997160

Farooq, M., Khaliq, A., Cheema, Z., and Cheema, S. (2013). Application of allelopathy in crop production: success story from Pakistan. *Allelopath. Curr. Trends Futur. Appl.*, 113–143. doi: 10.1007/978-3-642-30595-5_6

Farooq, M., Khan, I., Nawaz, A., Cheema, M. A., and Siddique, K. H. (2020). Using sorghum to suppress weeds in autumn planted maize. *Crop Prot.* 133, 105162. doi: 10.1016/j.cropro.2020.105162

Fay, P. A., Hui, D., Procter, A., Johnson, H. B., Polley, H. W., and Jackson, R. B. (2006). "December. Photosynthetic Water Use Efficiency in it Sorghastrum nutans (C4) and it Solidago canadensis (C3) in Three Soils Along a CO2 Concentration Gradient," in *AGU Fall Meeting Abstracts*, Vol. 2006. B41B–0187. Available at: https://ui.adsabs.harvard.edu/abs/2006AGUFM.B41B0187F/abstract.

Fisher, J. B., Sitch, S., Malhi, Y., Fisher, R. A., Huntingford, C., and Tan, S.-Y. (2010). Carbon cost of plant nitrogen acquisition: A mechanistic, globally applicable model of plant nitrogen uptake, retranslocation, and fixation. *Global Biogeochem Cycles* 24, GB1014. doi: 10.1029/2009GB003621

Florens, F. V., Baider, C., Seegoolam, N. B., Zmanay, Z., and Strasberg, D. (2017). Long-term declines of native trees in an oceanic island's tropical forests invaded by alien plants. *Appl. Veg. Sci.* 20, 94–105. doi: 10.1111/avsc.12273

Frost, C. M., Allen, W. J., Courchamp, F., Jeschke, J. M., Saul, W. C., and Wardle, D. A. (2019). Using network theory to understand and predict biological invasions. *Trends Ecol. Evol.* 34, 831–843. doi: 10.1016/j.tree.2019.04.012

Gazoulis, I., Antonopoulos, N., Kanatas, P., Karavas, N., Bertoncelj, I., and Travlos, I. (2022). Invasive alien plant species—Raising awareness of a threat to biodiversity and ecological connectivity (EC) in the adriatic-ionian region. *Diversity* 14, 387. doi: 10.3390/d14050387

Gholami, S., Minbashi, M., Zand, E., and Noormohammadi, G. (2013). Non chemical management of weeds effects on forage sorghum production. *Int. J. Adv. Biol. Biomed. Res.* 1, 614–623. doi: 10.26655/ijabbr.2017.9.6

Głąb, L., Sowiński, J., Bough, R., and Dayan, F. E. (2017). Allelopathic potential of sorghum (*Sorghum bicolor* (L.) Moench) in weed control: a comprehensive review. *Adv. Agron.* 145, 43–95. doi: 10.1016/bs.agron.2017.05.001

Gonzalez, V. M., Kazimir, J., Nimbal, C., Weston, L. A., and Cheniae, G. M. (1997). Inhibition of a photosystem II electron transfer reaction by the natural product sorgoleone. *J. Agric. Food Chem.* 45, 1415–1421. doi: 10.1021/jf960733w

Guan, M., Pan, X.-C., Sun, J.-K., Chen, J.-X., Kong, D.-L., and Feng, Y.-L. (2023). Nitrogen acquisition strategy and its effects on invasiveness of a subtropical invasive plant. *Front. Plant Sci.* 14. doi: 10.3389/fpls.2023.1243849

Guo, X., Ma, J.-Y., Liu, L.-L., Li, M.-Y., Wang, H., Sun, Y.-K., et al. (2023). Effects of salt stress on interspecific competition between an invasive alien plant Oenothera biennis and three native species. *Front. Plant Sci.* 14. doi: 10.3389/fpls.2023.1144511

Hess, L., and De Kroon, H. (2007). Effects of rooting volume and nutrient availability as an alternative explanation for root self/non-self discrimination. *J. Ecol.* 95, 241–251. doi: 10.1111/j.1365-2745.2006.01204.x

Hodge, A. (2005). "Nitrogen in soil/plant uptake," in *Encyclopedia of Soils in the Environment*, Elsevier, Radarweg 29, 1043 NX Amsterdam, The Netherlands. 00159–00154. doi: 10.1016/B0-12-348530-4/00159-4

Huang, P., Shen, F., Abbas, A., Wang, H., Du, Y., Du, D., et al. (2022). Effects of different nitrogen forms and competitive treatments on the growth and antioxidant system of Wedelia trilobata and Wedelia chinensis under high nitrogen concentrations. *Front. Plant Sci.* 13. doi: 10.3389/fpls.2022.851099

Huang, X., Yu, J., Liu, S., Xie, H., He, H., and Li, K. (2021). Plant morphological traits and competition index comparisons of three invasive and native submerged plants. *Knowledge Manage. Aquat. Ecosyst.* 422, 11. doi: 10.1051/kmae/2021012

Jabran, K., and Farooq, M. (2012). "Implications of potential allelopathic crops in agricultural systems," in *Allelopathy: Current trends and future applications* (Springer Berlin Heidelberg, Berlin, Heidelberg), 349–385. doi: 10.1007/978-3-642-30595-5_15

Jiang, Z., Zhao, C., Yu, S., Liu, S., Cui, L., Wu, Y., et al. (2019). Contrasting root length, nutrient content and carbon sequestration of seagrass growing in offshore carbonate and onshore terrigenous sediments in the South China Sea. *Sci. Total Environ.* 662, 151–159. doi: 10.1016/j.scitotenv.2019.01.175

Kato-Noguchi, H. (2023). The Impact and Invasive Mechanisms of *Pueraria montana* var. lobata, One of the World's Worst Alien Species. *Plants* 12, 3066. doi: 10.3390/plants12173066

Kelly, C. L., Schwarzkopf, L., Gordon, I. J., and Hirsch, B. (2021). Population growth lags in introduced species. *Ecol. Evol.* 11, 4577–4587. doi: 10.1002/ece3.7352

Khan, I. U., Qi, S. S., Gul, F., Manan, S., Rono, J. K., Naz, M., et al. (2023a). A green approach used for heavy metals 'Phytoremediation' Via invasive plant species to mitigate environmental pollution: A review. *Plants* 12, 725. doi: 10.3390/plants12040725

Khan, I. U., Zhang, Y. F., Shi, X. N., Qi, S. S., Zhang, H. Y., Du, D. L., et al. (2023b). Dose dependent effect of nitrogen on the phyto extractability of Cd in metal contaminated soil using *Wedelia trilobata*. *Ecotoxicol Environ. Saf.* 264, 115419. doi: 10.1016/j.ecoenv.2023.115419

Lai, H. R., Mayfield, M. M., Gay-des-combes, J. M., Spiegelberger, T., and Dwyer, J. M. (2015). Distinct invasion strategies operating within a natural annual plant system. *Ecol. Lett.* 18, 336–346. doi: 10.1111/ele.12414

Leger, E. A., and Rice, K. J. (2003). Invasive California poppies (*Eschscholzia californica* Cham.) grow larger than native individuals under reduced competition. *Ecol. Lett.* 6, 257–264. doi: 10.1046/j.1461-0248.2003.00423.x

Li, B., Li, Q., Xiong, L., Kronzucker, H. J., Krämer, U., and Shi, W. (2012). Arabidopsis plastid AMOS1/EGY1 integrates abscisic acid signaling to regulate global gene expression response to ammonium stress. *Plant Physiol.* 160, 2040–2051. doi: 10.1104/pp.112.206508

Li, S. X., Wang, Z. H., and Stewart, B. (2013). Responses of crop plants to ammonium and nitrate N. *Adv. Agron.* 118, 205–397. doi: 10.1016/B978-0-12-405942-9.00005-0

Liu, D., Chen, L., Chen, C., Zhou, Y., Xiao, F., Wang, Y., et al. (2022). Effect of plant VOCs and light intensity on growth and reproduction performance of an invasive and a native Phytolacca species in China. *Ecol. Evol.* 12, e8522. doi: 10.1002/ece3.8522

Liu, P. C., Peacock, W. J., Wang, L., Furbank, R., Larkum, A., and Dennis, E. S. (2020). Leaf growth in early development is key to biomass heterosis in Arabidopsis. *J. Exp. Bot.* 71, 2439–2450. doi: 10.1093/jxb/eraa006

Liu, Y., and von Wirén, N. (2017). Ammonium as a signal for physiological and morphological responses in plants. *J. Exp. Bot.* 68, 2581–2592. doi: 10.1093/jxb/erx086

Meng, T. T., Wang, H., Harrison, S. P., Prentice, I. C., Ni, J., and Wang, G. (2015). Responses of leaf traits to climatic gradients: adaptive variation versus compositional shifts. *Biogeosci.* 12, 5339–5352. doi: 10.5194/bg-12-5339-2015

Miranda, R. D. S., Alvarez-Pizarro, J. C., Araújo, C. M. S., Prisco, J. T., and Gomes-Filho, E. (2013). Influence of inorganic nitrogen sources on K+/Na+ homeostasis and salt tolerance in sorghum plants. *Acta Physiologiae Plantarum* 35, 841–852. doi: 10.1007/s11738-012-1128-2

Mitryasova, O., and Koszelnic, P. (2021). *Climate Change & Sustainable Development: New Challenges of the Century*. Available online at: https://dspace.chmnu.edu.ua/jspui/handle/123456789/1120. (Accessed June 30, 2024).

Mohd Ghazi, R., Nik Yusoff, N. R., Abdul Halim, N. S., Wahab, I. R., Ab Latif, N., Hasmoni, S. H., et al. (2023). Health effects of herbicides and its current removal strategies. *Bioengineered* 14, 2259526. doi: 10.1080/21655979.2023.2259526

Mrid, R. B., Omari, R. E., and Nhiri, M. (2016). Effect of nitrogen source and concentration on growth and activity of nitrogen assimilation enzymes in roots of a moroccan sorghum ecotype. *Plant* 4, 71. doi: 10.11648/j.plant.20160406.14

Narwal, S., and Haouala, R. (2013). Role of allelopathy in weed management for sustainable agriculture. Allelopathy. *Curr. Trends Future Appl.*, 217–249. doi: 10.1007/978-3-642-30595-5

Nawaz, M., Sun, J., Shabbir, S., Khattak, W. A., Ren, G., Nie, X., et al. (2023). A review of plants strategies to resist biotic and abiotic environmental stressors. *Sci. Total Environ.*, 165832. doi: 10.1016/j.scitotenv.2023.165832

Oswald, A., Ransom, J. K., Kroschel, J., and Sauerborn, J. (2001). Transplanting maize and sorghum reduces Striga hermonthica damage. *Weed Sci.* 49, 346–353. Available at: http://www.jstor.org/stable/4046316.

Pan, L., He, F., Liang, Q., Bo, Y., Lin, X., Javed, Q., et al. (2023). Allelopathic Effects of Caffeic Acid and Its Derivatives on Seed Germination and Growth Competitiveness of Native Plants (*Lantana indica*) and Invasive Plants (*Solidago canadensis*). *Agric.* 13, 1719. doi: 10.3390/agriculture13091719

Powell, K. I., Chase, J. M., and Knight, T. M. (2013). Invasive plants have scale-dependent effects on diversity by altering species-area relationships. *Science* 339, 316–318. doi: 10.1126/science.1226817

Qi, S., Wang, J., Wan, L., Dai, Z., da Silva Matos, D. M., Du, D., et al. (2022). Arbuscular mycorrhizal fungi contribute to phosphorous uptake and allocation strategies of *Solidago canadensis* in a phosphorous-deficient environment. *Front. Plant Sci.* 13. doi: 10.3389/fpls.2022.831654

Ren, G.-Q., Li, Q., Li, Y., Li, J., Adomako, M. O., Dai, Z.-C., et al. (2019). The enhancement of root biomass increases the competitiveness of an invasive plant against a co-occurring native plant under elevated nitrogen deposition. *Flora* 261, 151486. doi: 10.1016/j.flora.2019.151486

Ren, G., Yang, B., Cui, M., Yu, H., Fan, X., Dai, Z., et al. (2022). Additive effects of warming and nitrogen addition on the performance and competitiveness of invasive *Solidago canadensis* L. *Front. Plant Sci.* 13. doi: 10.3389/fpls.2022.1017554

Roth, C. M., Shroyer, J. P., and Paulsen, G. M. (2000). Allelopathy of sorghum on wheat under several tillage systems. *Agron. J.* 92, 855–860. doi: 10.2134/agronj2000.925855x

Sanchez-Zabala, J., González-Murua, C., and Marino, D. (2015). Mild ammonium stress increases chlorophyll content in Arabidopsis thaliana. *Plant Signal Behav.* 10, e991596. doi: 10.4161/15592324.2014.991596

Sarasketa, A., González-Moro, M. B., González-Murua, C., and Marino, D. (2014). Exploring ammonium tolerance in a large panel of Arabidopsis thaliana natural accessions. *J. Exp. Bot.* 65, 6023–6033. doi: 10.1093/jxb/eru342

Shan, Z., Zhou, S., Shah, A., Arafat, Y., Rizvi, S. A. H., and Shao, H. (2023). Plant allelopathy in response to biotic and abiotic factors. *Agronomy* 13, 2358. doi: 10.3390/agronomy13092358

Shen, G., Song, Z., Xu, J., Zou, L., Huang, L., and Li, Y. (2023). Are ecosystem services provided by street trees at parcel level worthy of attention? A case study of a campus in Zhenjiang, China. *Int. J. Environ. Res. Public Health* 20, 880. doi: 10.3390/ijerph20010880

Smart, A. J., Larson, G. E., and Bauman, P. J. (2012). Grass and Canada goldenrod (*Solidago canadensis*) competition and implications for management in the northern tallgrass Prairie. *Prairie Nat.* 45, 4–12. Available at: https://digitalcommons.unl.edu/cgi/viewcontent.cgi?article=1125&context=tpn.

Smil, V. (1999). Nitrogen in crop production: An account of global flows. *Global biogeochemical cycles* 13, 647–662. doi: 10.1029/1999GB900015

Szabó, A. K., Várallyay, É., Demian, E., Hegyi, A., Galbács, Z. N., Kiss, J., et al. (2020). Local aphid species infestation on invasive weeds affects virus infection of nearest crops under different management systems–a preliminary study. *Front. Plant Sci.* 11. doi: 10.3389/fpls.2020.00684

Tian, Z., Cheng, J., Xu, J., Feng, D., Zhong, J., Yuan, X., et al. (2023). Cytogeography of naturalized *Solidago canadensis* populations in Europe. *Plants* 12, 1113. doi: 10.3390/plants12051113

Valone, T. J., and Weyers, D. P. (2019). Invasion intensity influences scale-dependent effects of an exotic species on native plant diversity. *Sci. Rep.* 9, 18769. doi: 10.1038/s41598-019-55165-z

Venkateswaran, K., Elangovan, M., and Sivaraj, N. (2019). "Origin, domestication and diffusion of *Sorghum bicolor*," in *Breeding Sorghum for diverse end uses* (Radarweg 29, 1043 NX Amsterdam, The Netherlands: Elsevier), 15–31. doi: 10.1016/B978-0-08-101879-8.00002-4

Wang, C., Cheng, H., Wang, S., Wei, M., and Du, D. (2021). Plant community and the influence of plant taxonomic diversity on community stability and invasibility: A case study based on *Solidago canadensis* L. *Sci. Total Environ.* 768, 144518. doi: 10.1016/j.scitotenv.2020.144518

Wang, S., Cheng, H. Y., Wei, M., Wu, B. D., and Wang, C. Y. (2020). Litter decomposition process dramatically declines the allelopathy of *Solidago canadensis* L. on the seed germination and seedling growth of *Lactuca sativa* L. *Int. J. Phytoremed.* 22, 1295–1303. doi: 10.1080/15226514.2020.1765140

Wang, C., Guo, L., Li, Y., and Wang, Z. (2012). Systematic comparison of C3 and C4 plants based on metabolic network analysis. *BMC Syst. Biol.* 6, 1–14. doi: 10.1186/1752-0509-6-S2-S9

Wang, R., Wan, F., and Li, B. (2017). Roles of Chinese government on prevention and management of invasive alien species. *Biol. Invasions Its Manage. China* 1, 149–156. doi: 10.1007/978-94-024-0948-2_7

Wang, W., Zhu, Q., Dai, S., Meng, L., He, M., Chen, S., et al. (2023). Effects of *Solidago canadensis* L. @ on mineralization-immobilization turnover enhance its nitrogen competitiveness and invasiveness. *Sci. Total Environ.* 882, 163641. doi: 10.1016/j.scitotenv.2023.163641

Weidenhamer, J. D. (2005). Biomimetic measurement of allelochemical dynamics in the rhizosphere. *J. Chem. Ecol.* 31, 221–236. doi: 10.1007/s10886-005-1337-x

Werner, P. A., GROSS, R. S., and BRADBURY, I. K. (1980). The biology of canadian weeds.: 45. Solidago canadensis L. *Can. J. Plant Sci.* 60, 1393–1409. doi: 10.4141/cjps80-194

Yan, P., Song, Y. H., Zhang, K. Y., Zhang, F., Tang, Y. J., Zhao, X. N., et al. (2023). Interaction of genotype-ecological type-plant spacing configuration in sorghum [*Sorghum bicolor* (L.) Moench] in China. *Front. Plant Sci.* 13. doi: 10.3389/fpls.2022.1076854

Yau, S. K., and Hamblin, J. (1994). Relative yield as a measure of entry performance in variable environments. *Crop Sci*. 34, 813–817. doi: 10.2135/cropsci1994.0011183X003400030038x

Ying, L., Maohua, M., Zhi, D., Bo, L., Ming, J., Xianguo, L., et al. (2023). Light–acquisition traits link aboveground biomass and environment in inner saline–alkaline herbaceous marshes. *Sci. Total Environ*. 857, 159660. doi: 10.1016/j.scitotenv.2022.159660

Young, K. J., and Long, S. P. (2000). Crop ecosystem responses to climatic change: maize and sorghum. *Climate Change Global Crop productivity*, 107–131. doi: 10.1079/9780851994390.0107

Yu, Y., Cheng, H., Xu, Z., Zhong, S., Wang, C., and Guo, E. (2022). Invasion intensity modulates the allelopathic impact of Solidago canadensis L. leaves and roots against Lactuca sativa L. during germination and early seedling stage. *Internat. J. Environ. Res.* 16, 48. doi: 10.1007/s41742-022-00428-3

Zeng, H., Di, T., Zhu, Y., and Subbarao, G. V. (2016). Transcriptional response of plasma membrane H+-ATPase genes to ammonium nutrition and its functional link to the release of biological nitrification inhibitors from sorghum roots. *Plant Soil* 398, 301–312. doi: 10.1007/s11104-015-2675-2

Zhang, R., Yue, Z., Chen, X., Huang, R., Zhou, Y., and Cao, X. (2023). Effects of waterlogging at different growth stages on the photosynthetic characteristics and grain yield of sorghum (*Sorghum bicolor* L.). *Sci. Rep.* 13, 7212. doi: 10.1038/s41598-023-32478-8

Zhao, D., Reddy, K. R., Kakani, V. G., and Reddy, V. R. (2005). Nitrogen deficiency effects on plant growth, leaf photosynthesis, and hyperspectral reflectance properties of sorghum. *Europ. J. Agron.* 22, 391–403. doi: 10.1016/j.eja.2004.06.005

Zhao, Q., Wang, P., Smith, G. R., Hu, L., Liu, X., Tao, T., et al. (2023). Nitrogen redistribution and seasonal trait fluctuation facilitate plant N conservation and ecosystem N retention. *J. Ecol.* 00, 1–13. doi: 10.1111/1365-2745.14246

Zucareli, V., Coelho, E., Fernandes, W., Peres, E., and Stracieri, J. (2019). Allelopathic potential of *Sorghum bicolor* at different phenological stages. *Planta daninha* 37, 1–8. doi: 10.1590/s0100-83582019370100019

frontiers | Frontiers in Plant Science

TYPE Original Research
PUBLISHED 21 November 2024
DOI 10.3389/fpls.2024.1472439



OPEN ACCESS

EDITED BY
Xiang Liu,
Lanzhou University, China

REVIEWED BY
László Erdős,
Hungarian Academy of Science, Hungary
Puchang Wang,
Guizhou Normal University, China

*CORRESPONDENCE
Haijing Shi
shihaijingcn@nwafu.edu.cn
Zhongming Wen
zmwen@ms.iswc.ac.cn

RECEIVED 29 July 2024
ACCEPTED 30 October 2024
PUBLISHED 21 November 2024

CITATION
Zheng C, Yuan L, Shi H, Duan G, Liu Y and Wen Z (2024) Understanding the impact of introduction of *Robinia pseudoacacia* on community functional structure and moisture regulation in the Loess Plateau, China, using a trait-based approach.
*Front. Plant Sci.* 15:1472439.
doi: 10.3389/fpls.2024.1472439



# Understanding the impact of introduction of *Robinia pseudoacacia* on community functional structure and moisture regulation in the Loess Plateau, China, using a trait-based approach

Cheng Zheng[1], Liuhuan Yuan[1], Haijing Shi[2,3]*, Gaohui Duan[1], Yangyang Liu[1] and Zhongming Wen[1,2]*

[1]College of Grassland Agriculture, Northwest A&F University, Yangling, Shaanxi, China, [2]Institute of Soil and Water Conservation, Chinese Academy of Sciences and Ministry of Water Resources, Yangling, Shaanxi, China, [3]Institute of Soil and Water Conservation, Northwest A&F University, Yangling, Shaanxi, China

Depending on specific environmental conditions, *Robinia pseudoacacia* plantations can have a positive or negative impact on ecosystem function. Numerous studies have demonstrated that *R. pseudoacacia* plantations on the Loess Plateau has decreased the water levels in this area, increasing the risks of water resource security. Understanding the ecosystem function of the *R. pseudoacacia* plantations is thought to be critical to vegetation restoration in the Loess Plateau. However, no consensus exists on the mechanism by which afforestation affects moisture regulation under varying environmental conditions nor on how to manage *R. pseudoacacia* plantations to maintain the ecosystem function. In this study, we used the response–effect trait approach to examine the evolving relationship between community functional composition and water regulation by collecting community samples from *R. pseudoacacia* plantations and natural ecosystems across three vegetation zones (steppe, forest–steppe, and forest). Our goal was to clarify how the afforestation of *R. pseudoacacia* impacts functional composition and, consequently, moisture regulation. The findings indicated that *R. pseudoacacia* negatively impacts community structure and moisture regulation in the drier steppe and forest-steppe ($P<0.05$). Afforestation of *R. pseudoacacia* increases specific leaf area (SLA), leaf nitrogen content (LNC), and plant height (H), while weakening the trait correlations within the community, which is the main cause of the negative effect. Furthermore, we discovered that response and effect traits overlapped (leaf tissue density, LTD) in natural ecosystems but not in afforested ecosystems within the response–effect traits framework. In conclusion, our findings indicated that the functional structure of communities and moisture regulation are impacted *R. pseudoacacia* plantations in drier habitats. Additionally, because response–effect traits do not overlap and trait coordination declines, afforestation increases instability in the moisture regulation maintenance. The introduction of *R. pseudoacacia* weakens the coordination and coupling relationships between traits. We advise giving

preference to native species over *R. pseudoacacia* for restoration in the dry steppe and forest-steppe zones. Trait-based restoration approaches can enhance the efficacy of restoration measure in achieving desired ecosystem functions.

KEYWORDS

**response-effect trait framework, degraded ecosystem, moisture regulation, diversity, afforestation, forest management**

## 1 Introduction

Afforestation has emerged as a key nature-based solution for restoring degraded(1) ecosystems worldwide (Yu et al., 2019; Lu et al., 2020; Yan et al., 2023). Since 1999, China has completed 7.07 million hectares of afforestation, with the Loess Plateau accounting for 40% of the new green area (Han et al., 2020). This large-scale afforestation has significantly altered the material and energy balance of land surface, as evidenced by decreased erosion and sedimentation, increased vegetation coverage, and regional climate change (Liu et al., 2016; Wang et al., 2016; Fang et al., 2019). However, the rapid increase in the vegetation coverage on the Loess Plateau consumed substantial water resources, and water availability is approaching its upper limit (Feng et al., 2016; Jin et al., 2019). The excessive depletion of water resources from afforestation not only jeopardizes its sustainability (Vallejo et al., 2012; Lu et al., 2018; Liu et al., 2022) but also poses great risks to social and economic development (Cao et al., 2009). As a result, understanding community structure and moisture regulation has become critical in afforestation management and ecosystem function enhancement (Benayas et al., 2009).

*Robinia pseudoacacia* was introduced to the Loess Plateau in the 1950s and quickly became a pioneer tree species for vegetation restoration due to its rapid growth and high drought tolerance (Shangguan, 2007; Wang et al., 2020). *Robinia pseudoacacia* is widely planted as a plantation species around the world. Nevertheless, there is an ongoing debate concerning the ecological value of *R. pseudoacacia* plantations (Wu et al., 2015; Zhao et al., 2017; Ho et al., 2023). On the Loess Plateau, *R. pseudoacacia* plantations frequently exhibit degraded growth during the late-successional recovery stage, such as low biomass accumulation and small tree diameters. These plantations frequently become stunted and aged, producing trees with low ecological and economic benefits (Deng et al., 2016), thus failing to meet expected ecological functions. The primary reason for the low afforestation effectiveness and high water consumption is that afforestation often fails to consider site conditions (Tölgyesi et al., 2020). Mismatching the species with site may lead to significant soil drying due to its strong water absorption capacity (Liang et al., 2018; Yang et al., 2022). A thorough understanding of the structure and function of afforested ecosystems under various site conditions is critical for reversing the negative impact of *R. pseudoacacia* afforestation and improving afforestation management practices.

The introduction of *R. pseudoacacia* alters the original community structure and site conditions, influencing moisture regulation (Sitzia et al., 2012; Slabejova et al., 2019). The effects of *R. pseudoacacia* on plant diversity and composition have attracted significant interest from ecologists and conservationists (Sitzia et al., 2012; Piwczynski et al., 2016). However, species-based studies are often too slow to detect environmental changes and fail to provide real-time insights into afforestation's impact on the ecosystem structure. In contrast to species composition, plant functional traits are more responsive to environmental changes (Koide et al., 2014; Swenson, 2016). Functional traits link individual plants to their environment (Chai et al., 2015; Funk et al., 2017). Correlations between plant functional traits have been used to identify functional constraints and trade-offs that underpin key plant ecological strategies in vegetation (Reich, 2014; Li et al., 2015). These functional traits are individual adaptations to change in in local or regional environmental gradients (Ackerly, 2004; Violle et al., 2007). Plant functional traits have been shown to be closely linked to soil moisture (Gross et al., 2008). To adapt to environmental spatial heterogeneity, individuals must adjust specific leaf area, leaf thickness, leaf dry matter content, and other traits in response to varying soil moisture conditions (Herberich et al., 2017; Li et al., 2021). Functional trait-based approaches, which focus on ecological processes and species' quick responses to environmental changes, can transcend species classifications and thus the species status in restoration ecology (Laughlin, 2014; Rosenfield and Muller, 2017). In fact, there are still very few case studies that use functional traits to guide restoration efforts in restoration ecology.

Functional traits are divided into response traits and effect traits (Violle et al., 2007). Response traits are biological characteristics related to environmental factors, such as disturbances and resources, whereas effect traits determine the impact of a species on one or more ecosystem functions (Lavorel and Garnier, 2002; Suding and Goldstein, 2008). The response–effect trait framework uses this trait classification to determine how environmental change affects plant community traits, which, in turn, may impact ecosystem functioning (Klumpp and Soussana, 2009; Solé-Senan et al., 2017; Hu et al., 2021).The response–effect trait framework is used to quantify species interactions and ecosystem functions

(Lindo, 2015; Refsland and Fraterrigo, 2017). The relationships between response and effect traits may overlap, be correlated, or be independent, depending on the context, traits, and ecosystem functions selected (Suding et al., 2008; Zirbel et al., 2017). Trait associations at the community level reveal community assembly processes, which are important for understanding community structure and functional processes (Silvertown, 2004; Kooyman et al., 2010; Gotzenberger et al., 2012). For instance, Lasky et al. (2014) found that stable niche differences related to specific leaf area and leaf dry matter content mediate competition. As a result, we present a theoretical framework based on response–effect traits, which includes both direct effects of environmental changes and the indirect effects mediated by functional traits on ecosystem functions (Figure 1). By comparing the response–effect model of *R. pseudoacacia* plantations and natural ecosystems along the same vegetation gradient, we explored the mechanisms by which *R. pseudoacacia* plantations affect moisture regulation and provided recommendations for vegetation restoration practices.

Water resource security is a primary concern in arid and semi-arid regions worldwide (Jia et al., 2017; Zhang et al., 2021). Issues caused by afforestation on the Loess Plateau have drawn widespread attention (Deng et al., 2016; Liu et al., 2018; Han et al., 2020). However, while macro-environmental changes affect water resource distribution, it remains uncertain how changes in community structure due to afforestation influence water resource distribution. There is no consensus on how to manage existing plantations to ensure long-term moisture regulation. Using the response–effect trait framework, this study compared *R. pseudoacacia* plantations and natural ecosystems (steppe, forest-steppe, and forest according to environmental gradients) in the Yanhe River Basin (YRB) of the Loess Plateau. We investigated soil moisture and community samples and relationship between the community structure and soil moisture of the *R. pseudoacacia* plantations and natural ecosystems, aiming to clarify three key issues: (1) to investigate the impact of the introduction of *R. pseudoacacia* on the vegetation community structure and moisture regulation under different vegetation zones, (2) to reveal the mechanisms by which afforestation affects moisture regulation by comparing trait associations, and (3) to use the response–effect trait framework to compare ecosystem function maintenance processes in *R. pseudoacacia* plantations and natural ecosystems.

## 2 Materials and methods

### 2.1 Study area and sampling sites

The study was conducted across the loess hilly-gullied landscape of Yanhe River Basin (YRB), which is located in the middle area of the Loess Plateau of China (latitude, 36°21′–37°19′N; longitude, 108°38′–110°29′E). It covers an area of 7,725 $km^2$ (Figure 2), with annual temperature ranging from 8.8°C to 10.2°C and annual precipitation ranging from 450 mm to 500 mm over the last decade. The spatial and temporal variation of precipitation and temperature in YRB is obvious, which affects regional vegetation distribution. The dominant vegetation types are forest, forest–steppe, and steppe. The forest zone is dominated by *Quercus mongolica*, the forest–steppe zone by *Periloca sepium* and

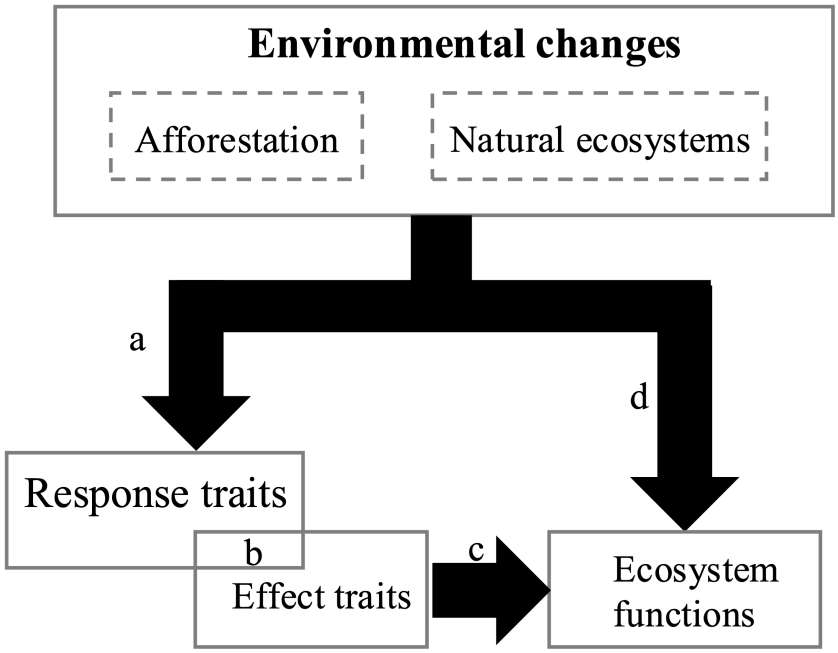


FIGURE 1
Conceptual framework of response effect traits: **(A)** environmental influence on traits. **(B)** Relationship between response traits and effect traits. **(C)** Effects traits on ecosystem function. **(D)** Independent effects of environment on ecosystem functions.

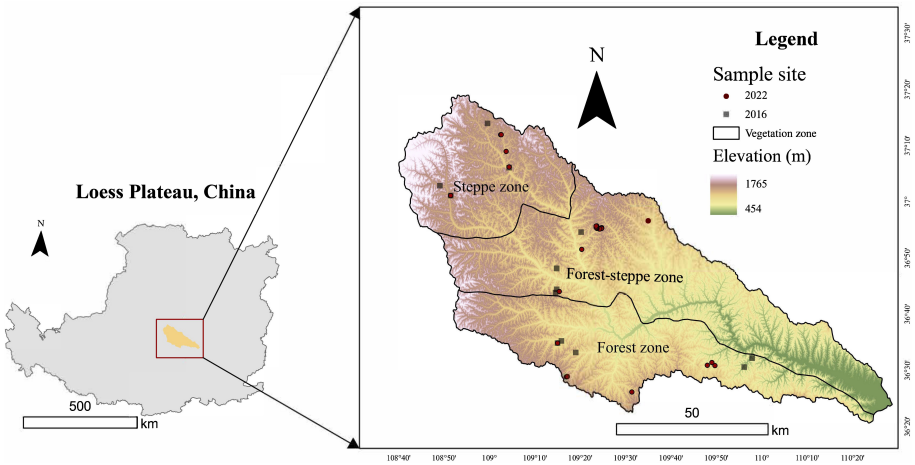


FIGURE 2
The spatial distribution map of the study sampling sites.

*Buddleja alternifolia*, and the steppe zone by *Stipa bungeana*, *Bothriochloa ischaemum*, *Poa sphondylodes*, and *Cleistogenes caespitosa*. YRB is one of the areas with the highest rate of soil and water loss on the Loess Plateau, with the soil and water loss area accounting for 80% of the basin area. The most commonly planted tree is *R. pseudoacacia*.

We selected 40 sites within the basin that had both natural ecosystems and *R. pseudoacacia* plantations in close proximity to ensure that biotic and abiotic conditions are comparable. We make sure that these natural ecosystems are far away from roads and settlements, minimizing human disturbance as much as possible. *Robinia pseudoacacia* plantations were planted more than 20 years ago and are adjacent to the natural ecosystem. Of these sites, 13 were from the 2016 field survey and 27 were from the 2022 survey. Figure 2 shows the distribution of the study sites.

## 2.2 Sampling design

For each site, we created two 10 m × 10 m plots for investigation and sampling: one for *R. pseudoacacia* plantations and the other for natural vegetation. For sampling, three 1 m ×1 m subplots were used for the herbaceous layers (arranged diagonally in the large plot) and a 5 m×5 m subplot for shrubs (positioned in the middle of the large plot).

We investigated the height, abundance, coverage, and biomass of each species in each subplot. A total of 10 leaves of each species were collected and packed into plastic bags at the plot. They were then brought to the laboratory in an icebox to be measured for the leaf area and thickness. We collected at least 20 g of leaves from the plants and put them into plastic bags. All the samples were dried at 65°C for 48 h until they reached a constant weight, after which they were crushed. Finally, the carbon, nitrogen, and phosphorus content of the leaves was measured.

To measure soil moisture, we used the S-type route to select 5 points in the plot and collected the soil samples with a soil drill at three depths (0–10 cm, 10–20 cm, and 20–40 cm). The soil samples from the same depth were then mixed, placed in plastic bags, and brought back to the laboratory.

## 2.3 Functional traits and functional diversity

To estimate the functional structure of plant communities, we focused on six growth-related functional traits: plant height (H, cm), which is associated with a plant's ability to compete for light, and specific leaf area (SLA, $mm^2/g$), leaf tissue density (LTD, $mg/mm^3$), leaf nitrogen content (LNC), leaf carbon content (LCC), and leaf phosphorus content (LPC), which indicate a species' resource-use strategy. Plant functional trait data were collected from field sampling to avoid potential confounding effects arising from within-species trait variation. Species were derived from plot-scale species, which included nearly all local dominant species and rare species.

We calculated community-weighted means [CWMs, Garnier et al. (2004)], which are the average trait values of plant communities, and reflect the importance of species. The formulas for calculating CWMs are as follows:

$$P_i = \frac{Ra+Rb+Rc}{3} \quad (1)$$

$$CWM_{ij} = \sum_{i=1}^{n} p_{ij} \times trait_{ij} \quad (2)$$

where $p_{ij}$ is the importance value of species i in plot j, Ra is the relative abundance, $R_b$ is the relative biomass, and $R_c$ is the relative coverage in plot j (Zheng et al., 2010). $Trait_{ij}$ is the mean trait value of species i in plot j and n is the number of species in the plot. Functional diversity was assessed using the quadratic entropy index and functional diversity (FRic), which quantifies the species dissimilarity based on functional trait values (Luo et al., 2019). FRic of different traits was calculated by the functional range index proposed by Mason et al. (2005). Its calculation formula is:

$$FRic = \frac{SFci}{Rc} \quad (3)$$

$SF_{ci}$ is the niche space filled by the species within the community; $R_c$ is the absolute range of the trait.

The Rao Quadratic Entropy (RaoQ) index is calculated using a distance matrix of functional traits and the relative importance value of species, where d*ij* represents the difference in functional traits between species i and j, and Pi and Pj represent the relative abundance of species i and j, respectively.

$$RaoQ = \sum_{i=1}^{S}\sum_{j=1}^{S} d_{ij}p_i p_j \quad (4)$$

## 2.4 Statistical analysis

To assess the impact of introduction of *R. pseudoacacia* on plant community structure and soil moisture, we compared the soil moisture, functional traits, and diversity between *R. pseudoacacia* plantations and natural ecosystems, within each vegetation zone separately, using *t*-test. To assess the effect of major environmental gradients, we compared the soil moisture, functional traits, and diversity among the three vegetation zones (steppe vs. forest–steppe vs. forest), for both the *R. pseudoacacia* plantations and natural ecosystems separately, using homogeneity test of variance and ANOVA. The Pearson correlation coefficient was used to analyze trait association. The response–effects framework is built using mixed-effects models that look at both response and effect traits. To detect response traits, the change of vegetation zone was used as a fixed effect, and different years were used as a random effect to explain the non-independence of time effects, and various traits were tested. We estimated the parameters using restricted maximum likelihood estimation to, and we tested the model's significance with the chi-square test. In the effect trait test, we used the MuMIn package to build a complete model including all of the traits tested. The lme4 package was used to complete the mixed effect model, and the optimal model is chosen using the Akaike Information Criterion (AIC) (Zuur et al., 2010). All statistical analyses were conducted using R.

# 3 Results

## 3.1 Functional composition and soil moisture distribution

In comparison to natural ecosystems, *R. pseudoacacia* plantations had significantly lower soil moisture in all vegetation zones ($p<0.05$) (Figure 3A). In terms of functional diversity, we found that FRic of natural ecosystems are higher than that of *R. pseudoacacia* plantations in all zones, and RaoQ of natural ecosystems are higher in the steppe. Moreover, CWM.SLA and CWM.LNC are smaller in natural ecosystems than in *R. pseudoacacia* plantations in all zones; CWM.LCC is higher in natural ecosystems than in *R. pseudoacacia* plantations in the forest–steppe, CWM.LPC is smaller in natural ecosystems than in *R. pseudoacacia* plantations in the forest, and CWM.LTD is bigger in natural ecosystems than in *R. pseudoacacia* plantations in the steppe.

## 3.2 Trait association

We found varying degrees of correlation between CWM trait values across our ecosystems (Figure 4). In *R. pseudoacacia* plantations, CWM.LPC was negatively correlated with CWM.H and CWM.LTD, positively correlated with CWM.SLA and CWM.LNC, and CWM.LTD was negatively correlated with CWM.SLA, while CWM.H and CWM.SLA were positively correlated. In natural ecosystems, there is also a close correlation between leaf stoichiometry (CWM.LCC is positively correlated with CWM.LNC and CWM.LPC) and plant height (CWM.H was positively correlated with CWM.LNC and CWM.LPC) ($P<0.05$).

## 3.3 Responses of soil moisture and functional indicators to vegetation zones

Vegetation zones influence community functional structure of natural ecosystems (from steppe to forest). We found that soil moisture content and functional diversity metrics were lower in the steppe zone than in the forest zone (Figure 3). The mixed effects model shows that vegetation zone gradient was positively correlated with FRic and RaoQ, while CWM.H and CWM.SLA are negatively correlated with CWM.LTD and CWM.LPC. Other traits were not significant in the full model ($p < 0.05$) (Table 1).

The relationship between functional traits of *R. pseudoacacia* plantations along the vegetation zones is similar to that of natural ecosystems, with the exception of CWM.LTD and CWM.LPC, which were not significant in the full model test ($p < 0.05$) (Table 1).

## 3.4 Effect of functional diversity and functional traits to soil moisture

A full mixed-effects model that integrated functional diversity and functional traits revealed that higher CWM.LTD was associated with lower soil moisture in natural ecosystems. Functional diversity (FRic) had a positive effect on soil moisture in the *R. pseudoacacia* plantations, while CWM.LNC had a negative effect ($p < 0.05$) (Table 2).

# 4 Discussion

Understanding how community functional structure determines ecosystem function is a major goal of restoration ecology (Yang et al., 2019). Manipulating community structure to achieve functional goals is a key aspect of restoring degraded ecosystem (Laughlin, 2014). We present, to our knowledge, the

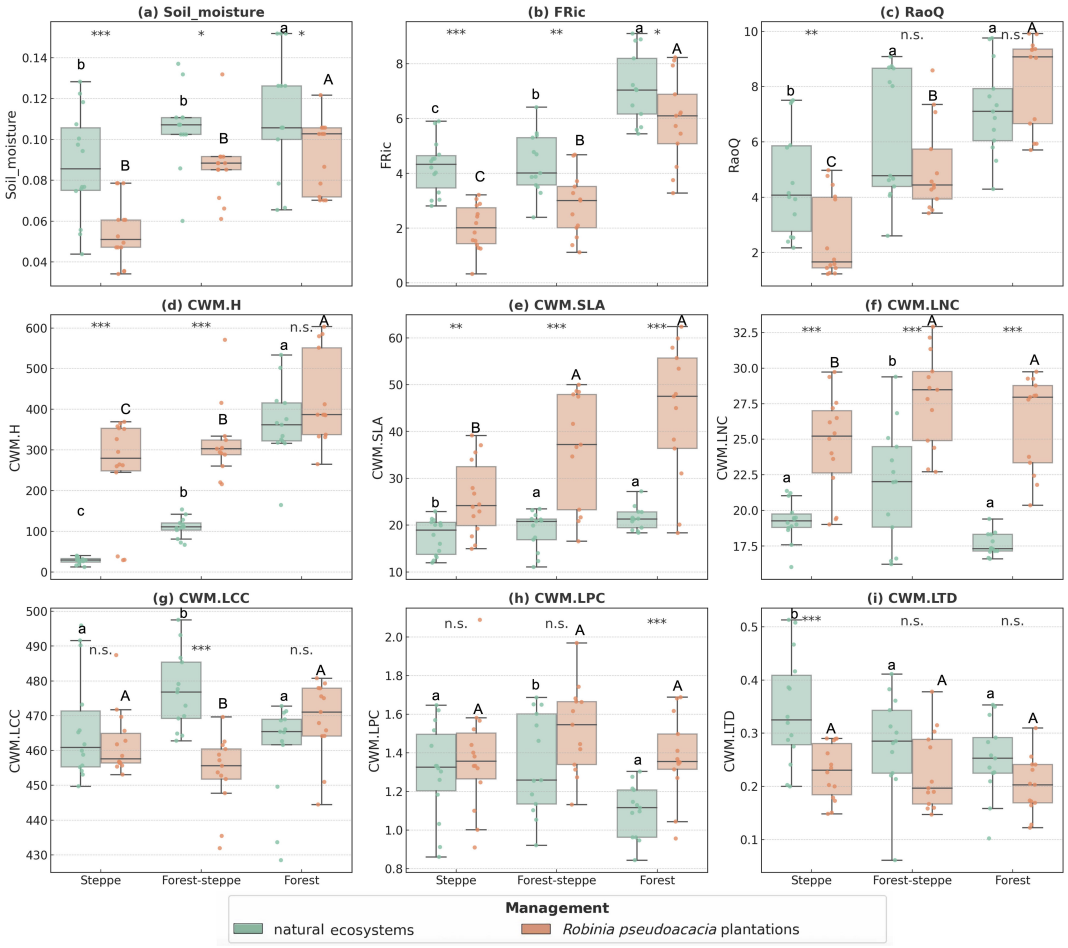


FIGURE 3
Functional composition indices and soil moisture distribution of *Robinia pseudoacacia* plantations and natural ecosystems. *, **, and *** indicate that the difference are significant at $p < 0.05$, $p < 0.01$ and $p < 0.001$. The same below. Lowercase and capital letters denote the variations among the vegetation zones for both natural ecosystems and plantations, separately. Panels **(A)** Soil moisture, **(B)** FRic, **(C)** RaoQ, **(D)** CWM.H, **(E)** CWM.SLA, **(F)** CWM.LNC, **(G)** CWM.LCC, **(H)** CWM.LPC and **(I)** CWM.LTD.

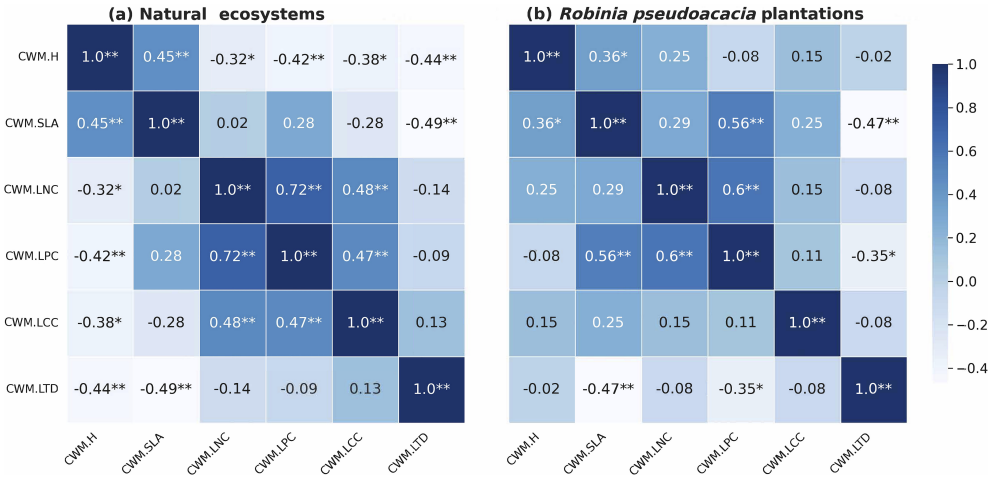


FIGURE 4
Correlogram of CWM metrics Pearson correlation. Correlation coefficients are shown in color and significance is marked. * and ** indicate the difference are significant at $P < 0.05$ and $P < 0.01$. Panels **(A, B)** represent the natural ecosystems and the *Robinia pseudoacacia* plantations, respectively.

TABLE 1 Linear mixed effect models testing the response of functional traits and functional diversity of (a) natural ecosystems and (b) *Robinia pseudoacacia* plantations to vegetation zones.

| Response variable | RaoQ | FRic | CWM.H | CWM.SLA | CWM.LTD | CWM.LCC | CWM.LNC | CWM.LPC |
|---|---|---|---|---|---|---|---|---|
| (a) Natural ecosystems | **1.28 (<0.01)** | **1.43 (<0.01)** | **167.79 (<0.01)** | **1.81(<0.01)** | **−0.04 (0.01)** | −2.98(0.30) | −0.81(0.16) | **−0.11 (<0.01)** |
| (b) *Robinia pseudoacacia* plantations | **2.82 (<0.01)** | **1.96 (<0.01)** | **87.08(<0.01)** | **8.72(<0.01)** | −0.01(0.29) | 3.29(0.15) | 0.82(0.24) | −0.01(0.90) |

Estimates of coefficients, their 95% intervals (in parentheses), with bold indicating statistical significance ($p < 0.05$).

TABLE 2 Linear mixed effect models testing the response of functional diversity and functional traits of (a) natural ecosystems and (b) *Robinia pseudoacacia* plantations to soil moisture (log-transformed).

| Response variable | RaoQ | Fric | CWM.H | CWM.SLA | CWM.LTD | CWM.LCC | CWM.LNC | CWM.LPC |
|---|---|---|---|---|---|---|---|---|
| natural ecosystems | 0.003 (0.17) | 0.005 (0.15) | −0.0001(0.03) | −0.004 (0.10) | **−0.17 (<0.01)** | −0.0005(0.27) | −0.0003(0.92) | −0.06 (0.18) |
| *Robinia pseudoacacia* plantations | 1.580e−03 (0. 30) | **6.168e −03(<0.01)** | −2.867e −05 (0.29) | 5.615e −04 (0.20) | 6.461e −02 (0.18) | **−1.085e −03 (<0.01)** | 1.781e −03 (0.09) | −2.452e −02 (0.18) |

Estimates of coefficients, their 95% intervals (in parentheses), with bold indicating statistical significance ($p < 0.05$).

first response–effect trait framework that integrates *R. pseudoacacia* plantations and natural ecosystems. Using quantitative trait-based approaches to explain community structure and ecosystem function yields more generalizable predictable outcome (Cadotte, 2017). First, we used natural ecosystems as a reference to investigate the effects of afforestation on community structure and moisture regulation in different vegetation zones. Afforestation alters the relationship between community structure and soil moisture, indicating that it has an impact on ecosystem. Second, we detected differences in trait correlations between natural ecosystems and *R. pseudoacacia* plantations, indicating that afforestation affects the community assembly and, consequently, ecosystem function. This finding provides important implications for understanding the relationship between community structure and ecosystem function. Finally, we used a mixed effects model to construct a response–effect trait framework for both ecosystems, which can support ecosystem management and restoration efforts, ultimately resulting in the desired ecosystem functions.

## 4.1 Effects of afforestation on community structure and soil moisture

Soil moisture varied significantly between vegetation zones. In most cases, we found the highest soil moisture in the forest zone and the lowest soil moisture in the steppe zone, indicating the spatial heterogeneity of regional precipitation (Yuan et al., 2023). Additionally, soil moisture in *R. pseudoacacia* plantations was significantly lower than in natural ecosystems across three vegetation zones, which is consistent with reports by Deng et al. (2016) and Dang et al. (2022). Afforestation is likely to coincide with the desiccation of deeper soil layers, leading to insufficient ground water recharge (Tölgyesi et al., 2020). One explanation is that *R. pseudoacacia* has larger roots and absorb more water for growth (Perez-Harguindeguy et al., 2013). Another explanation is that *R. pseudoacacia* has a larger canopy and broader leaves than native species, trapping rainfall and increasing evapotranspiration (Yang et al., 2014). We found that the overconsumption of water due to afforestation was more pronounced in arid steppe zone than in forest zone.

*Robinia pseudoacacia* plantations reduced functional diversity (FRic) in the relatively arid steppe and forest–steppe zones. *Robinia pseudoacacia* is an alien species that competes for resources and absorbs more water than native species (Weiher et al., 1999; Su and Shangguan, 2019). Ho et al. (2023) found that the *R. pseudoacacia* plantations had lower Shannon diversity and functional diversity than near-natural forests. The introduction of *R. pseudoacacia* altered resource allocation within the community, leading to changes in its functional structure (Cierjacks et al., 2013). In the arid loess hilly areas, water resource competition largely determines community composition. On the other hand, the introduction of *R. pseudoacacia* alters both biological and abiotic habitat environment, affecting factors such as soil microbial communities and microclimates (Zhou et al., 2022; Zhang et al., 2023). The functional diversity in afforested ecosystems is lower than in natural ecosystems, indicating that the *R. pseudoacacia* exerts a strong filtering effect on community structure (Pysek et al., 2012). In the forest zones, however, the impact of *R. pseudoacacia* plantations on functional diversity is comparable to that of natural ecosystems. This is consistent with the findings of Hu et al. (2021), indicating that *R. pseudoacacia* is expected to have less negative effect in environments with better hydrothermal conditions. To avoid depletion of water resource, we advocate for reducing the area of *R. pseudoacacia* plantations in arid areas.

The effects of afforestation on plant community structure and moisture regulation are closely related to plant functional traits (Qin et al., 2016). Non-native species have functional traits that differ from native species (Dyderski and Jagodzinski, 2019). Our findings showed that *R. pseudoacacia* plantations had higher CWM.SLA, CWM.H, CWM.LNC, and CWM.LPC than natural ecosystems. The values of these functional traits indicate how adaptable a species is to its surroundings (Cornelissen et al., 2003). Significant differences in functional traits were also noted

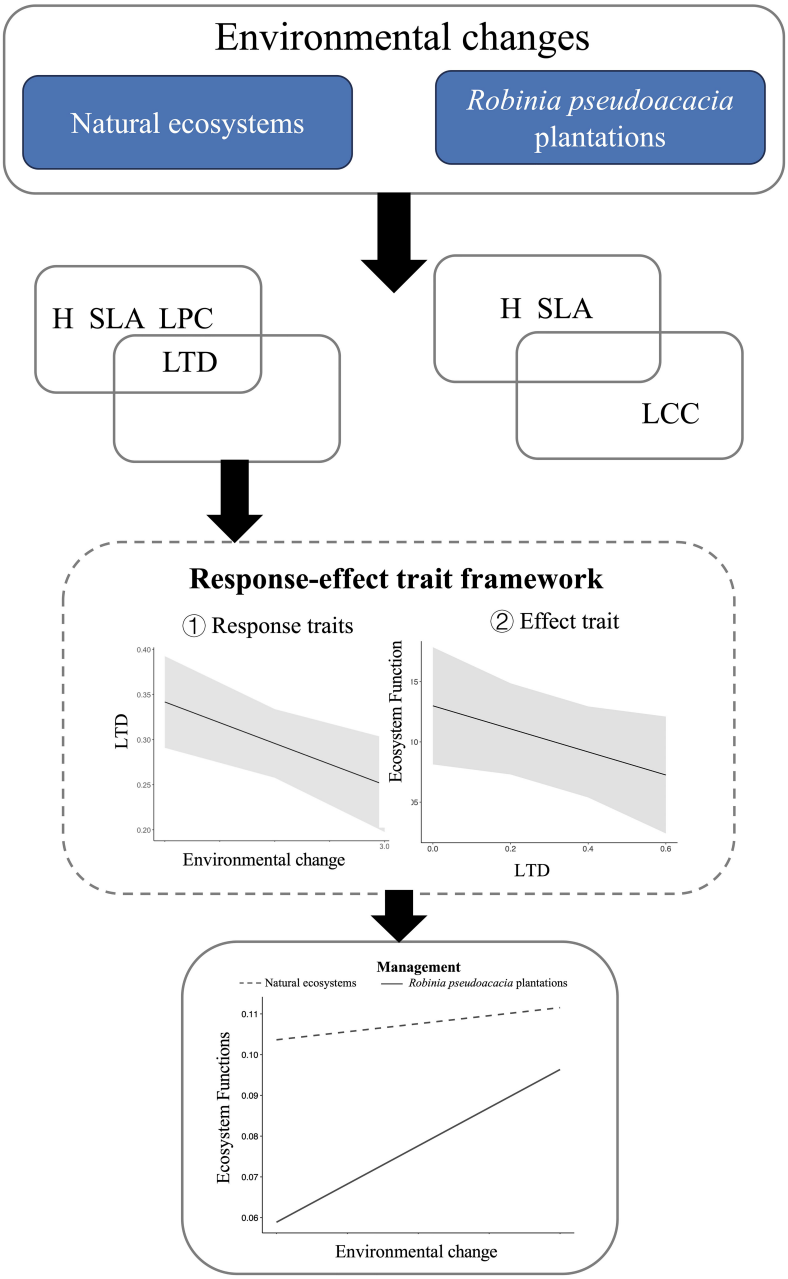


FIGURE 5
Summary of the effects of afforestation on changes in water resource availability, based on a response effect trait framework.

across different vegetation zones, indicating that plant communities in these zones use distinct functional trait strategies to adapt to environmental variation (Luo et al., 2016; Ahrens et al., 2020). In comparison to forest zone, *R. pseudoacacia* plantations usually had a lower CWM.SLA in the arid steppe zone. Our hypothesis was that by affecting the community resource allocation in the steppe zone, *R. pseudoacacia* plantations may shifted the investment strategy of leaves from conservative to economical one. In addition, the environment conditions of different vegetation zones determine how *R. pseudoacacia* plantations impact the structure of plant communities. In the arid steppe zone with poor habitat conditions, *R. pseudoacacia* plantations had the most significant effect on soil moisture and functional diversity. In contrast, in the forest zone, where water conditions were favorable, the effects of *R. pseudoacacia* plantations were weak or even negligible. This suggests that *R. pseudoacacia's* strong water-competitive ability under poor water conditions likely suppresses the native plant growth and interferes with the functioning of ecosystem. However, in the more resource-rich forest zone, the water scarcity is reduced, reducing *R. pseudoacacia*'s competitive advantage. In these conditions, *R. pseudoacacia* may even promote nutrient cycling and enhance ecosystem functions. This study highlights

the risks of afforestation without considering habitat conditions and the traits of introduced species. It is essential to assess the ecological impacts of introduced species under changing environmental conditions to develop effective afforestation management strategies that enhance ecosystem service value.

## 4.2 Effect of afforestation on trait associations

Plant functional strategies are typically achieved through the simultaneous expression of various traits, and their associations are likely shaped by environmental filtering (Candeias and Fraterrigo, 2020). The coordinated expression of functional traits has an adaptive value, particularly when it comes to optimizing traits to water conservation. Numerous investigations have demonstrated that resource-limited environments restrict the variation and distribution of plant functional traits (Laliberté et al., 2014). Plants often adopt traits combinations to cope with environmental stresses (He et al., 2020). In arid hilly areas, stable correlations between sets of traits are common (Yin et al., 2018). In the natural ecosystems of the loess hilly region, the content of nitrogen and phosphorus in leaves changes closely and synergistically, which is consistent with the prediction of plant ecological stoichiometric theory: to achieve functional balance during plant growth, nitrogen and phosphorus must be coupled to form a stable nitrogen and phosphorus ratio (Gusewell, 2004). In addition, Burns and Beaumont (2009) discovered a coupling relationship between the maximum plant height and the leaf economic traits. The reason may be that the complex terrain in hilly areas affects the distribution of water and heat factors, which in turn affects plant photosynthesis and drought resistance adaptation mechanisms. However, the relationships among functional traits in *R. pseudoacacia* plantations were significantly weaker than those in natural ecosystems. The reason is that *R. pseudoacacia*, a nitrogen-fixing plant, disrupts ecosystem's nutrient cycle, weakening the coordination between leaf chemical traits, especially the decoupling leaf nitrogen content with phosphorus content in *R. pseudoacacia* plantations.

## 4.3 Response–effect trait framework

In this study, we employed a response–effect trait framework to identify which combinations of functional trait structures achieve desired ecological benefits in *R. pseudoacacia* plantations ecosystems and natural ecosystems. In natural ecosystems, most leaf morphological traits responded significantly to environmental changes, as previously reported (Guo et al., 2021; Zheng et al., 2024). This is not surprising given that environment filtering is associated with functional traits (Lebrija-Trejos et al., 2010). Leaf functional traits either increased or decreased along the vegetation zone gradient. The introduction of *R. pseudoacacia* altered the relationship between some traits and the vegetation gradient. For instance, the significant relationships involving CWM.LTD and CWM.LPC disappeared. Regarding the effect traits, only CWM.LTD was significantly associated with soil moisture in the natural ecosystems, while no significant association was found between any functional trait and soil moisture in the *R. pseudoacacia* plantations.

In this study, the response–effect trait framework for natural ecosystems revealed that CWM.LTD is a functional trait in which response traits and effect traits overlap. To avoid excessive consumption of water resources in natural ecosystems, a combination of species with CWM.LTD as small as possible should be selected. Furthermore, species with small LTD may be able to adapt to environmental changes. Nevertheless, afforestation is more likely to increase water resource consumption and impact moisture regulation in the drier steppe and forest–steppe zones of the YRB (Figure 5). In *R. pseudoacacia* plantations, we did not find any trait that would be a response trait and an effect trait simultaneously. Currently, the response–effect trait framework in *R. pseudoacacia* plantations is more about the diversity of multiple functional traits rather than single functional traits. This framework proposed a management strategy for the existing problem of afforestation ecosystems in the Loess Plateau, namely, selecting specific components with high functional diversity to reduce the excessive consumption of water resources or reducing the planting area of *R. pseudoacacia* plantations.

The correlation between response traits and effect traits is crucial for understanding how community assembly processes indirectly affect ecosystem functions (Zirbel et al., 2017). When response and effect traits are identical or related, predictability can be established based on the relationship between trait set and functions (Lavorel and Garnier, 2002). In degraded ecosystems, restoration practitioners can use management techniques to modify specific environmental conditions to achieve targeted ecosystem services (Fu et al., 2023). However, response and effect traits may not be correlated, limiting the ability to predict ecosystem functions. For example, in *R. pseudoacacia* plantations, we found no effect traits associated with response traits. In such cases, predicting moisture regulation based on commonly measured functional traits or trait response mechanisms may not be possible. Future work should consider additional traits that may influence community assembly and ecosystem functions, for example, root traits and taxonomic traits. *Robinia pseudoacacia* is not the only tree species used for revegetation in YRB. One of the urgent tasks in ecology research is comparing the ecological value of afforestation with different species.

# 5 Conclusions

The introduction of *R. pseudoacacia* has a significant influence on the functional structure and moisture regulation of the dry steppe and forest–steppe zones. Our results showed that *R. pseudoacacia* plantations affected the distribution of traits and weakened the correlation between traits compared to the natural ecosystems, affecting community structure and moisture regulation. In addition, we propose a practical transformation scheme for forest management to achieve ecosystem functional expectations by introducing a trait response–effect framework for both natural ecosystems and *R. pseudoacacia* plantations, despite the fact that

our findings did not find response–effect traits in *R. pseudoacacia* plantations. The afforestation area of *R. pseudoacacia* plantations in the steppe and the forest–steppe zones must be reduced if soil moisture balance is to be maintained during ecological restoration.

## Data availability statement

The original contributions presented in the study are included in the article/supplementary material, further inquiries can be directed to the corresponding authors.

## Author contributions

CZ: Writing – original draft, Conceptualization, Data curation, Formal analysis, Funding acquisition, Investigation, Methodology, Project administration, Resources, Software, Supervision, Validation, Visualization, Writing – review & editing. ZW: Conceptualization, Writing – review & editing, Writing – original draft. LY: Investigation, Methodology, Supervision, Conceptualization, Data curation, Formal analysis, Project administration, Software, Validation, Writing – review & editing. HS: Data curation, Methodology, Writing – review & editing. GD: Conceptualization, Resources, Software, Writing – review & editing. YL: Formal analysis, Funding acquisition, Resources, Visualization, Writing – original draft.

## Funding

The author(s) declare that financial support was received for the research, authorship, and/or publication of this article. This study was financially supported by the CAS 'light of West China' program (XAB2020YN04) and the Natural Science Foundation of China (41977077 and41671289).

## Acknowledgments

We would like to thank Kai Tan and Yandan Liu for providing help of English writing. We gratefully acknowledge the data support from the Loess Plateau Science Data Center, National Earth System Science Data Sharing Infrastructure, National Science & Technology Infrastructure of China (http://loess.geodata.cn). Special thanks to the reviewers whose constructive feedback significantly improved the quality of this manuscript.

## Conflict of interest

The authors declare that the research was conducted in the absence of any commercial or financial relationships that could be construed as a potential conflict of interest.

## Publisher's note



## References

Ackerly, D. (2004). Functional strategies of chaparral shrubs in relation to seasonal water deficit and disturbance. *Ecol. Monogr.* 74, 25–44. doi: 10.1890/03-4022

Ahrens, C. W., Andrew, M. E., Mazanec, R. A., Ruthrof, K. X., Challis, A., Hardy, G., et al. (2020). Plant functional traits differ in adaptability and are predicted to be differentially affected by climate change. *Ecol. Evol.* 10, 232–248. doi: 10.1002/ece3.5890

Benayas, J. M. R., Newton, A. C., Diaz, A., and Bullock, J. M. (2009). Enhancement of biodiversity and ecosystem services by ecological restoration: A meta-analysis. *Science* 325, 1121–1124. doi: 10.1126/science.1172460

Burns, K. C., and Beaumont, S. (2009). Scale-dependent trait correlations in a temperate tree community. *Austral Ecol.* 34, 670–677. doi: 10.1111/j.1442-9993.2009.01973.x

Cadotte, M. W. (2017). Functional traits explain ecosystem function through opposing mechanisms. *Ecol. Lett.* 20, 989–996. doi: 10.1111/ele.12796

Candeias, M., and Fraterrigo, J. (2020). Trait coordination and environmental filters shape functional trait distributions of forest understory herbs. *Ecol. Evol.* 10, 14098–14112. doi: 10.1002/ece3.7000

Cao, S. X., Chen, L., and Yu, X. X. (2009). Impact of China's Grain for Green Project on the landscape of vulnerable arid and semi-arid agricultural regions: a case study in northern Shaanxi Province. *J. Appl. Ecol.* 46, 536–543. doi: 10.1111/j.1365-2664.2008.01605.x

Chai, Y. F., Zhang, X. F., Yue, M., Liu, X., Li, Q., Shang, H. L., et al. (2015). Leaf traits suggest different ecological strategies for two Quercus species along an altitudinal gradient in the Qinling Mountains. *J. For. Res.* 20, 501–513. doi: 10.1007/s10310-015-0496-z

Cierjacks, A., Kowarik, I., Joshi, J., Hempel, S., Ristow, M., von der Lippe, M., et al. (2013). Biological flora of the british isles: robinia pseudoacacia. *J. Ecol.* 101, 1623–1640. doi: 10.1111/1365-2745.12162

Cornelissen, J. H. C., Cerabolini, B., Castro-Diez, P., Villar-Salvador, P., Montserrat-Marti, G., Puyravaud, J. P., et al. (2003). Functional traits of woody plants: correspondence of species rankings between field adults and laboratory-grown seedlings? *J. Vegetation Sci.* 14, 311–322. doi: 10.1111/j.1654-1103.2003.tb02157.x

Dang, H., Li, J. H., Xu, J. S., Chu, G. C., Zhang, J., Yu, Y. L., et al. (2022). Differences in soil water and nutrients under catchment afforestation and natural restoration shape herbaceous communities on the Chinese Loess Plateau. *For. Ecol. Manage.* 505, 119925. doi: 10.1016/j.foreco.2021.119925

Deng, L., Yan, W. M., Zhang, Y. W., and Shangguan, Z. P. (2016). Severe depletion of soil moisture following land-use changes for ecological restoration: Evidence from northern China. *For. Ecol. Manage.* 366, 1–10. doi: 10.1016/j.foreco.2016.01.026

Dyderski, M. K., and Jagodzinski, A. M. (2019). Functional traits of acquisitive invasive woody species differ from conservative invasive and native species. *Neobiota* 41), 91–113. doi: 10.3897/neobiota.41.31908

Fang, W., Huang, S. Z., Huang, Q., Huang, G. H., Wang, H., Leng, G. Y., et al. (2019). Probabilistic assessment of remote sensing-based terrestrial vegetation vulnerability to drought stress of the Loess Plateau in China. *Remote Sens. Environ.* 232, 111290. doi: 10.1016/j.rse.2019.111290

Feng, X. M., Fu, B. J., Piao, S., Wang, S. H., Ciais, P., Zeng, Z. Z., et al. (2016). Revegetation in China's Loess Plateau is approaching sustainable water resource limits. *Nat. Climate Change* 6, 1019–101+. doi: 10.1038/nclimate3092

Fu, D. G., Wu, X. N., Hu, L. Y., Ma, X. D., Shen, C. J., Shang, H. Y., et al. (2023). Plant traits guide species selection in vegetation restoration for soil and water conservation. *Biology-Basel* 12, 618. doi: 10.3390/biology12040618

Funk, J. L., Larson, J. E., Ames, G. M., Butterfield, B. J., Cavender-Bares, J., Firn, J., et al. (2017). Revisiting the Holy Grail: using plant functional traits to understand ecological processes. *Biol. Rev.* 92, 1156–1173. doi: 10.1111/brv.12275

Garnier, E., Cortez, J., Billès, G., Navas, M. L., Roumet, C., Debussche, M., et al. (2004). Plant functional markers capture ecosystem properties during secondary succession. *Ecology* 85, 2630–2637. doi: 10.1890/03-0799

Gotzenberger, L., de Bello, F., Brathen, K. A., Davison, J., Dubuis, A., Guisan, A., et al. (2012). Ecological assembly rules in plant communities-approaches, patterns and prospects. *Biol. Rev.* 87, 111–127. doi: 10.1111/j.1469-185X.2011.00187.x

Gross, N., Robson, T. M., Lavorel, S., Albert, C., Le Bagousse-Pinguet, Y., and Guillemin, R. (2008). Plant response traits mediate the effects of subalpine grasslands on soil moisture. *New Phytol.* 180, 652–662. doi: 10.1111/j.1469-8137.2008.02577.x

Guo, Q., Wen, Z. M., Zheng, C., Li, W., Fan, Y. M., and Zhu, D. J. (2021). Effects of Robinia pseudoacacia on the undergrowth of herbaceous plants and soil properties in the Loess Plateau of China. *J. Plant Ecol.* 14, 896–910. doi: 10.1093/jpe/rtab041

Gusewell, S. (2004). N: P ratios in terrestrial plants: variation and functional significance. *New Phytol.* 164, 243–266. doi: 10.1111/j.1469-8137.2004.01192.x

Han, Z. M., Huang, S. Z., Huang, Q., Bai, Q. J., Leng, G. Y., Wang, H., et al. (2020). Effects of vegetation restoration on groundwater drought in the Loess Plateau, China. *J. Hydrology* 591, 125566. doi: 10.1016/j.jhydrol.2020.125566

He, N. P., Li, Y., Liu, C. C., Xu, L., Li, M. X., Zhang, J. H., et al. (2020). Plant trait networks: improved resolution of the dimensionality of adaptation. *Trends Ecol. Evol.* 35, 908–918. doi: 10.1016/j.tree.2020.06.003

Herberich, M. M., Gayler, S., Anand, M., and Tielborger, K. (2017). Hydrological niche segregation of plant functional traits in an individual-based model. *Ecol. Model.* 356, 14–24. doi: 10.1016/j.ecolmodel.2017.04.002

Ho, K. V., Kröel-Dulay, G., Tölgyesi, C., Bátori, Z., Tanács, E., Kertész, M., et al. (2023). Non-native tree plantations are weak substitutes for near-natural forests regarding plant diversity and ecological value. *For. Ecol. Manage.* 531, 120789. doi: 10.1016/j.foreco.2023.120789

Hu, S., Jiao, J., Kou, M., Wang, N., Garcia-Fayos, P., and Liu, S. (2021). Quantifying the effects of Robinia pseudoacacia afforestation on plant community structure from a functional perspective: New prospects for management practices on the hilly and gullied Loess Plateau, China. *Sci. Total Environ.* 773, 144878. doi: 10.1016/j.scitotenv.2020.144878

Jia, X. X., Wang, Y. Q., Shao, M. A., Luo, Y., and Zhang, C. C. (2017). Estimating regional losses of soil water due to the conversion of agricultural land to forest in China's Loess Plateau. *Ecohydrology* 10, 1851. doi: 10.1002/eco.1851

Jin, Z., Guo, L., Fan, B. H., Lin, H., Yu, Y. L., Zheng, H., et al. (2019). Effects of afforestation on soil and ambient air temperature in a pair of catchments on the Chinese Loess Plateau. *Catena* 175, 356–366. doi: 10.1016/j.catena.2018.12.036

Klumpp, K., and Soussana, J. F. (2009). Using functional traits to predict grassland ecosystem change: a mathematical test of the response-and-effect trait approach. *Global Change Biol.* 15, 2921–2934. doi: 10.1111/j.1365-2486.2009.01905.x

Koide, R. T., Fernandez, C., and Malcolm, G. (2014). Determining place and process: functional traits of ectomycorrhizal fungi that affect both community structure and ecosystem function. *New Phytol.* 201, 433–439. doi: 10.1111/nph.12538

Kooyman, R., Cornwell, W. K., and Westoby, M. (2010). Plant functional traits in Australian subtropical rain forest: partitioning within-community from cross-landscape variation. *J. Ecol.* 98, 517–525. doi: 10.1111/j.1365-2745.2010.01642.x

Laliberté, E., Zemunik, G., and Turner, B. L. (2014). Environmental filtering explains variation in plant diversity along resource gradients. *Science* 345, 1602–1605. doi: 10.1126/science.1256330

Lasky, J. R., Uriarte, M., Boukili, V. K., and Chazdon, R. L. (2014). Trait-mediated assembly processes predict successional changes in community diversity of tropical forests. *Proc. Natl. Acad. Sci. United States America* 111, 5616–5621. doi: 10.1073/pnas.1319342111

Laughlin, D. C. (2014). Applying trait-based models to achieve functional targets for theory-driven ecological restoration. *Ecol. Lett.* 17, 771–784. doi: 10.1111/ele.12288

Lavorel, S., and Garnier, E. (2002). Predicting changes in community composition and ecosystem functioning from plant traits: revisiting the Holy Grail. *Funct. Ecol.* 16, 545–556. doi: 10.1046/j.1365-2435.2002.00664.x

Lebrija-Trejos, E., Perez-Garcia, E. A., Meave, J. A., Bongers, F., and Poorter, L. (2010). Functional traits and environmental filtering drive community assembly in a species-rich tropical system. *Ecology* 91, 386–398. doi: 10.1890/08-1449.1

Li, L., McCormack, M. L., Ma, C. G., Kong, D. L., Zhang, Q., Chen, X. Y., et al. (2015). Leaf economics and hydraulic traits are decoupled in five species-rich tropical-subtropical forests. *Ecol. Lett.* 18, 899–906. doi: 10.1111/ele.12466

Li, S. J., Wang, H., Gou, W., White, J. F., Kingsley, K. L., Wu, G. Q., et al. (2021). Leaf functional traits of dominant desert plants in the Hexi Corridor, Northwestern China: Trade-off relationships and adversity strategies. *Global Ecol. Conserv.* 28, e01666. doi: 10.1016/j.gecco.2021.e01666

Liang, H. B., Xue, Y. Y., Li, Z. S., Wang, S., Wu, X., Gao, G. Y., et al. (2018). Soil moisture decline following the plantation of forests: Evidence from the Loess Plateau. *For. Ecol. Manage.* 412, 62–69. doi: 10.1016/j.foreco.2018.01.041

Lindo, Z. (2015). Linking functional traits and network structure to concepts of stability. *Community Ecol.* 16, 48–54. doi: 10.1556/168.2015.16.1.6

Liu, H. Y., Xu, C. Y., Allen, C. D., Hartmann, H., Wei, X. H., Yakir, D., et al. (2022). Nature-based framework for sustainable afforestation in global drylands under changing climate. *Global Change Biol.* 28, 2202–2220. doi: 10.1111/gcb.16059

Liu, Y., Miao, H. T., Huang, Z., Cui, Z., He, H. H., Zheng, J. Y., et al. (2018). Soil water depletion patterns of artificial forest species and ages on the Loess Plateau (China). *For. Ecol. Manage.* 417, 137–143. doi: 10.1016/j.foreco.2018.03.005

Liu, Z. P., Wang, Y. Q., Shao, M. G., Jia, X. X., and Li, X. L. (2016). Spatiotemporal analysis of multiscalar drought characteristics across the Loess Plateau of China. *J. Hydrology* 534, 281–299. doi: 10.1016/j.jhydrol.2016.01.003

Lu, C. X., Zhao, T. Y., Shi, X. L., and Cao, S. X. (2018). Ecological restoration by afforestation may increase groundwater depth and create potentially large ecological and water opportunity costs in arid and semiarid China. *J. Cleaner Production* 176, 1213–1222. doi: 10.1016/j.jclepro.2016.03.046

Lu, J. B., Wang, H., Qin, S. H., Cao, L., Pu, R. L., Li, G. L., et al. (2020). Estimation of aboveground biomass of forest in the Yellow River Delta based on UAV and Backpack LiDAR point clouds. *Int. J. Appl. Earth Observation Geoinformation* 86, 102014. doi: 10.1016/j.jag.2019.102014

Luo, Y. H., Cadotte, M. W., Burgess, K. S., Liu, J., Tan, S. L., Zou, J. Y., et al. (2019). Greater than the sum of the parts: how the species composition in different forest strata influence ecosystem function. *Ecol. Lett.* 22, 1449–1461. doi: 10.1111/ele.13330

Luo, Y. J., Yuan, Y. F., Wang, R. Q., Liu, J., Du, N., and Guo, W. H. (2016). Functional traits contributed to the superior performance of the exotic species Robinia pseudoacacia: a comparison with the native tree Sophora japonica. *Tree Physiol.* 36, 345–355. doi: 10.1093/treephys/tpv123

Mason, N. W. H., Mouillot, D., Lee, W. G., and Wilson, J. B. (2005). Functional richness, functional evenness and functional divergence: the primary components of functional diversity. *Oikos* 111, 112–118. doi: 10.1111/j.0030-1299.2005.13886.x

Perez-Harguindeguy, N., Diaz, S., Garnier, E., Lavorel, S., Poorter, H., Jaureguiberry, P., et al. (2013). New handbook for standardised measurement of plant functional traits worldwide. *Aust. J. Bot.* 61, 167–234. doi: 10.1071/Bt12225

Piwczynski, M., Puchalka, R., and Ulrich, W. (2016). Influence of tree plantations on the phylogenetic structure of understorey plant communities. *For. Ecol. Manage.* 376, 231–237. doi: 10.1016/j.foreco.2016.06.011

Pysek, P., Chytry, M., Pergl, J., Sadlo, J., and Wild, J. (2012). Plant invasions in the Czech Republic: current state, introduction dynamics, invasive species and invaded habitats. *Preslia* 84, 575–629. doi: 10.1016/j.precamres.2012.01.016

Qin, J., Xi, W. M., Rahmlow, A., Kong, H. Y., Zhang, Z., and Shangguan, Z. P. (2016). Effects of forest plantation types on leaf traits of Ulmus pumila and Robinia pseudoacacia on the Loess Plateau, China. *Ecol. Eng.* 97, 416–425. doi: 10.1016/j.ecoleng.2016.10.038

Refsland, T. K., and Fraterrigo, J. M. (2017). Both canopy and understory traits act as response-effect traits in fire-managed forests. *Ecosphere* 8, e02036. doi: 10.1002/ecs2.2036

Reich, P. B. (2014). The world-wide 'fast-slow' plant economics spectrum: a traits manifesto. *J. Ecol.* 102, 275–301. doi: 10.1111/1365-2745.12211

Rosenfield, M. F., and Muller, S. C. (2017). Predicting restored communities based on reference ecosystems using a trait-based approach. *For. Ecol. Manage.* 391, 176–183. doi: 10.1016/j.foreco.2017.02.024

Shangguan, Z. P. (2007). Soil desiccation occurrence an its impact on forest vegetation in the Loess Plateau of China. *Int. J. Sustain. Dev. World Ecol.* 14, 299–306. doi: 10.1080/13504500709469730

Silvertown, J. (2004). Plant coexistence and the niche. *Trends Ecol. Evol.* 19, 605–611. doi: 10.1016/j.tree.2004.09.003

Sitzia, T., Campagnaro, T., Dainese, M., and Cierjacks, A. (2012). Plant species diversity in alien black locust stands: A paired comparison with native stands across a north-Mediterranean range expansion. *For. Ecol. Manage.* 285, 85–91. doi: 10.1016/j.foreco.2012.08.016

Slabejova, D., Bacigal, T., Hegedusova, K., Majekova, J., Medvecka, J., Mikulova, K., et al. (2019). Comparison of the understory vegetation of native forests and adjacent Robinia pseudoacacia plantations in the Carpathian-Pannonian region. *For. Ecol. Manage.* 439, 28–40. doi: 10.1016/j.foreco.2019.02.039

Solé-Senan, X. O., Juárez-Escario, A., Robleño, I., Conesa, J. A., and Recasens, J. (2017). Using the response-effect trait framework to disentangle the effects of agricultural intensification on the provision of ecosystem services by Mediterranean arable plants. *Agric. Ecosyst. Environ.* 247, 255–264. doi: 10.1016/j.agee.2017.07.005

Su, B. Q., and Shangguan, Z. P. (2019). Decline in soil moisture due to vegetation restoration on the Loess Plateau of China. *Land Degradation Dev.* 30, 290–299. doi: 10.1002/ldr.3223

Suding, K. N., and Goldstein, L. J. (2008). Testing the Holy Grail framework: using functional traits to predict ecosystem change. *New Phytol.* 180, 559–562. doi: 10.1111/j.1469-8137.2008.02650.x

Suding, K. N., Lavorel, S., Chapin, F. S., Cornelissen, J. H. C., Diaz, S., Garnier, E., et al. (2008). Scaling environmental change through the community-level: a trait-based response-and-effect framework for plants. *Global Change Biol.* 14, 1125–1140. doi: 10.1111/j.1365-2486.2008.01557.x

Swenson, N. G. (2016). Plant functional diversity: organism traits, community structure, and ecosystem properties. *Ecology* 97, 3556–3558. doi: 10.1002/ecy.1608

Tölgyesi, C., Török, P., Hábenczyus, A. A., Bátori, Z., Valkó, O., Deák, B., et al. (2020). Underground deserts below fertility islands? Woody species desiccate lower soil layers in sandy drylands. *Ecography* 43, 848–859. doi: 10.1111/ecog.04906

Vallejo, V. R., Smanis, A., Chirino, E., Fuentes, D., Valdecantos, A., and Vilagrosa, A. (2012). Perspectives in dryland restoration: approaches for climate change adaptation. *New Forests* 43, 561–579. doi: 10.1007/s11056-012-9325-9

Violle, C., Navas, M. L., Vile, D., Kazakou, E., Fortunel, C., Hummel, I., et al. (2007). Let the concept of trait be functional! *Oikos* 116, 882–892. doi: 10.1111/j.2007.0030-1299.15559.x

Wang, S. A., Fu, B. J., Piao, S. L., Lu, Y. H., Ciais, P., Feng, X. M., et al. (2016). Reduced sediment transport in the Yellow River due to anthropogenic changes. *Nat. Geosci.* 9, 38–3+. doi: 10.1038/Ngeo2602

Wang, X., Zhong, Z. K., Li, W. J., Liu, W. C., Zhang, X. Y., Wu, S. J., et al. (2020). Effects of afforestation on aggregate size distribution and organic C dynamics in the central Loess Plateau of China: A chronosequence approach. *J. Environ. Manage.* 268, 110558. doi: 10.1016/j.jenvman.2020.110558

Weiher, E., van der Werf, A., Thompson, K., Roderick, M., Garnier, E., and Eriksson, O. (1999). Challenging Theophrastus: A common core list of plant traits for functional ecology. *J. Vegetation Sci.* 10, 609–620. doi: 10.2307/3237076

Wu, Y. Z., Huang, M. B., and Warrington, D. N. (2015). Black locust transpiration responses to soil water availability as affected by meteorological factors and soil texture. *Pedosphere* 25, 57–71. doi: 10.1016/S1002-0160(14)60076-X

Yan, Y., Wang, J., Ding, J. Y., Zhang, S. R., and Zhao, W. W. (2023). Afforestation promotes ecosystem multifunctionality in a hilly area of the Loess Plateau. *Catena* 223, 106905. doi: 10.1016/j.catena.2022.106905

Yang, Y., Dou, Y. X., Cheng, H., and An, S. S. (2019). Plant functional diversity drives carbon storage following vegetation restoration in Loess Plateau, China. *J. Environ. Manage.* 246, 668–678. doi: 10.1016/j.jenvman.2019.06.054

Yang, Y. T., Fan, Y. M., Basang, C. M. J., Lu, J. X., Zheng, C., and Wen, Z. M. (2022). Different biomass production and soil water patterns between natural and artificial vegetation along an environmental gradient on the Loess Plateau. *Sci. Total Environ.* 814, 152839. doi: 10.1016/j.scitotenv.2021.152839

Yang, L., Wei, W., Chen, L. D., Chen, W. L., and Wang, J. L. (2014). Response of temporal variation of soil moisture to vegetation restoration in semi-arid Loess Plateau, China. *Catena* 115, 123–133. doi: 10.1016/j.catena.2013.12.005

Yin, Q. L., Wang, L., Lei, M. L., Dang, H., Quan, J. X., Tian, T. T., et al. (2018). The relationships between leaf economics and hydraulic traits of woody plants depend on water availability. *Sci. Total Environ.* 621, 245–252. doi: 10.1016/j.scitotenv.2017.11.171

Yu, Z., Liu, S. R., Wang, J. X., Wei, X. H., Schuler, J., Sun, P. S., et al. (2019). Natural forests exhibit higher carbon sequestration and lower water consumption than planted forests in China. *Global Change Biol.* 25, 68–77. doi: 10.1111/gcb.14484

Yuan, Y. J., Gao, X. R., Huang, K. J., Wang, J. C., Zhao, X. H., Gao, X. D., et al. (2023). Evolution of the water-carbon relationship at basin scale under the background of a vegetation restoration program. *Land Degradation Dev.* 34, 2975–2989. doi: 10.1002/ldr.4661

Zhang, M., Bai, X. X., Wang, Y., Li, Y., Cui, Y. X., Hu, S. L., et al. (2023). Soil microbial trait-based strategies drive the storage and stability of the soil carbon pool in plantations. *Catena* 222, 106894. doi: 10.1016/j.catena.2022.106894

Zhang, X. Y., Xu, D. Y., and Wang, Z. Y. (2021). Optimizing spatial layout of afforestation to realize the maximum benefit of water resources in arid regions: A case study of Alxa, China. *J. Cleaner Production* 320, 128827. doi: 10.1016/j.jclepro.2021.128827

Zhao, C. L., Shao, M. A., Jia, X. X., and Zhu, Y. J. (2017). Estimation of spatial variability of soil water storage along the south-north transect on China's Loess Plateau using the state-space approach. *J. Soils Sediments* 17, 1009–1020. doi: 10.1007/s11368-016-1626-8

Zheng, X. X., Liu, G. H., Fu, B. J., Jin, T. T., and Liu, Z. F. (2010). Effects of biodiversity and plant community composition on productivity in semiarid grasslands of Hulunbeir, Inner Mongolia, China. *Ecol. Complexity Sustainability* 1195, E52–E64. doi: 10.1111/j.1749-6632.2009.05405.x

Zheng, C., Zhang, F., Lin, Z. Q., Yuan, L. H., Yao, H. B., Duan, G. H., et al. (2024). Using the response-effect trait framework to disentangle the effects of environmental change on the ecosystem services. *J. Plant Ecol.* 17, 1-13. doi: 10.1093/jpe/rtae024

Zhou, S., Wang, J. Y., Chen, L., Wang, J., and Zhao, F. Z. (2022). Microbial community structure and functional genes drive soil priming effect following afforestation. *Sci. Total Environ.* 825, 153925. doi: 10.1016/j.scitotenv.2022.153925

Zirbel, C. R., Bassett, T., Grman, E., and Brudvig, L. A. (2017). Plant functional traits and environmental conditions shape community assembly and ecosystem functioning during restoration. *J. Appl. Ecol.* 54, 1070–1079. doi: 10.1111/1365-2664.12885

Zuur, A. F., Ieno, E. N., Walker, N. J., Saveliev, A. A., and Smith, G. M. (2010). *Mixed effects models and extensions in ecology with R.* (New York, NY:Springer New York).

frontiers | Frontiers in Plant Science

TYPE Original Research
PUBLISHED 21 January 2025
DOI 10.3389/fpls.2024.1531654



OPEN ACCESS

EDITED BY
Hui Zhang,
Hainan University, China

REVIEWED BY
Zuoqiang Yuan,
Northwestern Polytechnical University, China
Yin Li,
Sanming University, China

*CORRESPONDENCE
Yunquan Wang
yqwang@vip.126.com

RECEIVED 20 November 2024
ACCEPTED 30 December 2024
PUBLISHED 21 January 2025

CITATION
Bian Y, Wu Q, Zheng R, Fu J, Chen J, Mi X, Yu M and Wang Y (2025) Temporal and habitat-specific variations in drivers of aboveground biomass dynamics in a Chinese subtropical forest.
*Front. Plant Sci.* 15:1531654.
doi: 10.3389/fpls.2024.1531654



# Temporal and habitat-specific variations in drivers of aboveground biomass dynamics in a Chinese subtropical forest

Yuxuan Bian[1], Qi Wu[1], Rong Zheng[1], Jiaqin Fu[1], Jianhua Chen[1], Xiangcheng Mi[2], Mingjian Yu[3] and Yunquan Wang[1,3,4]*

[1]College of Life Sciences, Zhejiang Normal University, Jinhua, China, [2]Zhejiang Qianjiangyuan Forest Biodiversity National Observation and Research Station, State Key Laboratory of Vegetation and Environmental Change, Institute of Botany, The Chinese Academy of Sciences, Beijing, China, [3]College of Life Sciences, Zhejiang University, Hangzhou, China, [4]The Administration Center of Zhejiang Jiulongshan National Nature Reserve, Lishui, China

Understanding the mechanisms governing biodiversity-biomass relationships across temporal and spatial scales is essential for elucidating how abiotic and biotic factors influence ecosystem function in natural forests. However, the simultaneous contributions of multiple abiotic (e.g., topography) and biotic factors (e.g., structural diversity) to aboveground biomass dynamics (ΔAGB) over time and across habitat types remain inadequately understood. To address this gap, we evaluated changes in aboveground biomass across a decade and various habitats, disentangling the relative influences of topography and multidimensional diversity on ΔAGB through datasets from forest inventories conducted between 2007 and 2017, along with phylogenetic relatedness, functional traits, and environmental variables from a subtropical forest in China. Our findings indicate that aboveground biomass at community level experienced a significant decline followed by an increase over the decade, predominantly driven by changes in the low-valley habitat. In contrast, no statistically significant alterations were detected in the aboveground biomass of mid-hillside and high-ridge habitats. Furthermore, the determinants of ΔAGB exhibited temporal variation. During the 2007-2012 period, ΔAGB was primarily influenced by functional and structural diversity, accounting for 66.11% and 21.35% of relative importance, respectively. In the subsequent 2012-2017 period, phylogenetic and structural diversity emerged as key factors, explaining 48.46% and 36.43% of relative importance, respectively. Additionally, we observed that the drivers and effects impacting ΔAGB exhibited significant variability across different habitat types. In summary, our study underscores the significant spatiotemporal dependence of abiotic and biotic drivers on biomass dynamics within forest ecosystems, thereby enhancing our understanding of the complex biodiversity-ecosystem functioning relationships.

KEYWORDS

**ecosystem functioning, functional diversity, evolutionary diversity, structural diversity, niche complementarity, disturbance**

# 1 Introduction

Anthropogenic global climate change and habitat destruction have exacerbated biodiversity loss worldwide (Synes et al., 2020; Richardson et al., 2023), resulting in irreversible negative impacts on species coexistence, services and functions of ecosystems (Isbell et al., 2017; He et al., 2024). Given that forests are indispensable to the worldwide carbon cycle and maintenance of carbon neutrality (Canadell and Raupach, 2008; Pan et al., 2011), the biodiversity-ecosystem functioning (BEF) relationships in forest communities have garnered considerable attention and pose a significant challenge in ecology (Gamfeldt et al., 2013; Liang et al., 2016; Ray et al., 2023; Zemp et al., 2023). Theoretically, a positive BEF relationship is expected when biodiversity promotes niche complementarity (i.e. the complementary effect) or the average competitive ability of species (i.e. the positive selection effect) (Lasky et al., 2014). Alternatively, a negative BEF relationship may occur if increased biodiversity results in a decrease of the average competitive ability of species (i.e. the negative selection effect) (Huston, 1997; Tilman, 1999). However, the relationship between biodiversity and aboveground biomass (AGB) within forest communities is complex and context-dependent, and potentially varying over time and across spatial scales (Cardinale et al., 2007; Reich et al., 2012; Forrester and Bauhus, 2016; Gottschall et al., 2022). It remains ambiguous how multiple abiotic and biotic factors simultaneously contribute to aboveground biomass dynamics (ΔAGB) over temporal scales and across various habitat types.

Considering multiple dimensions of biodiversity concurrently is able to facilitate a comprehensive and accurate insight into the ecological mechanism underlying BEF relationships (Cadotte et al., 2009; Srivastava et al., 2012; Wang et al., 2024). Previous researchers have already investigated how species and functional diversity influence AGB, revealing that species richness alone may inadequately capture the ecological differences or similarities among species (van der Sande et al., 2017; Yuan et al., 2019). In comparison to species diversity, functional diversity plays a more crucial role in ecosystem functions by reflecting a suite of core attributes essential for plant growth and reproduction within a community (Petchey and Gaston, 2002; Lian et al., 2022). A higher diversity of traits related to resource uptake enables a community to utilize resources more effectively, with resource use complementarity serving as an underlying mechanism linking functional diversity to ecosystem function (Fotis et al., 2018; Chen et al., 2023).

Structural diversity and phylogenetic diversity have been recognized as critical drivers of ecosystem functions (Dănescu et al., 2016; Yuan et al., 2018; Yang et al., 2024), as they offer insights into resource use efficiency and evolutionary history in forest communities, respectively (Cadotte et al., 2009; Zhu et al., 2021). Notably, due to its capacity to estimate both the actual volumetric occupancy and arrangement within niche spaces, stand structure is increasingly acknowledged in the context of the BEF relationship (Ali, 2019; Chen et al., 2023). Although it has been demonstrated that changes in BEF relationships may arise from the complementary trends in resource use strategies among species over time (Huang et al., 2018; Zheng et al., 2024), our understanding of how multiple dimensions of biodiversity contribute to ΔAGB over time remains limited. In the context of climate change, exploring the impact of multidimensional biodiversity on ΔAGB across temporal scales in natural forests is essential for elucidating the variation in biodiversity effects (Kardol et al., 2018).

The critical role of abiotic factors in shaping BEF relationships has been extensively examined (Ferry et al., 2010; McEwan et al., 2011; Quesada et al., 2012; Werner and Homeier, 2015). The "multivariate productivity-diversity hypothesis" posits that environmental conditions indirectly influence community productivity by affecting species diversity, thereby providing a theoretical framework for understanding spatial variation in BEF relationships (Cardinale et al., 2009). Habitat types comprehensively reflect topographic factors (e.g., elevation, slope, aspect, and convexity), which mediate microclimates and soil nutrients (Man et al., 2011; Lin et al., 2012), thus potentially impacting the ΔAGB of forests both directly or indirectly (McEwan et al., 2011; Lin et al., 2012; Zhang et al., 2024). For instance, certain habitat types such as ridges and steep slopes may experience periodic water stress, poor soil nutrients availability, and strong winds, where only species with stress-tolerant life history strategies can thrive (Paoli, 2006; Tanner et al., 2014). Distinct environmental factors across various habitats influence the species composition of plant communities as well as the growth performance of species, which in turn indirectly affect the AGB within forest communities (Chadwick and Asner, 2016; Jucker et al., 2018). Therefore, we argue that considering habitat types could further elucidate the spatial variation in diversity-ΔAGB relationships.

Subtropical forests, despite their relatively limited global distribution (Fang et al., 2001), rank second only to tropical forests in terms of species richness and serve as a significant carbon sink on the earth (Houghton, 2005; Piao et al., 2009; Li et al., 2019). They are essential in the worldwide carbon cycle and climate regulation (Yu et al., 2014). The forest within the Gutianshan National Nature Reserve exemplifies typical subtropical evergreen broad-leaved mature forest of China (Jiang et al., 2022), and large sustained forest dynamics monitoring plots with systematic vegetation inventories here facilitate the critical framework for linking abiotic and biotic drivers of carbon dynamics to spatiotemporal variation (Lin et al., 2012; Mi et al., 2021). To evaluate the potential contributions of multiple abiotic and biotic factors to ΔAGB over time and across habitat types in the subtropical forest, we examined the changes of AGB over time and across habitat types, disentangling the comparative impacts of these factors on ΔAGB across different temporal periods and habitat types. Specifically, we focused on the following three questions: (1) How did the AGB vary over time and across habitats during the past decade? (2) How did the abiotic and biotic determinants and their influences on ΔAGB differ across temporal periods? and (3) how did they vary across different habitat types?

# 2 Materials and methods

## 2.1 Study site and plot data

Our study was conducted within the Gutianshan National Nature Reserve in Quzhou City, Zhejiang Province, southeastern

China, with a total area of 8107 hectares. The reserve is distinguished by its subtropical humid monsoon climate, exhibiting an average annual temperature of 15.3 °C and an average annual precipitation of 1963.7 mm (Yu et al., 2001). The predominant soil types in the area comprise red soil, yellow-red soil, red-yellow soil, as well as swamp soil, with a pH ranging mostly between 5.5 and 6.5. The evergreen broad-leaved forest, dominated by *Castanopsis eyrei* and *Schima superba*, is the main vegetation type in Gutianshan, commonly found below 800 meters and characterized as typical subtropical zonal vegetation (Yu et al., 2001; Legendre et al., 2009).

The 5-ha forest plot was established in 2002 according to the standard of the CTFS-ForestGEO protocol. The plot spans 200 meters in an east-west direction and 250 meters in a north-south orientation, containing two hillsides on the northern and southern sides and a valley in the middle, with a cross-section resembling an irregular "V" shape (Jiang et al., 2022). In this plot, all woody stems with DBH (diameter at breast height, 1.3 m) ≥ 1 cm were tagged, spatially mapped, identified to species, and measured DBH, number of sprouts and branches. Tree census is conducted every 5 years for the 5-ha long-term forest dynamics monitoring plot. More than 18000 free-standing individuals belonging to 161 plant species were recorded during the 2007-2017 period (Table 1).

## 2.2 Estimation of aboveground biomass

To estimate aboveground biomass (AGB), the tree height was first calculated by referring to Lin et al. (2012) (Equation 1). There were 47 species-specific tree height equations fitted in our study site, and an equation based on combined data from all species was used for the remaining 114 species. Then the AGB of each tree and branch was calculated by using the allometric growth equation improved by Chave et al. (2014) (Equation 2):

$$H = aD^b \times CF \quad (1)$$

$$AGB = 0.0673 \times (WD \times D^2 \times H)^{0.976} \quad (2)$$

Where $D$ is DBH (cm), $a$ and $b$ are estimated species-specific coefficients and CF is the correction factor. The wood density (WD) was obtained mainly from Liu (2012) *in-situ* measured data and through the search of the TRY database (Kattge et al., 2020). Among them, 14.9% of species without WD data were replaced by the mean WD of species of the same genus or family in the same climate region.

## 2.3 Abiotic variables

We defined abiotic factors within the context of topography and habitat types in our study. Four topographic variables were calculated (i.e. elevation, slope, aspect, and convexity) for every 20 m × 20 m plot following Harms et al. (2001). To test how the drivers of ΔAGB vary with habitat types, the 5-ha forest plot was divided into three habitat types at 20 m × 20 m scale (The extra 20 m × 10 m is not included): low-valley (H1, 50 plots), mid-hillside (H2, 45 plots), and high-ridge (H3, 25 plots). More detailed information about habitat classification could be found in Jiang et al. (2022).

## 2.4 Biotic variables

To test the impacts of biotic factors on ΔAGB, we measured four dimensions of biodiversity indices: species (taxonomic) diversity, structural diversity, phylogenetic diversity, and functional diversity. Species diversity was measured by Shannon-Wiener index ($H$), Simpson index ($D$) and Pielou evenness index ($J$) (Ma and Liu, 1994). The change values of Shannon-Wiener index (cH), Simpson index (cD), and Pielou evenness index (cJ) were represented as the differences between each 5-year period (the same below). Stand density (SD) and the coefficient of variation of DBH ($CV_{DBH}$) were calculated for structural diversity variables (Ren et al., 2021). SD was the number of individual plants with DBH ≥1 cm per unit area (quadrat). The equation for the $CV_{DBH}$ is as follows (Zhang and Chen, 2015):

$$CV_{DBH} = \sigma/\mu \quad (3)$$

TABLE 1 The species richness and individual abundance of the whole plot and different habitat types from 2007 to 2017.

| Year | Whole plot | | Low-valley habitat | | Mid-hillside habitat | | High-ridge habitat | |
|---|---|---|---|---|---|---|---|---|
| | total | mean ± sd | total | mean ± sd | total | mean ± sd | total | mean ± sd |
| Species richness | | | | | | | | |
| 2007 | 149 | 32.98 ± 7.31 | 133 | 31.90 ± 6.50 | 133 | 32.51 ± 8.21 | 98 | 36 ± 6.01 |
| 2012 | 159 | 34.66 ± 8.67 | 144 | 32.68 ± 6.96 | 140 | 34.6 ± 10.12 | 113 | 38.72 ± 7.19 |
| 2017 | 160 | 33.15 ± 8.53 | 143 | 30.76 ± 6.72 | 141 | 32.35 ± 8.70 | 115 | 39.36 ± 8.30 |
| Individual abundance | | | | | | | | |
| 2007 | 17673 | 147.28 ± 49.49 | 6828 | 136.56 ± 44.45 | 6030 | 134 ± 45.25 | 4815 | 192.6 ± 37.71 |
| 2012 | 18901 | 157.51 ± 54.52 | 7295 | 145.9 ± 47.02 | 6443 | 143.18 ± 53.20 | 5163 | 206.52 ± 39.88 |
| 2017 | 16143 | 134.53 ± 51.05 | 5849 | 116.98 ± 37.18 | 5431 | 120.69 ± 43.42 | 4863 | 194.52 ± 41.06 |

Where $\sigma$ is the standard deviation of DBH in the quadrat, $\mu$ is the mean DBH in the quadrat, and the change values of SD (cSD) and $CV_{DBH}$ ($cCV_{DBH}$) were calculated at the same time.

According to the Angiosperm Phylogeny Group IV (APG IV), a phylogenetic tree was first constructed (Jin and Qian, 2022), and then the mean pairwise distance (MPD) and mean nearest taxon distance (MNTD) were calculated for all species in the community (Webb et al., 2002; Swenson et al., 2006):

$$MPD = \frac{MPD_{sample} - meanMPD_{null}}{sdMPD_{null}} \quad (4)$$

$$MNTD = \frac{MNTD_{sample} - meanMNTD_{null}}{sdMNTD_{null}} \quad (5)$$

Where $MPD_{sample}$ and $MNTD_{sample}$ are the actual observed values, while $MPD_{null}$ and $MNTD_{null}$ are the values of MPD and MNTD for randomly generated null communities under the null model, $sdMPD_{null}$ and $sdMNTD_{null}$ are the standard deviations of these values, $meanMPD_{null}$ and $meanMNTD_{null}$ are the average of these values. The change values of MPD (cMPD) and MNTD (cMNTD) were also calculated.

The WD, maximum tree height, and life form of plant species are closely related to forest AGB and are considered important functional traits (Ruiz-Benito et al., 2014; Ouyang et al., 2019). Therefore, we used these three types of functional traits to assess functional diversity. The WD used the data previously employed for calculating the AGB. The maximum tree height and species life form data were sourced from the Flora of Zhejiang (New Edition) (Li, 2021) and Flora of China (Wu et al., 1994-2009), with life forms categorized into three types: evergreen broad-leaved, deciduous broad-leaved, and coniferous. Then we calculated Rao's quadratic entropy (RaoQ) and Functional dispersion (FDis) for functional diversity (Laliberté and Legendre, 2010). And the trait mean pairwise distance (traitMPD) and trait mean nearest taxon distance (traitMNTD) were calculated based on the functional trait dendrogram (Swenson et al., 2006; Shui et al., 2022):

$$traitMPD = -1 \times \frac{traitMPD_{sample} - meantraitMPD_{null}}{sdtraitMPD_{null}} \quad (6)$$

$$traitMNTD = -1 \times \frac{traitMNTD_{sample} - meantraitMNTD_{null}}{sdtraitMNTD_{null}} \quad (7)$$

Where $traitMPD_{sample}$ and $traitMNTD_{sample}$ are the actual observed values, while $traitMPD_{null}$ and $traitMNTD_{null}$ are the values of traitMPD and traitMNTD for randomly generated null communities under the null model, $sdtraitMPD_{null}$ and $sdtraitMNTD_{null}$ are the standard deviations of these values, $meantraitMPD_{null}$ and $meantraitMNTD_{null}$ are the average of these values. The change values of FDis (cFDis), RaoQ (cRaoQ), traitMPD (ctraitMPD) and traitMNTD (ctraitMNTD) were also calculated.

## 2.5 Statistical analysis

First, we used the Wilcoxon rank-sum test to determine if there were significant differences in AGB across the three tree censuses. Second, the generalized linear model was used to examine the impact of biotic (including the change values of them) and abiotic variables on ΔAGB. The ΔAGB was represented as the difference in AGB between each 5-year period. We divided the study decade (2007-2017) into two 5-year periods (2007-2012 and 2012-2017) to investigate the temporal changes in the drivers of ΔAGB. Furthermore, the plot was categorized into three habitats, and we examined the relationship between the explanatory variables and the response variables within them. The initial values and the change values were used for all biotic variables. To enhance the comparative analysis among drivers and models, all variables were scaled and variables with too high collinearity of variance inflation factor (VIF) >5 were removed (Fox and Weisberg, 2018). Finally, we selected our optimal models with lowest Akaike information criterion (AIC) (Bartoń, 2012), then performed hierarchical partition on them to assess the relative importance of all variables influencing ΔAGB (Lai et al., 2022; Lai et al., 2023). Some variables are not represented in our figures because they are not included in the optimal model. The initial data proofreading and organization were completed in Excel 16.0, while the subsequent calculations of indices, data analysis, and plotting were all conducted in R (version 4.2.2).

# 3 Results

## 3.1 The changes of aboveground biomass over time and habitats

By estimating the AGB in Gutianshan 5-ha plot, we found that the AGB at community level showed a significant decrease followed by a nonsignificant increase from 2007 to 2017 (Table 2, Figure 1A), which was mainly driven by the biomass change in low-valley habitat (H1) (Table 2, Figure 1B). The AGB in the mid-hillside (H2) and high-ridge habitats (H3) from 2007 to 2017 also showed a decreasing and then increasing change, but variations at each stage were not significant (Table 2, Figures 1C, D).

## 3.2 The changes of drivers influencing aboveground biomass dynamics over time

The main impact factors on ΔAGB were functional diversity (66.11% of relative importance) and structural diversity (21.35% of relative importance) during 2007-2012 period (Figure 2A). Specifically,

TABLE 2 The aboveground biomass of the whole plot and different habitat types from 2007 to 2017.

| Year | Whole plot | Low-valley habitat | Mid-hill-side habitat | High-ridge habitat |
|---|---|---|---|---|
| Aboveground biomass (± sd) (Mg $ha^{-1}$) | | | | |
| 2007 | 212.45 (± 75.37) | 204.84 (± 71.38) | 219.00 (± 71.96) | 215.87 (± 89.77) |
| 2012 | 188.27 (± 73.20) | 178.33 (± 57.62) | 191.86 (± 76.26) | 201.69 (± 93.33) |
| 2017 | 195.89 (± 78.57) | 183.10 (± 62.04) | 204.01 (± 85.52) | 206.87 (± 93.56) |

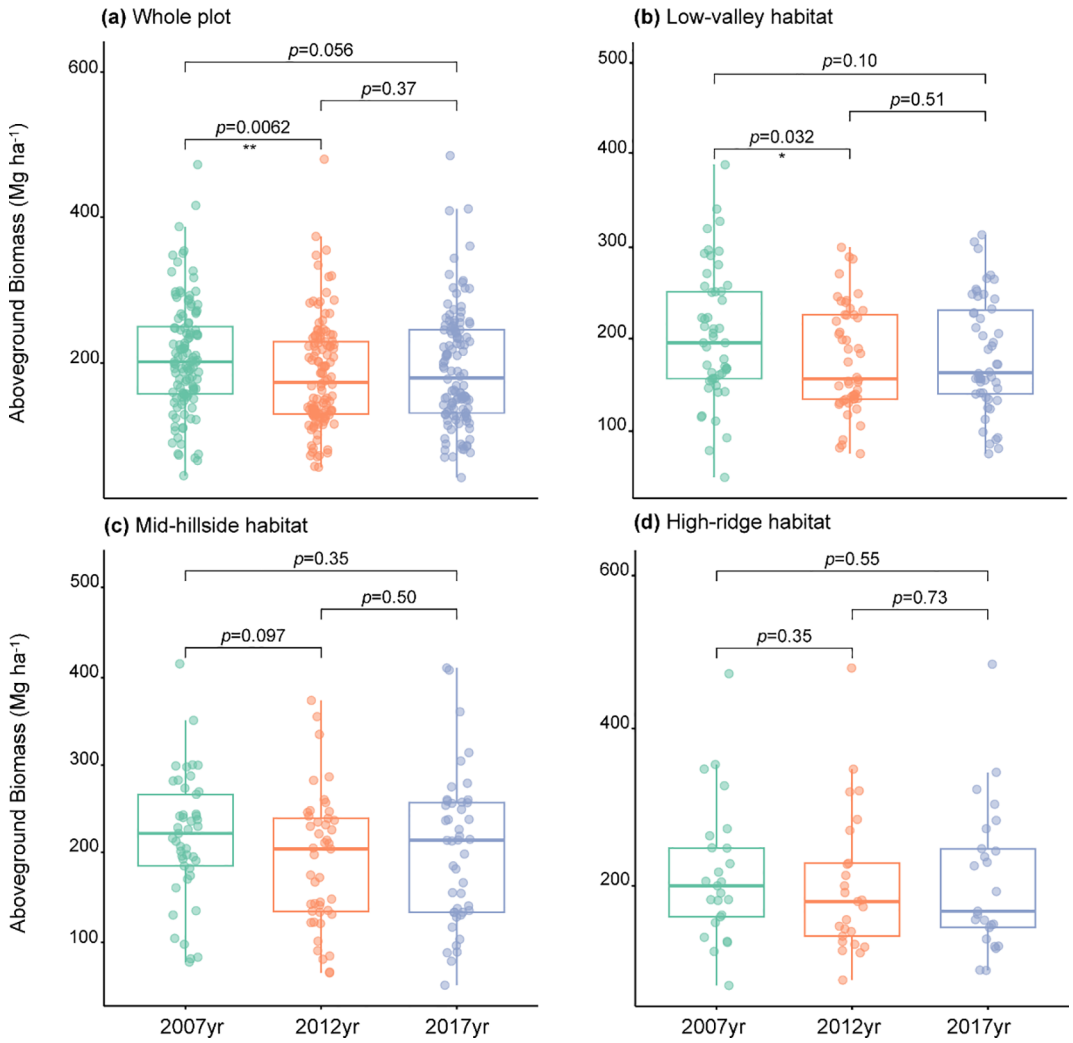


FIGURE 1
The aboveground biomass changes of the whole plot **(A)**, Low-valley habitat **(B)**, Mid-hillside habitat **(C)** and High-ridge habitat **(D)** from 2007 to 2017. *p< 0.05, **p< 0.01, ***p< 0.001.

ΔAGB was significantly negatively correlated with SD, FDis and ctraitMPD, but significantly positively correlated with ctraitMNTD. However, during 2012-2017 period, ΔAGB was mainly affected by phylogenetic diversity (48.46% of relative importance) and structural diversity (36.43% of relative importance) (Figure 2B). It showed a significant positive relationship with cMPD and $cCV_{DBH}$, but a significant negative relationship with cSD and cMNTD.

## 3.3 The changes of drivers influencing aboveground biomass dynamics across habitats

The main impact factors on ΔAGB in low-valley habitat were similar to the whole plot (Figures 3A, B). Moreover, we also found that it was significantly negatively correlated with aspect and elevation, but significantly positively correlated with convexity (Figure 3B). ΔAGB in mid-hillside habitat was significantly positively affected by phylogenetic diversity (Figures 3C, D). Besides, ΔAGB was significantly negatively associated with traitMPD but significantly positively associated with ctraitMNTD (Figure 3D). In high-ridge habitat, all dimensions of biodiversity as well as topographic factors showed significant effects on ΔAGB (Figures 3E, F). Specifically, ΔAGB was significantly negatively influenced by H, MNTD, cMNTD, cSD and slope, but was significantly positively influenced by cFDis, FDis, $cCV_{DBH}$, MPD, SD and elevation. Whereas $CV_{DBH}$ had a variable relationship with ΔAGB.

# 4 Discussion

## 4.1 Changes of aboveground biomass over the decade

The AGB at community level in Gutianshan showed a significant decrease during the 2007-2012 period. The large-scale ice storm occurred in this region in 2008 killed many trees especially the larger-diameter trees with higher biomass (Jin et al., 2015), which might cause a significant decrease in AGB of the plot (Zhang

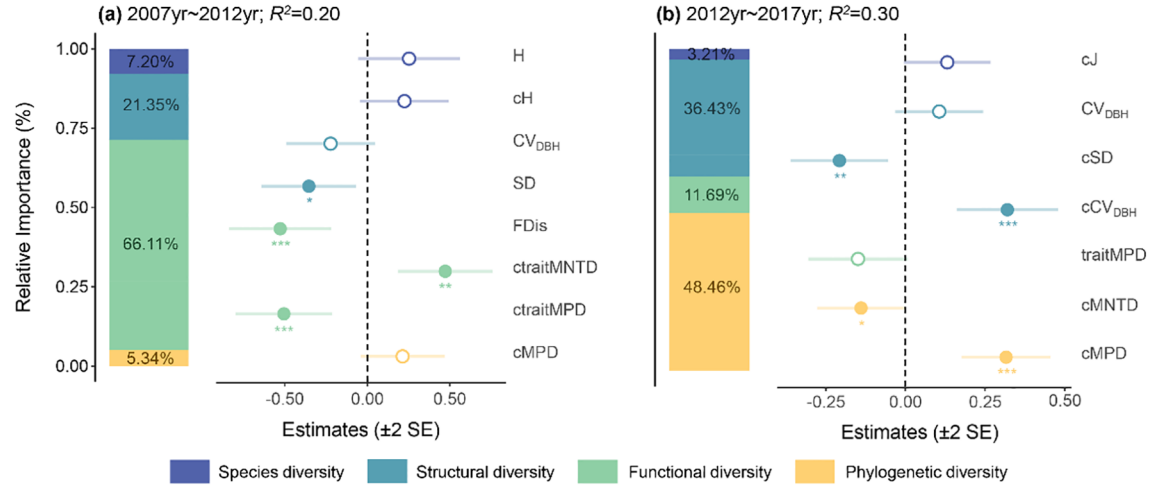


FIGURE 2
The main impact factors of aboveground biomass dynamics from 2007 to 2012 **(A)** and 2012 to 2017 **(B)**. Solid and open circles indicate significant or nonsignificant community diversity effects at $p < 0.05$, respectively. H, Shannon-Wiener index; $CV_{DBH}$, coefficient of variation in DBH; SD, stand density; FDis, functional dispersion; MPD, mean pairwise distance; MNTD, mean nearest taxon distance; traitMPD and traitMNTD, trait mean pairwise distance and trait mean nearest taxon distance; J, Pielou evenness index. c indicates the change values of each variable. *$p < 0.05$, **$p < 0.01$, ***$p < 0.001$.

et al., 2012). During the 2012-2017 period, the AGB increased but did not recover to the initial level, which was probably due to the stable forest type here. Most of the forest here is in the middle and late successional stages, with well-developed, typical, and stable vegetation, belonging to a mature subtropical evergreen broad-leaved forest (Legendre et al., 2009). However, the more stable a forest is before a disaster, the slower it recovers afterwards (Sun et al., 2012). Furthermore, the restoration of some forest ecosystem functions, such as the AGB and carbon sequestration, could span decades or potentially even longer periods (Amiro et al., 2010).

After examining the AGB across the three habitats within the plot, our results revealed that the trend of AGB variation at the community level was primarily driven by changes in low-valley habitat. In contrast, the AGB in mid-hillside and high-ridge habitats showed nonsignificant variation, indicating that the damage to trees in low-altitude valley was more severe than in mid- and high-altitude regions (Man et al., 2011). This was not aligned with the established impact of natural disasters on forest vegetation (Zhang et al., 2012; Tanner et al., 2014). The discrepancy may be due to the fact that the elevation differences within this plot are not substantial enough to reflect the influence of altitude. Additionally, the impact of elevation on the severity of damage to forest vegetation after disasters can be shaped by the distinctive characteristics of the local environment (Man et al., 2011).

## 4.2 Changes of drivers and effects on aboveground biomass dynamics across temporal scales

Changes in community performance may be attributed to plant ecological strategies, which impact the efficacy and interplay of species, thereby affecting the ecological processes and functions of ecosystem (Huang et al., 2018; Zheng et al., 2024). Our study showed that the factors influencing ΔAGB varied across time scales. During the 2007-2012 period, the main influencing factors on ΔAGB were functional diversity and structural diversity. It is generally believed that both functional diversity and structural diversity are beneficial for increasing ecosystem biomass accumulation or productivity (Li et al., 2019; Lian et al., 2022) as both can promote the resource use efficiency of the community (Zhu et al., 2021; Chen et al., 2023). However, in our study, functional diversity and structural diversity were mainly negatively correlated with ΔAGB. This is likely because of the negative relationship between plant diversity and resource availability in natural ecosystems due to resource constraints and interspecific competition (Fraser et al., 2015). The communities in the study plots are mostly in the middle and late successional stages, where resources are relatively limited (Lasky et al., 2014). In addition, the increase of plant diversity and individuals at this stage tended to intensify interspecific competition (Table 1), which further reduced the available resources for species and ultimately resulted in a decrease of community productivity (Wu et al., 2018). As a result, a negative BEF relationship occurred during this period.

In the subsequent period of 2012-2017, we found that the main impact factors on ΔAGB shifted to phylogenetic diversity and structural diversity. This is in line with previous studies suggesting that BEF relationships in forests could change over time (Lasky et al., 2014; Gottschall et al., 2022). The shift could be a consequence of the formation of canopy gaps in this forest (Man et al., 2011), which could increase the light availability of understory vegetation (Zhu et al., 2014; Song et al., 2018). This increase could promote the recruitment of early-successional species that struggle to reproduce under low light conditions, as well as the regeneration of late-successional species (Song et al., 2018). As a result, phylogenetic diversity might have encapsulated certain inherent functional characteristics that were not directly assessed during this period, including traits related to roots or herbivores (Cadotte et al., 2009; Liu et al., 2015). The ΔAGB was

10.3389/fpls.2024.1531654

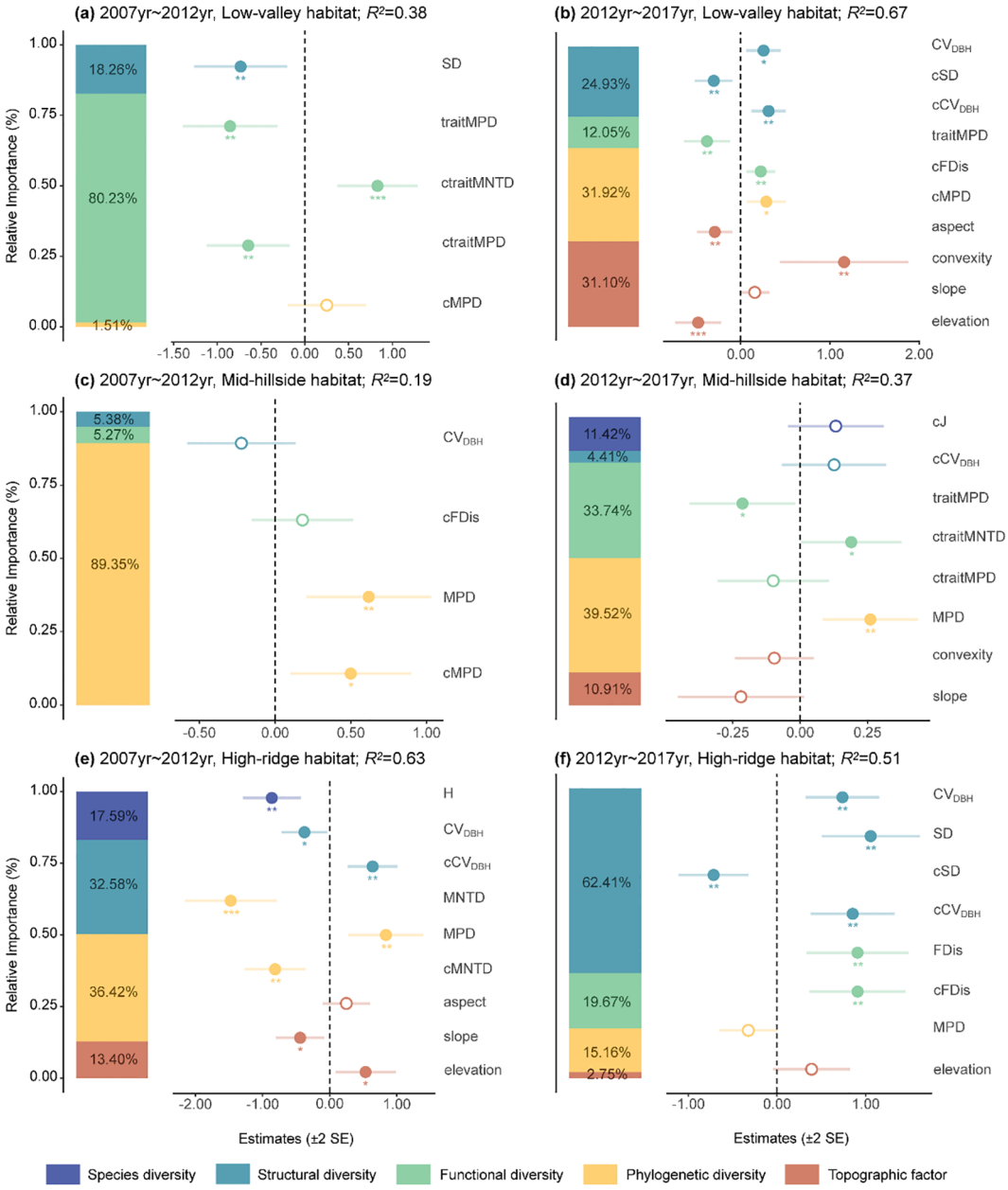


FIGURE 3
The main impact factors of aboveground biomass dynamics in Low-valley habitat **(A, B)**, Mid-hillside habitat **(C, D)**, and High-ridge habitat **(E, F)** from 2007 to 2017. Solid and open circles indicate significant or nonsignificant community diversity effects at p< 0.05, respectively. The meanings of abbreviations are the same as in Figure 2. *p< 0.05, **p< 0.01, ***p< 0.001.

mainly positively correlated with phylogenetic diversity and structural diversity during the 2012-2017 period. This could be attributed to the balance achieved between the high productivity but high mortality rates of early-successional species (acquisition strategy), and the lower productivity but also low mortality rates of late-successional species (conservative strategy), resulting in an increase in community productivity (Lasky et al., 2014; Zhang et al., 2023). However, we also found that ΔAGB was significantly negatively correlated with cSD and cMNTD. The variability observed in the correlations between various biodiversity indices and ΔAGB could be due to the varying capacities of each metric to capture the intensity of interactions within the forest ecosystems being studied, rather than an inherent ecological process (Yuan et al., 2018). Our results underscore the important role of multidimensional biodiversity and community context in elucidating the dynamic BEF relationships across temporal scales.

## 4.3 Changes of drivers and effects on aboveground biomass dynamics across habitat types

The spatial heterogeneity in resource supply rates can directly influence the biomass of producers, or indirectly impact producer biomass by limiting the variety of species that can coexist within an

ecosystem (Cardinale et al., 2009; Ferry et al., 2010). Our results revealed that both the drivers and effects on ΔAGB significantly varied across different habitat types. The factors influencing ΔAGB in low-valley habitat were extremely similar to those of the whole plot, possibly because this habitat has the highest number of plots (50), closely resembling the resource supply and utilization patterns of the whole plot. The result does not align with the discoveries from the low-altitude area in Dinghai, Zhejiang Province, where a nonsignificant relationship was found between biodiversity and biomass or productivity (Wu et al., 2018). This inconsistency may be a result of different dimensions of biodiversity, or the complex mediating role of environmental factors in the BEF relationship (Zhu et al., 2021). Additionally, we found that ΔAGB was significantly negatively correlated with aspect and elevation, but significantly positively correlated with convexity in this habitat. The low-valley habitat is defined by its significant topographical heterogeneity, featuring prominent rocks and small streams, making it particularly prone to regular disturbances like tree falls and seasonal stream flooding (Xu et al., 2015). Therefore, topographic factors had a significant effect on ΔAGB in this period.

In mid-hillside habitat, ΔAGB mainly showed a significant positive relationship with phylogenetic diversity. Liu et al. (2022) also found that phylogenetic diversity reaches its maximum in the mid-elevation region. It may be because the mid-hillside habitat serves as a transitional area between the low-valley and high-ridge habitats, where the favorable supply of light and water resources allows for the growth of most species in this environment (Legendre et al., 2009; Coomes et al., 2014). In addition, there were many broken and uprooted large trees found in slopes perhaps due to steep hillsides and shallow soil (Ferry et al., 2010; Xu et al., 2015), which could increase the openness of the canopy gaps, resulting in rapid regeneration of understory species (Song et al., 2018). Such an environment might offer opportunities for species with greater phylogenetic distance and different life history strategies to survive. In summary, it can be concluded that such ecological environment and resource supply enhance the positive effect of phylogenetic diversity on ΔAGB.

In high-ridge habitat, we found that ΔAGB was significantly influenced by all dimensions of biodiversity and topographical factors, which is consistent with the findings of most studies (Lasky et al., 2014; Yuan et al., 2018; Tiwari et al., 2023). The relationships among species in high-ridge habitat (high-altitude area) tend to be more intimate (Liu et al., 2022). The canopy gaps might increase the opportunities for species less associated with the vegetation in high-ridge habitat to recolonize from neighboring areas (Roxburgh et al., 2004). Given that the habitat is less disturbed (Man et al., 2011), the diversity of communities could reach the maximum and the coexistence of species will be promoted according to the Intermediate Disturbance Hypothesis (IDH) (Roxburgh et al., 2004). Moreover, the competition for resources especially light is minimal due to the lower stand density within high-ridge habitat (Ullah et al., 2021; Su et al., 2023), providing favorable conditions for the growth of recolonizing species. Overall, the increase in diversity had enhanced their influence on ΔAGB (Table 1). Synthesizing the results garnered from the various habitat types examined, our findings highlight that habitat heterogeneity constitutes a pivotal driver influencing the BEF relationship, providing a plausible perspective for investigating the spatial variations in BEF relationships.

## 5 Conclusions

In the present study, our comprehensive analysis elucidates the intricate interplay between multidimensional diversity and ΔAGB within natural forest ecosystems. We have demonstrated that both abiotic factors, such as topography, and biotic factors including functional diversity, phylogenetic diversity and structural diversity exert a significant influence on the ΔAGB over time and across various habitat types. Our decade-long analysis revealed a notable decline followed by an increase in community-level AGB, primarily within low-valley habitat, with no significant alterations observed in mid-hillside and high-ridge habitats. The determinants of ΔAGB exhibited substantial temporal shifts; functional and structural diversity were pivotal during the earlier period, while phylogenetic and structural diversity became increasingly influential in the subsequent period. Moreover, the drivers and effects on ΔAGB significantly varied across different habitat types. Our findings underscore the necessity of considering the spatiotemporal variability of both abiotic and biotic factors when assessing ecosystem function. This study not only addresses a critical gap in our understanding of BEF relationships but also provides valuable insights for conservation and management strategies aimed at preserving the health and resilience of forest ecosystems.

## Data availability statement

The original contributions presented in the study are included in the article/supplementary material. Further inquiries can be directed to the corresponding author.

## Author contributions

YB: Conceptualization, Formal analysis, Methodology, Visualization, Writing – original draft, Writing – review & editing. QW: Validation, Visualization, Writing – original draft. RZ: Data curation, Formal analysis, Investigation, Writing – original draft. JF: Formal analysis, Methodology, Visualization, Writing – original draft. JC: Conceptualization, Data curation, Supervision, Writing – review & editing. XM: Data curation, Investigation, Writing – review & editing. MY: Data curation, Funding acquisition, Investigation, Writing – review & editing. YW: Conceptualization, Data curation, Funding acquisition, Investigation, Methodology, Validation, Writing – original draft, Writing – review & editing.

## Funding

The author(s) declare financial support was received for the research, authorship, and/or publication of this article. This study

was financially supported by the "Pioneer" and "Leading Goose" R&D Program of Zhejiang (2023C03137), Zhejiang Undergraduate Science and Technology Innovation Activity Program (Xinmiao Talents Program) (2024R404A014) and Zhejiang Provincial Natural Science Foundation of China (LQ22C030001).

## Conflict of interest

The authors declare that the research was conducted in the absence of any commercial or financial relationships that could be construed as a potential conflict of interest.

## Generative AI statement

The author(s) declare that no Generative AI was used in the creation of this manuscript.

## Publisher's note



## References

Ali, A. (2019). Forest stand structure and functioning: Current knowledge and future challenges. *Ecol. Indic.* 98, 665–677. doi: 10.1016/j.ecolind.2018.11.017

Amiro, B. D., Barr, A. G., Barr, J., Black, T. A., Bracho, R., Brown, M., et al. (2010). Ecosystem carbon dioxide fluxes after disturbance in forests of North America. *J. Geophys. Res.* 115, G00K02. doi: 10.1029/2010JG001390

Bartoń, K. (2012). MuMIn: Multi-model inference. R package version 1.7.2 Available online at: http://CRAN.R-project.org/package=MuMIn (Accessed September 1, 2022).

Cadotte, M. W., Cavender-Bares, J., Tilman, D., and Oakley, T. H. (2009). Using phylogenetic, functional and trait diversity to understand patterns of plant community productivity. *PloS One* 4, e5695. doi: 10.1371/journal.pone.0005695

Canadell, J. G., and Raupach, M. R. (2008). Managing forests for climate change mitigation. *Science* 320, 1456–1457. doi: 10.1126/science.1155458

Cardinale, B. J., Bennett, D. M., Nelson, C. E., and Gross, K. (2009). Does productivity drive diversity or vice versa? A test of the multivariate productivity-diversity hypothesis in streams. *Ecology* 90, 1227–1241. doi: 10.1890/08-1038.1

Cardinale, B. J., Wright, J. P., Cadotte, M. W., Carroll, I. T., Hector, A., Srivastava, D. S., et al. (2007). Impacts of plant diversity on biomass production increase through time because of species complementarity. *Proc. Natl. Acad. Sci. U.S.A.* 104, 18123–18128. doi: 10.1073/pnas.0709069104

Chadwick, K. D., and Asner, G. P. (2016). Tropical soil nutrient distributions determined by biotic and hillslope processes. *Biogeochemistry* 127, 273–289. doi: 10.1007/s10533-015-0179-z

Chave, J., Réjou-Méchain, M., Búrquez, A., Chidumayo, E., Colgan, M. S., Delitti, W. B., et al. (2014). Improved allometric models to estimate the aboveground biomass of tropical trees. *Glob. Change Biol.* 20, 3177–3190. doi: 10.1111/gcb.12629

Chen, G. P., Cai, Q., Ma, S. H., Feng, Y. H., Fang, W. J., Ji, C. J., et al. (2023). Climate and forest attributes influence above-ground biomass of deciduous broadleaf forests in China. *J. Ecol.* 111, 495–508. doi: 10.1111/1365-2745.14042

Coomes, D. A., Flores, O., Holdaway, R., Jucker, T., Lines, E. R., and Vanderwel, M. C. (2014). Wood production response to climate change will depend critically on forest composition and structure. *Glob. Change Biol.* 20, 3632–3645. doi: 10.1111/gcb.12622

Dănescu, A., Albrecht, A. T., and Bauhus, J. (2016). Structural diversity promotes productivity of mixed, uneven-aged forests in southwestern Germany. *Oecologia* 182, 319–333. doi: 10.1007/s00442-016-3623-4

Fang, J. Y., Chen, A. P., Peng, C. H., Zhao, S. Q., and Ci, L. J. (2001). Changes in forest biomass carbon storage in China between 1949 and 1998. *Science* 292, 2320–2322. doi: 10.1126/science.1058629

Ferry, B., Morneau, F., Bontemps, J. D., Blanc, L., and Freycon, V. (2010). Higher treefall rates on slopes and waterlogged soils result in lower stand biomass and productivity in a tropical rain forest. *J. Ecol.* 98, 106–116. doi: 10.1111/j.1365-2745.2009.01604.x

Forrester, D. I., and Bauhus, J. (2016). A review of processes behind diversity-productivity relationships in forests. *Curr. For. Rep.* 2, 45–61. doi: 10.1007/s40725-016-0031-2

Fotis, A. T., Murphy, S. J., Ricart, R. D., Krishnadas, M., Whitacre, J., Wenzel, J. W., et al. (2018). Above-ground biomass is driven by mass-ratio effects and stand structural attributes in a temperate deciduous forest. *J. Ecol.* 106, 561–570. doi: 10.1111/1365-2745.12847

Fox, J., and Weisberg, S. (2018). *An R companion to applied regression* (USA: Sage publications).

Fraser, L. H., Pither, J., Jentsch, A., Sternberg, M., Zobel, M., Askarizadeh, D., et al. (2015). Worldwide evidence of a unimodal relationship between productivity and plant species richness. *Science* 349, 302–305. doi: 10.1126/science.aab3916

Gamfeldt, L., Snäll, T., Bagchi, R., Jonsson, M., Gustafsson, L., Kjellander, P., et al. (2013). Higher levels of multiple ecosystem services are found in forests with more tree species. *Nat. Commun.* 4, 1340. doi: 10.1038/ncomms2328

Gottschall, F., Cesarz, S., Auge, H., Kovach, K. R., Mori, A. S., Nock, C. A., et al. (2022). Spatiotemporal dynamics of abiotic and biotic properties explain biodiversity-ecosystem-functioning relationships. *Ecol. Monogr.* 92, e01490. doi: 10.1002/ecm.1490

Harms, K. E., Condit, R., Hubbell, S. P., and Foster, R. B. (2001). Habitat associations of trees and shrubs in a 50-ha neotropical forest plot. *J. Ecol.* 89, 947–959. doi: 10.1111/j.1365-2745.2001.00615.x

He, J. Y., Lu, L. Q., He, H. J., Zhang, Z. H., Hao, M. H., Zhang, C. Y., et al. (2024). Estimating the dynamics of ecosystem functions under climate change in a temperate forest region. *Ecol. Indic.* 166, 112353. doi: 10.1016/j.ecolind.2024.112353

Houghton, R. (2005). Aboveground forest biomass and the global carbon balance. *Glob. Change Biol.* 11, 945–958. doi: 10.1111/j.1365-2486.2005.00955.x

Huang, Y. Y., Chen, Y. X., Castro-Izaguirre, N., Baruffol, M., Brezzi, M., Lang, A., et al. (2018). Impacts of species richness on productivity in a large-scale subtropical forest experiment. *Science* 362, 80–83. doi: 10.1126/science.aat6405

Huston, M. A. (1997). Hidden treatments in ecological experiments: re-evaluating the ecosystem function of biodiversity. *Oecologia* 110, 449–460. doi: 10.1007/s004420050180

Isbell, F., Gonzalez, A., Loreau, M., Cowles, J., Díaz, S., Hector, A., et al. (2017). Linking the influence and dependence of people on biodiversity across scales. *Nat. Commun.* 546, 65–72. doi: 10.1038/nature22899

Jiang, C. C., Fu, J. Q., Wang, Y. Q., Chai, P. T., Yang, Y. D., Mi, X. C., et al. (2022). The habitat type and scale dependences of interspecific associations in a subtropical evergreen broad-leaved forest. *Forests* 13, 1334. doi: 10.3390/f13081334

Jin, Y., Chen, J. H., Mi, X. C., Ren, H. B., Ma, K. P., and Yu, M. J. (2015). Impacts of the 2008 ice storm on structure and composition of an evergreen broad-leaved forest community in eastern China. *Biodivers. Sci.* 23, 610. doi: 10.17520/biods.2015051

Jin, Y., and Qian, H. (2022). V. PhyloMaker2: An updated and enlarged R package that can generate very large phylogenies for vascular plants. *Plant Divers.* 44, 335–339. doi: 10.1016/j.pld.2022.05.005

Jucker, T., Bongalov, B., Burslem, D. F., Nilus, R., Dalponte, M., Lewis, S. L., et al. (2018). Topography shapes the structure, composition and function of tropical forest landscapes. *Ecol. Lett.* 21, 989–1000. doi: 10.1111/ele.12964

Kardol, P., Fanin, N., and Wardle, D. A. (2018). Long-term effects of species loss on community properties across contrasting ecosystems. *Nature* 557, 710–713. doi: 10.1038/s41586-018-0138-7

Kattge, J., Bönisch, G., Díaz, S., Lavorel, S., Prentice, I. C., Leadley, P., et al. (2020). TRY plant trait database-enhanced coverage and open access. *Glob. Change Biol.* 26, 119–188. doi: 10.1111/gcb.14904

Lai, J. S., Zhu, W. J., Cui, D. F., and Mao, L. F. (2023). Extension of the glmm.hp package to zero-inflated generalized linear mixed models and multiple regression. *J. Plant Ecol.* 16, rtad038. doi: 10.1093/jpe/rtad038

Lai, J. S., Zou, Y., Zhang, S., Zhang, X. G., and Mao, L. F. (2022). glmm. hp: an R package for computing individual effect of predictors in generalized linear mixed models. *J. Plant Ecol.* 15, 1302–1307. doi: 10.1093/jpe/rtac096

Laliberté, E., and Legendre, P. (2010). A distance-based framework for measuring functional diversity from multiple traits. *Ecology* 91, 299–305. doi: 10.1890/08-2244.1

Lasky, J. R., Uriarte, M., Boukili, V. K., Erickson, D. L., John Kress, W., and Chazdon, R. L. (2014). The relationship between tree biodiversity and biomass dynamics changes with tropical forest succession. *Ecol. Lett.* 17, 1158–1167. doi: 10.1111/ele.12322

Legendre, P., Mi, X. C., Ren, H. B., Ma, K. P., Yu, M. J., Sun, I. F., et al. (2009). Partitioning beta diversity in a subtropical broad-leaved forest of China. *Ecology* 90, 663–674. doi: 10.1890/07-1880.1

Li, G. Y. (2021). *Flora of zhejiang (New edition)* (Hangzhou: Zhejiang Science and Technology Publishing House).

Li, Y., Bao, W., Bongers, F., Chen, B., Chen, G., Guo, K., et al. (2019). Drivers of tree carbon storage in subtropical forests. *Sci. Total Environ.* 654, 684–693. doi: 10.1016/j.scitotenv.2018.11.024

Lian, Z. H., Wang, J., Fan, C. Y., and Von Gadow, K. (2022). Structure complexity is the primary driver of functional diversity in the temperate forests of northeastern China. *For. Ecosyst.* 9, 100048. doi: 10.1016/j.fecs.2022.100048

Liang, J. J., Crowther, T. W., Picard, N., Wiser, S., Zhou, M., Alberti, G., et al. (2016). Positive biodiversity-productivity relationship predominant in global forests. *Science* 354, aaf8957. doi: 10.1126/science.aaf8957

Lin, D. M., Lai, J. S., Muller-Landau, H. C., Mi, X. C., and Ma, K. P. (2012). Topographic variation in aboveground biomass in a subtropical evergreen broad-leaved forest in China. *PloS One* 7, e48244. doi: 10.1371/journal.pone.0048244

Liu, X. J. (2012). *Distribution pattern of functional traits of woody plants in subtropical forests and their relationship with the environment*. University of the Chinese Academy of Sciences, Beijing.

Liu, J. J., Zhang, X. X., Song, F. F., Zhou, S. R., Cadotte, M. W., and Bradshaw, C. J. (2015). Explaining maximum variation in productivity requires phylogenetic diversity and single functional traits. *Ecology* 96, 176–183. doi: 10.1890/14-1034.1

Liu, M. X., Zhang, G. J., Yin, F. L., Wang, S. Y., and Li, L. (2022). Relationship between biodiversity and ecosystem multifunctionality along the elevation gradient in alpine meadows on the eastern Qinghai-Tibetan plateau. *Ecol. Indic.* 141, 109097. doi: 10.1016/j.ecolind.2022.109097

Ma, K. P., and Liu, Y. M. (1994). Measurement of biotic community diversity I α diversity (Part 2). *Biodivers. Sci.* 2, 231–239. doi: 10.17520/biods.1994038

Man, X. X., Mi, X. C., and Ma, K. P. (2011). Effects of an ice storm on community structure of an evergreen broad-leaved forest in Gutianshan National Nature Reserve, Zhejiang Province. *Biodivers. Sci.* 19, 197. doi: 10.3724/SP.J.1003.2011.09220

McEwan, R. W., Lin, Y. C., Sun, I. F., Hsieh, C. F., Su, S. H., Chang, L. W., et al. (2011). Topographic and biotic regulation of aboveground carbon storage in subtropical broad-leaved forests of Taiwan. *For. Ecol. Manage.* 262, 1817–1825. doi: 10.1016/j.foreco.2011.07.028

Mi, X. C., Feng, G., Hu, Y. B., Zhang, J., Chen, L., Corlett, R. T., et al. (2021). The global significance of biodiversity science in China: an overview. *Natl. Sci. Rev.* 8, nwab032. doi: 10.1093/nsr/nwab032

Ouyang, S., Xiang, W. H., Wang, X. P., Xiao, W. F., Chen, L., Li, S. G., et al. (2019). Effects of stand age, richness and density on productivity in subtropical forests in China. *J. Ecol.* 107, 2266–2277. doi: 10.1111/1365-2745.13194

Pan, Y. D., Birdsey, R. A., Fang, J. Y., Houghton, R., Kauppi, P. E., Kurz, W. A., et al. (2011). A large and persistent carbon sink in the world's forests. *Science* 333, 988–993. doi: 10.1126/science.1201609

Paoli, G. D. (2006). Divergent leaf traits among congeneric tropical trees with contrasting habitat associations on Borneo. *J. Trop. Ecol.* 22, 397–408. doi: 10.1017/S0266467406003208

Petchey, O. L., and Gaston, K. J. (2002). Functional diversity (FD), species richness and community composition. *Ecol. Lett.* 5, 402–411. doi: 10.1046/j.1461-0248.2002.00339.x

Piao, S. L., Fang, J. Y., Ciais, P., Peylin, P., Huang, Y., Sitch, S., et al. (2009). The carbon balance of terrestrial ecosystems in China. *Nature* 458, 1009–1013. doi: 10.1038/nature07944

Quesada, C. A., Phillips, O. L., Schwarz, M., Czimczik, C. I., Baker, T. R., Patiño, S., et al. (2012). Basin-wide variations in Amazon forest structure and function are mediated by both soils and climate. *Biogeosciences* 9, 2203–2246. doi: 10.5194/bg-9-2203-2012

Ray, T., Delory, B. M., Beugnon, R., Bruelheide, H., Cesarz, S., Eisenhauer, N., et al. (2023). Tree diversity increases productivity through enhancing structural complexity across mycorrhizal types. *Sci. Adv.* 9, eadi2362. doi: 10.1126/sciadv.adi2362

Reich, P. B., Tilman, D., Isbell, F., Mueller, K., Hobbie, S. E., Flynn, D. F., et al. (2012). Impacts of biodiversity loss escalate through time as redundancy fades. *Science* 336, 589–592. doi: 10.1126/science.1217909

Ren, S., Ali, A., Liu, H., Yuan, Z., Yang, Q., Shen, G., et al. (2021). Response of community diversity and productivity to canopy gap disturbance in subtropical forests. *For. Ecol. Manage.* 502, 119740. doi: 10.1016/j.foreco.2021.119740

Richardson, K., Steffen, W., Lucht, W., Bendtsen, J., Cornell, S. E., Donges, J. F., et al. (2023). Earth beyond six of nine planetary boundaries. *Sci. Adv.* 9, eadh2458. doi: 10.1126/sciadv.adh2458

Roxburgh, S. H., Shea, K., and Wilson, J. B. (2004). The intermediate disturbance hypothesis: patch dynamics and mechanisms of species coexistence. *Ecology* 85, 359–371. doi: 10.1890/03-0266

Ruiz-Benito, P., Gómez-Aparicio, L., Paquette, A., Messier, C., Kattge, J., and Zavala, M. A. (2014). Diversity increases carbon storage and tree productivity in S panish forests. *Glob. Ecol. Biogeogr.* 23, 311–322. doi: 10.1111/geb.12126

Shui, W., Feng, J., Li, H., Jiang, C., Sun, X., Liu, Y. M., et al. (2022). Phylogeny and functional traits structure of plant communities with different slope aspects in the degraded karst tiankeng. *Acta Ecol. Sin.* 42, 8050–8060. doi: 10.5846/stxb202107201965

Song, X. Y., Hogan, J., Lin, L. X., Wen, H. D., Cao, M., and Yang, J. (2018). Canopy openness and topographic habitat drive tree seedling recruitment after snow damage in an old-growth subtropical forest. *For. Ecol. Manage.* 429, 493–502. doi: 10.1016/j.foreco.2018.07.038

Srivastava, D. S., Cadotte, M. W., Macdonald, A. A. M., Marushia, R. G., and Mirotchnick, N. (2012). Phylogenetic diversity and the functioning of ecosystems. *Ecol. Lett.* 15, 637–648. doi: 10.1111/j.1461-0248.2012.01795.x

Su, L., Heydari, M., Omidipour, R., Soheili, F., Cheraghi, J., Villa, P. M., et al. (2023). Stand structural diversity and elevation rather than functional diversity drive aboveground biomass in historically disturbed semiarid oak forests. *For. Ecol. Manage.* 543, 121139. doi: 10.1016/j.foreco.2023.121139

Sun, Y., Gu, L. H., Dickinson, R. E., and Zhou, B. Z. (2012). Forest greenness after the massive 2008 Chinese ice storm: integrated effects of natural processes and human intervention. *Environ. Res. Lett.* 7, 35702. doi: 10.1088/1748-9326/7/3/035702

Swenson, N. G., Enquist, B. J., Pither, J., Thompson, J., and Zimmerman, J. K. (2006). The problem and promise of scale dependency in community phylogenetics. *Ecology* 87, 2418–2424. doi: 10.1890/0012-9658(2006)87[2418:TPAPOS]2.0.CO;2

Synes, N. W., Ponchon, A., Palmer, S. C., Osborne, P. E., Bocedi, G., Travis, J. M., et al. (2020). Prioritising conservation actions for biodiversity: Lessening the impact from habitat fragmentation and climate change. *Biol. Conserv.* 252, 108819. doi: 10.1016/j.biocon.2020.108819

Tanner, E. V., Rodriguez-Sanchez, F., Healey, J. R., Holdaway, R. J., and Bellingham, P. J. (2014). Long-term hurricane damage effects on tropical forest tree growth and mortality. *Ecology* 95, 2974–2983. doi: 10.1890/13-1801.1

Tilman, D. (1999). The ecological consequences of changes in biodiversity: a search for general principles. *Ecology* 80, 1455–1474. doi: 10.1890/0012-9658(1999)080[1455:TECOCI]2.0.CO;2

Tiwari, R. M., Liu, J. L., Xie, Y. C., Yao, S. H., Liu, S. L., Wu, S. M., et al. (2023). Decoupling the impact of biodiversity and environmental factors on the biomass and biomass growth of trees in subtropical forests. *J. Plant Ecol.* 16, rtac040. doi: 10.1093/jpe/rtac040

Ullah, F., Gilani, H., Sanaei, A., Hussain, K., and Ali, A. (2021). Stand structure determines aboveground biomass across temperate forest types and species mixture along a local-scale elevational gradient. *For. Ecol. Manage.* 486, 118984. doi: 10.1016/j.foreco.2021.118984

van der Sande, M. T., Peña-Claros, M., Ascarrunz, N., Arets, E. J., Licona, J. C., Toledo, M., et al. (2017). Abiotic and biotic drivers of biomass change in a Neotropical forest. *J. Ecol.* 105, 1223–1234. doi: 10.1111/1365-2745.12756

Wang, S. P., Hong, P. B., Adler, P. B., Allan, E., Hautier, Y., Schmid, B., et al. (2024). Towards mechanistic integration of the causes and consequences of biodiversity. *Trends Ecol. Evol.* 39, 689–700. doi: 10.1016/j.tree.2024.02.008

Webb, C. O., Ackerly, D. D., Mcpeek, M. A., and Donoghue, M. J. (2002). Phylogenies and community ecology. *Annu. Rev. Ecol. Syst.* 33, 475–505. doi: 10.1146/annurev.ecolsys.33.010802.150448

Werner, F. A., and Homeier, J. (2015). Is tropical montane forest heterogeneity promoted by a resource-driven feedback cycle? Evidence from nutrient relations, herbivory and litter decomposition along a topographical gradient. *Funct. Ecol.* 29, 430–440. doi: 10.1111/1365-2435.12351

Wu, C. P., Han, W. J., Jiang, B., Liu, B. W., Yuan, W. G., Shen, A. H., et al. (2018). Relationships between species richness and biomass/productivity depend on environmental factors in secondary forests of Dinghai, Zhejiang Province. *Biodivers. Sci.* 26, 545. doi: 10.17520/biods.2017320

Wu, Z. Y., Raven, P. H., and Hong, D. Y. (1994-2009). *Flora of China* (Beijing and St Louis: Science Press and Missouri Botanical Garden Press).

Xu, Y. Z., Franklin, S., Wang, Q. G., Shi, Z., Luo, Y., Lu, Z. J., et al. (2015). Topographic and biotic factors determine forest biomass spatial distribution in a subtropical mountain moist forest. *For. Ecol. Manage.* 357, 95–103. doi: 10.1016/j.foreco.2015.08.010

Yang, B., Ma, R. H., Zhai, J., Du, J. R., Bai, J. H., and Zhang, W. H. (2024). Stand spatial structure is more important than species diversity in enhancing the carbon sink of fragile natural secondary forest. *Ecol. Indic.* 158, 111449. doi: 10.1016/j.ecolind.2023.111449

Yu, G. R., Chen, Z., Piao, S. L., Peng, C. H., Ciais, P., Wang, Q. F., et al. (2014). High carbon dioxide uptake by subtropical forest ecosystems in the East Asian monsoon region. *Proc. Natl. Acad. Sci. U.S.A.* 111, 4910–4915. doi: 10.1073/pnas.1317065111

Yu, M. J., Hu, Z. H., Yu, J. P., Ding, B. Y., and Fang, T. (2001). Forest vegetation types in Gutianshan natural reserve in Zhejiang. *J. Zhejiang. Univ. Agric. Life Sci.* 27, 375–380. Available online at: https://www.zjujournals.com/agr/CN/Y2001/V27/I4/375.

Yuan, Z. Q., Ali, A., Jucker, T., Ruiz-Benito, P., Wang, S. P., Jiang, L., et al. (2019). Multiple abiotic and biotic pathways shape biomass demographic processes in temperate forests. *Ecology* 100, e02650. doi: 10.1002/ecy.2650

Yuan, Z. Q., Wang, S. P., Ali, A., Gazol, A., Ruiz-Benito, P., Wang, X. G., et al. (2018). Aboveground carbon storage is driven by functional trait composition and stand structural attributes rather than biodiversity in temperate mixed forests recovering from disturbances. *Ann. For. Sci.* 75, 1–13. doi: 10.1007/s13595-018-0745-3

Zemp, D. C., Guerrero-Ramirez, N., Brambach, F., Darras, K., Grass, I., Potapov, A., et al. (2023). Tree islands enhance biodiversity and functioning in oil palm landscapes. *Nature* 618, 316–321. doi: 10.1038/s41586-023-06086-5

Zhang, Y., and Chen, H. Y. (2015). Individual size inequality links forest diversity and above-ground biomass. *J. Ecol.* 103, 1245–1252. doi: 10.1111/1365-2745.12425

Zhang, Y. H., Jin, B. C., Zhang, X. L., Wei, H. H., Chang, Q. Q., Huang, F. Q., et al. (2023). Grazing alters the relationships between species diversity and biomass during community succession in a semiarid grassland. *Sci. Total Environ.* 887, 164155. doi: 10.1016/j.scitotenv.2023.164155

Zhang, R., Li, S. F., Huang, X. B., Li, C., Xu, C. H., and Su, J. R. (2024). Diversity-biomass relationships are shaped by tree mycorrhizal associations and stand structural diversity at different spatial scales. *For. Ecosyst.* 11, 100234. doi: 10.1016/j.fecs.2024.100234

Zhang, F., Zhou, G. Y., Hiratsuka, M., Tanaka, K., and Morikawa, Y. (2012). Influence of an ice storm on aboveground biomass of subtropical evergreen broadleaf forest in Lechang, Nanling mountains of Southern China. *Int. J. For. Res.* 2012, 467848. doi: 10.1155/2012/467848

Zheng, L. T., Barry, K. E., Guerrero-Ramírez, N. R., Craven, D., Reich, P. B., Verheyen, K., et al. (2024). Effects of plant diversity on productivity strengthen over time due to trait-dependent shifts in species overyielding. *Nat. Commun.* 15, 2078. doi: 10.1038/s41467-024-46355-z

Zhu, J. J., Lu, D. L., and Zhang, W. D. (2014). Effects of gaps on regeneration of woody plants: a meta-analysis. *J. For. Res.* 25, 501–510. doi: 10.1007/s11676-014-0489-3

Zhu, J., Wu, A. C., Zou, S., Xiong, X., Liu, S. Z., Chu, G. W., et al. (2021). Relationships between tree diversity and biomass/productivity and their influence factors in a lower subtropical evergreen broad-leaved forest. *Biodivers. Sci.* 29, 1435. doi: 10.17520/biods.2021014

frontiers | Frontiers in Plant Science

TYPE Original Research
PUBLISHED 20 February 2025
DOI 10.3389/fpls.2025.1553886



OPEN ACCESS

EDITED BY
Xiang Liu,
Lanzhou University, China

REVIEWED BY
Yongxiu Sun,
Yan'an University, China
Xianfeng Yang,
Chinese Academy of Tropical Agricultural Sciences, China

*CORRESPONDENCE
Hui Zhang
13925183735@139.com
Cui Chen
421656231@qq.com
Qingqing Yang
xiaohua.chen@hnaf.ac.cn
Wenfeng Gong
gwf101@163.com

†These authors have contributed equally to this work

RECEIVED 31 December 2024
ACCEPTED 27 January 2025
PUBLISHED 20 February 2025

CITATION
Mao J, Xue P, Chen Y, Xiang T, Zhang H, Chen C, Yang Q and Gong W (2025) Wood density can best predict carbon stock in the forest aboveground biomass following restoration in a post open limestone mining in a tropical region.
*Front. Plant Sci.* 16:1553886.
doi: 10.3389/fpls.2025.1553886



# Wood density can best predict carbon stock in the forest aboveground biomass following restoration in a post open limestone mining in a tropical region

Junyang Mao[1†], Peipei Xue[2†], Yuxin Chen[1], Ting Xiang[1], Hui Zhang[3*], Cui Chen[4*], Qingqing Yang[5*] and Wenfeng Gong[1*]

[1]School of Ecology, Hainan University, Haikou, China, [2]Chongqing Academy of Forestry, Wulingshan Forest Eco-station, Chongqing, China, [3]Wanning Tropical Lowland Rainforest Restoration and Utilization, Hainan Observation and Research Station, Haikou, China, [4]School of Geography and Tourism, Huanggang Normal University, Huanggang, Hubei, China, [5]Hainan Academy of Forestry (Hainan Academy of Mangrove), Haikou, China

**Introduction:** Reforestation has been widely considered to best solve this problem, but this requires an accurate estimation of carbon stocks in the forest aboveground biomass (AGB) at a large scale. AGB models based on traits and remote sensing indices (moisture vegetation index (MVI)) are the two good methods for this purpose. But limited studies have developed them to estimate carbon stock in AGB during restoration of degraded mining areas.

**Methods:** Here, we have successfully addressed this challenge as we have developed trait-based and MVI-based AGB models to estimate carbon stock in the AGB after performing reforestation in a 0.2 $km^2$ degraded tropical mining area in Hainan Island in China. During this reforestation, seven non-native fast-growing tree species were planted, which has successfully recovered soil processes (including soil microorganisms, nematodes and chemical and physical properties).

**Results and discussions:** By using these two models to evaluate carbon stock in AGB, we have found that an average of 78.18 Mg C $hm^{-2}$ could be accumulated by our reforestation exercise. Moreover, wood density could predict AGB for this restored tropical mining site, and indicated that strategies of planting fast-growing species leads to fast-growing strategies (indicated by wood density) which in turn determined the largely accumulated carbon stocks in the AGB during restoration. This restoration technology (multiple-planting of several non-native fast-growing tree species) and the two accurate and effective AGB models (trait-based and MVI-based AGB models) developed by us could be applied to 1) restore other degraded tropical mining area in China, and 2) estimate carbon stock in forest AGB after performing restoration.

KEYWORDS

**carbon emission, carbon stock, functional traits, land use, vegetation**

# 1 Introduction

Variations in global carbon stocks are largely determined by terrestrial ecosystem (Migliavacca et al., 2021; Tang et al., 2022). Globally, industrial mining has destroyed nearly 2 million hectares of land (FAO, 2015), and the changes in land use and cover as a consequence of mining are considered as a main driver of terrestrial carbon loss (Baier et al., 2022; Tagesson et al., 2020). Mining activities have influenced approximately 11.5% of the global terrestrial area (Luckeneder et al., 2021). Thus, ecological degradation and emission of greenhouse gases throughout the world may be aggravated by mining, which in turn influence the global climate and pose a serious threat to the ecological safety (Zhu et al., 2024).

Two potential ways have been assumed to be effective in balancing the global C cycle. The first involves cutting the carbon emissions, whereas the second warrants an increase in the natural C sink to offset the increased carbon emissions (Ahirwal et al., 2017). The loss of forest-cover due to open strip mining activities have significantly increased the C level in the atmosphere (Mukhopadhyay and Maiti, 2014). Increasing forest area could be a sustainable tool to mitigate elevated atmospheric $CO_2$ concentration (IPCC, 2001). As a result, performing reforestation in degraded mining area to increase forest cover has widely been suggested to decrease the potential carbon emission due to mining (Ahirwal et al., 2017; Yuan et al., 2023; Zhu et al., 2024). Tropical forests contain 55% of the global stores of aboveground forest carbon (Pan et al., 2011; Philipson et al., 2020). Mining constitute one of the biggest threats to vegetation and soil in the tropical forests, which thereby gives rise to a large amount of carbon emission (Ahirwal et al., 2017; Zhang et al., 2024a). Thus, it is very necessary to perform reforestation in degraded tropical mining area to enlarge natural C sink to prevent the increase in the atmospheric $CO_2$ level.

Accurate estimation of forest aboveground biomass (AGB) can directly determine the C accumulation capacity of the tree species in the restored mining area. The greater estimates of AGB indicate a high C accumulation capacity of the plants (Zhao et al., 2014; Ahirwal et al., 2017). Traditionally, AGB is estimated by harvesting multiple individuals of several tree species to obtain diameter at breast height (DBH) and height (H) for developing an estimation model [$AGB = a \times (DBH^2 \times H^b)$] (Chave et al., 2005). Then, by measuring DBH and H for all the individuals of every tree species in an ecosystem could accurately estimate the AGB for an ecosystem. However, this method could only be used at a small scale, because it takes a long time to measure DBH and H of all trees of every species in a forest.

Two more ABG models could be developed for a forest ecosystem, (1) a remote sensing indices-based AGB model; and (2) a trait-based AGB model. Vegetation indices obtained from remote sensing (moisture vegetation index (MVI)) are highly related to forest AGB in tropical forests (Boyd, 1999; Foody et al., 2003; Freitas et al., 2005). MVI, at large and regional scales, could be easily obtained from remote sensing images. Therefore, MVI-based model is more effective than a traditional model for estimating AGB for a forest ecosystem. Functional traits that are correlated with the growth rate of individual plants (Perez-Harguindeguy et al., 2013) are also expected to be mechanistically related to primary productivity of the vegetation (Garnier et al., 2004). It has been found that key traits (for example, specific leaf area (SLA), and wood density) not only directly determine AGB, they also indicate the mechanisms that result in alterations in AGB in the tropical forests (Baker et al., 2004; Nam et al., 2018; Phillips et al., 2019; Finegan et al., 2015; Wang and Ali, 2021). Functional traits could only be measured for 3-5 individuals of one tree species (Garnier et al., 2004; Zhang et al., 2018). Consequently, compared to a traditional model, a trait-based model is also more effective for the estimation of AGB for tropical forests. However, relatively few studies have developed these two models to accurately and effectively estimating AGB for tropical forests, let alone for restored tropical mining area.

Since 2013, a reforestation project has been initiated to restore a 0.2 $km^2$ degraded tropical limestone mining area near the southern edge of Hainan Island (Figures 1A–C, Zhang et al., 2024a, b). Limestone mining for the cement industry had been performed for two decades in this area, which had converted an original tropical rainforest into an open-mining area (bare rocky substrates, without any plants; Figures 1B, C, Zhang et al., 2023, 2024a). By mix-planting one non-native shrub species and seven non-native fast-growing tree species, this open-mining area now has been successfully restored into a secondary tropical rainforest, whose soil microorganisms, nematodes and physical and chemical properties are comparable to those of an adjacent undisturbed tropical rainforest (Zhang et al., 2024a, b).

Limestone mining and the global production of cement has grown in tandem with economic development (Uwasu et al., 2014; Farfan et al., 2019). The exponential increase in cement production and export in recent decades has resulted in a global annual quarrying of over 178 million metric tons, with huge areas being mined for limestone, particularly in Asia (Hughes et al., 2017). The production of cement at this scale has enormous environmental implications as it utilizes about 1.9% of the global electricity production and contributes 5-8% of the global $CO_2$ emissions (Farfan et al., 2019).

Moreover, China has become a major mining country, which in turn may lead it to be one of the largest carbon emitters (assessment of carbon sequestration potential of mining areas under ecological restoration in China). Recovering the degraded mining areas, preventing the geological hazards and performing reforestation to recover the green landscape in the mining areas are the main focus in China (Chen et al., 2022; Zhu et al., 2024). However, it remains unclear whether restored mining areas could increase carbon sequestration potential (assessment of carbon sequestration potential of mining areas under ecological restoration in China). Thus, the above-mentioned restored tropical limestone mining area (in the Hainan Island) provide us with a perfect platform to develop trait-based and MVI-based AGB models to determine the amount of carbon accumulated by this successful reforestation. For achieving this goal, we first harvested a total of 35 trees (five individuals for each of the seven native tree species) to obtain DBH and H so that we could develop a traditional AGB model. Then, we measured six key functional traits (transpiration rate (mmol $m^{-2}$ $s^{-1}$), stomatal conductance (mmol $m^{-2}$ $s^{-1}$), leaf hydraulic conductance (mmol $m^{-1}$ $s^{-1}$ $MPa^{-1}$), photosynthesis rate (μmol $m^{-1}$ $s^{-1}$), specific leaf area

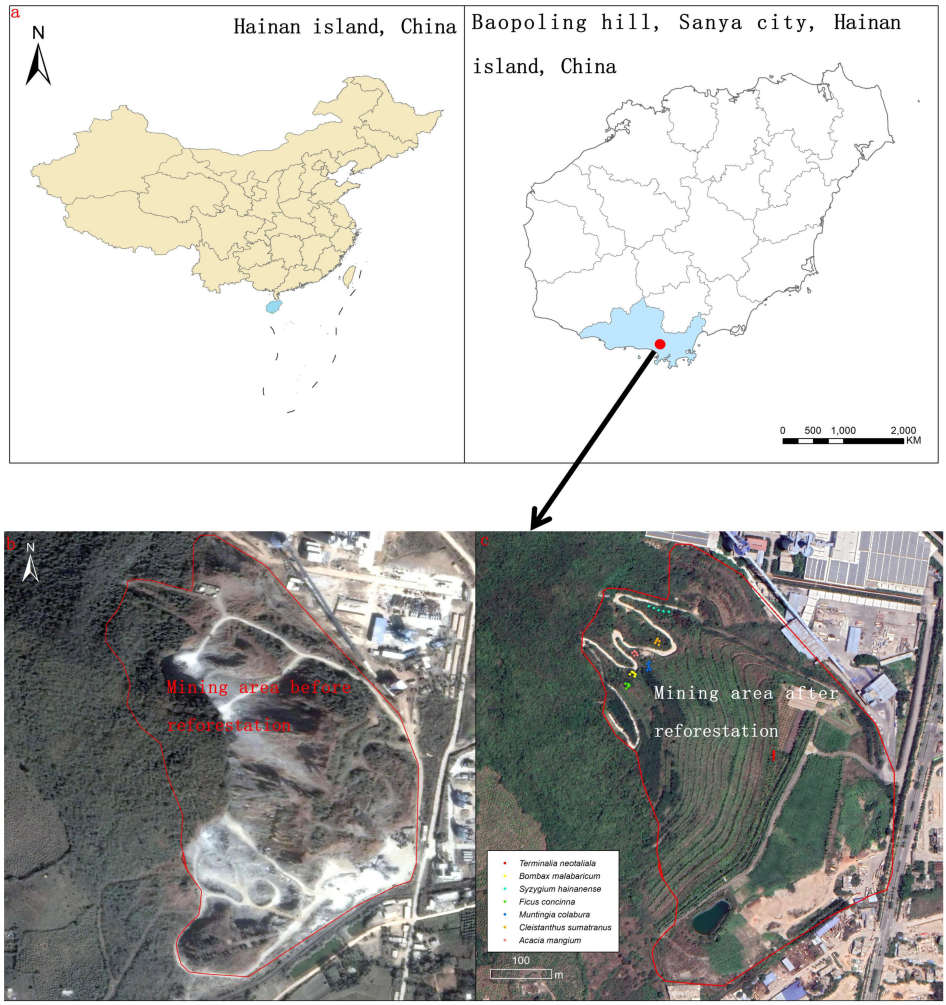


FIGURE 1
The location of the study sites **(A)**, landscape for mining area before and after reforestation, and the location of our sampled 35 trees of the seven species (5 individuals for each tree species) that were used for our reforestation and generating the aboveground biomass (AGB) model **(B, C)**.

(cm $g^{-1}$) and wood density (g $m^{-3}$) and obtained the MVI from the remote sensing images for this restored tropical mining area. Finally, we utilized data on six functional traits, and the MVI to further generate more effective trait-based and MVI-based AGB models. These two models could not only accurately estimate how much carbon stock was accumulated by our reforestation, but also provide two useful tools for estimating AGB for other restored tropical mining areas in China.

# 2 Materials and methods

## 2.1 Study sites

The study site was located in a limestone mountain near Sanya City of Hainan Island, China (110°58′01′′E, 19° 38′48′′N; Baopoling Mountain; 300 m a.s.l). The area has a tropical monsoon oceanic climate, with a mean annual temperature of 28° C, and 1500 mm of mean annual precipitation, about 91% of which occurs between the months of June to October (Zhang et al., 2024a). The natural vegetation of the area is classified as broadleaf tropical rainforest (Zhang et al., 2024a). In this area, limestone was extensively mined between 1995 to 2015 (Zhang et al., 2023). We reforested a degraded mine area of about 0.2 $km^2$, whose mining history and our reforestation efforts has been described in detail in a recent study (Zhang et al., 2023).

## 2.2 Harvesting of trees and sampling of functional traits in the restored mining area

Since seven non-native tree species (*Terminalia neotaliala*, *Bombax ceiba*, *Ficus concinna*, *Muntingia colabura*, *Cleistanthus sumatranus*, *Acacia mangium* and *Syzygium hainanense*) were used in our restoration, we harvest 35 trees (five individuals for each species). First, we measured the DBH and height for all the individuals for all the seven tree species in the restored site and calculated the mean DBH and height for each of the seven non-native tree species. Then, for each species, we randomly selected 5 individuals whose DBH and height were comparable to the mean

DBH and height; their locations were shown in detail in Figure 1C. Finally, we harvested the aboveground parts of all 35 selected trees and obtained their dry weight as AGB. We also used these 35 selected trees/individuals to measure six functional traits (transpiration rate, stomatal conductance, leaf hydraulic conductance, photosynthesis rate, specific leaf area and wood density). The details of measurements of these six functional traits have been described in previous studies (Li et al., 2015; Shen et al., 2016; Zhang et al., 2018), and further summarized in the Supplementary Material.

### 2.3 The developments of traditional, trait-based and MVI-based AGB models

Following Chave et al. (2005), we first used the following equation ($AGB= a\times(DBH^2\times H)^b$) to develop a traditional AGB model. Then, we used a penalization on the number of parameters, the Akaike information criterion (AIC) to get the best parameter (a and b). Specifically, the best a and b should be derived at the minimum AIC. We also provided the residual standard error (RSE) to be used as an alternative statistic.

For developing a MVI-based AGB model, we first collected the remote sensing images for the restored mining areas, which are from Landsat8 OLI (http://glovis.usgs.gov/) and Jilin-1 (https://www.jl1mall.com/store/). The ENVI software was used to perform a series of processing, such as radiometric correction, atmospheric correction, and terrain correction, for the remote sensing images of the mining areas from Landsat8 OLI. The ENVI software was also first used for completing the radiometric and atmospheric corrections for Jilin-1. Then, topographic maps (1:10000), the RTK sampling of the ground point coordinates, and the DEM data for the whole of the restored mining area were utilized to finish the orthorectified processing of Jilin-1, with a resampling resolution of 0.75m. By using the Jilin-1 image as the reference, automatic registration module in the ENVI software was used to complete the dynamic matching processing of Landsat8 OLI and Jilin-1 remote sensing images, and the fusion processing of Landsat8 OLI and Jilin-1 was completed to generate the high-resolution remote sensing data, whose map projection coordinate system was WGS1984-UTM_Zone49N. Following Freitas et al. (2005), this study selected the following combinations of red band (0.63-0.69 μ m) and short infrared band (1.55-1.75 μ m) to analyze the generated high-resolution remote sensing data to get the moisture vegetation index (MVI). The following equation was used: $MVI5 = (NIR - MIR5)/(NIR + MIR5)$, where NIR and MIR5 represent the near-infrared band and mid-infrared band, respectively. Specifically, the unit for unit size for extracting the Moisture Vegetation Index (MVI) is based on each 0.75 ×0.75 $m^2$ image. With the support of ArcGIS Pro software, the mean DBH and H for the mining area were used to develop the model between MVI and DBH, and between MVI and H. Specifically, the DBH-MVI and H-MVI models are $DBH=1.1770\times MVI5_m00 + 11.7964$ and $H=44.171\times MVI5_r01$-10.06405 and respectively (Supplementary Figures S1 and S2). Finally, the MIV-based AGB model was directly obtained by using the developed traditional AGB mode.

In terms of trait-based AGB model, we only used the linear regression to quantify the relationship between AGB and each of the six functional traits (transpiration rate, stomatal conductance, leaf hydraulic conductance, photosynthesis rate, specific leaf area and wood density). Our main purpose was to find out which trait could best determine AGB.

## 3 Results

By using the measured mean DBH and H values for the restored mining area, and AGB for the harvested 35 individuals for the seven tree species, we finally derived the traditional AGB model as following: $AGB= 34.8279\times(DBH^2\times H)^{0.1117}$ (Figure 2). By using the measured mean DBH and H for the restored mining area and the generated high-resolution remote sensing data, which is derived from Landsat8 OLI and Jilin-1, first, we got the model between the DBH and MVI ($DBH=1.770\times MVI5_m00 + 11.7964$; the generated mean DBH of the whole mining area is presented in Figure 3A). Also, we obtained a model between H and MVI as ($H=44.4171\times MVI5_r01$-10.0650511.7964; the generated mean H for the whole of the mining area is presented in Figure 3B). Here, $MVI5_m00$ and $MVI5_r01$ represent the mean MVI in the wet and dry season, respectively. Then, by using the developed traditional AGB model, we finally obtained the MVI-based AGB model as ($AGB= 34.8279\times((1.770\times MVI5_m00 + 11.7964)^2\times(44.4171\times MVI5_r01$-$10.0650511.7964))^{0.1117}$, Figure 4). We also provided the actual AGB (ranging from 65.0426-87.5317, Figure 3C) and predicted the AGB (ranging from 70.6116-83.0665, Figure 3D), which are based on both traditional and the MVI-based AGB models.

Our linear regression analysis clearly demonstrated that among the six functional traits, only wood density could determine the AGB. Wood density was significantly positively related to AGB (Figure 5), whereas the other five traits were not significantly associated (Figure 5).

## 4 Discussion

A greater AGB indicates a high C accumulation capacity of the plants (Zhao et al., 2014; Ahirwal et al., 2017; Zhu et al., 2024). Developing trait-based and MVI-based AGB models could directly indicate the amount of C that could be accumulated during the reforestation of degraded tropical mining areas. In this study, we have successfully developed trait-based and MVI-based AGB models for accurately estimating the carbon stock in the AGB of a successfully restored 0.2 $km^2$ tropical limestone mining area. By using these two models, we have found that an average of 78.18 Mg C $hm^{-2}$ could have been accumulated during our reforestation exercise. This value is much higher than those in the other restored tropical mining areas. For example, Ahirwal et al. (2017) showed that a restored tropical mining area could only accumulate 23.7 Mg C $hm^{-2}$. Similarly, Agus et al. (2016) had demonstrated that recovered tropical mining area was able to accumulate less than 30

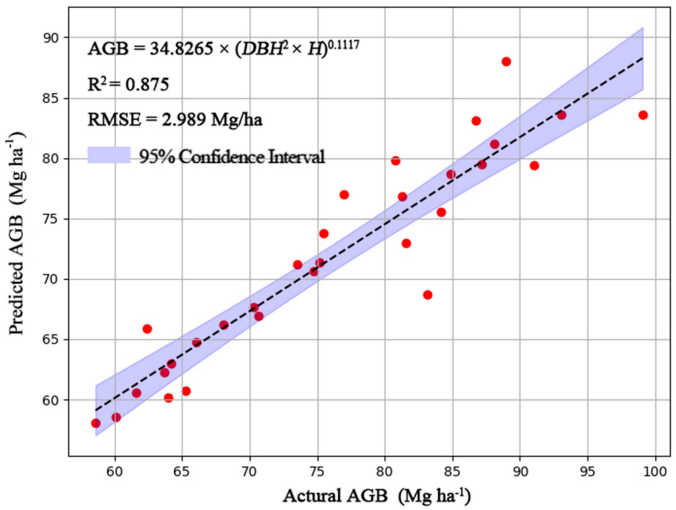


FIGURE 2
Development of a traditional AGB model (AGB= 34.8279×(DBH$^2$×H)$^{0.1117}$) on the basis of AGB, DBH and height for our sampled 35 individuals for the seven tree species.

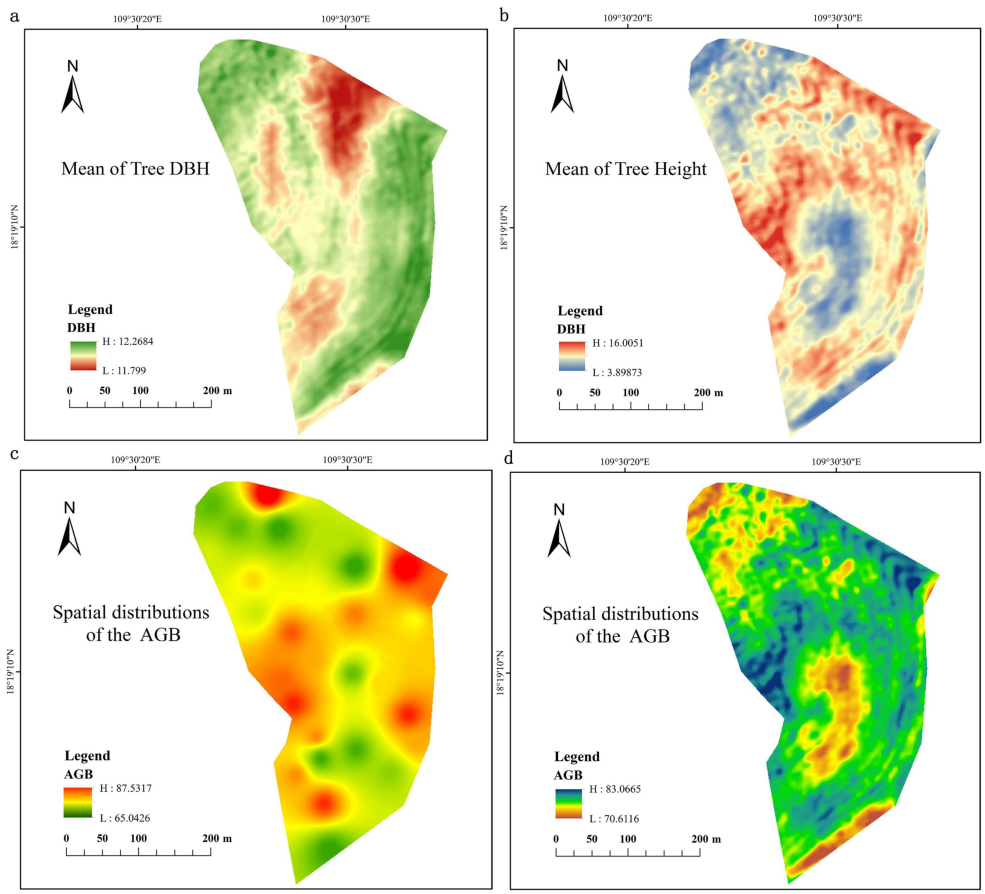


FIGURE 3
Predicted mean height **(A)** and DBH **(B)** that were used along with the remote sensing images. Actual AGB **(C)** and predicted AGB **(D)**, which are based on traditional AGB model, are presented.

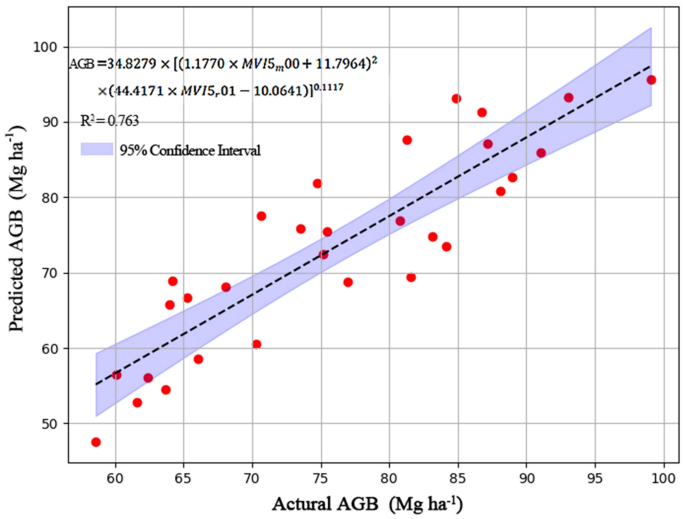


FIGURE 4
Development of a MVI-based AGB model (AGB= 34.8279×((1.770×MVI5$_m$00 + 11.7964)$^2$×(44.4171×MVI5$_r$01-10.0650511.7964))$^{0.1117}$).

Mg C hm$^{-2}$. It has been found that mature tropical forests can accumulate 57-375 Mg C hm$^{-2}$ across the tropics (Lewis et al., 2013; Niiyama et al., 2010). In these scenarios, our reforestation exercise was able to achieve high levels of accumulated carbon stocks. Consequently, we recommend that our tropical limestone mining restoration program should be expanded to other degraded tropical limestone mining areas.

Vegetation indices (MVI) has been widely used to estimate AGB at large scale (Freitas et al., 2005). But to the best of our knowledge, limited studies have developed a MVI-based model for estimating AGB in a restored tropical mining area. By combining the use of a traditional AGB model and a MVI obtained from remote sensing images, for the first time, our study has successfully developed a MVI-based AGB model (AGB= 34.8279×((1.770×MVI5$_m$00 + 11.7964)$^2$×(44.4171×MVI5$_r$01-10.0650511.7964))$^{0.1117}$). This model can be applied to estimate the amount of carbon that has been stored after the reforestation of the degraded tropical mining areas.

The relationships between the six traits and the AGB clearly demonstrated that only wood density could predict AGB for our restored limestone mining area. This result is consistent with other findings (Iida et al., 2012; King et al., 2006; Poorter et al., 2008). This also further confirms that wood density can determine AGB for tropical forests (Baker et al., 2004; Nam et al., 2018; Phillips et al., 2019). We found wood density is significantly positively related to AGB in our restored tropical mining area. This observation supports the findings in Chave et al. (2008), who show that the species with higher wood densities could attain more AGB than those with low wood density in different forest sites in three continents (Africa, America and Asia). Wood density is considered as a key trait for capturing growth of tropical forest species, with higher wood density indicating fast-growing strategies (Nam et al., 2018). Thus, this results also clearly elucidated fast-growing strategies determined the accumulation of C in all the tree species. The other five functional traits are highly associated with plant photosynthesis and hydrology (Li et al., 2015; Shen et al., 2016; Zhang et al., 2018). However, they were not good predictors of AGB in our restored tropical mining area. Thus, strategies of plant photosynthesis and hydrology may not be the good predictor of C accumulation in our restored tropical mining area. However, future control experiments of light and water environments are required to further verify this.

The choice of tree species for initial planting are primarily based on the goals of the restoration (de Souza Barbosa et al., 2021). But a natural recommendation is to plant native species to recover original biodiversity and function (Cunningham et al., 2015). Importantly, it has been amply demonstrated that restoration could contribute greatly to achieving the multiple sustainable development goals (SDGs) of the United Nations (Ahirwal and Maiti, 2022; Ghosh and Maiti, 2021a, b). Land supports the resources and provides the matrix for achieving multiple SDGs, which include climate action, life on land, reduction of poverty and hunger, human health and wellbeing, as well as affordable and clean energy (Ghosh and Maiti, 2021a). So, the goals of restoration could be very broad and comprehensive. Irrespective of the set of goals and the choice of tree species for initial planting, the basic ecological processes of colonization and establishment by native species, and the natural ecological successions are bound to operate and contribute to plant community development (Ahirwal et al., 2017).

Generally when the reforestation begins at an open-site conditions, fast-growing, and native early successional species are a natural choice for their better growth and survival and also their facilitation for recovering original biodiversity and function (Nunes et al., 2020; Reid et al., 2015). However, the choice of species may often be limited by the availability of seeds and seedlings for planting (Nunes et al., 2020; Osorio-Salomón et al., 2021). Therefore, non-native tree species have often been used in the initial planting for restoration (Cunningham et al., 2015; Damptey et al., 2020; Nunes et al., 2020). Planting non-native species may result in a poor or slow recovery of attributes like biodiversity, soil physical and biological structure (for example, soil bulk density and

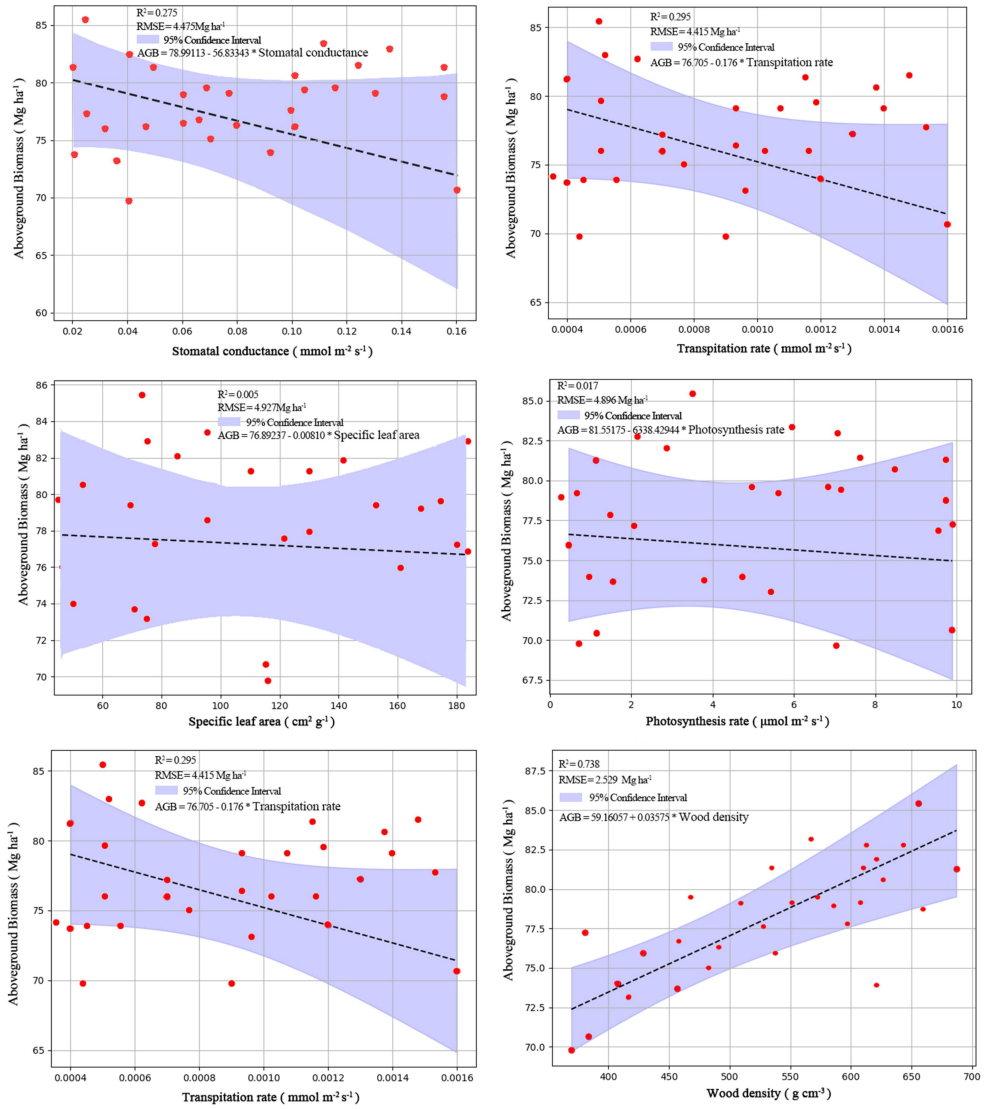


FIGURE 5
The relationships between the six functional traits (transpiration rate, stomatal conductance, leaf hydraulic conductance, photosynthesis rate, specific leaf area and wood density) and AGB. Specifically the responding trait-based model for these six traits are shown respectively as: AGB=59.16057 + 0.03575×WD (wood density), AGB=76.705-0.176×A (transpiration rate), AGB=76.89237 + 0.00810×SLA (specific leaf area), AGB=85.55175 + 6338.4294×E (photosynthesis rate), AGB=78.99113 + 56.83343×gsw (stomatal conductance), and AGB=81.98104 + 435.44942×Kleaf (leaf hydraulic conductance).

microorganism), soil water content, and soil fertility (Cunningham et al., 2015; Liu et al., 2021; Zhao et al., 2021). However, non-native species could greatly improve the recovery of biomass at a speed at which restoration can be achieved. Based on this scenario, we finally mix-plant seven non-native fast-growing tree species, to restore our degraded tropical mining area. This type of restoration has successfully restored this degraded tropical mining area into a secondary tropical rainforest, whose soil microorganisms, nematodes and physical and chemical properties are comparable to those of an adjacent undisturbed tropical rainforest (Zhang et al., 2024a, b). More important, we further demonstrate that this type of reforestation may result in very high carbon accumulation. As a result, multiple non-native fast-growing tree species should be utilized to perform restoration of degraded tropical mining area in China. However future comparison experiments should be performed whether planting native tree species can achieve more carbon stock than planting-non-native tree species.

## 5 Conclusion

The restoration of mined areas has been widely assumed as a good way to reduce carbon emission that result from mining. By using a successfully recovered tropical limestone mining platform, we have demonstrated that this restoration could indeed accumulate high levels of C, and thereby could facilitate in reducing C emissions. This restoration technology, along with the two accurate (and effective) AGB models (trait-based and MVI-based AGB models)

developed in this study, can be applied to 1) restore other degraded tropical mining area in China, and 2) to evaluate carbon stocks in the forest AGB in other restored mining area.

## Data availability statement

The raw data supporting the conclusions of this article will be made available by the authors, without undue reservation.

## Author contributions

JM: Conceptualization, Data curation, Formal analysis, Investigation, Methodology, Project administration, Resources, Validation, Writing – original draft, Writing – review & editing. PX: Conceptualization, Data curation, Formal analysis, Funding acquisition, Methodology, Project administration, Validation, Writing – original draft, Writing – review & editing. YC: Conceptualization, Investigation, Software, Writing – original draft. TX: Conceptualization, Investigation, Software, Writing – original draft. CC: Conceptualization, Formal analysis, Investigation, Methodology, Project administration, Supervision, Validation, Writing – original draft, Writing – review & editing, Software. HZ: Conceptualization, Data curation, Formal analysis, Funding acquisition, Investigation, Methodology, Project administration, Supervision, Validation, Writing – original draft, Writing – review & editing. QY: Investigation, Methodology, Project administration, Software, Supervision, Validation, Writing – original draft, Writing – review & editing. WG: Formal analysis, Investigation, Methodology, Project administration, Software, Supervision, Validation, Writing – original draft, Writing – review & editing.

## Funding

The author(s) declare financial support was received for the research, authorship, and/or publication of this article. This work was funded by the Hainan Province Science and Technology Special Fund (ZDYF2022SHFZ320), Hainan Provincial Natural Science Foundation of China (422CXTD508), the National Natural Science Foundation of China (No. 32360386) and the National Key Research and Development Program "Microhabitat Regulation and Mixed Forest Management Techniques for the Configuration of Companion Species in Low-Productivity Plantations (2023YFF1305202-5).

## Conflict of interest

The authors declare that the research was conducted in the absence of any commercial or financial relationships that could be construed as a potential conflict of interest.

## Generative AI statement

The author(s) declare that no Generative AI was used in the creation of this manuscript.

## Publisher's note



## Supplementary material

The Supplementary Material for this article can be found online at: https://www.frontiersin.org/articles/10.3389/fpls.2025.1553886/full#supplementary-material

## References

Agus, C., Putra, P. B., Faridah, E., Wulandari, D., and Napitupulu, R. R. (2016). Organic carbon stock and their dynamics in rehabilitation ecosystem areas of post open coal mining at tropical region. *Proc. Eng.* 159, 329337. doi: 10.1016/j.proeng.2016.08.201

Ahirwal, J., and Maiti, S. K. (2022). Restoring coal mine degraded lands in India for achieving the United Nations-Sustainable Development Goals. *Restor. Ecol.* 30, e13606. doi: 10.1111/rec.13606

Ahirwal, J., Maiti, S. K., and Singh, A. K. (2017). Changes in ecosystem carbon pool and soil $CO_2$ flux following post-mine reclamation in dry tropical environment, India. *Sci. Total Environ.* 583, 153–162. doi: 10.1016/j.scitotenv.2017.01.043

Baier, C., Modersohn, A., Jalowy, F., Glaser, B., and Gross, A. (2022). Effects of recultivation on soil organic carbon sequestration in abandoned coal mining sites: a meta-analysis. *Sci. Rep.* 12, 20090. doi: 10.1038/s41598-022-22937-z

Baker, T. R., Phillips, O. L., Malhi, Y., Almeida, S., Arroyo, L., Di Fiore, A., et al. (2004). Variation in wood density determines spatial patterns inAmazonian forest biomass. *Glob. Change Biol.* 10, 545–562. doi: 10.1111/j.1365-2486.2004.00751.x

Boyd, D. S. (1999). The relationship between the biomass of Cameroonian tropical forests and radiation reflected in middle infrared wavelengths (3.0-5.0 mu m). *Int. J. Remote. Sens.* 20, 1017–1023. doi: 10.1080/014311699213055

Chave, J., Andalo, C., Brown, S., Cairns, M. A., Chambers, J. Q., Eamus, D., et al. (2005). Tree allometry and improved estimation of carbon stocks and balance in tropical forests. *Oecologia* 145, 87–99. doi: 10.1007/s00442-005-0100-x

Chave, J., Condit, R., Muller-Landau, H. C., Thomas, S. C., Ashton, P. S., Bunyavejchewin, S., et al. (2008). Assessing evidence for a pervasive alteration in tropical tree communities. *PloS Biol.* 6, e45. doi: 10.1371/journal.pbio.0060045

Chen, Z., Yang, Y., Zhou, L., Hou, H., Zhang, Y., Liang, J., et al. (2022). Ecological restoration in mining areas in the context of the Belt and Road initiative: Capability and challenges. *Environ. Impact Assess. Rev.* 95, 106767. doi: 10.1016/j.eiar.2022.106767

Cunningham, S. C., Mac Nally, R., Baker, P. J., Cavagnaro, T. R., Beringer, J., Thomson, J. R., et al. (2015). Balancing the environmental benefits of reforestation in agricultural regions. *Perspect. Plant Ecol. Evol. Syst.* 17, 301–317. doi: 10.1016/j.ppees.2015.06.001

Damptey, F. G., Birkhofer, K., Nsiah, P. K., and de la Riva, E. G. (2020). Soil properties and biomass attributes in a former gravel mine area after two decades of forest restoration. *Land* 9, 209. doi: 10.3390/land9060209

de Souza Barbosa, R., Pereira, G. F. M., Ribeiro, S. S., Hage, A. L. F., Costa, G. F., Salomão, R. P., et al. (2021). Key species selection for forest restoration after bauxite mining in the Eastern Amazon. *Ecol. Eng.* 162, 106190. doi: 10.1016/j.ecoleng.2021.106190

FAO (2015). *FAOStat: Food and Agriculture Organization of the United Nations-Statistics Division*. (Food and Agriculture Organization of the United Nations).

Farfan, J., Fasihi, M., and Breyer, C. (2019). Trends in the global cement industry and opportunities for long-term sustainable CCU potential for Power-to-X. *J. Clean. Prod.* 217, 821–835. doi: 10.1016/j.jclepro.2019.01.226

Finegan, B., Peña-Claros, M., de Oliveira, A., Ascarrunz, N., Bret-Harte, M. S., Carreño-Rocabado, G., et al. (2015). Does functional trait diversity predict above-ground biomass and productivity of tropical forests? Testing three alternative hypotheses. *J. Ecol.* 103, 191–201. doi: 10.1111/1365-2745.12346

Foody, G. M., Boyd, D. S., and Cutler, M. E. (2003). Predictive relations of tropical forest biomass from Landsat TM data and their transferability between regions. *Remote. Sens. Environ.* 85, 463–474. doi: 10.1016/S0034-4257(03)00039-7

Freitas, S. R., Mello, M. C., and Cruz, C. B. (2005). Relationships between forest structure and vegetation indices in Atlantic Rainforest. *For. Ecol. Manage.* 218, 353–362. doi: 10.1016/j.foreco.2005.08.036

Garnier, E., Cortez, J., Billès, G., Navas, M. L., Roumet, C., Debussche, M., et al. (2004). Plant functional markers capture ecosystem properties during secondary succession. *Ecology* 85, 2630–2637. doi: 10.1890/03-0799

Ghosh, D., and Maiti, S. K. (2021a). Biochar-assisted eco-restoration of coal mine degraded land to meet United Nation Sustainable Development Goals. *Land Degrad. Dev.* 32, 4494–4508. doi: 10.1002/ldr.4055

Ghosh, D., and Maiti, S. K. (2021b). Eco-restoration of coal mine spoil: biochar application and carbon sequestration for achieving UN sustainable development goals 13 and 15. *Land* 10, 1112. doi: 10.3390/land10111112

Hughes, T. P., Kerry, J. T., Álvarez-Noriega, M., Álvarez-Romero, J. G., Anderson, K. D., Baird, A. H., et al. (2017). Global warming and recurrent mass bleaching of corals. *Nature* 543, 373–377. doi: 10.1038/nature21707

Iida, Y., Poorter, L., Sterck, F. J., Kassim, A. R., Kubo, T., Potts, M. D., et al. (2012). Wood density explains architectural differentiation across 145 co-occurring tropical tree species. *Funct. Ecol.* 26, 274–282. doi: 10.1111/j.1365-2435.2011.01921.x

IPCC. (2001). Climate change 2001:mitigation. Third Assessment Report (TAR) of the Intergovernmental Panel on Climate Change (IPCC). Available online at: http://www.grida.no/climate/ipcc_tar/wg3/pdf/TAR-total.pdf (Accessed May, 2024).

King, D. A., Davies, S. J., Tan, S., and Noor, N. S. M. (2006). The role of wood density and stem support costs in the growth and mortality of tropical trees. *Funct. Ecol.* 94, 670–680. doi: 10.1111/j.1365-2745.2006.01112.x

Lewis, S. L., Sonké, B., Sunderland, T., Begne, S. K., Lopez-Gonzalez, G., van der Heijden, G. M., et al. (2013). Above-ground biomass and structure of 260 African tropical forests. *Philos. Trans. R. Soc B Biol. Sci.* 368, 20120295. doi: 10.1098/rstb.2012.0295

Li, R., Zhu, S., Chen, H. Y., John, R., Zhou, G., Zhang, D., et al. (2015). Are functional traits a good predictor of global change impacts on tree species abundance dynamics in a subtropical forest? *Ecol. Lett.* 18, 1181–1189. doi: 10.1111/ele.12497

Liu, T., Jiang, K., Tan, Z., He, Q., Zhang, H., and Wang, C. (2021). A method for performing reforestation to effectively recover soil water content in extremely degraded tropical rain forests. *Front. Ecol. Evol.* 9. doi: 10.3389/fevo.2021.643994

Luckeneder, S., Giljum, S., Schaffartzik, A., Maus, V., and Tost, M. (2021). Surge in global metal mining threatens vulnerable ecosystems. *Glob. Environ. Change* 69, 102303. doi: 10.1016/j.gloenvcha.2021.102303

Migliavacca, M., Musavi, T., Mahecha, M. D., Nelson, J. A., Knauer, J., Baldocchi, D. D., et al. (2021). The three major axes of terrestrial ecosystem function. *Nature* 598, 468–472. doi: 10.1038/s41586-021-03939-9

Mukhopadhyay, S., and Maiti, S. K. (2014). Soil $CO_2$ flux in grassland, afforested land and reclaimed coalmine overburden dumps: a case study. *Land Degrad. Dev.* 25, 216–227. doi: 10.1002/ldr.1161

Nam, V. T., Anten, N. P., and van Kuijk, M. (2018). Biomass dynamics in a logged forest: the role of wood density. *J. Plant Res.* 131, 611–621. doi: 10.1007/s10265-018-1042-9

Niiyama, K., Kajimoto, T., Matsuura, Y., Yamashita, T., Matsuo, N., Yashiro, Y., et al. (2010). Estimation of root biomass based on excavation of individual root systems in a primary dipterocarp forest in Pasoh Forest Reserve, Peninsular Malaysia. *J. Trop. Ecol.* 26, 271–284. doi: 10.1017/S0266467410000040

Nunes, S., Gastauer, M., Cavalcante, R. B. L., Ramos, S. J., Caldeira, C. F., Silva, D., et al. (2020). Challenges and opportunities for large-scale reforestation in the Eastern Amazon using native species. *For. Ecol. Manage.* 466, 118120. doi: 10.1016/j.foreco.2020.118120

Osorio-Salomón, K., Bonilla-Moheno, M., López-Barrera, F., and Martínez-Garza, C. (2021). Accelerating tropical cloud forest recovery: Performance of nine late-successional tree species. *Ecol. Eng.* 166, 106237. doi: 10.1016/j.ecoleng.2021.106237

Pan, Y., Birdsey, R. A., Fang, J., Houghton, R., Kauppi, P. E., Kurz, W. A., et al. (2011). A large and persistent carbon sink in the world's forests. *Science* 333, 988–993. doi: 10.1126/science.120160

Perez-Harguindeguy, N., Dıaz, S., Garnier, E., Lavorel, S., Poorter, H., Jaureguiberry, P., et al. (2013). New handbook for standardised measurement of plant functional traits worldwide. *Aust. J. Bot.* 61, 167–234. doi: 10.1071/BT12225

Philipson, C. D., Cutler, M. E., Brodrick, P. G., Asner, G. P., Boyd, D. S., Moura Costa, P., et al. (2020). Active restoration accelerates the carbon recovery of human-modified tropical forests. *Science* 369, 838–841. doi: 10.1126/science.aay4490

Phillips, O. L., Sullivan, M. J., Baker, T. R., Monteagudo Mendoza, A., Vargas, P. N., and Vásquez, R. (2019). Species matter: wood density influences tropical forest biomass at multiple scales. *Surv. Geophys.* 40, 913–935. doi: 10.1007/s10712-019-09540-0

Poorter, L., Wright, S. J., Paz, H., Ackerly, D. D., Condit, R., and Ibarra-Manríquez, G. (2008). Are functional traits good predictors of demographic rates? Evidence from five neotropical forests. *Ecology* 89, 1908–1920. doi: 10.1890/07-0207.1

Reid, J. L., Holl, K. D., and Zahawi, R. A. (2015). Seed dispersal limitations shift over time in tropical forest restoration. *Ecol. Appl.* 25, 1072–1082. doi: 10.1890/14-1399.1

Shen, Y., Yu, S. X., Lian, J. Y., Shen, H., Cao, H. L., Lu, H. P., et al. (2016). Inferring community assembly processes from trait diversity across environmental gradients. *J. Trop. Ecol.* 32, 290–299. doi: 10.1017/S0266467416000262

Tagesson, T., Schurgers, G., Horion, S., Ciais, P., Tian, F., Brandt, M., et al. (2020). Recent divergence in the contributions of tropical and boreal forests to the terrestrial carbon sink. *Nat. Ecol. Evol.* 4, 202–209. doi: 10.1038/s41559-019-1090-0

Tang, R., He, B., Chen, H. W., Chen, D., Chen, Y., Fu, Y. H., et al. (2022). Increasing terrestrial ecosystem carbon release in response to autumn cooling and warming. *Nat. Clim. Change* 12, 380–385. doi: 10.1038/s41558-022-01304-w

Uwasu, M., Hara, K., and Yabar, H. (2014). World cement production and environmental implications. *Environ. Dev.* 10, 36–47. doi: 10.1016/j.envdev.2014.02.005

Wang, L. Q., and Ali, A. (2021). Climate regulates the functional traits–aboveground biomass relationships at a community-level in forests: A global meta-analysis. *Sci. Total Environ.* 761, 143238. doi: 10.1016/j.scitotenv.2020.143238

Yuan, C., Wu, F., Wu, Q., Fornara, D. A., Heděnec, P., Peng, Y., et al. (2023). Vegetation restoration effects on soil carbon and nutrient concentrations and enzymatic activities in post-mining lands are mediated by mine type, climate, and former soil properties. *Sci. Total Environ.* 879, 163059. doi: 10.1016/j.scitotenv.2023.163059

Zhang, H., Chen, H. Y., Lian, J., John, R., Ronghua, L. I., Liu, H., et al. (2018). Using functional trait diversity patterns to disentangle the scale-dependent ecological processes in a subtropical forest. *Funct. Ecol.* 32, 1379–1389. doi: 10.1111/1365-2435.13079

Zhang, H., He, M., Pandey, S. P., Liu, L., and Zhou, S. (2023). Soil fungal community is more sensitive than bacterial to mining and reforestation in a tropical rainforest. *Land Degrad. Dev.* 34, 4035–4045. doi: 10.1002/ldr.4734

Zhang, H., Kuzyakov, Y., Yu, H., Pei, X., Hou, W., Wang, C., et al. (2024b). Root traits drive the recovery of soil nematodes during restoration of open mines in a tropical rainforest. *Sci. Total Environ.* 953, 176178. doi: 10.1016/j.scitotenv.2024.176178

Zhang, H., Li, Y., Xu, Y., and John, R. (2024a). The recovery of soil N-cycling and P-cycling following reforestation in a degraded tropical limestone mine. *J. Clean. Prod.* 448, 141580. doi: 10.1016/j.jclepro.2024.141580

Zhao, J., Kang, F., Wang, L., Yu, X., Zhao, W., Song, X., et al. (2014). Patterns of biomass and carbon distribution across a chronosequence of Chinese pine (*Pinus tabulaeformis*) forests. *PloS One* 9, e94966. doi: 10.1371/journal.pone.0094966

Zhao, Y., Zou, Y., Wang, L., Su, R., He, Q., Jiang, K., et al. (2021). Tropical rainforest successional processes can facilitate successfully recovery of extremely degraded tropical forest ecosystems following intensive mining operations. *Front. Envir. Sci.* 9. doi: 10.3389/fenvs.2021.701210

Zhu, Y., Wang, L., Ma, J., Hua, Z., Yang, Y., and Chen, F. (2024). Assessment of carbon sequestration potential of mining areas under ecological restoration in China. *Sci. Total Environ.* 921, 171179. doi: 10.1016/j.scitotenv.2024.171179

frontiers | Frontiers in Plant Science

TYPE Original Research
PUBLISHED 26 March 2025
DOI 10.3389/fpls.2025.1548664



OPEN ACCESS

EDITED BY
Robert John,
Indian Institute of Science Education and Research Kolkata, India

REVIEWED BY
Pu Jia,
South China Normal University, China
Mu Liu,
Lanzhou University, China

*CORRESPONDENCE
Yikang Cheng
ykcheng@hainanu.edu.cn
Shurong Zhou
zhshrong@hainanu.edu.cn

RECEIVED 20 December 2024
ACCEPTED 04 March 2025
PUBLISHED 26 March 2025

CITATION
Yang C, Liao R, Huang S, Cheng Y and Zhou S (2025) Wind speed and soil properties drive the height-diameter allometric pattern of island plants.
*Front. Plant Sci.* 16:1548664.
doi: 10.3389/fpls.2025.1548664



# Wind speed and soil properties drive the height-diameter allometric pattern of island plants

Chengfeng Yang[1], Renfu Liao[1], Shengzhuo Huang[2], Yikang Cheng[3*] and Shurong Zhou[3*]

[1]Key Laboratory of Genetics and Germplasm Innovation of Tropical Special Forest Trees and Ornamental Plants, Ministry of Education, School of Tropical Agriculture and Forestry, Hainan University, Haikou, China, [2]Hainan Key Laboratory for Research and Development of Natural Products from Li Folk Medicine, Institute of Tropical Bioscience and Biotechnology, Chinese Academy of Agricultural Sciences, Haikou, China, [3]School of Ecology, Hainan University, Haikou, China

**Introduction:** Island ecosystems, due to their geographical isolation and unique environmental conditions, often serve as natural laboratories for ecological research and are also sensitive to global climate change and biodiversity loss. The allometric relationship between plant height-diameter reflects the adaptive growth strategy of plants under different environmental conditions, particularly in response to biomechanical constraints (e.g., wind resistance) and resource availability. This study aims to explore the key driving factors of the height-diameter allometry of island plants, focusing on how island area, soil properties, and climatic factors (e.g., wind speed, temperature, and precipitation) affect plant growth strategy.

**Methods:** We analyzed plant data from 20 tropical islands, using SMA regression to calculate the allometric exponent and intercept for each island's plants, and evaluated the effects of island area, soil properties, and climatic factors (wind speed, temperature, and precipitation) on the height-diameter allometric relationship.

**Results:** The results show that island area has no significant effect on plant allometry, while climatic factors, particularly wind speed, and soil properties significantly influence the allometric exponent and intercept, respectively. Specifically, wind speed is the primary driver of the height-diameter allometric exponent, regulating plant growth proportions through mechanical stress and canopy limitation. In contrast, soil properties predominantly govern changes in the allometric intercept, reflecting their critical role in determining baseline growth conditions, such as resource allocation and initial morphological adaptation. The effects of temperature and precipitation are relatively weak, likely due to the buffering effects of the tropical climate and marine moisture supplementation.

**Discussion:** Overall, this study highlights the key roles of wind speed and soil in shaping the allometry of island plants, providing new insights into the adaptive strategies of island plants under resource limitations and climatic pressures, as well as offering important scientific evidence for island ecological conservation and restoration.

KEYWORDS

**height-diameter allometry, island plants, island area, soil, wind speed, temperature**

## 1 Introduction

Allometric relationships, particularly between height and diameter, are crucial in plant growth and ecological adaptation (King, 1996; Chave et al., 2005). They reflect how plants optimize their morphological structure to cope with environmental pressures (e.g., wind, temperature) and resource limitations, thereby enhancing their competitive ability and ecological adaptability through adaptive growth strategies (Chave et al., 2005, 2014; Thomas et al., 2015; Xiao et al., 2021). Island ecosystems are one of the hotspots of biodiversity loss, and the growth patterns of insular plants are more susceptible to environmental changes due to the unique environmental and geographical conditions. Thus, there is an urgent need for a thorough study of island ecosystems in the context of global change and increasing human disturbance (MacArthur and Wilson, 1967; Whittaker et al., 2017; Fernández-Palacios et al., 2021; Manes et al., 2021). Indeed, plant growth strategies vary among species and environments, and these strategies can influence allometric relationships, thereby helping plants maximize their survival and reproductive capacities under limited resources (West et al., 1999; Thomas et al., 2015). Therefore, studying the height-diameter allometric relationship of island plants is of great significance for predicting how plants respond to environmental changes, as well as guiding the conservation and restoration of island ecosystems (Tilman, 1988; Whittaker et al., 2017).

Height and diameter are core indicators of plant growth, playing key roles in resource acquisition and structural stability (Tilman, 1988; Poorter et al., 2012). Specifically, plant height directly affects the ability to capture light resources and is a primary determinant of carbon sequestration capacity (Moles et al., 2009), while diameter relates to the mechanical support and water transport efficiency (Niklas, 1993; Vizcaíno-Palomar et al., 2016). The dynamic balance between these height and diameter determines the plant growth pattern and performance (Chave et al., 2005; Qiu et al., 2021). The allometric relationship between height and diameter is typically expressed in the power function form: $H=a D^b$, where H is the tree height, $D$ is the diameter of a cross-section of a tree trunk 1.3 meters above the ground (i.e., DBH) for trees, or the basal diameter for forbs; $a$ is the constant coefficient, or intercept meaning the height when $D$ =1, and $b$ is the height-diameter allometric exponent (West et al., 1999; Brown et al., 2004). When the allometric exponent $b$=1, height and diameter grow at the same rate, the plant height and diameter increase proportionally. When $b$<1, the growth rate of height is lower than that of diameter, indicating a greater emphasis on enhancing the supporting structure (Figure 1a). The height-diameter allometric relationship reflects plant adaptation strategies under different environmental conditions, with plants tending to increase diameter under resource limitation and height under resource availability. Xiao et al. (2021) found that nitrogen addition affects plant allometry, subsequently altering species diversity and community structure, highlighting the close relationship between allometric relationship, resource use efficiency, and competitive ability. Additionally, the logarithmic form of the function is often used to analyze the relationship between height and diameter: log (H) = log ($a$) + $b$ log (D), this form facilitates a clearer understanding of the height-diameter allometric pattern through regression analysis (Thomas et al., 2015; Xiao et al., 2021) (Figure 1b). In this equation, $b$ still represents the height-diameter allometric exponent, and $a$ is the intercept, which reflects the initial proportional relationship between the two variables (i.e., height and diameter) in the allometric equation. It reveals the differences in the growth starting points or baseline levels of plants under varying environmental conditions (Feldpausch et al., 2011).

Mechanistically, many theories suggest that the allometric relationship of plants would be influenced by various biological factors such as metabolism, biomechanical constraints, and hydraulic transport, making the relationship generally predictable. For example, $b$ = 3/2 is often cited (McMahon, 1973; West et al., 1997; Brown et al., 2004). However, more evidence now shows that the allometric relationship exhibits a certain degree of plasticity, with abiotic factors such as climate conditions, soil properties, and geographical traits, potentially overriding the predictability of biological factors, thereby exerting a strong influence on allometry (Hulshof et al., 2015; Thomas et al., 2015; Zhang et al., 2020; Xiao et al., 2021). For instance, a previous study has shown that the height of all trees in Spain was shorter than predicted by biomechanical models (Lines et al., 2012). Due to the unique environmental conditions, such as resource limitation, soil infertility, and extreme climate variations, this could lead to more significant changes in height-diameter allometric relationships (Hulshof et al., 2015;

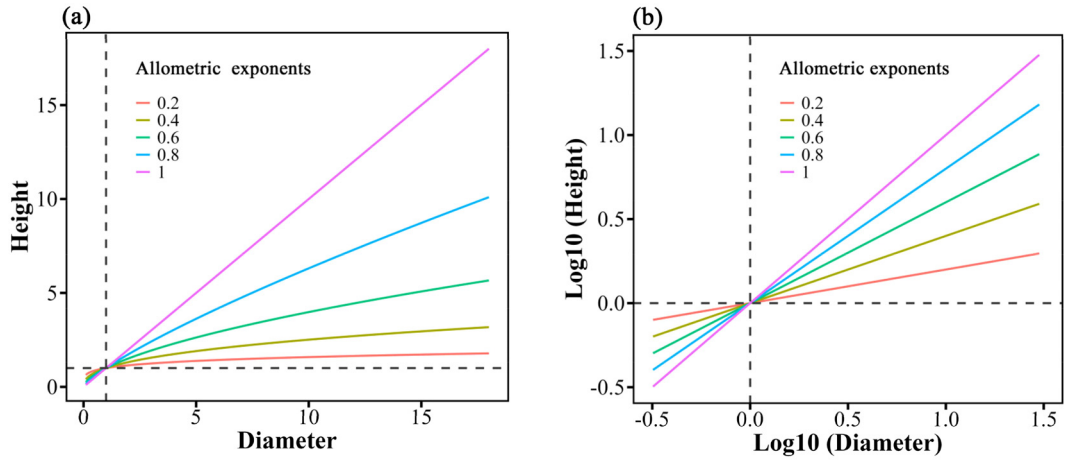


FIGURE 1
Schematic of allometry for different heights and diameters, illustrating the power-law expression **(a)** and its log10-transformed expression **(b)**. Lines of different colors represent different height-diameter allometric exponent **(b)** values. a: $H = aD^b$. b: Log (H) = log (*a*) + *b* log (D).

Thomas et al., 2015). Therefore, island ecosystems are an excellent place to explore the potential driving mechanisms of height-diameter allometric relationships.

Island area is one of the most important features of island ecosystems, and the positive relationship between island size and species richness has been widely confirmed (MacArthur and Wilson, 1967; Zhou et al., 2024). With further research, many studies have found that island area not only influences species richness (Whittaker et al., 2017; Ottaviani et al., 2020), but also exerts significant effects on various ecological processes, such as community structure, species interactions, and the process of species succession across multiple trophic levels (Patiño et al., 2017; Zhou et al., 2024). Thus, island size may be a potential factor affecting the plant growth relationships. However, whether and how the island area influences the plant height-diameter allometric relationship remains unclear.

Furthermore, soil properties and nutrient availability are critical for plant height growth, which may, in turn, affect height-diameter growth relationships. Indeed, nutrient-rich soils could promote vertical growth in plants (Givnish et al., 2014), while nutrient-poor soils may drive plants to alter their growth strategies (Cramer, 2012), subsequently altering their allometric relationships (Xiao et al., 2021; Xu et al., 2022). On the other hand, many studies have been conducted on the effects of climate factors (e.g., temperature and precipitation) on plant allometry (Olson et al., 2018; Fortin et al., 2019; Liu et al., 2021). For example, there is considerable variation in the height-diameter allometric relationships of trees across America, and temperature and precipitation have been confirmed as the main contributing factors (Hulshof et al., 2015). Likewise, temperature has been found to be the primary factor influencing the tree height-diameter relationship in the southern and northeastern regions of China (Wang et al., 2006; Zhang et al., 2019). Further, Liu et al. (2021) also found that tree height was mainly positively influenced by precipitation in Arizona. In island ecosystems, particularly in tropical regions, wind speed not only differs significantly from that on mainland, but islands are also more prone to tropical storms (Young et al., 2011; Jiang et al., 2022). Indeed, high wind speeds and strong biomechanical disturbances may affect plant morphology and survival strategies, such as the formation of bent tree shapes, deepening of root systems, or horizontal growth (King, 1986; Meng et al., 2006; Niklas and Spatz, 2006; Jackson et al., 2021). A study on Dominica Island in the West Indies, one of the regions with the highest wind speeds in the tropical zone, found that tree heights were 30-116% shorter than those in other tropical regions, and the height-diameter allometric relationship showed a distinct depression compared to other areas (Thomas et al., 2015). Nevertheless, there is limited research on the impact of climate conditions, especially wind speed, on plant height-diameter allometric relationship in island ecosystems (Watt and Kirschbaum, 2011; Thomas et al., 2015; Young et al., 2011).

Many studies have also shown that extreme climate factors (such as precipitation in the wettest month, temperature in the warmest month, and wind speed in the windiest month) often have a more significant impact on plant growth than average climate indicators. Intense environmental stress or more favorable conditions are more likely to lead to changes in plant growth patterns in terms of tree height and diameter (Cunningham and Read, 2002; Frank et al., 2015; Rudley et al., 2023). For example, a global-scale study on plant height found that precipitation in the wettest month was the best explanatory factor for plant height variation (Moles et al., 2009). Moreover, maximum wind speed and extreme events such as tropical storms have a strong impact on plant height and survival (Thomas et al., 2015; Bauman et al., 2022). Given the intensifying global climate change, understanding the influence of these extreme environmental variables on plant growth mechanisms has become especially important. Therefore, we conducted research in the South China Sea region, investigating the height-diameter allometric relationships of plants surveyed on twenty islands. The study aims to address the following questions: 1) What is the relationship between island area, soil properties, various climate variables, and the height-diameter allometric

relationship of island plants? 2) What are the key factors influencing the height-diameter allometric relationship of plants on islands in the South China Sea region?

# 2 Materials and methods

## 2.1 Study site and sampling method

As an important tropical marine ecosystem in China, the South China Sea comprises a rich array of islands, coral reefs, and shallow marine areas, showcasing diverse marine environments and abundant biodiversity. The South China Sea not only provides favorable conditions for the survival of numerous marine species but also serves as a habitat and breeding ground for tropical and subtropical plants. The plant communities on the islands in this region exhibit significant variations due to island area, soil type, and climatic conditions (Zhou et al., 2024). Despite more than 50 islands occurring within this region, considering factors such as whether the island is suitable for investigation (with a certain area to allow for sampling plots, and suitable woody plant communities rather than just a few herbaceous species) and whether it is easy to climb the islands, we ultimately selected the 20 most representative islands with a size varies from 1ha to 400ha for detailed surveys, which were conducted from April 2023 to May 2024.

For each island, we established different numbers of permanent 20m × 20m sampling plots, after logarithmically transforming the area of the islands we planned to survey, we adjusted the number of plots based on the actual situation, ensuring that the number of plots on each island is proportional to the transformed island area. To minimize spatial autocorrelation effects, we ensured that the distance between any two sampling plots on the same island exceeded 100 meters. Additionally, the vegetation status and habitat differences of the island were considered as supplementary information when selecting the sampling plots. For the smallest islands, where the limited area prevented the establishment of plots more than 100 meters apart, we maintained a minimum distance of 40 meters between plots. In total, we established 87 sampling plots on 20 islands in this region.

Within these plots, we conducted plant surveys and soil sampling. The plot setup was based on RTK (Real-Time Kinematic) positioning provided by Xunwei Positioning, which allowed for more precise positioning compared to traditional methods and avoided the influence of slope on the projected area of the plots. RTK was used to locate the four corners of each plot, and rubber tubing and red plastic rope were used to mark and fix the boundaries of the plots. Within each plot, we inventoried all woody plants rooted within the plots and recorded plant height and diameter, Plant height was measured using a height pole, with the height recorded by aligning the top of the canopy with the marked scale on the pole. Stem diameter was measured at breast height (1.3 m above the ground) using a diameter tape. Species were identified on-site using morphological methods, and further identification was done with reference to the Flora of Chinese (2019). Soil samples were collected using a diagonal sampling method. Three 2m × 2 m subplots were evenly distributed along the diagonal of each plot, and four soil samples (10 cm in depth) were randomly taken from each subplot. Then, all samples were combined and homogenized within a plot into one composite sample. In total, 261 soil samples were collected.

## 2.2 Data acquisition

In this study, we used a logarithmic regression model to calculate the height-diameter allometric relationship of plants, which describes the growth relationship between plant height and diameter. Specifically, we used the standard major axis (SMA) regression to estimate the height-diameter allometric exponent and intercept for the plants surveyed on each island. SMA regression is preferred for allometric studies as it accounts for measurement error in both the independent (diameter) and dependent (height) variables. To facilitate subsequent analysis, we calculated the height-diameter allometric exponent ($b$) and intercept ($a$) for each plant species surveyed across the islands. The logarithmic linear model used in this study is as follows:

$$\log(H) = a + b \log(D)$$

Where H represents plant height (in meters), D represents plant diameter (in centimeters), $a$ is the intercept of the regression equation, reflecting the initial proportional relationship between height and diameter, $b$ is the height-diameter allometric exponent, which represents the scaling relationship between diameter and height. For the SMA regression, we used the sma() function from the smatr package in R with the argument robust = T, which provides robust estimates of the slope and intercept, minimizing the influence of outliers. This method allows us to derive the strength and trend of the relationship between diameter and height for each plant species on different islands, ensuring more accurate allometric calculations.

We measured five soil physicochemical properties that may influence plant communities, with the specific measurement methods as follows: Soil pH was measured using the Metter-S210 SevenCompact pH analyzer, with a soil-to-water ratio of 1:2.5; Soil organic carbon (SOC) content was determined by the K2Cr2O7 redox titration method; Total nitrogen (TN) content was measured using the semi-micro Kjeldahl method; Total phosphorus (TP) concentration was determined by colorimetric analysis using a UV-Visible spectrophotometer; Total potassium (TK) content was extracted with 1 M ammonium acetate and analyzed by inductively coupled plasma technology.

Climate data were sourced from the WorldClim Global Climate and Weather Data (Fick and Hijmans, 2017). We downloaded bioclimatic variables including temperature and precipitation data, as well as wind speed datasets. Subsequently, we used the "***terra***" package to process the downloaded TIF files. To explore the impact of extreme climate factors on plant height-diameter allometric relationship, we extracted the annual maximum temperature of the hottest month (hereafter temperature), the

annual precipitation of the wettest month (hereafter precipitation), and the annual wind speed of the windiest month from the dataset (hereafter wind).

## 2.3 Statistical analysis

Before analysis, we applied Principal Component Analysis (PCA) to the five soil variables (SOC, N, P, K, pH) to simplify the data structure (Abdi and Williams, 2010; Ren et al., 2022). We retained the first PCA axis as the integrated predictor for each group of variables, as the first principal component explained the largest percentage of variance in soil properties ($PC_{soil}$).

Then we used linear regression to analyze the effects of island characteristics (i.e., area), environmental conditions (i.e., PCsoil), and climatic factors (i.e., wind speed, temperature, and precipitation) on plant height-diameter allometric relationship. We treated the allometric exponent *b* and intercept *a* as dependent variables, with abiotic factors as independent variables, to investigate the relationship between island environmental conditions and plant height-diameter allometric exponent and intercept. This approach aimed to explain the link between plant height-diameter allometric relationship and island conditions.

To investigate the relative importance of island area, soil properties, and climate factors on the height-diameter allometric exponent and intercept of plant height-diameter relationships, we estimated the relative importance of each variable using the "glmm.hp" function (Lai et al., 2022). All variables were standardized using the "scale" function. All statistical analyses were performed in R v.4.4.1 (R Core Team, 2013).

# 3 Results

## 3.1 The effects of island area and soil factors on island plant allometric relationship

Linear regression analysis revealed that island area had no significant effect on either the allometric exponent or intercept ($P > 0.05$) (Figures 2a, c). Likewise, soil factors also exerted an insignificant effect on the allometric exponent ($P > 0.05$) (Figure 2b), while their influence on the intercept approached significance ($P = 0.029$) (Figure 2d). This result suggests that soil properties may influence the plant height-diameter allometric relationship by regulating the intercept.

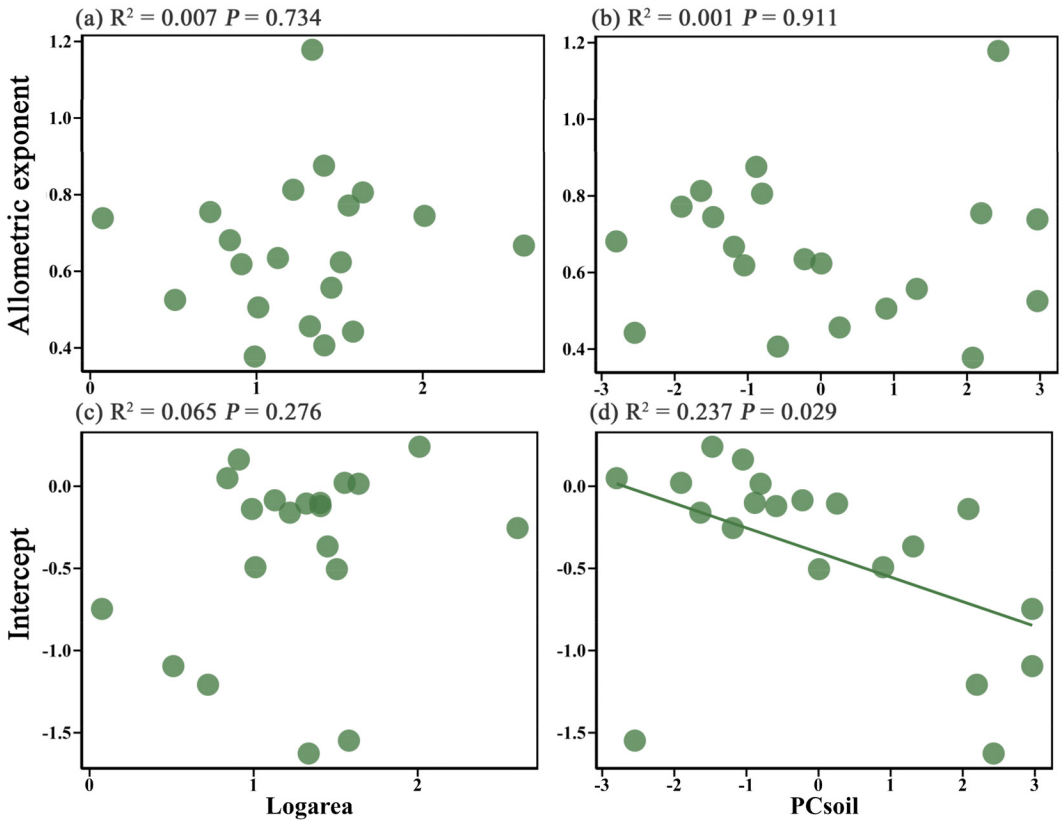


FIGURE 2
Effect of island area on the height-diameter allometric exponent **(a)** and intercept **(c)** of island plants, and the effect of soil properties ($PC_{soil}$) on the height-diameter allometric exponent **(b)** and intercept **(d)** of island plants.

## 3.2 The effects of climate factors on island plant allometric relationship

Regression analysis results showed that wind speed, precipitation, and temperature had different effects on the height-diameter allometric exponent and intercept of plants. Specifically, wind speed had a significant effect on the height-diameter allometric exponent ($P$ = 0.02) but no significant effect on the intercept ($P$ > 0.05) (Figures 3a, d). As wind speed increased, the height-diameter allometric exponent decreased, indicating a clear suppressive effect of wind speed on plant growth patterns. In contrast, temperature and precipitation showed no significant effects on either the height-diameter allometric exponent or intercept ($P$ > 0.05) (Figures 3b, c, e, f). This suggests that wind speed is the primary factor influencing the allometric relationship of island plants in the study area, while the effects of precipitation and temperature are relatively limited.

## 3.3 Relative importance of different factors affecting island plant allometric relationship

For the height-diameter allometric exponent of plants, island area, soil, and three climate variables explained approximately 47% of the variation in the height-diameter allometric exponent, and wind speed was the most important predictor, accounting for 64.8% of the variation in the exponent, followed by temperature, which accounted for 16.9%. The relative importance of soil factors, precipitation, and island area was low, with soil contributing 5.8%, precipitation 5.5%, and area 7% (Figure 4a). For the height-diameter allometric intercept of plants, the five variables explained approximately 49% of the variation in the intercept. Soil was the most important predictor, contributing 47.9% of the variation, followed by wind speed, which accounted for 17.3%. Temperature and precipitation contributed 13.3% and 14.2%, respectively, while area had the least explanation of just 7.3% (Figure 4b).

# 4 Discussion

The height-diameter allometric exponent and intercept reflect differences in growth strategies under varying environmental conditions, highlighting the plant adaptability to resource limitations and climate change. This study was conducted to investigate the key drivers of plant height-diameter allometric relationships in island ecosystems, mainly focusing on how island area, soil properties, and climate variables (such as wind speed, temperature, and precipitation) influence plant growth strategies. The results showed that island area had no statistically significant effect on plant height-diameter allometric relationship, while soil factors exhibited a significant influence on the intercept. Among the climate factors, wind speed significantly affected the height-diameter allometric exponent, whereas temperature and precipitation showed no significant effects. Therefore, soil and wind speed play more critical roles in regulating the growth patterns of island plants, while the influences of island area, temperature, and precipitation may be more indirect or limited within the study area.

Island area is generally considered an important factor influencing species richness and various ecological processes

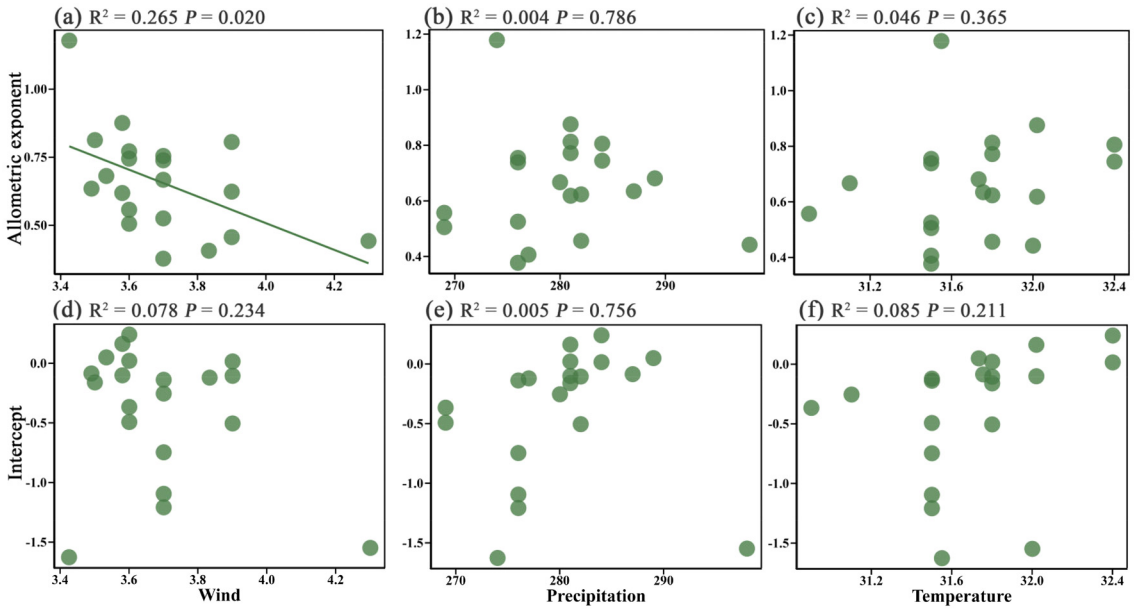


FIGURE 3
Effect of wind speed **(a, d)**, precipitation **(b, e)**, and temperature **(c, f)** on the height-diameter allometric exponent and intercept of island plants respectively.

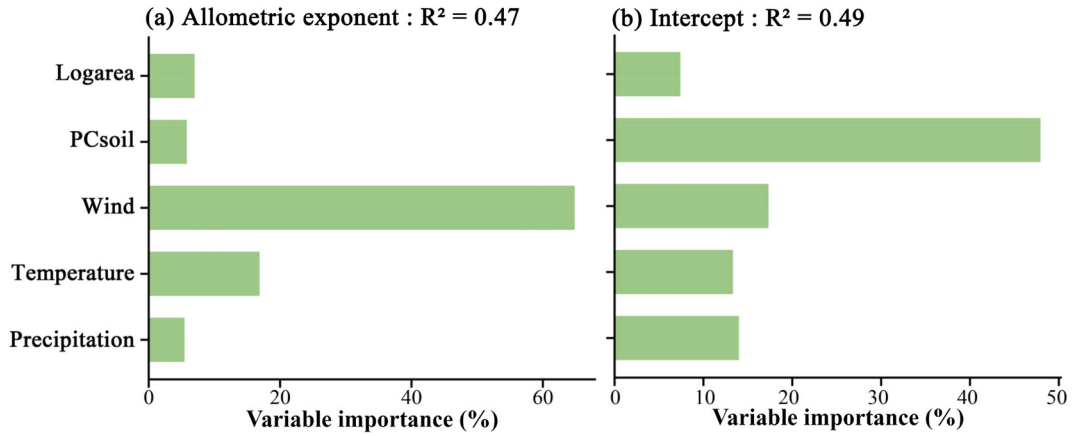


FIGURE 4
Relative importance of island area, soil properties, and climate factors (wind speed, temperature, and precipitation) in explaining the variation in the height-diameter allometric exponent **(a)** and intercept **(b)** of island plants.

(MacArthur and Wilson, 1967; Whittaker et al., 2017; Zhou et al., 2024). However, in this study, we found that the island area did not have a significant effect on the plant height-diameter allometric relationship. Although some studies have shown that island area would affect plant functional traits (Whittaker et al., 2014). We suggest that, although the direct effects are not significant, on larger islands, island area may indirectly influence ecological factors through its impact on soil, temperature, wind speed, and water vapor pressure. Larger islands typically feature more complex topography, better habitat quality, and fewer edge effects (MacArthur and Wilson, 1967; Patiño et al., 2017; Whittaker et al., 2017; Zhang et al, 2021; Zhou et al., 2024). For instance, studies have shown that trees in sheltered valleys are taller than those exposed to strong winds (Thomas et al., 2015), Future research could explore this indirect effect further on larger, more environmentally complex islands.

The influence of soil properties on the height-diameter allometric intercept reached a significant level ($P$ = 0.029), indicating that soil factors play an important role in regulating plant growth strategies. Specifically, soil characteristics such as nutrient content, pH, and organic carbon content may shape the height-diameter allometric relationships by influencing plant resource allocation and growth efficiency. Indeed, these soil properties have been shown to significantly affect plant growth rates and patterns across various ecosystems (Cramer, 2012; Givnish et al., 2014; Cysneiros et al., 2021; Xu et al., 2022). For instance, a previous study in the Brazilian forest ecosystem found that soil nutrients were one of the key predictors of tree height-diameter allometric relationship, with nutrient-rich forests supporting taller trees (Cysneiros et al., 2021). Additionally, the physical and chemical properties of soil may further regulate plant growth strategies by influencing the availability of water and nutrients (Li and Fang, 2016). Therefore, the impact of soil properties on plant height-diameter allometric relationship in island ecosystems cannot be overlooked, particularly in resource-limited environments where the role of soil may be even more pronounced.

In this study, climatic factors (i.e., wind speed, temperature, and precipitation) exhibited complex and significantly varying effects on the height-diameter allometric relationship of island plants. Specifically, unlike previous studies (Wang et al., 2006; Zhang et al., 2019), our findings showed that temperature and precipitation had no significant effects on either the height-diameter allometric exponent or the intercept of plants. Generally, rising temperatures accelerate plant metabolic processes and promote growth rates, potentially influencing height-diameter allometric relationships (Zhang et al., 2019; Wang et al., 2006; Hulshof et al., 2015). However, in the study area, variations in temperature did not significantly alter plant height-diameter allometric patterns, which may be related to the fact that the study region is a tropical oceanic island with a relatively narrow range of temperature fluctuations, insufficient to reach the threshold for significantly affecting plant height-diameter allometric relationship. Similarly, precipitation, a key factor influencing plant growth, typically plays a critical role in determining plant growth status by providing water (Hulshof et al., 2015; Cysneiros et al., 2021; Liu et al., 2021). However, in this study, precipitation also showed no significant effect, likely because the islands not only receive water through precipitation but also indirectly supplement moisture from the ocean (Gimeno et al., 2020), thereby mitigating the direct impact of precipitation on plant height-diameter allometric relationship. Nevertheless, under extreme temperature conditions, temperature may still play a crucial role in plant growth, such as extreme high temperatures potentially inhibiting metabolic activities or extreme low temperatures limiting growth rates. Similarly, under extreme precipitation conditions, precipitation may remain a critical factor for plant growth (Cysneiros et al., 2021; Seleiman et al., 2021).

Notably, wind speed exerted a significant negative effect on the height-diameter allometric exponent (Figure 3), indicating a

remarkably inhibitory effect on the growth patterns of island plants. This finding is partially consistent with the results of Thomas et al. (2015), where plants exposed to higher wind speeds exhibited lower height-diameter allometric exponents. On the one hand, high wind speeds cause mechanical disturbance, directly impacting plants through mechanical damage, leading to sustained mechanical stress and canopy restriction (King, 1986; Meng et al., 2006; Niklas and Spatz, 2006; Jackson et al., 2021);. Many studies have shown that wind speed is one of the main factors limiting canopy height, which in turn inhibits vertical growth (Takashima et al., 2009; Thomas et al., 2015). On the other hand, under high wind conditions, prolonged exposure to wind may drive plants to develop more wind-resistant traits, such as deeper root systems, tougher wood structures, and the formation of more branched growth forms rather than a single trunk (De Langre, 2008; Gardiner et al., 2016). These adaptive changes lead to a growth pattern that favors horizontal expansion rather than vertical growth, further reducing the height-diameter allometric exponent (Telewski, 2012; Gardiner et al., 2016).Although the effect of wind speed on the intercept was not statistically significant in this study, its significant impact on the height-diameter allometric exponent still suggests that wind speed is one of the key environmental factors regulating the growth strategies of island plants.

Based on the relative importance results, different factors exhibited distinct effects on the height-diameter allometric exponent and intercept of island plant height-diameter relationships. Specifically, wind speed among climatic factors and soil properties showed the highest explanatory power for the height-diameter allometric exponent and intercept, respectively. Although numerous studies have demonstrated that island area can directly or indirectly influence island plant communities (MacArthur and Wilson, 1967; Whittaker et al., 2017; Cysneiros et al., 2021; Zhou et al., 2024), its impact in this study was relatively weak. In contrast, among climatic factors, wind speed was the most significant predictor of the height-diameter allometric exponent (contributing 64.8% of the variation), indicating its dominant role in shaping plant growth strategies through mechanical stress and canopy limitation (King, 1986; Niklas and Spatz, 2006; Takashima et al., 2009). On the other hand, soil properties had the strongest influence on the intercept (contributing 47.9% of the variation), reflecting their critical role in determining baseline growth conditions, such as resource allocation and initial morphological adaptation (Cramer, 2012; Cysneiros et al., 2021; Xu et al., 2022). The effects of temperature and precipitation were relatively mild (contributing 16.9% and 5.5% to the exponent, and 13.3% and 14.2% to the intercept, respectively), likely due to the buffering effects of the oceanic climate and moisture supplementation (Gimeno et al., 2020). These results suggest that wind-driven physical constraints (e.g., mechanical damage, canopy limitation, and structural adaptation) primarily regulate the proportional relationship between plant height and diameter (allometric exponent), while soil-mediated resource availability (e.g., nutrient content, pH, and organic matter) predominantly shapes the baseline growth trajectory (intercept). This mechanistic decoupling reveals a multi-dimensional regulatory pattern of plant height-diameter allometric relationship in island ecosystems: wind speed directly influences plant morphological development through external mechanical pressures, forcing plants to tradeoff between vertical growth and horizontal expansion, while soil regulates the starting point and early developmental strategies of plants through resource allocation and initial growth conditions. This distinction not only emphasizes the multi-layered influence of environmental factors on plant growth strategies but also provides new insights into the adaptive evolution of island plants under resource limitations and climatic pressures. Future research could further explore the spatiotemporal dynamics of these driving mechanisms, particularly how the synergistic or antagonistic effects of wind speed and soil resources influence the long-term adaptability of island plants in the context of global climate change.

## 5 Conclusion

Overall, this study reveals the critical roles of wind speed among climatic factors and soil properties in shaping the height-diameter allometric patterns of island plants in the South China Sea region. Wind speed emerged as the primary driver influencing the height-diameter allometric exponent, while soil properties predominantly governed changes in the height-diameter allometric intercept. In contrast, the effects of island area and other climatic factors, such as temperature and precipitation, were relatively weak. These findings uncover the multi-dimensional adaptive strategies of island plants under resource limitations and climatic pressures: wind speed directly shapes plant morphological development through external mechanical stress, whereas soil regulates the starting point of plant growth via resource allocation. The results provide new insights into the driving mechanisms of plant height-diameter allometric relationship in island ecosystems, particularly in the context of global climate change, where the synergistic or antagonistic effects of wind speed and soil resources may influence the long-term adaptability of island plants. These discoveries not only deepen our understanding of plant growth strategies in island ecosystems but also offer important scientific evidence for island ecological conservation and restoration.

## Data availability statement

The raw data supporting the conclusions of this article will be made available by the authors, without undue reservation.

## Author contributions

CY: Conceptualization, Data curation, Formal Analysis, Investigation, Methodology, Visualization, Writing – original draft. RL: Investigation, Writing – review & editing. SH: Investigation, Writing – review & editing. YC: Conceptualization, Data curation, Investigation, Methodology, Supervision, Visualization, Writing – original draft, Writing – review & editing. SZ: Conceptualization, Data curation, Funding acquisition, Investigation, Methodology,

Resources, Supervision, Visualization, Writing – original draft, Writing – review & editing.

## Funding

The author(s) declare that financial support was received for the research and/or publication of this article. This study was supported by the Hainan Province Science and Technology Special Fund (Grant no. ZDYF2022SHFZ320).

## Acknowledgments

We are grateful to Lan Liu, Lingbing Wu, and Nianxun Xi from Hainan University for their guidance in experimental design and implementation. We also appreciate Haifeng Ding, Bo Zhang, and Yu Nie for their assistance and valuable suggestions during data analysis. Our thanks go to Hao Qin, Jingyan Zhao, Shuxin Liu, Zhen Zhang, and Run Zhang for their help in fieldwork.

## Conflict of interest

The authors declare that the research was conducted in the absence of any commercial or financial relationships that could be construed as a potential conflict of interest.

## Generative AI statement

The author(s) declare that no Generative AI was used in the creation of this manuscript.

## Publisher's note



## References

Abdi, H., and Williams, L. J. (2010). Principal component analysis. *Wiley Interdiscip. Rev.: Comput. Stat* 2, 433–459. doi: 10.1002/wics.101

Bauman, D., Fortunel, C., Delhaye, G., Malhi, Y., Cernusak, L. A., Bentley, L. P., et al. (2022). Tropical tree mortality has increased with rising atmospheric water stress. *Nature* 608, 528–533. doi: 10.1038/s41586-022-04737-7

Brown, J. H., Gillooly, J. F., Allen, A. P., Savage, V. M., and West, G. B. (2004). Toward a metabolic theory of ecology. *Ecology* 85, 1771–1789. doi: 10.1890/03-9000

Chave, J., Andalo, C., Brown, S., Cairns, M. A., Chambers, J. Q., Eamus, D., et al. (2005). Tree allometry and improved estimation of carbon stocks and balance in tropical forests. *Oecologia* 145, 87–99. doi: 10.1007/s00442-005-0100-x

Chave, J., Réjou-Méchain, M., Búrquez, A., Chidumayo, E., Colgan, M. S., Delitti, W. B., et al. (2014). Improved allometric models to estimate the aboveground biomass of tropical trees. *Global Change Biol.* 20, 3177–3190. doi: 10.1111/gcb.2014.20.issue-10

Cramer, M. D. (2012). Unravelling the limits to tree height: a major role for water and nutrient trade-offs. *Oecologia* 169, 61–72. doi: 10.1007/s00442-011-2177-8

Cunningham, S., and Read, J. (2002). Comparison of temperate and tropical rainforest tree species: photosynthetic responses to growth temperature. *Oecologia* 133, 112–119. doi: 10.1007/s00442-002-1034-1

Cysneiros, V. C., de Souza, F. C., Gaui, T. D., Pelissari, A. L., Orso, G. A., do Amaral MaChado, S., et al. (2021). Integrating climate, soil and stand structure into allometric models: An approach of site-effects on tree allometry in Atlantic Forest. *Ecol. Indic.* 127, 107794. doi: 10.1016/j.ecolind.2021.107794

De Langre, E. (2008). Effects of wind on plants. *Annu. Rev. Fluid Mech.* 40, 141–168. doi: 10.1146/annurev.fluid.40.111406.102135

Feldpausch, T. R., Banin, L., Phillips, O. L., Baker, T. R., Lewis, S. L., Quesada, C. A., et al. (2011). Height-diameter allometry of tropical forest trees. *Biogeosciences* 8, 1081–1106. doi: 10.5194/bg-8-1081-2011

Fernández-Palacios, J. M., Kreft, H., Irl, S. D., Norder, S., Ah-Peng, C., Borges, P. A., et al. (2021). Scientists' warning–The outstanding biodiversity of islands is in peril. *Global Ecol. Conserv.* 31, e01847. doi: 10.1016/j.gecco.2021.e01847

Fick, S. E., and Hijmans, R. J. (2017). WorldClim 2: new 1km spatial resolution climate surfaces for global land areas. *Int. J. Climatol.* 37, 4302–4315. doi: 10.1002/joc.2017.37.issue-12

Flora of Chinese (2019). Available online at: https://www.iplant.cn/foc (Accessed September 15, 2024).

Fortin, M., Van Couwenberghe, R., Perez, V., and Piedallu, C. (2019). Evidence of climate effects on the height-diameter relationships of tree species. *Ann. For. Sci.* 76, 1–20. doi: 10.1007/s13595-018-0784-9

Frank, D., Reichstein, M., Bahn, M., Thonicke, K., Frank, D., Mahecha, M. D., et al. (2015). Effects of climate extremes on the terrestrial carbon cycle: concepts, processes and potential future impacts. *Global Change Biol.* 21, 2861–2880. doi: 10.1111/gcb.2015.21.issue-8

Gardiner, B., Berry, P., and Moulia, B. (2016). Wind impacts on plant growth, mechanics and damage. *Plant Sci.* 245, 94–118. doi: 10.1016/j.plantsci.2016.01.006

Gimeno, L., Nieto, R., and Sorí, R. (2020). The growing importance of oceanic moisture sources for continental precipitation. *NPJ Climate Atmospher. Sci.* 3, 27. doi: 10.1038/s41612-020-00133-y

Givnish, T. J., Wong, S. C., Stuart-Williams, H., Holloway-Phillips, M., and Farquhar, G. D. (2014). Determinants of maximum tree height in Eucalyptus species along a rainfall gradient in Victoria, Australia. *Ecology* 95, 2991–3007. doi: 10.1890/14-0240.1

Hulshof, C. M., Swenson, N. G., and Weiser, M. D. (2015). Tree height–diameter allometry across the United States. *Ecol. Evol.* 5, 1193–1204. doi: 10.1002/ece3.2015.5.issue-6

Jackson, T. D., Shenkin, A. F., Majalap, N., Bin Jami, J., Bin Sailim, A., Reynolds, G., et al. (2021). The mechanical stability of the world's tallest broadleaf trees. *Biotropica* 53, 110–120. doi: 10.1111/btp.12850

Jiang, H., Zhang, H., Xin, D., Zhao, Y., Cao, J., Wu, B., et al. (2022). Field measurement of wind characteristics and induced tree response during strong storms. *J. Forest. Res.* 33, 1505–1516. doi: 10.1007/s11676-021-01427-4

King, D. A. (1986). Tree form, height growth, and susceptibility to wind damage in Acer saccharum. *Ecology* 67, 980–990. doi: 10.2307/1939821

King, D. A. (1996). Allometry and life history of tropical trees. *J. Trop. Ecol.* 12, 25–44. doi: 10.1017/S0266467400009299

Lai, J., Zou, Y., Zhang, S., Zhang, X., and Mao, L. (2022). glmm. hp: an R package for computing individual effect of predictors in generalized linear mixed models. *J. Plant Ecol.* 15, 1302–1307. doi: 10.1093/jpe/rtac096

Li, Z., and Fang, H. (2016). Impacts of climate change on water erosion: A review. *Earth-Science Rev.* 163, 94–117. doi: 10.1016/j.earscirev.2016.10.004

Lines, E. R., Zavala, M. A., Purves, D. W., and Coomes, D. A. (2012). Predictable changes in aboveground allometry of trees along gradients of temperature, aridity and competition. *Global Ecol. Biogeogr.* 21, 1017–1028. doi: 10.1111/j.1466-8238.2011.00746.x

Liu, S., Zhang, X., Li, J., and Zhu, K. (2021). Effects of climate and topography on height-diameter allometry of Pinus ponderosa. *Scandinav. J. For. Res.* 36, 434–441. doi: 10.1080/02827581.2021.1961016

MacArthur, R. H., and Wilson, E. O. (1967). *The theory of island biogeography* (Princeton, NJ: Princeton University Press).

Manes, S., Costello, M. J., Beckett, H., Debnath, A., Devenish-Nelson, E., Grey, K. A., et al. (2021). Endemism increases species' climate change risk in areas of global biodiversity importance. *Biol. Conserv.* 257, 109070. doi: 10.1016/j.biocon.2021.109070

McMahon, T. (1973). Size and shape in biology: elastic criteria impose limits on biological proportions, and consequently on metabolic rates. *Science* 179, 1201–1204. doi: 10.1126/science.179.4079.1201

Meng, S. X., Lieffers, V. J., Reid, D. E., Rudnicki, M., Silins, U., and Jin, M. (2006). Reducing stem bending increases the height growth of tall pines. *J. Exp. Bot.* 57, 3175–3182. doi: 10.1093/jxb/erl079

Moles, A. T., Warton, D. I., Warman, L., Swenson, N. G., Laffan, S. W., Zanne, A. E., et al. (2009). Global patterns in plant height. *J. Ecol.* 97, 923–932. doi: 10.1111/j.1365-2745.2009.01526.x

Niklas, K. J. (1993). The scaling of plant height: a comparison among major plant clades and anatomical grades. *Ann. Bot.* 72, 165–172. doi: 10.1006/anbo.1993.1095

Niklas, K. J., and Spatz, H. C. (2006). Allometric theory and the mechanical stability of large trees: proof and conjecture. *Am. J. Bot.* 93, 824–828. doi: 10.3732/ajb.93.6.824

Olson, M. E., Soriano, D., Rosell, J. A., Anfodillo, T., Donoghue, M. J., Edwards, E. J., et al. (2018). Plant height and hydraulic vulnerability to drought and cold. *Proc. Natl. Acad. Sci.* 115, 7551–7556. doi: 10.1073/pnas.1721728115

Ottaviani, G., Keppel, G., Götzenberger, L., Harrison, S., Opedal, Ø.H., Conti, L., et al. (2020). Linking plant functional ecology to island biogeography. *Trends Plant Sci.* 25, 329–339. doi: 10.1016/j.tplants.2019.12.022

Patiño, J., Whittaker, R. J., Borges, P. A., Fernández-Palacios, J. M., Ah-Peng, C., Araújo, M. B., et al. (2017). A roadmap for island biology: 50 fundamental questions after 50 years of The Theory of Island Biogeography. *J. Biogeogr.* 44, 963–983. doi: 10.1111/jbi.12986

Poorter, L., Lianes, E., Moreno-de Las Heras, M., and Zavala, M. A. (2012). Architecture of Iberian canopy tree species in relation to wood density, shade tolerance and climate. *Plant Ecol.* 213, 707–722. doi: 10.1007/s11258-012-0032-6

Qiu, H., Liu, S., Zhang, Y., and Li, J. (2021). Variation in height-diameter allometry of ponderosa pine along competition, climate, and species diversity gradients in the western United States. *For. Ecol. Manage.* 497, 119477. doi: 10.1016/j.foreco.2021.119477

R Core Team (2013). *R: A language and environment for statistical computing*. Vienna, Austria: R Foundation for Statistical Computing. Available online at: https://www.R-project.org/

Ren, S., Song, C., Ye, S., Cheng, C., and Gao, P. (2022). The spatiotemporal variation in heavy metals in China's farmland soil over the past 20 years: A meta-analysis. *Sci. Total Environ.* 806, 150322. doi: 10.1016/j.scitotenv.2021.150322

Rudley, D., DeSoto, L., Rodríguez-Echeverría, S., and Nabais, C. (2023). Climate effect on the growth and hydraulic traits of two shrubs from the top of a Mediterranean mountain. *Sci. Total Environ.* 902, 165911. doi: 10.1016/j.scitotenv.2023.165911

Seleiman, M. F., Al-Suhaibani, N., Ali, N., Akmal, M., Alotaibi, M., Refay, Y., et al. (2021). Drought stress impacts on plants and different approaches to alleviate its adverse effects. *Plants* 10, 259. doi: 10.3390/plants10020259

Takashima, A., Kume, A., Yoshida, S., Murakami, T., Kajisa, T., and Mizoue, N. (2009). Discontinuous DBH–height relationship of Cryptomeria japonica on Yakushima Island: effect of frequent typhoons on the maximum height. *Ecol. Res.* 24, 1003–1011. doi: 10.1007/s11284-008-0574-1

Telewski, F. W. (2012). Is windswept tree growth negative thigmotropism? *Plant Sci.* 184, 20–28. doi: 10.1016/j.plantsci.2011.12.001

Thomas, S. C., Martin, A. R., and Mycroft, E. E. (2015). Tropical trees in a wind-exposed island ecosystem: Height-diameter allometry and size at onset of maturity. *J. Ecol.* 103, 594–605. doi: 10.1111/jec.2015.103.issue-3

Tilman, D. (1988). *Plant strategies and the dynamics and structure of plant communities* (Princeton, NJ: Princeton University Press).

Vizcaíno-Palomar, N., Ibáñez, I., González-Martínez, S. C., Zavala, M. A., and Alía, R. (2016). Adaptation and plasticity in aboveground allometry variation of four pine species along environmental gradients. *Ecol. Evol.* 6, 7561–7573. doi: 10.1002/ece3.2016.6.issue-21

Wang, X., Fang, J., Tang, Z., and Zhu, B. (2006). Climatic control of primary forest structure and DBH–height allometry in Northeast China. *For. Ecol. Manage.* 234, 264–274. doi: 10.1016/j.foreco.2006.07.007

Watt, M. S., and Kirschbaum, M. U. (2011). Moving beyond simple linear allometric relationships between tree height and diameter. *Ecol. Model.* 222, 3910–3916. doi: 10.1016/j.ecolmodel.2011.10.011

West, G. B., Brown, J. H., and Enquist, B. J. (1997). A general model for the origin of allometric scaling laws in biology. *Science* 276, 122–126. doi: 10.1126/science.276.5309.122

West, G. B., Brown, J. H., and Enquist, B. J. (1999). A general model for the structure and allometry of plant vascular systems. *Nature* 400, 664–667. doi: 10.1038/23251

Whittaker, R. J., Fernández-Palacios, J. M., Matthews, T. J., Borregaard, M. K., and Triantis, K. A. (2017). Island biogeography: taking the long view of nature's laboratories. *Science* 357, eaam8326. doi: 10.1126/science.aam8326

Whittaker, R. J., Rigal, F., Borges, P. A., Cardoso, P., Terzopoulou, S., Casanoves, F., et al. (2014). Functional biogeography of oceanic islands and the scaling of functional diversity in the Azores. *Proc. Natl. Acad. Sci.* 111, 13709–13714. doi: 10.1073/pnas.1218036111

Xiao, Y., Liu, X., Zhang, L., Song, Z., and Zhou, S. (2021). The allometry of plant height explains species loss under nitrogen addition. *Ecol. Lett.* 24, 553–562. doi: 10.1111/ele.13673

Xu, M., Zhao, Z., Zhou, H., Ma, L., and Liu, X. (2022). Plant allometric growth enhanced by the change in soil stoichiometric characteristics with depth in an alpine meadow under climate warming. *Front. Plant Sci.* 13, 860980. doi: 10.3389/fpls.2022.860980

Young, I. R., Zieger, S., and Babanin, A. V. (2011). Global trends in wind speed and wave height. *Science* 332, 451–455. doi: 10.1126/science.1197219

Zhang, X., Chhin, S., Fu, L., Lu, L., Duan, A., and Zhang, J. (2019). Climate-sensitive tree height–diameter allometry for Chinese fir in southern China. *Forest.: Int. J. For. Res.* 92, 167–176. doi: 10.1093/forestry/cpy043

Zhang, W. P., Zhao, L., Larjavaara, M., Morris, E. C., Sterck, F. J., and Wang, G. X. (2020). Height-diameter allometric relationships for seedlings and trees across China. *Acta Oecol.* 108, 103621. doi: 10.1016/j.actao.2020.103621

Zhang, A., Zheng, S., Didham, R. K., Holt, R. D., and Yu, M. (2021). Nonlinear thresholds in the effects of island area on functional diversity in woody plant communities. *J. Ecol.* 109, 2177–2189. doi: 10.1111/1365-2745.136321

Zhou, S., Qin, H., Liao, R., and Cheng, Y. (2024). Habitat quality drives the species–area relationship of plants and soil microbes in an ocean archipelago. *Oikos*, e10660. doi: 10.1111/oik.v2024.i11

frontiers | Frontiers in Plant Science

TYPE Original Research
PUBLISHED 02 April 2025
DOI 10.3389/fpls.2025.1566156



OPEN ACCESS

EDITED BY
Robert John,
Indian Institute of Science Education and Research Kolkata, India

REVIEWED BY
Xiao Xu,
Yunnan University, China
Tianyun Li,
Lanzhou University, China

*CORRESPONDENCE
Yikang Cheng
ykcheng@hainanu.edu.cn

RECEIVED 24 January 2025
ACCEPTED 17 March 2025
PUBLISHED 02 April 2025

CITATION
Yang C, Zhao J, Huang S, Zhou S and Cheng Y (2025) Distribution of different plant life forms on tropical islands: patterns and underlying mechanisms.
*Front. Plant Sci.* 16:1566156.
doi: 10.3389/fpls.2025.1566156



# Distribution of different plant life forms on tropical islands: patterns and underlying mechanisms

Chengfeng Yang[1], Jingyan Zhao[1], Shengzhuo Huang[2], Shurong Zhou[3] and Yikang Cheng[3]*

[1]Key Laboratory of Genetics and Germplasm Innovation of Tropical Special Forest Trees and Ornamental Plants, Ministry of Education, School of Tropical Agriculture and Forestry, Hainan University, Haikou, China, [2]Hainan Key Laboratory for Research and Development of Natural Products from Li Folk Medicine, Institute of Tropical Bioscience and Biotechnology, Chinese Academy of Agricultural Sciences, Haikou, China, [3]School of Ecology, Hainan University, Haikou, China

**Introduction:** Island biogeography theory posits that both island area and isolation significantly influence species distribution patterns and community structure. This study investigates the effects of island area and isolation on plant community structure, specifically focusing on the variation in species richness and abundance among different plant life forms (i.e., trees and shrubs) on tropical islands in the South China Sea.

**Methods:** We surveyed woody plants and collected soil samples from 20 tropical islands in the South China Sea, analyzing how island area, isolation, climate and soil factors influence plant communities across different life forms (trees vs. shrubs).

**Results:** The results indicate that species richness increases with island area and decreases with isolation, which aligns with the classic predictions of island biogeography. However, plant abundance exhibits a more complex pattern: tree abundance is positively correlated with island area and negatively correlated with isolation, while shrub abundance shows the opposite trend. Furthermore, the relative tree richness and abundance are predominant on larger, less isolated islands, whereas shrubs are more prevalent on smaller, more remote islands. These contrasting patterns suggest that different life forms adopt distinct ecological strategies within island ecosystems. The structural equation model (SEM) revealed that island area, isolation, and climatic factors directly affect the richness and abundance of trees but not shrubs. Additionally, the indirect effect of soil pH has proven to be a crucial environmental factor in shaping plant community structure.

**Discussion:** Overall, this study highlights the multifaceted roles of geographic, climatic, and soil factors in determining the composition of island plant communities across different life forms. The findings have important implications for island conservation, as they provide a deeper understanding of how plant communities respond to spatial and environmental factors, aiding in the management of biodiversity on tropical islands.

KEYWORDS

**ecological strategies, plants life forms, island area, island biogeography, island isolation, species abundance, species richness**

# 1 Introduction

Island biogeography theory plays a critical role in ecology, with its core principle being the positive correlation between area and species richness, as well as the negative correlation between isolation and species richness (MacArthur and Wilson, 1967). Island ecosystems, serve as "natural laboratories" for ecological research, providing unique conditions that enable scientists to investigate the mechanisms of species formation, extinction, and ecological adaptation, thereby enhancing our understanding of biodiversity maintenance and the dynamic processes of species distribution (Whittaker and Fernández-Palacios, 2007; Losos and Ricklefs, 2009; Whittaker et al., 2017). In the context of global change and increasing human disturbance, the significance of island studies have become even more pronounced (Fernández-Palacios et al., 2021; Manes et al., 2021).

Current research on island biogeography theory primarily focuses on the relationship between species richness and island area or isolation. However, community composition, including both species and functional diversity, is also highly sensitive to changes in island area, isolation, and environmental factors, which further influence ecosystem functions (MacArthur and Wilson, 1967; Warren et al., 2015; Spaak et al., 2017; Losos and Schluter, 2000; Schrader et al., 2020; Li X. et al., 2024). For instance, studies on plant abundance in contemporary ecological research are limited, yet abundance plays a crucial role in ecosystem functions, and its trends may not necessarily align with those of species richness (Ehrlén and Morris, 2015). A study on ecosystem services found that the abundance of common species is a major driver of ecosystem service functions, while species richness is not significantly correlated (Winfree et al., 2015). Additionally, a meta-analysis revealed that nitrogen enrichment reduced both plant species richness and abundance; however, the magnitude of the response varied due to differences in biodiversity indicators, environmental factors, and experimental contexts (Midolo et al., 2019).

Compared to mainland ecosystems, island ecosystems typically face more limited resources and harsher environmental conditions, which drive plants to develop unique and efficient adaptive strategies to cope with these challenges (Craine et al., 2012; Volaire, 2018). For example, in arid regions, short-lived plants fully exploit the periods each year when temperature and precipitation are moderately favorable for growth, completing their entire life cycle within this window and thus adopting a shortened life history strategy (Li et al., 2019; Tao et al., 2022). In island environments, the survival and reproduction of trees and shrubs necessitate more efficient resource utilization, which may, in turn, influence their distribution and diversity within the island ecosystem (Han et al., 2020). Trees are taller with larger root systems, enabling efficient resource capture and ecological stability. However, in relatively harsh island environments, their distribution is constrained by competition and growth conditions, making them more likely to concentrate in more favorable habitats (Shirima et al., 2016; Ziegler et al., 2024). In contrast, shrubs, with their shorter heights and dense branching structures, demonstrate greater adaptability and can achieve higher individual densities in competitive environments, thereby occupying more ecological niches and forming rich vegetation layers (Wilson, 1995; Götmark et al., 2016). Due to differing survival strategies and adaptations, plants with various life forms may respond differently to island area, isolation, and environmental factors (Xie et al., 2024). For instance, a study along an altitudinal gradient in the eastern Himalayas of Nepal found that plants of different life forms exhibited distinct relationships with various environmental factors (Bhattarai and Vetaas, 2003). Additionally, the relative abundance and density of different life forms within a community are crucial. The survival strategies and environmental responses of trees and shrubs differ, and their relative abundance and density can reveal their interrelationships and adaptation strategies within the ecosystem, the relative proportion of trees and shrubs reflects different successional stages of island vegetation and, to some extent, the stability of the island ecosystem (Morales et al., 2012; Yang et al., 2020). Some studies have shown that shrubs facilitate tree establishment in peat bogs, and once a certain number of trees are established, they further enhance shrub growth. The varying proportions of trees and shrubs within a community can have significant effects on its health and stability (Holmgren et al., 2015). Different relative proportions of trees and shrubs influence both species diversity and ecosystem function. Shrub dominance may aid soil restoration and expand habitat occupancy, while tree dominance enhances community stability and productivity (Lavorel and Garnier, 2002; Zizka et al., 2014). These ecological functions are vital for island ecosystem conservation, particularly through optimizing vegetation structure and fostering species interactions to improve ecosystem sustainability.

When exploring the relationship between species richness and island area, several mechanisms have been proposed, including the "passive sampling effect", which suggests that island size may influence species numbers primarily through limitations on sample space rather than ecological factors (Connor and McCoy, 1979); the "habitat diversity effect", which posits that species richness on islands is closely related to the diversity of habitat types and structures (Bracewell et al., 2018; Zhou et al., 2024); and "ecological drift", which implies that changes in species populations may result from random factors rather than selective pressures (Gilbert and Levine, 2017; Leibold and Chase, 2018). Numerous studies have demonstrated that these mechanisms play varying roles across different island systems (Li S. et al., 2024; Zhou et al., 2024). However, these mechanisms may overlook additional factors that could further explain island plant community composition, such as climatic conditions and habitat quality (e.g., soil nutrients, soil pH), which also influence island plant communities (Wu et al., 2022; Yuan et al., 2024; Zhou et al., 2024). A substantial body of evidence indicates that climate significantly affects plant growth, reproduction, and distribution (Cabral et al., 2014; Ramirez et al., 2020). Furthermore, soil properties, particularly soil nutrients and pH, exert distinct effects on plants, which vary across different ecosystems (Barker and Pilbeam, 2015; Barrow and Hartemink, 2023; Duan et al., 2023). By investigating the effects of island area, isolation, and climate, we can better understand how these factors

influence island plant species richness and the abundance of various plant life forms. This occurs directly or indirectly through soil characteristics, providing a more comprehensive understanding of the dynamic changes in island ecosystems and their responses to external pressures. This knowledge provides essential scientific insights for ecological conservation and resource management.

Due to the diverse adaptive strategies exhibited by different life forms, this study focuses on examining the varying responses of trees and shrubs to island area, isolation, and other environmental factors on the islands of the South China Sea. Specifically, the objectives of this study are to: 1) explore the relationships between plant species richness and the abundance of different life forms (trees and shrubs) in relation to island area and isolation; 2) assess how the relative abundance and relative density of trees and shrubs change with variations in island area and isolation; and 3) identify the key environmental and ecological factors that influence the richness, abundance, and relative distribution of trees and shrubs across different islands. Based on island biogeography theory, we hypothesize that larger and less isolated islands will have higher tree abundance, while smaller and more isolated islands will favor shrubs due to their superior adaptability and more efficient reproductive strategies. These insights will help clarify the mechanisms behind the composition of island plant communities and contribute to better understanding of the ecological dynamics at play in these unique environments.

# 2 Materials and methods

## 2.1 Study site and sampling method

As an important tropical marine ecosystem, the South China Sea is home to numerous islands, coral reefs, and shallows, exhibiting rich biodiversity and complex marine ecological environments. This region not only provides habitats and breeding grounds for a variety of marine organisms but also creates conditions conducive to the growth of diverse tropical and subtropical plant species. Despite the abundance of islands in this area, some are too small or lack sufficient vegetation to meet the criteria for plant surveys. Consequently, we selected 20 representative islands with woody vegetation that have experienced minimal disturbance for investigation from April 2023 to May 2024.

For each island, we established 20 m × 20 m permanent sampling plots, with the number of plots proportional to the logarithmic transformation of the island area (log10) (Supplementary Figure S1). Additionally, we took topography into account when selecting the specific locations of the plots, ensuring that the plot locations on the investigated islands covered all terrain types and different altitudes of the islands as much as possible. Additionally, we considered the vegetation conditions and habitat differences of the islands as supplementary information for plot selection. As a result, a total of 87 permanent plots were established across the 20 islands. To minimize the effects of spatial autocorrelation, we ensured that the distance between any two adjacent plots within each island exceeded 100 meters. For the smallest islands, while it was not entirely feasible to meet this standard, the distance between plots was maintained at over 40 meters.

On all selected islands, we conducted plant surveys and soil sampling within the established permanent plots. First, we utilized Real-Time Kinematic (RTK) positioning technology, provided by Xunwei Positioning, to accurately locate the four corners of each plot. We marked these positions by inserting white rubber tubes into the soil and enclosing the 20 m × 20 m plot with red plastic string. Within the marked plots, we surveyed all woody plants with a diameter at breast height (DBH) ≥ 1 cm, recording species names through morphological identification and subsequently calibrated the Chinese and Latin names of the species based on the "Flora of China" (Flora of Chinese, 2019).

To collect soil samples, we established three evenly distributed 2 m × 2 m quadrats along the diagonal of each plot, ensuring that the quadrats covered different microhabitats within the plot. In each quadrat, we randomly collected four soil samples to a depth of 0-10 cm from various locations within the quadrat. The soil samples from each quadrat were then combined and thoroughly mixed to create a composite sample for each quadrat. In total, 261 composite soil samples were obtained across all islands, corresponding to 87 plots and three quadrats per plot. For each soil sample, large particles were removed using a 2 mm sieve, and the samples were and stored at 4°C for subsequent measurements of their physicochemical properties.

## 2.2 Data acquisition

We classified these plants into tree or shrub categories based on their life forms, referencing the "Flora of China" (Flora of Chinese, 2019). Subsequently, we utilized the "vegan" package in R to calculate the species richness and abundance of all species, as well as those of trees and shrubs, respectively. Additionally, we assessed the relative richness and relative abundance of trees and shrubs for each plot.

We measured five physicochemical properties of soil from the collected samples that could potentially influence plant communities, using the following specific methods: Soil pH was determined with a Metter- S210 SevenCompact pH analyzer, employing a soil-to-water ratio of 1:2.5. Soil organic carbon (SOC) content was assessed using the K2Cr2O7 oxidation-reduction titration technique. Total nitrogen (TN) levels in the soil were quantified utilizing the semi-micro Kjeldahl method. Total phosphorus (TP) concentrations were measured through colorimetric analysis with a UV-visible spectrophotometer. Finally, total potassium (TK) content was extracted using 1 M ammonium acetate and analyzed via inductively coupled plasma technology.

Climate data were obtained from WorldClim's global climate and weather database (Fick and Hijmans, 2017), specifically the WorldClim 2.1 dataset for the period 1970-2000. This version was released in January 2020. Annual mean temperature and annual precipitation data were extracted from the bioclimatic variables bio1 and bio12 in the historical climate dataset. Wind speed data were sourced from a dataset with a spatial resolution of 2.5 arc minutes. We processed the downloaded TIFF files using the "terra" package in R to extract annual mean temperature, annual precipitation, and annual mean wind speed data for the 20 surveyed islands.

## 2.3 Statistic analysis

In this study, we employed linear regression to assess the effects of island area and isolation on plant community structure. We used logarithmically transformed island area and isolation as independent variables to analyze their linear relationships with species richness and abundance, including total species, trees, and shrubs, as well as the relative richness and relative abundance of different plant life forms.

We applied principal component analysis (PCA) to simplify the data structure of climate and soil nutrient variables. For climate, we used annual mean temperature, annual precipitation, and annual mean wind. For soil nutrients, we included total nitrogen (TN), total phosphorus (TP), total potassium (TK), and soil organic carbon (SOC). The first principal component (PC1) from each PCA was retained as a composite predictor, as it explained the largest proportion of the variance-56.0% for climate variables and 54.7% for soil nutrients. In $PC_{climate}$, annual precipitation (-0.711) contributed the most, while in $PC_{soil}$, both nitrogen (-0.658) and soil organic carbon (-0.653) had the largest contributions. These first principal components were used as composite predictors for climate and soil variables in subsequent analyses (Supplementary Table S1).

We employed a piecewise structural equation model (SEM) to assess the direct effects of island area, isolation, and climate variables ($PC_{climate}$) on total plant richness and abundance, as well as the absolute and relative richness and abundance of each life form. Additionally, we examined the indirect effects mediated by soil nutrients ($PC_{soil}$) and soil pH. The psem function in the piecewiseSEM package (Lefcheck, 2016) was utilized for the SEM analysis. Specifically, this method performs confirmatory path analysis based on the results of directed separation tests (Shipley, 2009, 2013). Model fit was evaluated using goodness-of-fit statistics, and the best model was selected by comparing the Akaike Information Criterion corrected for small sample size (AICc) values between the full model and simplified models (Grace, 2006). The model with the lowest AICc value was designated as the final model for the study (Shipley, 2013). Furthermore, the overall model fit was assessed using Fisher's C statistic (Supplementary Table S2). If the p-value of Fisher's C statistic exceeded 0.05 (i.e., the null hypothesis was accepted), the model was considered to have a good fit (Shipley, 2009). All statistical analyses were conducted using R 4.4.1.

# 3 Results

## 3.1 Response of richness of different life forms to island area and isolation

In terms of species richness, the richness of all species, trees, and shrubs exhibited similar trends in relation to island area and isolation. Specifically, with an increase in island area, the richness of all three groups significantly increased ($P < 0.05$) (Figures 1a-c). This phenomenon suggests that larger islands can provide more niches and resources, thereby supporting a greater number of species for survival and reproduction. Conversely, as isolation increased, the richness of all species, trees, and shrubs significantly decreased ($P < 0.05$) (Figures 1d-f). This trend may be related to the limitations on species dispersal abilities; more isolated islands often struggle to maintain high levels of species diversity. These results further emphasize the important influence of island area and isolation on plant community structure.

## 3.2 Response of abundance of different life forms to island area and isolation

In terms of species abundance, the relationships between the abundance of total species, trees, and shrubs with island area and isolation exhibited certain differences. Specifically, the abundance of total species did not show a significant relationship with either island area or isolation ($P = 0.251$, $P = 0.731$) (Figure 2a, d). However tree abundance increased significantly with island area, demonstrating a clear positive correlation ($P < 0.001$) (Figure 2b). Tree abundance, on the other hand, decreased with isolation ($P = 0.013$) (Figure 2e). In contrast, the trend for shrubs was opposite to that of trees. Shrub abundance showed a decreasing trend with island area ($P = 0.119$) (Figure 2c) but an increasing trend with isolation ($P = 0.075$) (Figure 2f), though the relationships were not statistically significant. These findings suggest that trees are more sensitive to the island area and isolation, possibly relying more on ecological spaces to maintain population stability. At the same time, the differing responses in abundance between trees and shrubs further reflect the diversity of adaptive strategies among different life forms in island environments.

## 3.3 Response of relative richness and relative abundance of different life forms to island area and isolation

As island area increases, both relative richness and relative abundance of trees significantly increased, while the relative richness and relative abundance of shrubs significantly decreased ($P < 0.001$, $P = 0.002$) (Figure 3a, c). This indicates that large island area favors the spread and colonization of trees, while reducing the relative dominance of shrubs. Conversely, as isolation increases, both the relative richness and relative abundance of trees significantly decreased, while the relative richness and relative

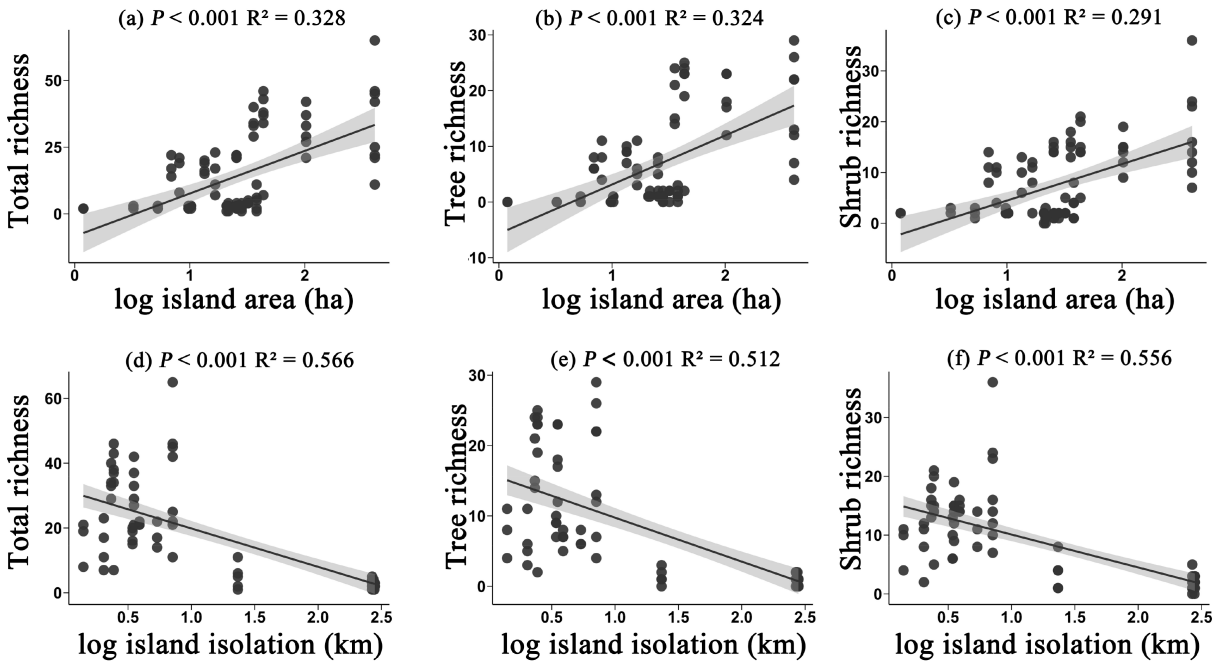


FIGURE 1
The effects of island area on the richness of all species **(a)**, tree richness **(b)**, and shrub richness **(c)**; and the effects of island isolation on the richness of all species **(d)**, tree richness **(e)**, and shrub richness **(f)**. Species richness refers to the taxonomic diversity within each plot, specifically the number of species present in a plot.

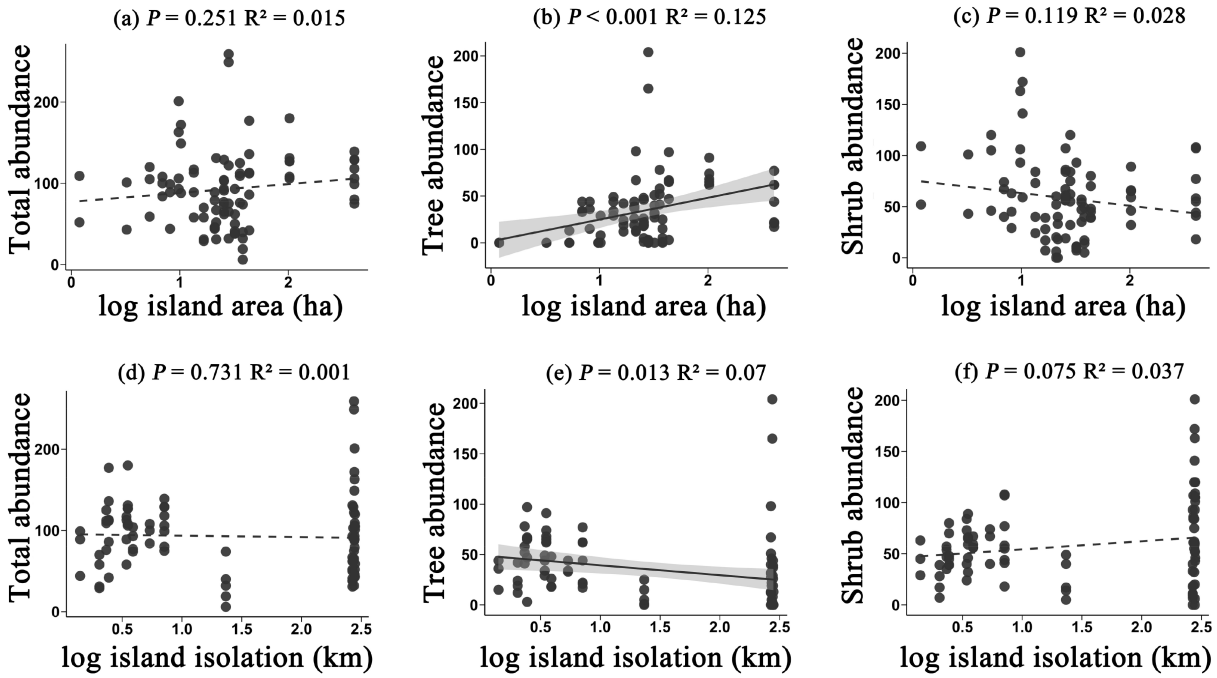


FIGURE 2
The effects of island area on the abundance of all species **(a)**, tree abundance **(b)**, and shrub abundance **(c)**; and the effects of island isolation on the abundance of all species **(d)**, tree abundance **(e)**, and shrub abundance **(f)**. Plant abundance refers to the number of individuals present in each plot.

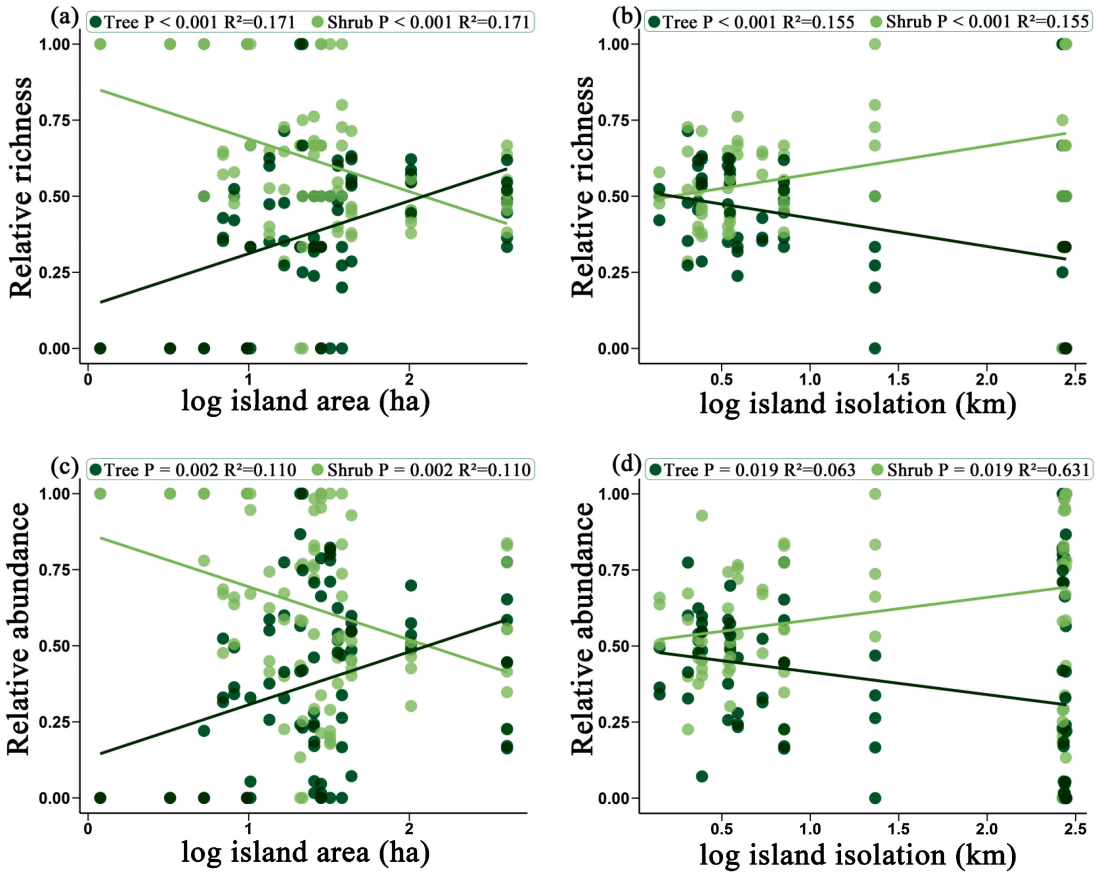


FIGURE 3
The effects of island area on the relative richness of trees and shrubs **(a)** and the relative abundance of trees and shrubs **(c)**; and the effects of island isolation on the relative richness of trees and shrubs **(b)** and the relative abundance of trees and shrubs **(d)**. Dark green represents trees, while light green represents shrubs.

abundance of shrubs significantly increased ($P < 0.001$, $P = 0.019$ (Figure 3b, d). This suggests that on highly isolated islands, shrubs have a higher relative proportion within the community. In comparison, trees are more severely constrained in highly isolated environments, leading to a decrease in their proportion within the community. In summary, island area and isolation have significant effects on the relative proportions of trees and shrubs in a plant community. An increase in island area favors the richness and abundance of trees, whereas increased isolation promotes the relative proportion of shrubs in the community.

## 3.4 Direct and indirect effects of island area, isolation, and climate on the absolute and relative plant richness and abundance

The final structural equation model (SEM) revealed that the direct and indirect effects of island area, isolation and climate on the richness and abundance of different life forms varied. For all the species, island geographical characteristics and climate mainly exerted indirect effects on island plant richness and abundance through their influence on soil pH, rather than soil nutrients Island area, isolation, and climate factors also directly influenced species richness. Species abundance, on the other hand, was only directly influenced by climate factors, while island area and isolation had no direct effect on it (Figure 4a, b). For trees, the effects of island area, isolation, and climate on their richness followed a similar pattern to that of total species richness, but with different coefficients. Tree abundance, however, was directly influenced only by island area, isolation, and climate (Figure 4c, d). For shrubs, richness was mainly directly influenced by island isolation, while abundance was neither directly nor indirectly affected by affected by island geographical characteristics and climate (Figure 4e, f). Since the relative richness and relative abundance of trees and shrubs sum to 1, they exhibited a negative correlation. Therefore, the trends for trees were opposite to those of shrubs (Supplementary Figures S2a, b). For the relative richness of trees, island area, isolation, and climate factors influenced it via soil pH. The relative richness of trees also increased with island area. Island isolation did not have a direct effect on relative richness of trees (Figure 4g). For relative abundance, the impact of island area was more pronounced, while island isolation and climate factors only influenced it indirectly through soil pH and had no direct effects (Figure 4h).

10.3389/fpls.2025.1566156

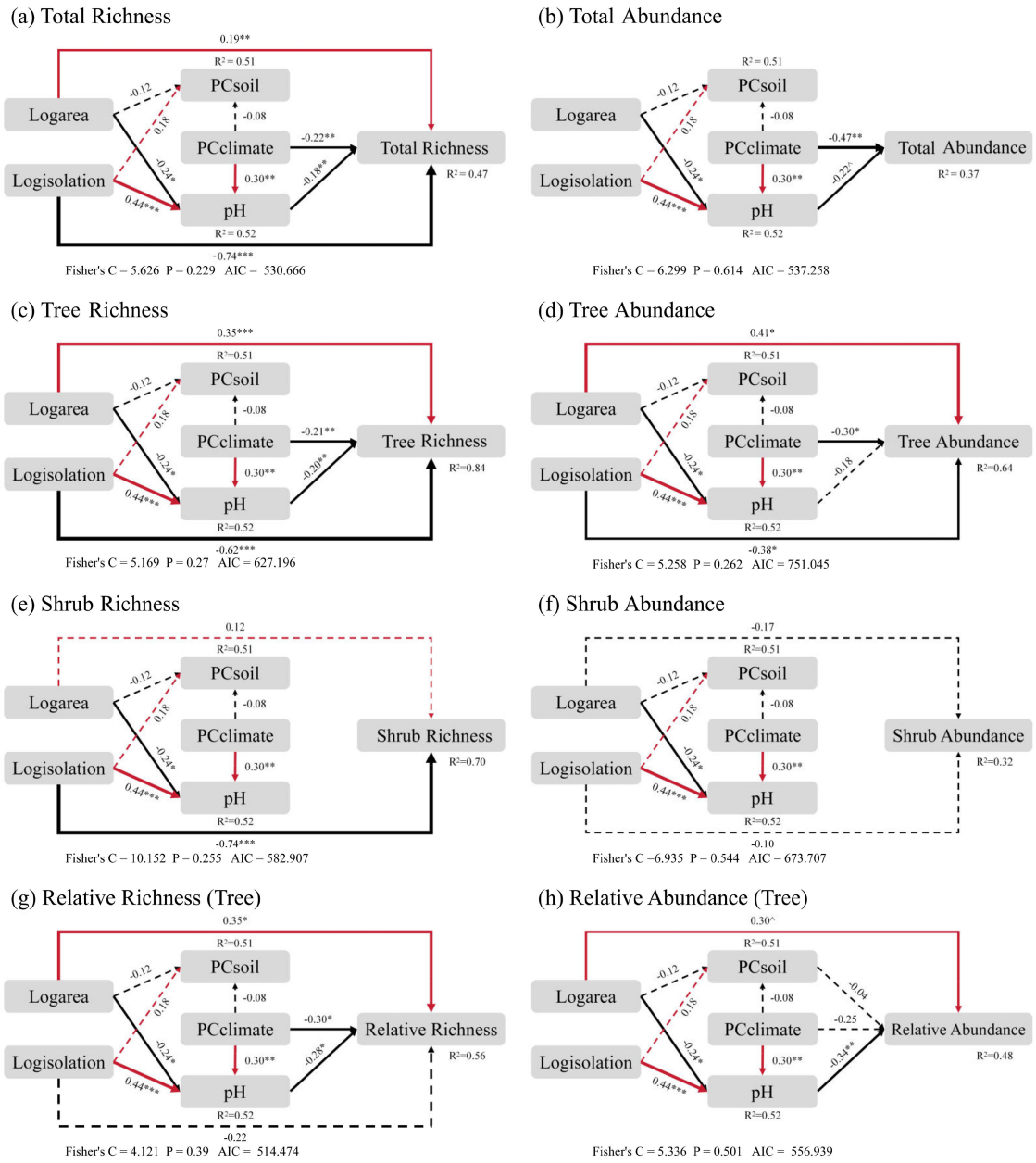


FIGURE 4
The final results of the Structural Equation Model (SEM) reveal the direct effects of island area, isolation, and climate on total species richness **(a)**, total species abundance **(b)**, tree species richness **(c)**, tree species abundance **(d)**, shrub species richness **(e)**, shrub species abundance **(f)**, relative richness of trees **(g)**, and relative abundance of trees **(h)**, as well as their indirect effects mediated by environmental factors such as soil nutrients and pH, respectively. Plant species richness was estimated based on the number of species observed in the plots, while abundance was estimated based on the number of individuals recorded. $PC_{climate}$ represents the climate factors after dimensionality reduction through Principal Component Analysis (PCA), $PC_{soil}$ refers to the soil nutrient factors after dimensionality reduction, and pH represents soil acidity. Red and black arrows are the standardized path coefficient variables, representing significant positive and negative pathways respectively, with the thickness of the line proportional to the strength of the path coefficient. $R^2$ is the marginal value that represents the proportion of variance explained for each fixed variable in the model. The symbols denote statistical significance (***$P < 0.001$; **$P < 0.01$; *$P < 0.05$; ^$P < 0.1$).

# 4 Discussion

## 4.1 Effects of island area and isolation on plant richness and abundance

While traditional studies in island biogeography have mainly focused on the relationship between species richness and island area or isolation, our study further explores the differences in the responses of plant community abundance to island area and isolation, revealing significant ecological adaptations between trees and shrubs. Overall, plant species richness significantly increased with larger island areas, while it decreased markedly with greater isolation, a trend that aligns with the classic predictions of island biogeography (MacArthur and Wilson, 1967). This positive correlation between island area and species richness, as well as the negative correlation between isolation and species richness, was observed for the entire plant community and when categorized by life forms (Weigelt and Kreft, 2013; Portillo et al., 2019). These findings suggest that both island area and isolation play an important role in influencing plant species richness, and these patterns remain consistent regardless of the classification of different plant life forms (Kubota et al., 2015; Xie et al., 2024). However, the trends in plant abundance on these islands did not fully correspond with species richness. Notable differences in abundance trends were observed between trees and shrubs across various plant life forms. Specifically, the trend in tree abundance was consistent with that of its species richness; tree abundance significantly increased with island area but decreased significantly on highly isolated islands. This indicates that the growth and expansion of trees may depend on the ample resources and habitats available on larger islands, while high levels of isolation hinder seed dispersal and colonization, further limiting the increase in tree population density on isolated islands (Whittaker and Fernández-Palacios, 2007; Shirima et al., 2016; Nogales et al., 2024).

In contrast, the relationship between shrub abundance and island area and isolation exhibited an opposite trend. On islands with greater isolation, shrub abundance was higher, although this trend was close to being statistically significant. This phenomenon may be attributed to the relative reduction of tree abundance and the ecological strategy of shrubs, which makes their abundance insensitive to island area and isolation, as well as the formation of high-density monocultures. For instance, shrubs typically possess high vegetative reproduction capabilities and rapid growth rates; many shrubs on islands exhibit rhizomes and stolons, which enable them to occupy habitats with limited resources or restricted seed dispersal, thereby enhancing species persistence (Wilson, 1995; Götmark et al., 2016; Ottaviani et al., 2020). As observed in this study, islands such as Beishazhou Island and Zhongshazhou Island, which are characterized by higher isolation and smaller areas, displayed relatively low species richness. However, plant abundance was particularly high due to the dominance of a single species, i.e., *Scaevola taccada*. This suggests that while soil and climatic conditions on highly isolated islands may not be suitable for the growth of all plant types, larger islands may also suppress or inhibit the growth of certain plants through resource competition, with trees and shrubs showing different adaptive responses.

It is important to note that the differing patterns in species abundance and species richness suggest that the number of species and the abundance of individuals may be driven by distinct ecological mechanisms. Therefore, a comprehensive examination of these patterns should take into account various ecological processes from multiple perspectives within island ecosystems.

## 4.2 The regulation of the relative proportions of trees and shrubs by island area and isolation

This study revealed that island area and isolation significantly influence the relative richness and abundance of different plant life forms within the plant community. As island area increases, the relative richness and abundance of trees significantly increased, while the relative richness and abundance of shrubs significantly decline. This phenomenon aligns with the classical "area effect" in island biogeography, where larger islands provide more habitats and resources, thereby facilitating the expansion and survival of species (Connor and McCoy, 1979; Leibold and Chase, 2018; Li S. et al., 2024). For trees, larger islands not only offer more habitat but also maintain more stable environmental conditions, particularly in resource-rich environments where trees may dominate interspecific competition, driving their relative abundance and richness upward (Yan et al., 2023). In contrast, the relative richness and abundance of shrubs are lower on larger islands, which may be attributed to the expansion and competition of tree populations (Barnes and Archer, 1999). On larger islands, trees may dominate due to their spatial requirements for growth and their efficiency in resource utilization, which limits the expansion of shrubs (Grime, 2006). However, on smaller islands, the plant community may be more strongly influenced by edge effects, which favor the competition of shrubs in lower-quality habitats, resulting in a noticeable increase in their relative richness and abundance (Harper et al., 2005).

The increase in island isolation significantly reduced the relative richness and abundance of trees, while the relative richness and abundance of shrubs significantly increased. This is likely due to differences in dispersal mechanisms and colonization success rates. On smaller and more isolated islands, the difficulty of plant colonization increases. Shrubs, compared to trees, possess more flexible dispersal mechanisms and stronger reproductive and adaptive abilities to survive in harsh environments (Zizka et al., 2014; Ehmet et al., 2021). For instance, one of the most frequently occurring species in this survey, *Scaevola taccada*, has heteromorphic fruits—one type with softwood and fleshy pulp, and another with only pulp—that can be dispersed both by seawater and indirectly by birds, greatly enhancing the species' dispersal efficiency (Emura et al., 2014). In cases where dispersal is challenging, shrubs may benefit relatively more from increased isolation, as their adaptive advantages are more pronounced in these environments (Gillespie et al., 2008). Shrub species, characterized by higher growth rates and the ability to rapidly

respond to environmental changes while tolerating local resource limitations, may quickly occupy new habitats, form dominant communities, and potentially further restrict the territorial expansion of trees (Fukami, 2015). These findings suggest that classical theories in island biogeography still play a significant role in shaping plant communities. However, the distribution and dynamics of plant populations are not determined solely by the physical environment; their ecological strategies and interspecies competition also contribute to shaping these patterns.

## 4.3 The driving mechanisms of island plant communities: the synergistic effects of geography, climate, and soil factors

Our results clearly indicate that the direct effects of island area and isolation are the most significant factors influencing plant communities on islands. The findings from the structural equation modeling (SEM) demonstrate that the direct effects of island area and isolation are highly significant, which is consistent with studies conducted on various islands. However, the impact of island area and isolation on species richness and abundance, as well as on different plant life forms, exhibits some variability (Schrader et al., 2020; Lee et al., 2022; Xie et al., 2024; Zhou et al., 2024). Specifically, species richness is more readily influenced by island area and isolation, while the responses of trees and shrubs to these two factors differ. The survival strategies of trees indicate a greater reliance on the favorable living conditions provided by larger island areas (Connor and McCoy, 1979). Furthermore, the influence of area and isolation on plant communities extends beyond direct effects to include indirect effects as well.

We also found that climatic factors, such as temperature, precipitation, and wind speed, directly influence the community structure of plants on islands, particularly affecting trees (Harter et al., 2015; Irl et al., 2020). Compared to mainland environments, oceanic islands, influenced by surrounding seas, may have more favorable conditions in terms of precipitation and temperature. However, the isolation and smaller size of islands made their plant communities more sensitive to changes in these climatic factors. Therefore, in the fragile island environment, climatic factors can still directly impact plant growth, survival, and distribution (Cabral et al., 2014; Ramirez et al., 2020). Interestingly, precipitation contributed the most in the $PC_{climate}$. However, trees and shrubs responded differently to precipitation. Structural equation modeling (SEM) revealed that trees were directly influenced by the precipitation-dominant $PC_{climate}$, while shrubs were not. This is likely related to the more robust adaptive strategies of shrubs. As observed in our study, on islands dominated by shrubs (with higher relative abundance and relative dominance of shrubs), the leaf thickness of these shrub species was greater, and in some cases, even succulent-like (e.g., *Scaevola taccada*, *Tournefortia argentea*), further corroborating the distinct ecological strategies of trees and shrubs on islands (Aneja et al., 2025). Although wind speed had a lower contribution to the climate principal component than precipitation, it remains an important factor. In tropical islands, intermittent extreme wind events, such as tropical storms or typhoons, can significantly impact plant communities, leading to tree falls or vegetation loss (Uriarte et al., 2019; Bauman et al., 2022). These disturbances may disrupt existing community structures and provide opportunities for more adaptable plants, such as shrubs or herbaceous species, to expand, thereby altering the species composition of the community (Murphy and Metcalfe, 2016). We also found that the effects of these climatic factors are not only reflected at the physiological level of plants but also indirectly influence plant communities by altering the soil pH on islands. For instance, changes in precipitation and temperature can cause fluctuations in soil acidity, which in turn affect nutrient uptake and plant growth rates (Jesus et al., 2015; Pugnaire et al., 2019).

We also found that climatic factors, such as temperature, precipitation, and wind speed, directly affect the community structure of plants on islands (Harter et al., 2015; Irl et al., 2020). Islands are more fragile than mainland environments, and temperature and precipitation directly influence plant growth, survival, and distribution (Cabral et al., 2014; Ramirez et al., 2020). However, these effects are not only reflected at the physiological level of plants; they also indirectly influence plant communities by affecting soil conditions on the islands, including soil nutrients and pH (Jesus et al., 2015; Pugnaire et al., 2019). Wind speed, as a unique climatic factor on islands, also has a significant impact on plant communities. Strong winds can directly affect the growth and stability of tall plants, such as trees, and alter species dispersal patterns by spreading seeds and pollen (Kuparinen et al., 2009; Bullock et al., 2012). Particularly in tropical islands, intermittent extreme wind events, such as tropical storms or typhoons, can significantly impact plant communities, leading to tree falls or vegetation loss (Uriarte et al., 2019; Bauman et al., 2022). Such disturbances may disrupt existing community structures and create opportunities for highly adaptable plants, such as shrubs or herbaceous species, to expand, thereby altering the species composition of the community (Murphy and Metcalfe, 2016).

Our study confirmed the important role of soil pH in influencing island plant communities. This is supported by the results from structural equation modeling (SEM), which indicated that soil nutrients (such as nitrogen and organic carbon) did not have a significant direct impact on plant community structure. Instead, island area, isolation, and climatic factors affected community structure through their influence on soil pH. As a key environmental factor in island plant communities, soil pH profoundly affects plant growth and species diversity. It influences plant communities through various ecological mechanisms, not only by directly restricting plant growth but also by indirectly shaping community structure through alterations in interactions among plants, the environment, and other organisms. Soil pH affects the efficiency of nutrient absorption by plants, particularly the availability of essential elements (Kemmitt et al., 2006; Penn and Camberato, 2019; Barrow and Hartemink, 2023). Furthermore, soil pH influences the diversity and functional activity of rhizosphere microorganisms, which further impacts plant community composition through plant-microbe interactions (Husson, 2013; Duan et al., 2023). At the community level, in soils with extreme

acidic or alkaline conditions, species with strong tolerance often dominate ecological niches, while pH-sensitive species may be excluded from the community (Barker and Pilbeam, 2015; Deinlein et al., 2014; Mann et al., 2023). This selective effect significantly alters the species composition of the community, particularly in isolated island environments, where regional variations in soil pH can increase the heterogeneity of plant communities across different islands, our study provides a new perspective for island ecology, emphasizing the critical role of soil as an ecological factor.

## 5 Conclusion

Although many traditional studies in island biogeography focus on the relationship between species diversity and island area or isolation, fewer investigations have refined the analysis of island plants based on different life forms. Most studies tend to address species richness without exploring other comprehensive indicators, such as plant community abundance, relative richness, and relative abundance. Our study represents a significant advancement in this area, revealing the distinct relationships between plant richness and abundance and island area and isolation. The observed trends in species richness align with traditional island biogeography theory, while plant abundance exhibits a more complex pattern, highlighting differential responses among various plant life forms. Specifically, trees are more sensitive to spatial limitations and their growth and dispersal are more dependent on the resources and habitat space provided by larger islands, whereas shrubs exhibit stronger dispersal abilities and faster reproductive mechanisms, showing greater adaptability in resource-limited and highly isolated environments. In addition, relative richness and relative abundance also show significant differences under variations in island area and isolation. On larger islands, the relative richness and relative abundance of trees significantly increase, while shrubs show a contrasting decline. These results indicate that increasing island area favors the expansion of trees, while higher island isolation promotes the dominance of shrubs within communities, revealing the distinct responses of different plant life forms to their ecological strategies in island environments. Structural equation modeling (SEM) further indicates that island area and isolation indirectly affect plant community richness and abundance by influencing soil pH, highlighting the mediating role of soil pH as a key environmental factor. This emphasizes the critical role of soil factors in shaping the structure of island plant communities. The direct effects of island geography and climate on plant communities are not limited to the physical environment but also act indirectly through their influence on the soil, affecting plant community composition and function. This finding provides new perspectives for the conservation and management of island plant communities. Island area and isolation directly influence the composition of plant communities, and different plant life forms respond differently to these factors. Therefore, island conservation strategies should be tailored to the needs of different plant communities, taking into account the size and isolation of the islands. Additionally, future research should focus on how island plant communities respond to climate change, particularly the regulation of key soil factors such as soil pH, to further optimize the management of island ecosystems and promote plant community diversity. Long-term monitoring and comparative studies across islands will help to better understand the complex relationships between island geography, soil properties, and plant community composition, providing a more scientific basis for island conservation.

## Data availability statement

The raw data supporting the conclusions of this article will be made available by the authors, without undue reservation.

## Author contributions

CY: Conceptualization, Data curation, Formal Analysis, Investigation, Methodology, Visualization, Writing – original draft. JZ: Investigation, Writing – review & editing. SH: Investigation, Writing – review & editing. SZ: Conceptualization, Funding acquisition, Investigation, Supervision, Writing – review & editing. YC: Conceptualization, Data curation, Formal Analysis, Investigation, Methodology, Supervision, Writing – original draft, Writing – review & editing.

## Funding

The author(s) declare that financial support was received for the research and/or publication of this article. This study was supported by the Hainan Province Science and Technology Special Fund (Grant no. ZDYF2022SHFZ320).

## Acknowledgments

We are grateful to Lan Liu, Lingbing Wu, and Nianxun Xi from Hainan University for their guidance in experimental design and implementation. We also appreciate Haifeng Ding, Bo Zhang, and Yu Nie for their assistance and valuable suggestions during data analysis. Our thanks go to Hao Qin, Renfu Liao, Shuxin Liu, Zhen Zhang, and Run Zhang for their help in fieldwork.

## Conflict of interest

The authors declare that the research was conducted in the absence of any commercial or financial relationships that could be construed as a potential conflict of interest.

## Generative AI statement

The author(s) declare that no Generative AI was used in the creation of this manuscript.

## Publisher's note

All claims expressed in this article are solely those of the authors and do not necessarily represent those of their affiliated organizations, or those of the publisher, the editors and the reviewers. Any product that may be evaluated in this article, or claim that may be made by its manufacturer, is not guaranteed or endorsed by the publisher.

## Supplementary material

The Supplementary Material for this article can be found online at: https://www.frontiersin.org/articles/10.3389/fpls.2025.1566156/full#supplementary-material

## References

Aneja, P., Sanyal, R., and Ranjan, A. (2025). Leaf growth in third dimension: a perspective of leaf thickness from genetic regulation to ecophysiology. *New Phytol.* 245, 989–999. doi: 10.1111/nph.v245.3

Barker, A. V., and Pilbeam, D. J. (Eds.) (2015). *Handbook of plant nutrition* (CRC press).

Barnes, P. W., and Archer, S. (1999). Tree-shrub interactions in a subtropical savanna parkland: competition or facilitation? *J. Vegetation. Sci.* 10, 525–536. doi: 10.2307/3237187

Barrow, N. J., and Hartemink, A. E. (2023). The effects of pH on nutrient availability depend on both soils and plants. *Plant Soil* 487, 21–37. doi: 10.1007/s11104-023-05960-5

Bauman, D., Fortunel, C., Delhaye, G., Malhi, Y., Cernusak, L. A., Bentley, L. P., et al. (2022). Tropical tree mortality has increased with rising atmospheric water stress. *Nature* 608, 528–533. doi: 10.1038/s41586-022-04737-7

Bhattarai, K. R., and Vetaas, O. R. (2003). Variation in plant species richness of different life forms along a subtropical elevation gradient in the Himalayas, east Nepal. *Global Ecol. Biogeogr.* 12, 327–340. doi: 10.1046/j.1466-822X.2003.00044.x

Bracewell, S. A., Clark, G. F., and Johnston, E. L. (2018). Habitat complexity effects on diversity and abundance differ with latitude: an experimental study over 20 degrees. *Ecology* 99, 1964–1974. doi: 10.1002/ecy.2018.99.issue-9

Bullock, J. M., White, S. M., Prudhomme, C., Tansey, C., Perea, R., and Hooftman, D. A. (2012). Modelling spread of British wind-dispersed plants under future wind speeds in a changing climate. *J. Ecol.* 100, 104–115. doi: 10.1111/j.1365-2745.2011.01910.x

Cabral, J. S., Weigelt, P., Kissling, W. D., and Kreft, H. (2014). Biogeographic, climatic and spatial drivers differentially affect α-, β-and γ-diversities on oceanic archipelagos. *Proc. R. Soc. B.: Biol. Sci.* 281, 20133246. doi: 10.1098/rspb.2013.3246

Connor, E. F., and McCoy, E. D. (1979). The statistics and biology of the species-area relationship. *Am. Nat.* 113, 791–833. doi: 10.1086/283438

Craine, J. M., Engelbrecht, B. M., Lusk, C. H., McDowell, N. G., and Poorter, H. (2012). Resource limitation, tolerance, and the future of ecological plant classification. *Front. Plant Sci.* 3, 246. doi: 10.3389/fpls.2012.00246

Deinlein, U., Stephan, A. B., Horie, T., Luo, W., Xu, G., and Schroeder, J. I. (2014). Plant salt-tolerance mechanisms. *Trends Plant Sci.* 19, 371–379. doi: 10.1016/j.tplants.2014.02.001

Duan, C., Li, X., Li, C., Yang, P., Chai, Y., and Xu, W. (2023). Positive effects of fungal β diversity on soil multifunctionality mediated by pH in the natural restoration succession stages of alpine meadow patches. *Ecol. Indic.* 148, 110122. doi: 10.1016/j.ecolind.2023.110122

Ehmet, N., Wang, Y. P., Zhao, X., Sun, K., and Hou, Q. Z. (2021). Adaptive response of reproductive characteristics of Trifolium repens on time scale. *Flora* 285, 151923. doi: 10.1016/j.flora.2021.151923

Ehrlén, J., and Morris, W. F. (2015). Predicting changes in the distribution and abundance of species under environmental change. *Ecol. Lett.* 18, 303–314. doi: 10.1111/ele.2015.18.issue-3

Emura, N., Denda, T., Sakai, M., and Ueda, K. (2014). Dimorphism of the seed-dispersing organ in a pantropical coastal plant, Scaevola taccada: heterogeneous population structures across islands. *Ecol. Res.* 29, 733–740. doi: 10.1007/s11284-014-1164-z

Fernández-Palacios, J. M., Kreft, H., Irl, S. D., Norder, S., Ah-Peng, C., Borges, P. A., et al. (2021). Scientists' warning–The outstanding biodiversity of islands is in peril. *Global Ecol. Conserv.* 31, e01847. doi: 10.1016/j.gecco.2021.e01847

Fick, S. E., and Hijmans, R. J. (2017). WorldClim 2: new 1km spatial resolution climate surfaces for global land areas. *Int. J. Climatol.* 37, 4302–4315. doi: 10.1002/joc.2017.37.issue-12

Flora of Chinese (2019). Available online at: https://www.iplant.cn/foc (Accessed September 15, 2024).

Fukami, T. (2015). Historical contingency in community assembly: integrating niches, species pools, and priority effects. *Annu. Rev. Ecol. Evol. Syst.* 46, 1–23. doi: 10.1146/annurev-ecolsys-110411-160340

Gilbert, B., and Levine, J. M. (2017). Ecological drift and the distribution of species diversity. *Proc. R. Soc. B.: Biol. Sci.* 284, 20170507. doi: 10.1098/rspb.2017.0507

Gillespie, R. G., Claridge, E. M., and Roderick, G. K. (2008). Biodiversity dynamics in isolated island communities: interaction between natural and human-mediated processes. *Mol. Ecol.* 17, 45–57. doi: 10.1111/j.1365-294X.2007.03466.x

Götmark, F., Götmark, E., and Jensen, A. M. (2016). Why be a shrub? A basic model and hypotheses for the adaptive values of a common growth form. *Front. Plant Sci.* 7, 1095. doi: 10.3389/fpls.2016.01095

Grace, J. B. (2006). *Structural equation modeling and natural systems*. (Boca Raton, FL, USA: Cambridge University Press).

Grime, J. P. (2006). *Plant strategies, vegetation processes, and ecosystem properties* (Hoboken, NJ, USA: John Wiley & Sons).

Han, Z. Q., Liu, T., Wang, T., Liu, H. F., Hao, X. R., Ouyang, Y. N., et al. (2020). Quantification of water resource utilization efficiency as the main driver of plant diversity in the water-limited ecosystems. *Ecol. Model.* 429, 108974. doi: 10.1016/j.ecolmodel.2020.108974

Harper, K. A., Macdonald, S. E., Burton, P. J., Chen, J., Brosofske, K. D., Saunders, S. C., et al. (2005). Edge influence on forest structure and composition in fragmented landscapes. *Conserv. Biol.* 19, 768–782. doi: 10.1111/j.1523-1739.2005.00045.x

Harter, D. E., Irl, S. D., Seo, B., Steinbauer, M. J., Gillespie, R., Triantis, K. A., et al. (2015). Impacts of global climate change on the floras of oceanic islands–Projections, implications and current knowledge. *Perspect. Plant Ecol. Evol. Syst.* 17, 160–183. doi: 10.1016/j.ppees.2015.01.003

Holmgren, M., Lin, C. Y., Murillo, J. E., Nieuwenhuis, A., Penninkhof, J., Sanders, N., et al. (2015). Positive shrub–tree interactions facilitate woody encroachment in boreal peatlands. *J. Ecol.* 103, 58–66. doi: 10.1111/jec.2015.103.issue-1

Husson, O. (2013). Redox potential (Eh) and pH as drivers of soil/plant/microorganism systems: a transdisciplinary overview pointing to integrative opportunities for agronomy. *Plant Soil* 362, 389–417. doi: 10.1007/s11104-012-1429-7

Irl, S. D., Obermeier, A., Beierkuhnlein, C., and Steinbauer, M. J. (2020). Climate controls plant life-form patterns on a high-elevation oceanic island. *J. Biogeogr.* 47, 2261–2273. doi: 10.1111/jbi.v47.10

Jesus, J. M., Danko, A. S., Fiúza, A., and Borges, M. T. (2015). Phytoremediation of salt-affected soils: a review of processes, applicability, and the impact of climate change. *Environ. Sci. pollut. Res.* 22, 6511–6525. doi: 10.1007/s11356-015-4205-4

Kemmitt, S. J., Wright, D., Goulding, K. W., and Jones, D. L. (2006). pH regulation of carbon and nitrogen dynamics in two agricultural soils. *Soil Biol. Biochem.* 38, 898–911. doi: 10.1016/j.soilbio.2005.08.006

Kubota, Y., Shiono, T., and Kusumoto, B. (2015). Role of climate and geohistorical factors in driving plant richness patterns and endemicity on the east Asian continental islands. *Ecography* 38, 639–648. doi: 10.1111/ecog.2015.v38.i6

Kuparinen, A., Katul, G., Nathan, R., and Schurr, F. M. (2009). Increases in air temperature can promote wind-driven dispersal and spread of plants. *Proc. R. Soc. B.: Biol. Sci.* 276, 3081–3087. doi: 10.1098/rspb.2009.0693

Lavorel, S., and Garnier, E. (2002). Predicting changes in community composition and ecosystem functioning from plant traits: revisiting the Holy Grail. *Funct. Ecol.* 16, 545–556. doi: 10.1046/j.1365-2435.2002.00664.x

Lee, M. K., Lee, H. S., Lee, H. I., Lee, S. W., Lee, Y. J., and Lee, C. B. (2022). Relative importance of landscape and climate factors to the species diversity of plant growth forms along an East Asian Archipelago. *Forests* 13, 218. doi: 10.3390/f13020218

Lefcheck, J. S. (2016). piecewiseSEM: Piecewise structural equation modelling in r for ecology, evolution, and systematics. *Methods Ecol. Evol.* 7, 573–579. doi: 10.1111/mee3.2016.7.issue-5

Leibold, M. A., and Chase, J. M. (2018). *Metacommunity ecology* Vol. 59 (Princeton University Press).

Li, X., Chen, Y., Liu, F., Cheng, X., Zhang, Q., and Zhang, K. (2024). Plant species composition and key-species abundance drive ecosystem multifunctionality. *J. Appl. Ecol.* 61 (9), 2100–2110. doi: 10.1111/1365-2664.14717

Li, S., Tu, T., Li, S., Yang, X., Zheng, Y., Guo, L. D., et al. (2024). Different mechanisms underlie similar species-area relationships in two tropical archipelagoes. *Plant Diversity* 46, 238–246. doi: 10.1016/j.pld.2023.08.006

Li, Y., Zhang, X. N., and Lv, G. H. (2019). Phylogeography of Ixiolirion songaricum, a spring ephemeral species endemic to Northwest China. *Plant Syst. Evol.* 305, 205–221. doi: 10.1007/s00606-018-1563-7

Losos, J. B., and Ricklefs, R. E. (2009). Adaptation and diversification on islands. *Nature* 457, 830–836. doi: 10.1038/nature07893

Losos, J. B., and Schluter, D. (2000). Analysis of an evolutionary species–area relationship. *Nature* 408, 847–850. doi: 10.1038/35048558

MacArthur, R. H., and Wilson, E. O. (1967). *The theory of island biogeography* Vol. 1 (Princeton, NJ, USA: Princeton university press).

Manes, S., Costello, M. J., Beckett, H., Debnath, A., Devenish-Nelson, E., Grey, K. A., et al. (2021). Endemism increases species' climate change risk in areas of global biodiversity importance. *Biol. Conserv.* 257, 109070. doi: 10.1016/j.biocon.2021.109070

Mann, A., Lata, C., Kumar, N., Kumar, A., Kumar, A., and Sheoran, P. (2023). Halophytes as new model plant species for salt tolerance strategies. *Front. Plant Sci.* 14, 1137211. doi: 10.3389/fpls.2023.1137211

Midolo, G., Alkemade, R., Schipper, A. M., Benítez-López, A., Perring, M. P., and De Vries, W. (2019). Impacts of nitrogen addition on plant species richness and abundance: A global meta-analysis. *Global Ecol. Biogeogr.* 28, 398–413. doi: 10.1111/geb.12856

Morales, A. I. G. C., Mendoza, J. M. O., Gozalbo, M. E., and Martínez, J. J. C. (2012). Arboreal and prostrate conifers coexisting in Mediterranean high mountains differ in their climatic responses. *Dendrochronologia* 30, 279–286. doi: 10.1016/j.dendro.2012.02.004

Murphy, H. T., and Metcalfe, D. J. (2016). The perfect storm: Weed invasion and intense storms in tropical forests. *Austral Ecol.* 41, 864–874. doi: 10.1111/aec.2016.41.issue-8

Nogales, M., McConkey, K. R., Carlo, T. A., Wotton, D. M., Bellingham, P. J., Traveset, A., et al. (2024). A review on the state of the art in frugivory and seed dispersal on islands and the implications of global change. *Bot. Rev.* 90 (2), 160–185. doi: 10.1007/s12229-023-09296-8

Ottaviani, G., Keppel, G., Götzenberger, L., Harrison, S., Opedal, Ø. H., Conti, L., et al. (2020). Linking plant functional ecology to island biogeography. *Trends Plant Sci.* 25, 329–339. doi: 10.1016/j.tplants.2019.12.022

Penn, C. J., and Camberato, J. J. (2019). A critical review on soil chemical processes that control how soil pH affects phosphorus availability to plants. *Agriculture* 9, 120. doi: 10.3390/agriculture9060120

Portillo, J. T. D. M., Ouchi-Melo, L. S., Crivellari, L. B., de Oliveira, T. A. L., Sawaya, R. J., and Duarte, L. D. S. (2019). Area and distance from mainland affect in different ways richness and phylogenetic diversity of snakes in Atlantic Forest coastal islands. *Ecol. Evol.* 9, 3909–3917. doi: 10.1002/ece3.2019.9.issue-7

Pugnaire, F. I., Morillo, J. A., Peñuelas, J., Reich, P. B., Bardgett, R. D., Gaxiola, A., et al. (2019). Climate change effects on plant-soil feedbacks and consequences for biodiversity and functioning of terrestrial ecosystems. *Sci. Adv.* 5, eaaz1834. doi: 10.1126/sciadv.aaz1834

Ramirez, A. R., De Guzman, M. E., Dawson, T. E., and Ackerly, D. D. (2020). Plant hydraulic traits reveal islands as refugia from worsening drought. *Conserv. Physiol.* 8, coz115. doi: 10.1093/conphys/coz115

Schrader, J., König, C., Triantis, K. A., Trigas, P., Kreft, H., and Weigelt, P. (2020). Species–area relationships on small islands differ among plant growth forms. *Global Ecol. Biogeogr.* 29, 814–829. doi: 10.1111/geb.13056

Shipley, B. (2009). Confirmatory path analysis in a generalized multilevel context. *Ecology* 90, 363–368. doi: 10.1890/08-1034.1

Shipley, B. (2013). The AIC model selection method applied to path analytic models compared using ad-separation test. *Ecology* 94, 560–564. doi: 10.1890/12-0976.1

Shirima, D. D., Totland, Ø., and Moe, S. R. (2016). The relative importance of vertical soil nutrient heterogeneity, and mean and depth-specific soil nutrient availabilities for tree species richness in tropical forests and woodlands. *Oecologia* 182, 877–888. doi: 10.1007/s00442-016-3696-0

Spaak, J. W., Baert, J. M., Baird, D. J., Eisenhauer, N., Maltby, L., Pomati, F., et al. (2017). Shifts of community composition and population density substantially affect ecosystem function despite invariant richness. *Ecol. Lett.* 20, 1315–1324. doi: 10.1111/ele.2017.20.issue-10

Tao, Y., Qiu, D., Gong, Y. M., Liu, H. L., Zhang, J., Yin, B. F., et al. (2022). Leaf-root-soil N: P stoichiometry of ephemeral plants in a temperate desert in Central Asia. *J. Plant Res.* 135, 55–67. doi: 10.1007/s10265-021-01355-8

Uriarte, M., Thompson, J., and Zimmerman, J. K. (2019). Hurricane María tripled stem breaks and doubled tree mortality relative to other major storms. *Nat. Commun.* 10, 1362. doi: 10.1038/s41467-019-09319-2

Volaire, F. (2018). A unified framework of plant adaptive strategies to drought: crossing scales and disciplines. *Global Change Biol.* 24, 2929–2938. doi: 10.1111/gcb.2018.24.issue-7

Warren, B. H., Simberloff, D., Ricklefs, R. E., Aguilée, R., Condamine, F. L., Gravel, D., et al. (2015). Islands as model systems in ecology and evolution: Prospects fifty years after MacArthur-Wilson. *Ecol. Lett.* 18, 200–217. doi: 10.1111/ele.2015.18.issue-2

Weigelt, P., and Kreft, H. (2013). Quantifying island isolation–insights from global patterns of insular plant species richness. *Ecography* 36, 417–429. doi: 10.1111/j.1600-0587.2012.07669.x

Whittaker, R. J., and Fernández-Palacios, J. M. (2007). *Island biogeography: ecology, evolution, and conservation* (Oxford, UK: Oxford University Press).

Whittaker, R. J., Fernández-Palacios, J. M., Matthews, T. J., Borregaard, M. K., and Triantis, K. A. (2017). Island biogeography: taking the long view of nature's laboratories. *Science* 357, eaam8326. doi: 10.1126/science.aam8326

Wilson, B. F. (1995). "Shrub stems: form and function," in *Plant stems* (Cambridge, MA, USA: Academic Press), 91–102.

Winfree, R., Fox, J. W., Williams, N. M., Reilly, J. R., and Cariveau, D. P. (2015). Abundance of common species, not species richness, drives delivery of a real-world ecosystem service. *Ecol. Lett.* 18, 626–635. doi: 10.1111/ele.2015.18.issue-7

Wu, L., Ren, Y., Wan, J. Z., Wang, M., Wang, Z., Fu, F., et al. (2022). Effects of precipitation change and nitrogen and phosphorus additions on traits and abundance of potentilla anserina in an alpine meadow. *Atmosphere* 13, 1820. doi: 10.3390/atmos13111820

Xie, Y., Huang, H., Xie, X., Ou, J., Chen, Z., Lu, X., et al. (2024). Landscape, human disturbance, and climate factors drive the species richness of alien invasive plants on subtropical islands. *Plants* 13, 2437. doi: 10.3390/plants13172437

Yan, Y., Jarvie, S., Zhang, Q., Han, P., Liu, Q., Zhang, S., et al. (2023). Habitat heterogeneity determines species richness on small habitat islands in a fragmented landscape. *J. Biogeogr.* 50, 976–986. doi: 10.1111/jbi.14594

Yang, J., Cooper, D. J., Li, Z., Song, W., Zhang, Y., Zhao, B., et al. (2020). Differences in tree and shrub growth responses to climate change in a boreal forest in China. *Dendrochronologia* 63, 125744. doi: 10.1016/j.dendro.2020.125744

Yuan, G., Levi, E. E., Davidson, T. A., Lauridsen, T. L., Søndergaard, M., Yang, Z., et al. (2024). Warming alters the network of physiological traits and their contribution to plant abundance. *Sci. Total. Environ.* 939, 173573. doi: 10.1016/j.scitotenv.2024.173573

Zhou, S., Qin, H., Liao, R., and Cheng, Y. (2024). Habitat quality drives the species–area relationship of plants and soil microbes in an ocean archipelago. *Oikos* 2024 (11), e10660. doi: 10.1111/oik.v2024.i11

Ziegler, C., Cochard, H., Stahl, C., Foltzer, L., Gérard, B., Goret, J. Y., et al. (2024). Residual water losses mediate the trade-off between growth and drought survival across saplings of 12 tropical rainforest tree species with contrasting hydraulic strategies. *J. Exp. Bot.* 75 (13), 4128–4147. doi: 10.1093/jxb/erae159

Zizka, A., Govender, N., and Higgins, S. I. (2014). How to tell a shrub from a tree: A life-history perspective from a South African savanna. *Austral Ecol.* 39, 767–778. doi: 10.1111/aec.2014.39.issue-7

frontiers | Frontiers in Plant Science

TYPE Original Research
PUBLISHED 15 September 2025
DOI 10.3389/fpls.2025.1587343



OPEN ACCESS

EDITED BY
Robert John,
Indian Institute of Science Education and Research Kolkata, India

REVIEWED BY
Congcong Shen,
Chinese Academy of Sciences (CAS), Beijing, China
JiaLuo Yu,
Chinese Academy of Sciences (CAS), China

*CORRESPONDENCE
Junpeng Rui
ruijp@lzu.edu.cn

†These authors have contributed equally to this work and share first authorship

RECEIVED 04 March 2025
ACCEPTED 27 August 2025
PUBLISHED 15 September 2025

CITATION
Rui J, Long X, Wang X, Xiong X and Zhu J (2025) Soil microclimate and vegetation dynamics shape elevational and seasonal variations of diazotrophic communities in alpine grasslands.
*Front. Plant Sci.* 16:1587343.
doi: 10.3389/fpls.2025.1587343



# Soil microclimate and vegetation dynamics shape elevational and seasonal variations of diazotrophic communities in alpine grasslands

Junpeng Rui[1,2,3*†], Xiaojian Long[4†], Xuemiao Wang[3,5], Xinyu Xiong[5] and Jianxiao Zhu[5]

[1]State Key Laboratory of Herbage Improvement and Grassland Agro-ecosystems, College of Ecology, Lanzhou University, Lanzhou, China, [2]Key Laboratory of Biodiversity and Environment on the Qinghai-Tibetan Plateau, Ministry of Education, School of Ecology and Environment, Tibet University, Lhasa, China, [3]Center for Grassland Microbiome, Lanzhou University, Lanzhou, China, [4]Gannan Tibetan Autonomous Prefecture Academy of Agriculture, Forestry and Animal Husbandry Grassland Science, Gannan, China, [5]College of Pastoral Agriculture Science and Technology, Lanzhou University, Lanzhou, China

**Introduction:** Diazotrophs play critical roles in maintaining ecosystem nitrogen (N) cycling in alpine grasslands. However, the elevational and seasonal variations of diazotrophic communities in these ecosystems remain poorly understood. This gap in knowledge limits our ability to predict how N fixation will respond to environmental change. Here, we investigated the seasonal dynamics of soil diazotrophic communities across a 3200-4000 m elevational gradient in Qinghai-Tibetan alpine grasslands during the growing season.

**Methods:** Soil samples were collected across an elevational gradient (3200-4000 m) throughout the growing season. The diazotrophic community composition was assessed by sequencing the nifH gene, which was also quantified using quantitative PCR. Soil nitrogenase activity was measured to assess N fixation potential. Key environmental variables, such as soil temperature, moisture, and plant biomass (particularly legume biomass), were monitored.

**Results and Discussion:** Our results revealed that diazotrophic alpha-diversity followed an inverted V-shaped pattern along the elevational gradient, primarily driven by soil temperature and moisture. Beta-diversity analyses demonstrated that diazotrophic communities generally exhibited similar elevational distribution patterns throughout the growing season, also primarily influenced by temperature and moisture. Seasonal variations in diazotrophic communities were more pronounced at lower elevations, primarily associated with plant biomass dynamics, including delayed legume emergence at 3200 m in June and their subsequent biomass accumulation after July. In contrast, soil microclimate (particularly temperature) dominated community shifts at higher elevations. Notably, *nifH* gene abundance and soil nitrogenase activity were higher in the early growing season, suggesting free-living diazotrophs may play a crucial role in N fixation. Abundant species were key contributors to diazotrophic

beta-diversity. Symbiotic *Mesorhizobium* was more abundant at low elevations, while free-living *Geobacter* at high elevations. Conversely, associative diazotrophs peaked later in the growing season, in contrast to *Geobacter*. Rare species played a key role in shaping alpha diversity, particularly at mid-elevations, where soil moisture was the highest. Our study underscores the complex interactions between soil microclimate change and plant dynamics in regulating diazotrophic communities. Furthermore, it highlights the essential roles of both abundant and rare species in sustaining ecosystem functions in alpine grasslands. These findings provide new insights into the biogeochemical processes supporting N cycling in alpine grasslands and highlight the potential impacts of vegetation and climate change on these fragile ecosystems.

KEYWORDS

**diazotroph, alpine grassland, altitudinal gradient, seasonal dynamics, nitrogen fixation, *nifH* gene, climate change, plant biomass**

## 1 Introduction

Biological nitrogen fixation (BNF) is a crucial process in terrestrial ecosystems that transforms atmospheric $N_2$ into plant-available nitrogen (N) (Herridge et al., 2008; Vitousek et al., 2013). N-fixing microorganisms comprise three types: symbiotic, associative, and free-living diazotrophs. Symbiotic and associative diazotrophs exhibit superior N fixation efficiency and have been the subject of more comprehensive research. Free-living diazotrophs, though less efficient, are extensively spread across ecosystems and are essential for N intake in N-limited environments (Houlton et al., 2008). Understanding the distribution and function of these N-fixing types across different ecosystems is critical for revealing the mechanisms of N cycling, especially in extreme environments such as alpine grasslands (Yang et al., 2014).

The diversity and N fixation activity of soil diazotrophic communities are regulated by multiple environmental factors, which can be categorized into climatic, edaphic, and biotic drivers. Among these, temperature and water conditions (e.g., precipitation, soil moisture) are recognized as the two most critical determinants, particularly in shaping large-scale distribution patterns (Zhao et al., 2020). In cold environments, low temperatures constrain nitrogenase activity, while warming can enhance enzymatic efficiency and subsequently reshape diazotrophic community structure (Rousk et al., 2017). Soil moisture influences diazotrophs both directly (by modulating microbial growth and metabolism) and indirectly (by altering soil oxygen diffusion, given the well-documented oxygen sensitivity of nitrogenase) (Smercina et al., 2021). Elevated soil available N (e.g., ammonium, and nitrate) suppresses N fixation, with free-living diazotrophs being particularly sensitive due to their preferential uptake of environmental N sources (Dynarski and Houlton, 2018). In contrast, symbiotic N fixation relies on legume-rhizobia interactions within root nodules (Holzmann and Haselwandter, 1988), while associative fixation depends on plant hosts (e.g., grasses) (Wickstrom and Garono, 2007). Consequently, shifts in plant community composition (including species identity and biomass) may significantly alter the structure and function of soil diazotrophic communities. Despite this mechanistic understanding of individual drivers, how these factors collectively regulate diazotroph communities remains a critical gap in alpine ecosystem ecology.

Alpine grasslands, situated in high-elevation regions, provide essential ecological services, including water regulation, and biodiversity preservation (Körner, 2004). These ecosystems are exceptionally sensitive to climate change, characterized by low temperatures, rendering biodiversity and ecological processes more vulnerable (Shangguan et al., 2024). The elevational gradient serves as an important platform for studying climate change impacts, differing elevations lead to substantial alterations in environmental variables including temperature and water conditions (e.g., precipitation and soil moisture) (Lomolino, 2001; Sundqvist et al., 2013). These changes not only affect plant growth but also have profound effects on microbial community structure and function. For instance, low-elevation areas are typically warmer, hence facilitating the proliferation of leguminous plants and potentially enhancing symbiotic N fixation (Tang et al., 2024).

Seasonal changes are crucial determinants of microbial community dynamics in alpine grasslands. High-elevation ecosystems typically exhibit a short growing season and experience large temperature fluctuations, resulting in a dramatic effect of seasonal shifts on microbial communities (Zhao and Hu, 2023). Changes in factors such as plant growth, temperature, and precipitation throughout a growing season may influence the structure and function of diazotrophic communities. For example, in early growing season, characterized by low temperatures and sluggish growth of leguminous plants, symbiotic N fixation may exhibit reduced efficiency (Chellem et al., 2024). Plants have diverse

N requirements at different stages of their growth cycle (Wang et al., 2024). Furthermore, the N-fixing capacity of legume root nodules also fluctuates (Daubech et al., 2017). Consequently, the seasonal fluctuations of various diazotroph types necessitate additional examination.

Microbial communities exhibit a characteristic structure where abundant species dominate in terms of biomass and functional contributions, while rare species, despite their low abundance, can play critical roles in maintaining community resilience and adaptability (Litchman et al., 2024). Despite these general trends, the specific roles of abundant and rare species in shaping microbial community diversity remain an area of active debate in the field (Ma et al., 2024; Ye et al., 2024). Abundant species in diazotrophic community, such as rhizobia and associative diazotrophs, have received more attention. However, despite the remarkably high diversity of soil diazotrophs, the ecological roles of rare species (e.g., numerous soil free-living diazotrophs) remain poorly understood. How they contribute specifically to diazotrophic communities in alpine ecosystems, in terms of both alpha and beta diversity, is still poorly understood and warrants further investigation.

Understanding the elevational-seasonal dynamics of diazotrophic communities is critical for predicting alpine ecosystem responses to climate change, as it may determine the stability of nitrogen inputs in these vulnerable systems. However, two key knowledge gaps remain: (1) whether the elevational patterns of diazotrophs persist throughout the growing season, given that most existing data come from single-timepoint surveys (Rui et al., 2022); and (2) how the relative importance of soil microclimatic (e.g., soil temperature and moisture) versus biotic (e.g., plant biomass) controls shifts across elevations.

Here, we address these gaps by systematically investigating soil diazotrophic communities along a 3200-4000 m elevational gradient during the growing season (June-September) in Qinghai-Tibetan alpine grasslands. We aim to answer three scientific questions: (1) Do diazotrophic communities exhibit consistent elevational distribution patterns throughout the growing season, and what are the key factors? (2) Are seasonal dynamics of diazotrophic communities elevation-dependent, and how do the controlling factors (e.g., soil microclimate vs. vegetation dynamics) vary with elevation? (3) What are the distinct roles of abundant versus rare species in maintaining diazotrophic community diversity across spatial and temporal scales? Our findings will provide mechanistic insights into how climate-vegetation interactions regulate N fixation potential in alpine ecosystems under rapid climate change.

# 2 Materials and methods

## 2.1 Study site description and soil sampling

The study site is located at the Haibei National Field Research Station of Alpine Grassland Ecosystem (101°12'E, 37°37'N, approximately 3200 m *a.s.l.*) on the northeastern Qinghai-Tibetan Plateau in Qinghai, China. The region experiences an annual average air temperature of -1.1°C and an average annual precipitation of 485 mm. More than 80% of the annual rainfall occurs in the growing season (Yang et al., 2014), which lasts from May to September. Due to persistent snow cover in high-elevation areas in early May, we collected soil samples at the beginning of June, July, August, and September 2021. The monthly precipitation at 3200 m during these months were 90, 64, 125, and 104 mm, respectively (Rui et al., 2023). Unfortunately, the precipitation data for the higher elevation sites were not collected.

The experimental plots were established at five elevations (3200, 3400, 3600, 3800, and 4000 m *a.s.l*). At each elevation, six 1 m × 1 m quadrats were designated as replicates with an interval of 10 m. The soils, classified as Mat-Gryic Cambisol, are primarily vegetated with perennial flora. Geographic coordinates and vegetation features for these elevations are available in our previous study (Rui et al., 2022). Five soil cores (0-10 cm depth) were randomly obtained from each quadrat, amalgamated into a single sample, and sieved through a 2-mm mesh. Concurrently, aboveground plant biomass and species richness were documented, with particular attention to leguminous species which were separately collected and weighed to quantify their biomass contribution. Soil temperature was measured with EM-50 devices (Decagon devices, USA) at a depth of 5 cm, and the average monthly temperature was computed. Methods for measuring soil moisture, pH, ammonium, and nitrate contents were reported previously (Rui et al., 2022). Soil C:N ratio denotes the ratio of total carbon to total N. Soil nitrogenase activity was determined using the acetylene reduction assay (Hardy et al., 1973).

## 2.2 DNA extraction, qPCR and sequencing

Genomic DNA was extracted from 1 g fresh soils using the PowerSoil DNA Isolation kit (MO BIO Laboratories, USA) in accordance with the manufacturer's guidelines. The universal *nifH* primers PolF (5'-TGC GAY CCS AAR GCB GAC TC-3') and PolR (5'-ATSGCCATCATYTCRCCGGA-3') were employed for amplicon sequencing and quantitative PCR (qPCR), adhering to the procedure established by Che et al (Che et al., 2018). Sequencing libraries were constructed using TruSeq® DNA Kit (Illumina, USA), and sequencing was conducted on the Illumina NovaSeq platform (Novogene, Beijing, China) with the Reagent Kit v2 (2 × 250 bp).

## 2.3 Sequencing data analysis

Paired-end reads were merged using FLASh v1.2.11 (Magoč and Salzberg, 2011). Primers were eliminated from the merged reads using the Perl script *trim_primer_in fq.pl*. Low quality reads and chimeras were eliminated utilizing Trimomatic v0.39 (Bolger et al., 2014) and Uchime, respectively. Frameshifts were corrected using FrameBot (Wang et al., 2013), and sequences that cannot be corrected through frameshift correction were removed. Amplicon Sequence Variants (ASVs) were deduced from the nucleotide sequences employing the Unoise algorithm (Edgar, 2016).

Representative ASV sequences were aligned against the local BLAST database mentioned before (Rui et al., 2022), and their taxonomic affiliations were ascertained using lowest common ancestor (LCA) algorithm in MEGAN 6 (Huson et al., 2016). Based on existing literature, diazotrophic genera were classified into three groups: symbiotic, associative, and free-living diazotrophs (Supplementary Table S1). For the ASV table, sequences from each sample were randomly subsampled to the same sequence depth (16227 reads per sample in this study) using the Perl script *subsample_in_table.pl*. ASVs were categorized as abundant (>0.1% average relative abundance across all samples), common (0.01–0.1%), or rare (<0.01%). Alpha-diversity indices, including observed species and Shannon diversity, were calculated with the script *alpha_diversity.pl*. All of the Perl scripts mentioned above have been described previously (Rui et al., 2023).

## 2.4 Statistical analyses

Generally, statistical analyses based on the ASV table and environmental factors were predominantly conducted using R (version 4.3.3) as outlined by Rui et al (Rui et al., 2022). To evaluate differences in diazotrophic communities across elevations or months, ANOVA with Tukey's *post hoc* test was applied using the *aov* function from *vegan* package and *HSD.test* from *agricolae*. Non-metric multidimensional scaling (NMDS) based on Bray-Curtis dissimilarity was performed using *metaMDS* from *vegan*, with environmental variables incorporated into the NMDS plots by the *envfit* function.

Community differences across elevational and seasonal gradients were evaluated using the PerMANOVA (i.e., Adonis) test through the *adonis2* function. Based on Bray-Curtis dissimilarity matrices, two-way Adonis design was implemented to assess the individual and interactive effects of elevation and season on diazotrophic community composition. One-way Adonis was used to assess the pairwise differences between specific elevations and monthly time points. The analysis employed 999 permutations to ensure robust significance testing.

Partial Mantel test was conducted using the *ecodist* package to assess the influence of environmental factors on community variances. When evaluating each factor's influence, the remaining factors were treated as covariates to isolate the independent effect.

We analyzed the effects of environmental factors on N-fixation related variables (alpha diversity, nitrogenase activity, *nifH* gene abundance, and relative abundances of specific diazotrophs) using linear mixed-effects models implemented in the *lme4* package, with plot as random effect. Temperature, soil moisture, plant biomass and soil properties were included as fixed effects. To obtain standardized effect sizes (β coefficients), all continuous predictors were z-score normalized (mean-centered and scaled by 1 standard deviation) prior to model fitting. Separate models were run to examine either elevational gradients (controlling for seasonal variation) or seasonal dynamics (controlling for elevation), respectively. The relative importance of each predictor was quantified using variance partitioning analysis through the *glmm.hp* package (Lai et al., 2022). This approach allowed us to assess both the direction and magnitude of environmental effects while accounting for spatial autocorrelation among plots.

# 3 Results

## 3.1 Plant dynamics and *nifH* gene abundance/nitrogenase activity

Aboveground biomass showed clear seasonal patterns across elevations (Supplementary Figure S1H), with consistently lower values in June (initial growth phase) than in July–September. Legumes (primarily *Oxytropis*, *Tibetia himalaica* and *Medicago*), representing <2.3% of total biomass, were scarce at higher elevations but increased substantially at 3200 m from July onward, after minimal presence in June (Supplementary Figure S1I).

The abundance of *nifH* genes (i.e., number of *nifH* gene copies) for each month exhibited an inverted V-shaped pattern along the elevational gradient, peaking at 3600 m (Supplementary Figure S1J), with significantly higher values in June compared to later months (July-September), particularly at 3600 m and 3200 m. There was no significant difference in *nifH* gene abundance between July and September. Across all samples, the abundance of *nifH* genes showed a significant positive correlation with soil moisture (Spearman's $\rho$ = 0.585, $P$<0.001), and a significant negative correlation with legume biomass (Spearman's $\rho$ = -0.677, $P$<0.001).

The soil nitrogenase activity from July to September also displayed an inverted V-shaped pattern along the elevation gradient, reaching its peak at 3600 m (Supplementary Figure S1K). However, in June, it was highest at both 3200 m and 3600 m, followed by 3400 m. At each elevation, the nitrogenase activity in June was consistently higher than that from July to September. It was the lowest in the high-elevation soils in September. The abundance of *nifH* gene showed the strongest correlation with soil nitrogenase activity (Spearman's $\rho$ = 0.52, $P$<0.001). The linear mixed-effects model results showed that soil moisture had significant positive effects on both nitrogenase activity and *nifH* gene abundance, explaining most of their elevational variations (Figure 1). Temperature also showed positive effects on the elevational patterns of nitrogenase activity. In contrast, Both temperature and plant biomass exhibited significant negative effects on the seasonal variations of nitrogenase activity.

## 3.2 The soil diazotrophic community composition in alpine grasslands

In this study, a total of 5131 *nifH* gene ASVs from 11 phyla were identified, dominated by Pseudomonadota and Thermodesulfobacteriota (Supplementary Figure S2). ASV numbers belonging to abundant, common, and rare ASVs were 192, 1078 and 4562, respectively. Abundant, common, and rare ASVs accounted for 58.3%, 33.5% and 8.3% of total abundance,

10.3389/fpls.2025.1587343

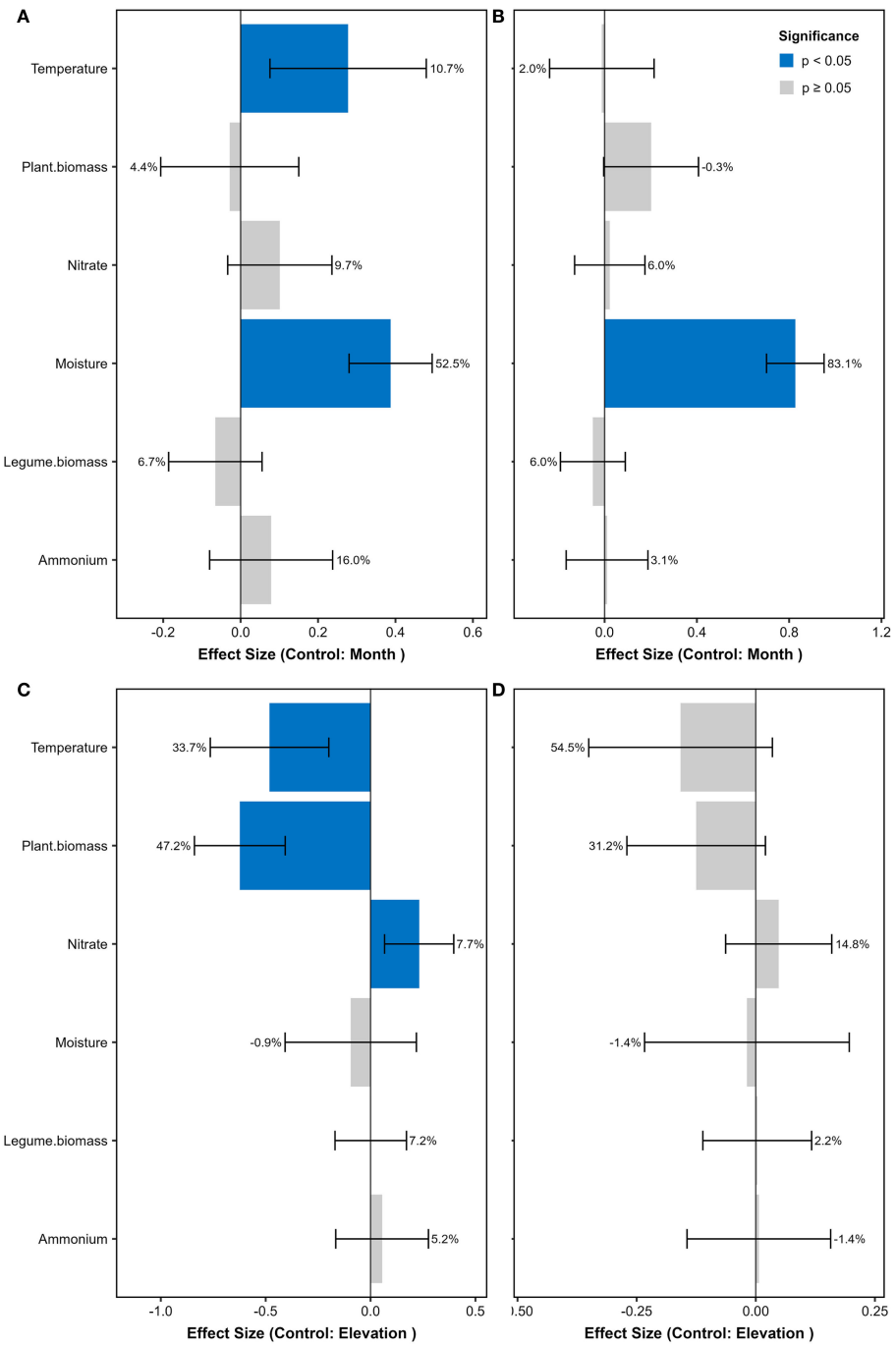


FIGURE 1
Standardized effects on nitrogenase activity and *nifH* gene abundance from linear mixed-effects models. **(A)** Nitrogenase activity patterns along elevational gradients (controlling for seasonal variation by month). **(B)** *nifH* gene abundance patterns along elevational gradients (controlling for season). **(C)** Nitrogenase activity seasonal dynamics (controlling for elevation). **(D)** *nifH* gene abundance seasonal dynamics (controlling for elevation). Predictors were z-score standardized prior to analysis. Blue bars indicate significant effects ($P < 0.05$; error bars show 95% CI), with adjacent percentages representing the proportion of variance explained by each predictor (from *glmm.hp* partitioning). Gray bars denote non-significant effects ($P \geq 0.05$). Positive β values denote enhancing effects, negative values indicate inhibitory effects. Models were fitted using *lme4* with plot as random intercept.

respectively. The abundant ASVs were exclusively classified into Pseudomonadota, Thermodesulfobacteriota, Myxococcota and Actinomycetota.

Pseudomonadota was the most abundant phylum, with an average relative abundance of 75%, comprising 3104 ASVs, primarily distributed in Alphaproteobacteria and Betaproteobacteria. The average relative abundance of Thermodesulfobacteriota was 21%, comprising 1286 ASVs, predominantly anaerobic free-living genus *Geobacter*. Each of the remaining phyla comprised fewer than 200 ASVs. In Myxococcota,

all ASVs were exclusively assigned to the anaerobic free-living genus *Anaeromyxobacter*. Within Verrucomicrobiota, the majority of ASVs were classified under the family Opitutaceae. For Actinomycetota, most ASVs (81%) were affiliated with the genus *Frankia*, while Cyanobacteriota ASVs were predominantly members of the order Nostocales.

Symbiotic diazotrophs were dominated by *Mesorhizobium*, followed by *Bradyrhizobium*, with lower relative abundances of *Frankia*, *Rhizobium*, and *Paraburkholderia* (Supplementary Figure S3). Associative diazotrophs were mainly represented by *Azospirillum*, followed by *Azoarcus*. Free-living diazotrophs were dominated by *Geobacter*, with other genera with average relative abundances greater than 1% including *Hydrogenophaga*, *Anaeromyxobacter*, *Dechloromonas*, and *Azonexus* (Supplementary Table S1).

## 3.3 Changes in the relative abundance of diazotrophic taxa

The relative abundance of dominant diazotrophs showed consistent elevational trends throughout the growing season. Pseudomonadota, (e.g., *Azospirillum*) followed a V-shaped pattern, reaching its lowest at 3600 m. In contrast, symbiotic diazotrophs (e.g., *Mesorhizobium* and *Bradyrhizobium*) exhibited the highest relative abundance at 3200 m, with no significant variation between 3400 and 4000 m. Conversely, Thermodesulfobacteriota showed an inverted V-shaped pattern, peaking at 3600 m, with *Geobacter* as a representative genus.

Many diazotrophs showed significant seasonal dynamics in relative abundance during the growing season. Diazotrophs affiliated to Pseudomonadota, Verrucomicrobiota, and Actinomycetota were significantly lowest in June, whereas Thermodesulfobacteriota showed the opposite trend (Supplementary Figure S2). Myxococcota (mainly *Anaeromyxobacter*) was the highest in August, especially at 3600 m. At 3200-3400 m, Actinomycetota (mainly Frankia) was the highest in July.

Along the altitudinal gradient, symbiotic diazotrophs exhibited the highest relative abundance in soils at 3200 m (Supplementary Figure S3). Associative diazotrophs showed a V-shaped pattern along elevation, whereas free-living diazotrophs displayed an inverted V-shaped pattern. Compared to other months, soils in June contained higher free-living and symbiotic diazotrophs, but lower associative diazotrophs. *Azoarcus*, the second highest associative diazotroph, was very low in June (Supplementary Figure S3E).

The linear mixed-effects models revealed that across both elevational gradients and seasonal dynamics, soil moisture showed significantly positive effects on free-living diazotrophs but negative effects on symbiotic diazotrophs (Figure 2). Conversely, soil temperature exhibited significantly negative effects on free-living diazotrophs and marginally positive effects on associative diazotrophs ($P < 0.1$). These results demonstrate that temperature and moisture collectively drive functional shifts in diazotrophic community structure.

## 3.4 Alpha diversity of diazotrophic community

Across the elevational gradient, both richness (i.e., observed species) and Shannon diversity of soil diazotrophs during the growing season followed an inverted V-shaped pattern, peaking between 3600 and 3800 m (Figure 3). Additionally, alpha diversity showed significant seasonal variations, higher in July and August than that in June and September, especially at 3200 and 4000 m.

Elevational and seasonal variations in alpha diversity (particularly richness) were predominantly driven by Pseudomonadota and Thermodesulfobacteriota (Figure 3C). Compared to abundant ASVs, common and rare ASVs contributed more to the elevational and seasonal variations in richness. For example, at low elevations (3200-3400 m) in June and September, the number of common and rare ASVs from these two phyla (especially for Thermodesulfobacteriota) was significantly lower than that at 3600-3800 m. At 3200 m in September, richness was lowest, with the lowest ASV numbers for Thermodesulfobacteriota. At 3600 m, rare ASVs of Thermodesulfobacteriota were mostly from *Geobacter*, while rare ASVs of Pseudomonadota were largely unclassified Alphaproteobacteria.

Temperature and soil moisture were the primary factors influencing the elevational pattern of diazotrophic richness, and temperature was also the primary factor affecting seasonal dynamics at most elevations (Supplementary Figure S4). In detail, temperature played a dominant role in June and July, whereas soil moisture was most important in August and September. At the same elevation, the main factors driving the seasonal dynamics of diazotrophic richness varied: temperature was the primary factor at 3200 m, 3600 m, and 4000 m, while aboveground biomass at 3400 m. No significant influencing factor was identified at 3800 m.

The linear mixed-effects models revealed distinct environmental controls on diazotrophic diversity. Soil moisture dominated elevational patterns (explaining 64.4% of richness variation), showing strong positive effects, while soil ammonium concentration exerted negative influences (17.5%) (Figure 2). Seasonally, temperature drove diversity dynamics (14.1% explained variation). These results demonstrate consistent positive effects of moisture (more spatially) and temperature (more temporally) on richness, contrasted by ammonium's suppressive role.

## 3.5 Beta diversity of diazotrophic community

The beta diversity of the diazotrophic community varied significantly with elevation and season (Figure 4). Specifically, elevation, season (i.e., months), and their interaction explained 26.5%, 13.8%, and 14.5% of the community variation, respectively. In each month, there were significant community differences among different elevations (Figures 5, 4C). Compared to 3200 m, community similarity did not decrease linearly with elevation; in other words, it did not fully conform to the distance-decay relationship. For instance, communities at 3200 m were more

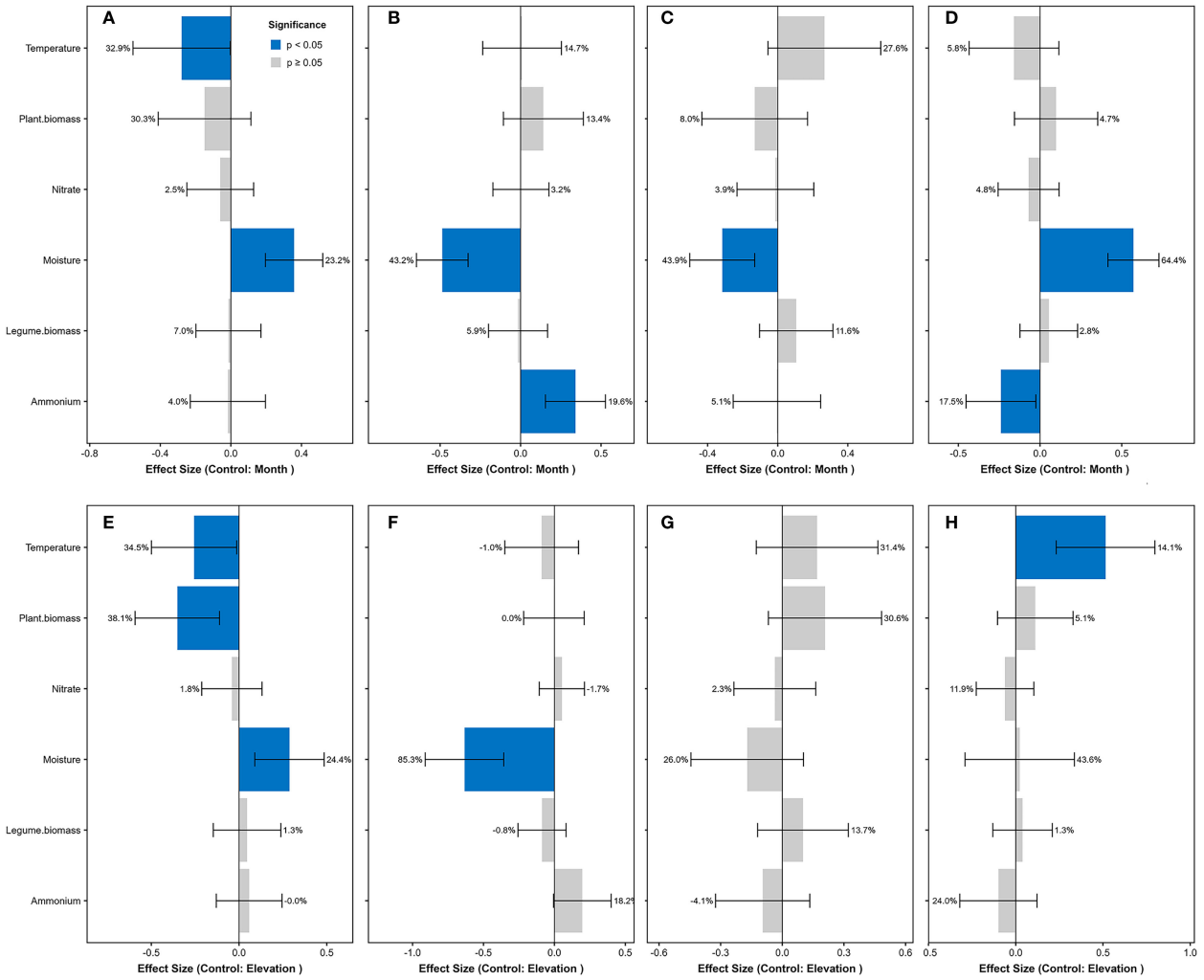


FIGURE 2
Standardized effects on diazotrophic functional groups and richness. Models controlling for seasonal variation (by month): **(A)** free-living, **(B)** symbiotic, **(C)** associative diazotrophs, and **(D)** diazotrophic richness. Models controlling for elevation: **(E)** free-living, **(F)** symbiotic, **(G)** associative diazotrophs, and **(H)** diazotrophic richness. Predictors were z-score standardized prior to analysis. Blue bars indicate significant effects ($P < 0.05$; error bars show 95% CI), with adjacent percentages representing the proportion of variance explained by each predictor (from *glmm.hp* partitioning). Gray bars denote non-significant effects ($P \geq 0.05$). Positive β values denote enhancing effects, negative values indicate inhibitory effects. Models were fitted using *lme4* with plot as random intercept.

similar to those at 4000 m than to those at 3600 m (Figure 4C). At each elevation, there were also significant community differences among different months (Figures 6, 4D). Seasonal dynamics of diazotrophic communities were more pronounced at low elevations (3200-3400 m), especially between June and other months (Figure 4A).

The distribution of abundant ASVs in NMDS plots showed that the dominant genera, such as *Mesorhizobium* and *Geobacter*, were the primary contributors to elevational and seasonal variation in beta diversity (Figure 4). Along the elevational gradient, ASVs belonging to *Mesorhizobium* were more abundant at 3200 m, while those belonging to *Geobacter* were more abundant at high elevations (Figures 5, 4A). Seasonally, ASVs belonging to these genera were more prevalent in June, contributing to the distinct community differences between June and other months (Figures 6, 4B). Additionally, ASVs of *Azospirillum* were clustered near the NMDS origin, indicating their relatively minor contribution to community differences. The V-shaped elevation changes of *Azospirillum* were most pronounced in June and July, while in August and September, the relative abundance of this genus increases at intermediate elevations, narrowing the differences between elevations. This results in the ASVs of this genus being closer to the origin position on the NMDS plot in August and September (Figure 5).

Three subcommunities, composed of abundant, common, and rare ASVs respectively, exhibited similar NMDS patterns. However, the Adonis test revealed that elevational and seasonal changes explained a greater proportion of the variation in the abundant subcommunity, while explaining the least variation in the rare subcommunity (Supplementary Figure S4).

10.3389/fpls.2025.1587343

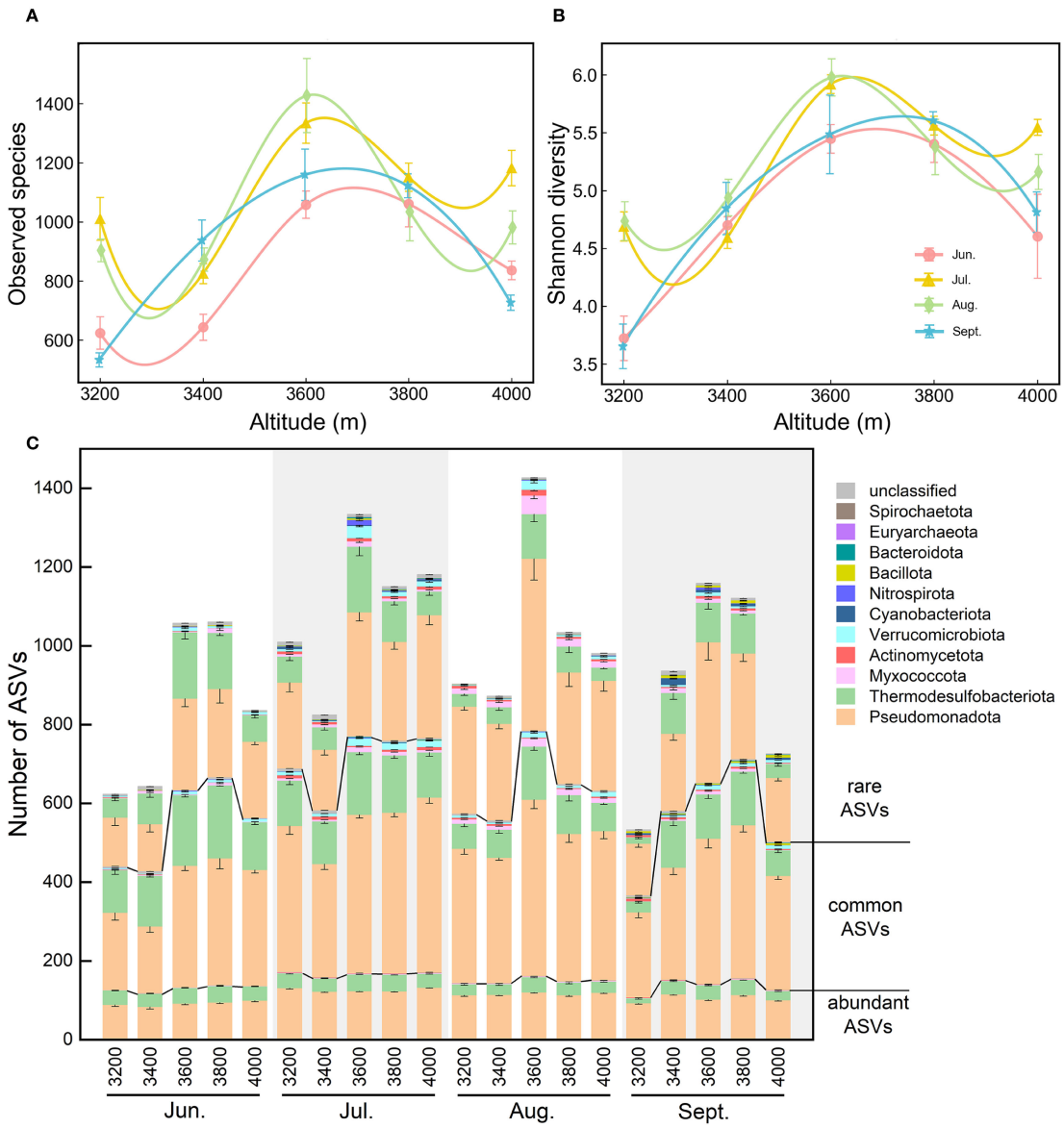


FIGURE 3
Elevational changes of alpha diversity indices during the growing season. **(A)** Observed species. **(B)** Shannon diversity. **(C)** Number of ASVs: ASVs from each elevation were sequentially classified by abundance category (abundant/common/rare ASVs), then by phylum affiliation. Error bars represent standard errors (n = 6).

## 3.6 Key factors driving elevational and seasonal variations of diazotrophic community

Soil moisture had the greatest impact on diazotrophic communities, followed by soil pH, ammonium, temperature, plant richness, aboveground biomass, and soil C:N ratio (Table 1). These factors were well-fitted on the NMDS plots, showing stronger associations with elevational variations than seasonal dynamics (Figure 4A).

To disentangle the effects of elevation and season, we separately assessed environmental factors influencing elevational and seasonal variations of diazotrophic communities (Figures 5, 6, Table 1). Partial Mantel test showed that temperature and moisture consistently influenced elevational variations across the growing season, with temperature having a greater effect. In contrast, key factors driving seasonal dynamics varied at different elevations. At low elevations (3200-3400 m), aboveground biomass was the primary factor, with legume biomass also being significant at 3200 m. However, at 3600 m and 4000 m, temperature was the primary factor. In fact, temperature was a significant factor at almost all elevations. In addition, moisture was the primary factor at 3800 m and also significant at 3400 m. Notably, soil C:N ratio was also significant at 4000 m and increased throughout the growing season at high elevations (Supplementary Figure S1F).

In summary, elevational variations were primarily driven by temperature and moisture, whereas seasonal dynamics depended more on plant growth at low elevations and climatic factors at higher sites.

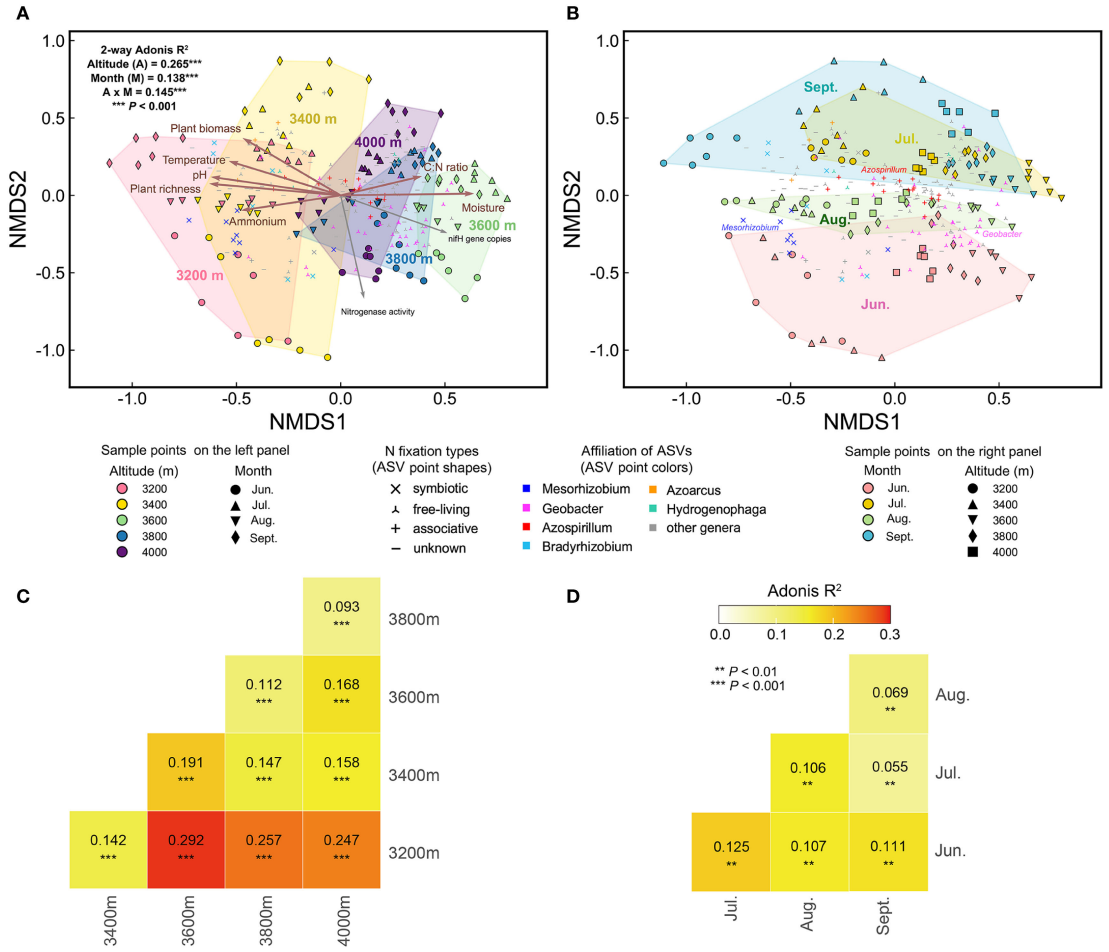


FIGURE 4
NMDS patterns and Adonis test for diazotrophic communities. **(A)** The NMDS plot colored by elevation. **(B)** The same NMDS plot colored by sampling month. **(C)** Adonis test for community differences across elevations. **(D)** Adonis test for community differences across the growing season. Environmental factors were fitted onto the NMDS plot. Brown arrows indicate factors which significantly influenced diazotrophic communities, as identified by partial Mantel test (Table 1). Gray arrows represent *nifH* gene copies and nitrogenase activity. Points representing abundant ASVs are displayed on the NMDS plots. Significance of Adonis test: * $P < 0.01$, ** $P < 0.001$.

# 4 Discussion

## 4.1 Elevational changes in diazotrophic communities driven by temperature and moisture

Our results indicated that elevational variation significantly affected soil diazotrophic community structures in alpine grasslands throughout the growing season, primarily driven by temperature and soil moisture. Low temperature is one of the limiting factors for BNF in alpine grasslands (Holzmann and Haselwandter, 1988). The higher temperature at low elevation not only enhances nitrogenase activity but also promotes plant growth, thereby altering the composition of soil diazotrophic communities (Wang et al., 2022). For example, low elevations are more favorable for the growth of leguminous plants, which increase the proportion and N fixation activity of symbiotic rhizobia, further raising soil ammonium concentration (Rui et al., 2022; Tang et al., 2024). BNF is an energy-intensive process (Norman and Friesen, 2017), and free-living diazotrophs require additional energy to overcome the toxic effects of oxygen on nitrogenase (Smercina et al., 2019). When available N is sufficient in the environment, free-living diazotrophs tend to avoid N fixation (Reed et al., 2011). Therefore, in soils at 3200 m, where legume biomass and ammonium concentration were highest, the relative abundance of free-living diazotrophs, soil nitrogenase activity (representing non-symbiotic N fixation activity), and *nifH* gene copies were all relatively low there (Figure 1).

Soil moisture is another important factor influencing the elevational variation. In mountainous environments, moisture typically follows an inverted V-shaped pattern along elevations (Rahbek, 1995). In our study sites, soil moisture also showed an inverted V-shaped pattern across elevations during the growing season (Supplementary Figure S1), as a result of orographic precipitation patterns (Xu et al., 2010). This pattern resulted in a non-linear variation of diazotrophic communities along the elevational gradient, with the most significant differences observed between the communities at 3600 m and those at

10.3389/fpls.2025.1587343

TABLE 1 Effects of environmental factors on elevational and seasonal variations of diazotrophic community based on partial Mantel test.

| | Ammonium | Nitrate | C:N ratio | Soil pH | Moisture | Temperature | Plant richness | Aboveground biomass | Legume biomass |
|---|---|---|---|---|---|---|---|---|---|
| all samples | **0.171***** | 0.036 | **0.079*** | **0.183***** | **0.225***** | **0.115**** | **0.167***** | **0.106**** | 0.048 |
| (a) grouped by month | | | | | | | | | |
| Jun. | **0.209**** | 0.162 | **0.293***** | **0.288**** | **0.195**** | **0.527***** | 0.048 | 0.056 | 0.085 |
| Jul. | 0.036 | 0.114 | 0.118 | 0.034 | **0.465***** | **0.628***** | 0.120 | 0.112 | **0.250**** |
| Aug. | **0.167*** | 0.073 | 0.107 | 0.044 | **0.220**** | **0.340**** | **0.160*** | 0.113 | 0.031 |
| Sept. | 0.003 | 0.150 | 0.022 | 0.115 | **0.166*** | **0.577***** | 0.074 | 0.074 | 0.131 |
| (b) grouped by elevation | | | | | | | | | |
| 3200 m | 0.110 | 0.065 | 0.023 | 0.059 | 0.100 | **0.184*** | 0.154 | **0.412***** | **0.222*** |
| 3400 m | 0.054 | 0.056 | 0.038 | 0.021 | **0.221*** | **0.156*** | 0.014 | **0.235**** | 0.074 |
| 3600 m | 0.187 | 0.139 | 0.049 | 0.189 | 0.032 | **0.329***** | 0.090 | 0.032 | 0.117 |
| 3800 m | 0.058 | 0.097 | 0.147 | 0.008 | **0.206*** | 0.072 | 0.124 | 0.019 | 0.014 |
| 4000 m | 0.040 | 0.127 | **0.182*** | **0.229*** | 0.113 | **0.333**** | 0.029 | 0.109 | 0.103 |

When one environmental factor was analyzed, the remaining environmental variables were controlled. Significant values are in bold: *$P<0.05$, ** $P<0.01$, *** $P<0.001$.

3200 m (Figure 4). The higher moisture at 3600 m hindered the growth of leguminous plants, leading to a very low relative abundance of rhizobia. Moreover, the relatively anaerobic and moist environment favors anaerobic free-living diazotrophs by reducing oxygen toxicity to nitrogenase (Smercina et al., 2019). This led to the highest relative abundance of *Geobacter*, soil nitrogenase activity, and *nifH* gene copies.

The effects of temperature and moisture on the elevational differentiation of diazotrophic communities are consistent with our previous study sampled in Sept. 2020 (Rui et al., 2022), indicating that diazotrophic communities generally exhibit similar elevational distribution patterns throughout the growing season. This study extends these findings by demonstrating that this pattern holds true across the entire growing season, highlighting the consistent role of temperature and moisture in regulating not only the species composition of diazotrophic communities but also the significant structural differences between communities at different elevations.

## 4.2 Seasonal dynamics of diazotrophic community driven by plant dynamics and microclimatic factors

Seasonal variations in diazotrophic communities of alpine grasslands across different elevations exhibited significant differences, primarily driven by seasonal dynamics of temperature, soil moisture, and plant dynamics. At lower elevations (3200 m and 3400 m), the dominant factor influencing seasonal dynamics of diazotrophic communities was the aboveground biomass. Additionally, legume biomass was also one of the significant influencing factors at 3200 m. This may be attributed to the greater seasonal variation in plant and legume biomass at lower elevations, particularly the significant difference between June and the other months of the growing season. Plant growth significantly influences soil microbial communities in grasslands through several mechanisms, such as changes in root exudates, nutrient uptake patterns, and litter input (Che et al., 2020; Steinauer et al., 2023). In our study, June marked the early growing season, during which plant biomass, including that of legumes, was lower at all elevations but significantly increased from July to September at lower elevations. At 3600 m and 4000 m, temperature was the most important factor, significantly influencing the seasonal changes in diazotrophic communities at all elevations except 3800 m. Seasonal variations in soil moisture were relatively minor, significantly affecting only the 3400 m and 3800 m sites. Therefore, seasonal changes in plant biomass and soil micoclimate factors, especially temperature, drive the dynamics of diazotrophic communities across elevations.

The soil nitrogenase activity and *nifH* gene copies were the highest in June (Figure 1), which indicated that free-living N fixation may play important roles in the early grow season. In habitats devoid of leguminous plants, free-living N fixation may represent the predominant form of BNF (Reed et al., 2011). Our sequencing results suggest that the alpine grasslands were primarily dominated by free-living diazotrophs in June, due to slower plant growth and the lack of legumes. From July to September, the contribution of associative N fixation increases. However, the high proportion of symbiotic diazotrophs in soils does not necessarily indicate high symbiotic N fixation in June, as this process occurs within root nodules. Studies have shown that rhizobia are released into the soil from ruptured root nodules at the end of the growing season (Poole et al., 2018; Krutylo and Nadkernychna, 2023). They live saprophytically in soils during the non-growing season, and infect legume roots again in the next growing season. This may explain the higher proportion of rhizobia in the soil in June.

The C:N ratio is an important indicator regulating N fixation activity of non-symbiotic diazotrophs, with a high C:N ratio favoring

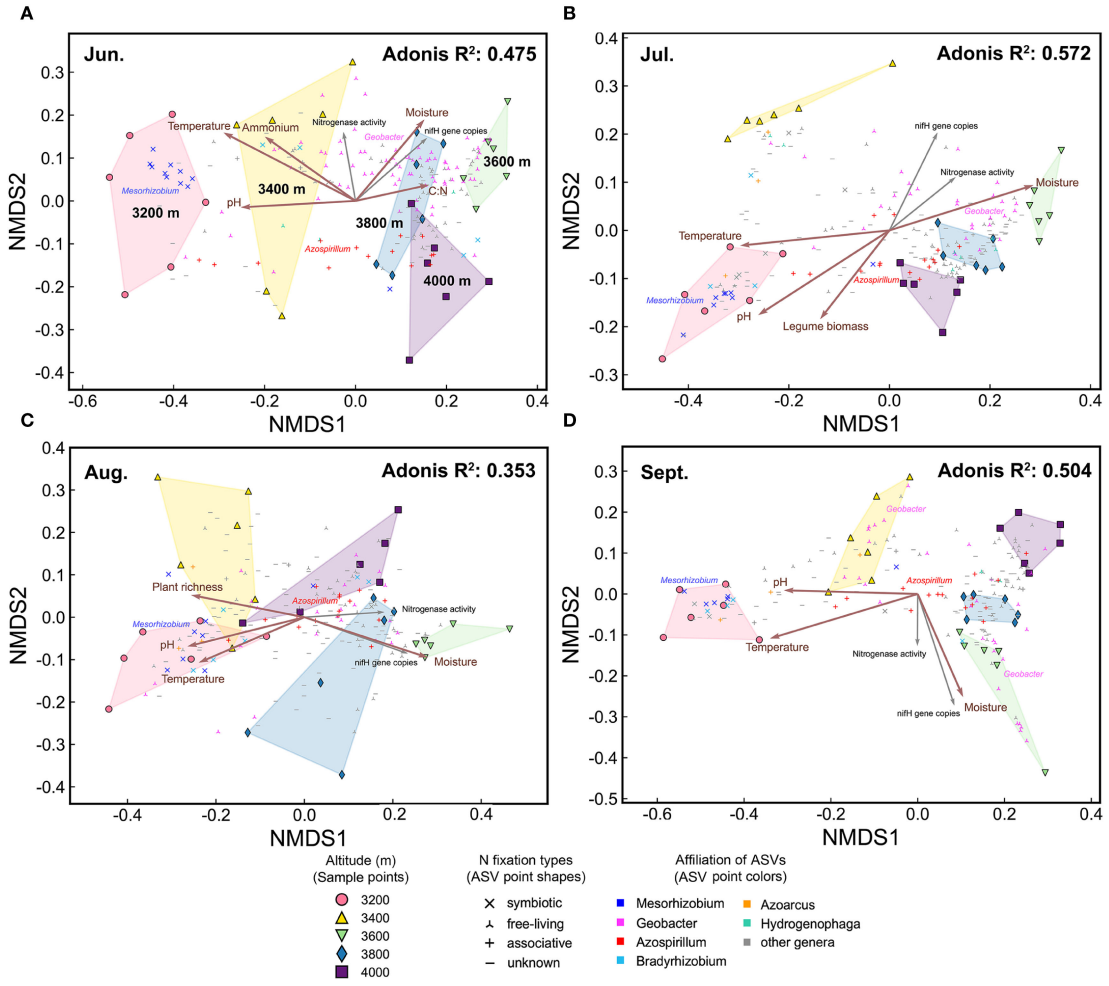


FIGURE 5
The NMDS plots of diazotrophic communities in each month. **(A)** June, **(B)** July, **(C)** August, and **(D)** September. Environmental factors are fitted onto the patterns. Brown arrows indicate factors which significantly influenced diazotrophic communities, as identified by partial Mantel test. Gray arrows represent *nifH* gene copies and nitrogenase activity. Points representing abundant ASVs are displayed on the NMDS plots. Adonis $P<0.001$.

N fixation (Reed et al., 2011; Inomura et al., 2018). We noted considerable variations in the soil C:N ratio across elevations, with that at 3200 m being significantly lower than at higher elevations (Supplementary Figure S1F). This suggests a relatively plentiful supply of N sources at lower elevations, perhaps attributable to increased symbiotic N fixation activity. As elevation ascends, the C:N ratio also rises while plant biomass diminishes, signifying a reduction in N availability. This highlights the important role of free-living diazotrophs in BNF at elevated elevations, especially under colder temperature circumstances. The temporal patterns of soil C:N ratio during the growing season differed between low and high elevations. At the low elevation (3600 m), the soil C:N ratio rose from June to August but declined to a lower level after September. This suggests that symbiotic and associative N fixation could meet plant N requirements throughout the growing season, thereby maintaining N balance. In contrast, the soil C:N ratio at high elevations (3600–4000 m) gradually increased from June to September, indicating that the rate of free-living N fixation could not keep up with plant N demand, exacerbating N limitation. The observed differences likely result from two key factors. First, the warmer conditions at lower altitudes enhance nitrogenase activity. Second, the inherent efficiency disparity between free-living and symbiotic N fixation. While symbiotic N fixation (e.g., rhizobia-legume associations in root nodules) achieves highly efficient N fixation, free-living diazotrophs must expend significantly more energy to mitigate oxygen toxicity, leading to substantially higher metabolic costs for N fixation (Smercina et al., 2019).

## 4.3 Contributions of abundant and rare species to diazotrophic community diversity

The diversity of diazotrophic communities depends not only on the richness and species composition of the community but also on the dynamics of abundant and rare species. We found that the beta diversity of diazotrophic communities was more strongly influenced by abundant species. Subcommunities composed of

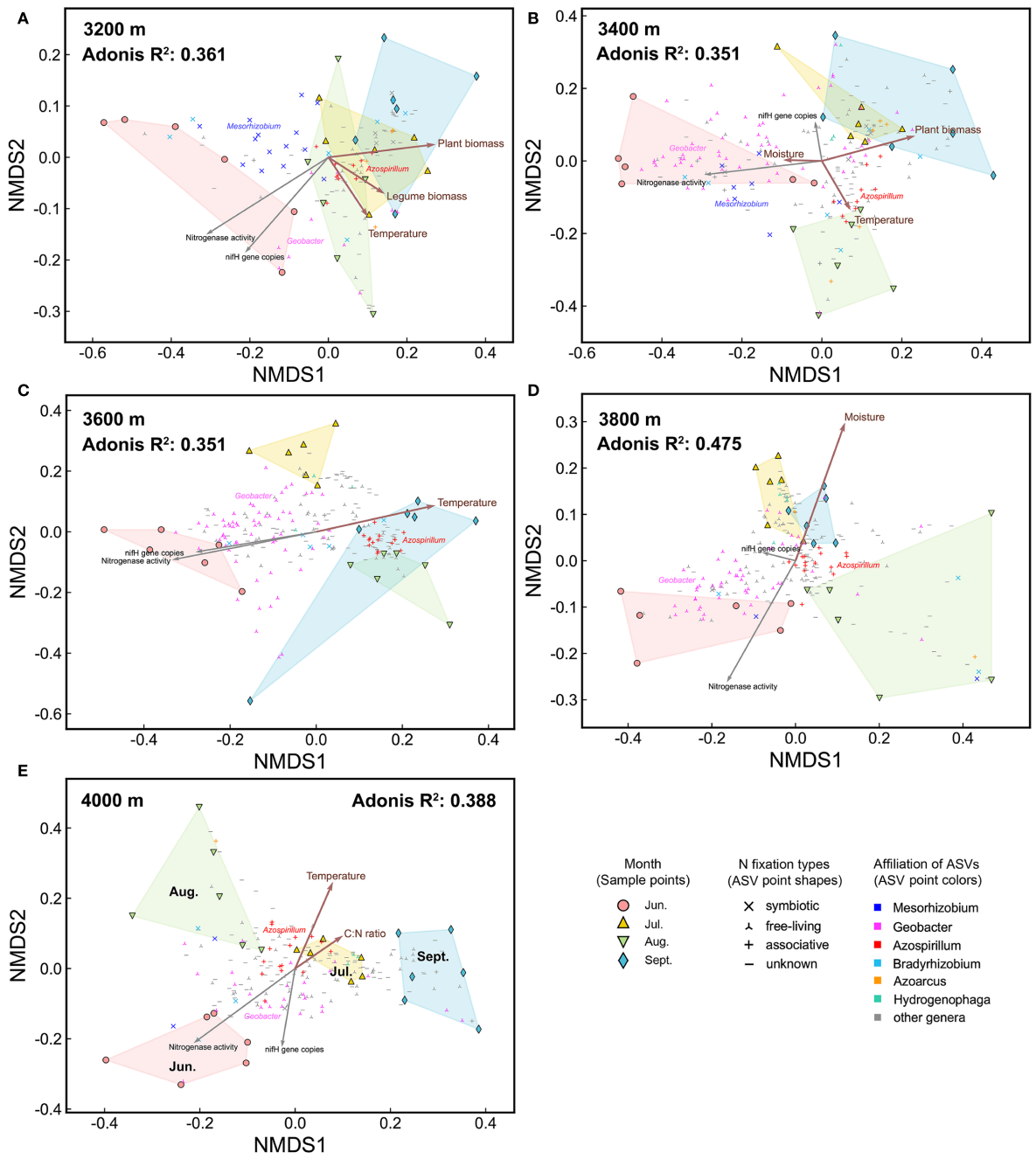


FIGURE 6
The NMDS plots of diazotrophic communities at each elevation. **(A)** 3200 m, **(B)** 3400 m, **(C)** 3600 m, **(D)** 3800 m, and **(E)** 4000 m. Environmental factors are fitted onto the patterns. Brown arrows indicate factors which significantly influenced diazotrophic communities, as identified by partial Mantel test. Gray arrows represent *nifH* gene copies and nitrogenase activity. Points representing abundant ASVs are displayed on the NMDS plots. Adonis $P<0.001$.

just 192 abundant ASVs effectively represent the beta diversity of the entire diazotrophic communities (Supplementary Figure S4). Abundant genera, such as *Geobacter*, *Mesorhizobium*, and *Azospirillum*, shaped the beta diversity of diazotrophic communities under different elevational and seasonal conditions, with their relative abundance changes driving notable differences in community composition along elevations. For example, *Geobacter* was predominant at middle elevations, while *Mesorhizobium* dominated at lower elevations, with both groups showing a stronger presence in June. Interestingly, compared to rare species, the subcommunity composed of abundant species can be better explained by changes in elevation and season (Supplementary Figure S4), suggesting that the species composition of abundant species may be more sensitive to environmental changes.

Rare species had a major impact on the alpha diversity of diazotrophic community, with their relative abundance being

notably higher at middle elevations compared to other elevations. These rare species primarily belonged to *Geobacter* and unclassified Alphaproteobacteria. Interestingly, the number of ASVs belonging to *Geobacter* also followed an inverted V-shaped pattern along the elevational gradient, positively correlated with its relative abundance. Geobacter possesses remarkable adaptive and evolutionary capabilities (Summers et al., 2012), which may explain the exceptionally high ASV richness of this genus at mid/high elevations. The relatively anaerobic soils at mid-elevations are less conducive to the majority of plants, including legumes, leading to the lowest relative abundances of both symbiotic and associative diazotrophs. However, the richness of rare diazotrophic species was highest in this zone. These rare species might play a potential role in the stability and adaptability of the community, possibly acting as key players in community recovery and ecological adaptation (Ma et al., 2024). The presence of rare species may enhance the functional redundancy of diazotrophic communities, particularly at higher elevations, where they may contribute N fixation through distinct physiological functions in N-limited environments. For example, *Geobacter* is considered a successful N fixer in nutrient-deficient conditions, utilizing ferric iron ($Fe^{3+}$) as the electron acceptor (Bazylinski et al., 2000). Therefore, rare species may play a crucial role in maintaining community diversity and significantly contribute to the ecological adaptation of diazotrophic community (Jain et al., 2014). The interaction between abundant and rare species is complex and multi-layered, reflecting not only the impact of environmental gradients on diazotrophic community structure but also the interaction and functional complementarity between different species communities in ecosystems.

## 5 Conclusion

This study highlights the dynamic characteristics of diazotrophic communities in alpine grasslands, accentuating their elevational and seasonal variations driven by soil microclimate factors and plant dynamics. Our findings indicated that diazotrophic communities typically display uniform elevational distribution patterns throughout the growing season, predominantly affected by temperature and moisture. Seasonal variations were more pronounced at lower elevations, driven by vegetation, while microclimate factors, particularly temperature, held greater significance at higher elevations. Additionally, *nifH* gene abundance and soil nitrogenase activity were higher in the early growing season, suggesting that free-living N fixation may play a crucial role in BNF before legumes and grasses reach maturity in grasslands. We also find that abundant species were key contributors to diazotrophic beta diversity, whereas rare species were instrumental in determining alpha diversity. These findings underscore the complexity of diazotrophic community dynamics and emphasize the need for a deeper understanding of the roles of both abundant and rare species in ecosystem functioning. However, a limitation of this study is that only soil nitrogenase activity was monitored, which primarily reflects the nitrogenase activity of free-living N fixation in soils. Future research should also monitor plant-associated N fixation rate in alpine grassland ecosystems.

## Data availability statement

The datasets presented in this study can be found in online repositories. The names of the repository/repositories and accession number(s) can be found below: https://ngdc.cncb.ac.cn, CRA021903.

## Author contributions

JR: Conceptualization, Data curation, Formal Analysis, Funding acquisition, Methodology, Project administration, Software, Supervision, Visualization, Writing – original draft, Writing – review & editing. XL: Data curation, Investigation, Validation, Writing – original draft, Writing – review & editing. XW: Investigation, Resources, Writing – original draft. XX: Investigation, Resources, Writing – original draft. JZ: Resources, Funding acquisition, Writing – review & editing.

## Funding

The author(s) declare financial support was received for the research and/or publication of this article. This work was supported by grants from the National Natural Science Foundation of China (No. 42477113, U24A20630), the Project Supported by the Open Fund of Key Laboratory of Biodiversity and Environment on the Qinghai-Tibet Plateau, Ministry of Education (No. KLBE2024007), Gansu Provincial Science and Technology Major Projects (23ZDNA009), and the Fundamental Research Funds for the Central Universities (lzujbky-2023-ct04).

## Acknowledgments

We thank Juan Du and Chao Li (Lanzhou University) for their assistance with soil property measurements. We also thank the Haibei National Field Research Station of Alpine Grassland Ecosystem for helping environmental data collection.

## Conflict of interest

The authors declare that the research was conducted in the absence of any commercial or financial relationships that could be construed as a potential conflict of interest.

## Generative AI statement

The author(s) declare that no Generative AI was used in the creation of this manuscript.

Any alternative text (alt text) provided alongside figures in this article has been generated by Frontiers with the support of artificial intelligence and reasonable efforts have been made to ensure accuracy, including review by the authors wherever possible. If you identify any issues, please contact us.

## Publisher's note

All claims expressed in this article are solely those of the authors and do not necessarily represent those of their affiliated organizations, or those of the publisher, the editors and the reviewers. Any product that may be evaluated in this article, or claim that may be made by its manufacturer, is not guaranteed or endorsed by the publisher.

## Supplementary material

The Supplementary Material for this article can be found online at: https://www.frontiersin.org/articles/10.3389/fpls.2025.1587343/full#supplementary-material

## References

Bazylinski, D. A., Dean, A. J., Schüler, D., Phillips, E. J., and Lovley, D. R. (2000). $N_2$-dependent growth and nitrogenase activity in the metal-metabolizing bacteria, *Geobacter* and *Magnetospirillum* species. *Environ. Microbiol.* 2, 266–273. doi: 10.1046/j.1462-2920.2000.00096.x

Bolger, A. M., Lohse, M., and Usadel, B. (2014). Trimmomatic: a flexible trimmer for Illumina sequence data. *Bioinformatics* 30, 2114–2120. doi: 10.1093/bioinformatics/btu170

Che, R., Deng, Y., Wang, F., Wang, W., Xu, Z., Hao, Y., et al. (2018). Autotrophic and symbiotic diazotrophs dominate nitrogen-fixing communities in Tibetan grassland soils. *Sci. Total Environ.* 639, 997–1006. doi: 10.1016/j.scitotenv.2018.05.238

Che, R., Liu, D., Qin, J., Wang, F., Wang, W., Xu, Z., et al. (2020). Increased litter input significantly changed the total and active microbial communities in degraded grassland soils. *J. Soils Sediments* 20, 2804–2816. doi: 10.1007/s11368-020-02619-x

Chellem, S. R., Kishore, C. V. L., Reddy, G. S. V., Akshay, D., Kalpana, K., Lavanya, P., et al. (2024). Symbiotic Relationships between Nitrogen-fixing Bacteria and Leguminous Plants Ecological and Evolutionary Perspectives: A Review. *Uttar Pradesh J. Zool* 45, 145–160. doi: 10.56557/upjoz/2024/v45i134143

Daubech, B., Remigi, P., Doin de Moura, G., Marchetti, M., Pouzet, C., Auriac, M.-C., et al. (2017). Spatio-temporal control of mutualism in legumes helps spread symbiotic nitrogen fixation. *eLife* 6, e28683. doi: 10.7554/eLife.28683.035

Dynarski, K. A., and Houlton, B. Z. (2018). Nutrient limitation of terrestrial free-living nitrogen fixation. *N. Phytol.* 217, 1050–1061. doi: 10.1111/nph.14905

Edgar, R. C. (2016). UNOISE2: improved error-correction for Illumina 16S and ITS amplicon sequencing. *BioRxiv*, 081257. doi: 10.1101/081257

Hardy, R., Burns, R. C., and Holsten, R. D. (1973). Applications of the acetylene-ethylene assay for measurement of nitrogen fixation. *Soil Biol. Biochem.* 5, 47–81. doi: 10.1016/0038-0717(73)90093-X

Herridge, D. F., Peoples, M. B., and Boddey, R. M. (2008). Global inputs of biological nitrogen fixation in agricultural systems. *Plant Soil* 311, 1–18. doi: 10.1007/s11104-008-9668-3

Holzmann, H.-P., and Haselwandter, K. (1988). Contribution of nitrogen fixation to nitrogen nutrition in an alpine sedge community (*Caricetum curvulae*). *Oecologia* 76, 298–302. doi: 10.1007/BF00379967

Houlton, B. Z., Wang, Y.-P., Vitousek, P. M., and Field, C. B. (2008). A unifying framework for dinitrogen fixation in the terrestrial biosphere. *Nature* 454, 327–330. doi: 10.1038/nature07028

Huson, D. H., Beier, S., Flade, I., Górska, A., El-Hadidi, M., Mitra, S., et al. (2016). MEGAN community edition-interactive exploration and analysis of large-scale microbiome sequencing data. *PLoS Comput. Biol.* 12, e1004957. doi: 10.1371/journal.pcbi.1004957

Inomura, K., Bragg, J., Riemann, L., and Follows, M. J. (2018). A quantitative model of nitrogen fixation in the presence of ammonium. *PLoS One* 13, e0208282. doi: 10.1371/journal.pone.0208282

Jain, M., Flynn, D. F. B., Prager, C. M., Hart, G. M., DeVan, C. M., Ahrestani, F. S., et al. (2014). The importance of rare species: a trait-based assessment of rare species contributions to functional diversity and possible ecosystem function in tall-grass prairies. *Ecol. Evol.* 4, 104–112. doi: 10.1002/ece3.915

Körner, C. (2004). Mountain biodiversity, its causes and function. *Ambio* 33, 11–17. doi: 10.1007/0044-7447-33.sp13.11

Krutylo, D., and Nadkernychna, O. (2023). Features of Local *Bradyrhizobia* Populations after Long-Term Period in the Soil without a Host Plant. *Mikrobiolohichnyi Zhurnal* 85, 20–30. doi: 10.15407/microbiolj85.05.020

Lai, J., Zou, Y., Zhang, S., Zhang, X., and Mao, L. (2022). glmm. hp: an R package for computing individual effect of predictors in generalized linear mixed models. *J. Plant Ecol.* 15, 1302–1307. doi: 10.1093/jpe/rtac096

Litchman, E., Villéger, S., Zinger, L., Auguet, J.-C., Thuiller, W., Munoz, F., et al. (2024). Refocusing the microbial rare biosphere concept through a functional lens. *Trends Ecol. Evol.* 39, 923–936. doi: 10.1016/j.tree.2024.06.005

Lomolino, M. V. (2001). Elevation gradients of species-density: historical and prospective views. *Global Ecol. Biogeogr* 10, 3–13. doi: 10.1046/j.1466-822x.2001.00229.x

Ma, L., Niu, W., Li, G., Du, Y., Sun, J., Zhang, Q., et al. (2024). Crucial role of rare taxa in preserving bacterial community stability. *Land Degrad. Dev.* 35, 1397–1410. doi: 10.1002/ldr.4994

Magoč, T., and Salzberg, S. L. (2011). FLASH: fast length adjustment of short reads to improve genome assemblies. *Bioinformatics* 27, 2957–2963. doi: 10.1093/bioinformatics/btr507

Norman, J. S., and Friesen, M. L. (2017). Complex N acquisition by soil diazotrophs: how the ability to release exoenzymes affects N fixation by terrestrial free-living diazotrophs. *ISME J.* 11, 315–326. doi: 10.1038/ismej.2016.127

Poole, P., Ramachandran, V., and Terpolilli, J. (2018). Rhizobia: from saprophytes to endosymbionts. *Nat. Rev. Microbiol.* 16, 291–303. doi: 10.1038/nrmicro.2017.171

Rahbek, C. (1995). The elevational gradient of species richness: a uniform pattern? *Ecography* 18, 200–205. doi: 10.1111/j.1600-0587.1995.tb00341.x

Reed, S. C., Cleveland, C. C., and Townsend, A. R. (2011). Functional ecology of free-living nitrogen fixation: a contemporary perspective. *Annu. Rev. Ecol Evol Syst* 42, 489–512. doi: 10.1146/annurev-ecolsys-102710-145034

Rousk, K., Pedersen, P. A., Dyrnum, K., and Michelsen, A. (2017). The interactive effects of temperature and moisture on nitrogen fixation in two temperate-arctic mosses. *Theor. Exp. Plant Physiol.* 29, 25–36. doi: 10.1007/s40626-016-0079-1

Rui, J., Hu, J., Wang, F., Zhao, Y., and Li, C. (2022). Altitudinal niches of symbiotic, associative and free-living diazotrophs driven by soil moisture and temperature in the alpine meadow on the Tibetan Plateau. *Environ. Res.* 211, 113033. doi: 10.1016/j.envres.2022.113033

Rui, J., Zhao, Y., Cong, N., Wang, F., Li, C., Liu, X., et al. (2023). Elevational distribution and seasonal dynamics of alpine soil prokaryotic communities. *Front. Microbiol.* 14, 1280011. doi: 10.3389/fmicb.2023.1280011

Shangguan, Z., Jing, X., Wang, H., Liu, H., Gu, H., and He, J. S. (2024). Plant biodiversity responds more strongly to climate warming and anthropogenic activities than microbial biodiversity in the Qinghai–Tibetan alpine grasslands. *J. Ecol.* 112, 110–125. doi: 10.1111/1365-2745.14222

Smercina, D. N., Evans, S. E., Friesen, M. L., and Tiemann, L. K. (2019). To fix or not to fix: controls on free-living nitrogen fixation in the rhizosphere. *Appl. Environ. Microbiol.* 85, e02546–e02518. doi: 10.1128/AEM.02546-18

Smercina, D. N., Evans, S. E., Friesen, M. L., and Tiemann, L. K. (2021). Temporal dynamics of free-living nitrogen fixation in the switchgrass rhizosphere. *GCB Bioenergy* 13, 1814–1830. doi: 10.1111/gcbb.12893

Steinauer, K., Thakur, M. P., Emilia Hannula, S., Weinhold, A., Uthe, H., van Dam, N. M., et al. (2023). Root exudates and rhizosphere microbiomes jointly determine temporal shifts in plant-soil feedbacks. *Plant Cell Environ.* 46, 1885–1899. doi: 10.1111/pce.14570

Summers, Z. M., Ueki, T., Ismail, W., Haveman, S. A., and Lovley, D. R. (2012). Laboratory evolution of Geobacter sulfurreducens for enhanced growth on lactate via a single-base-pair substitution in a transcriptional regulator. *ISME J.* 6, 975–983. doi: 10.1038/ismej.2011.166

Sundqvist, M. K., Sanders, N. J., and Wardle, D. A. (2013). Community and ecosystem responses to elevational gradients: processes, mechanisms, and insights for global change. *Annu. Rev. Ecol Evol. Syst* 44, 261–280. doi: 10.1146/annurev-ecolsys-110512-135750

Tang, J., Li, W., Wei, T., Huang, R., and Zeng, Z. (2024). Patterns and Mechanisms of Legume Responses to Nitrogen Enrichment: A Global Meta-Analysis. *Plants* 13, 3244. doi: 10.3390/plants13223244

Vitousek, P. M., Menge, D. N., Reed, S. C., and Cleveland, C. C. (2013). Biological nitrogen fixation: rates, patterns and ecological controls in terrestrial ecosystems. *Philos. Trans. R. Soc. B: Biol. Sci.* 368, 20130119. doi: 10.1098/rstb.2013.0119

Wang, Q., Li, S., Li, J., and Huang, D. (2024). The utilization and roles of nitrogen in plants. *Forests* 15, 1191. doi: 10.3390/f15071191

Wang, Q., Quensen Iii, J. F., Fish, J. A., Kwon Lee, T., Sun, Y., Tiedje, J. M., et al. (2013). Ecological patterns of *nifH* genes in four terrestrial climatic zones explored with targeted metagenomics using FrameBot, a new informatics tool. *mBio* 4, e00592–e00513. doi: 10.1128/mBio.00592-13

Wang, J., Yan, X., Zhang, F., Wu, Q., Li, Q., Liu, X., et al. (2022). Changes in community assembly processes and co-occurrence networks of soil diazotrophs along an elevational gradient in Tibetan alpine meadows. *Eur. J. Soil Biol.* 113, 103445. doi: 10.1016/j.ejsobi.2022.103445

Wickstrom, C. E., and Garono, R. J. (2007). Associative rhizosphere nitrogen fixation (acetylene reduction) among plants from Ohio peatlands. *Ohio Journal of Science*. 107, 39–43. Available online at: http://hdl.handle.net/1811/44819.

Xu, G., Hu, Y., Wang, S., Zhang, Z., Chang, X., Duan, J., et al. (2010). Effects of litter quality and climate change along an elevation gradient on litter mass loss in an alpine meadow ecosystem on the Tibetan plateau. *Plant Ecol.* 209, 257–268. doi: 10.1007/s11258-009-9714-0

Yang, Y., Gao, Y., Wang, S., Xu, D., Yu, H., Wu, L., et al. (2014). The microbial gene diversity along an elevation gradient of the Tibetan grassland. *ISME J.* 8, 430–440. doi: 10.1007/s11368-017-1792-3

Ye, G., Wang, Y., Cui, X., Jin, Y., Hu, H.-W., Liu, J., et al. (2024). High stochasticity in rare bacterial community assembly in rice-wheat rotation soils at a regional scale. *Soil Biol. Biochem.* 195, 109479. doi: 10.1016/j.soilbio.2024.109479

Zhao, Y.-D., and Hu, X. (2023). Seasonal freeze–thaw processes regulate and buffer the distribution of microbial communities in soil horizons. *Catena* 231, 107348. doi: 10.1016/j.catena.2023.107348

Zhao, W., Kou, Y., Wang, X., Wu, Y., Bing, H., and Liu, Q. (2020). Broad-scale distribution of diazotrophic communities is driven more by aridity index and temperature than by soil properties across various forests. *Global Ecol. Biogeogr.* 29, 2119–2130. doi: 10.1111/geb.13178

# Frontiers in
# Plant Science

**Cultivates the science of plant biology and its applications**

The most cited plant science journal, which advances our understanding of plant biology for sustainable food security, functional ecosystems and human health.

---

## Discover the latest Research Topics

See more →

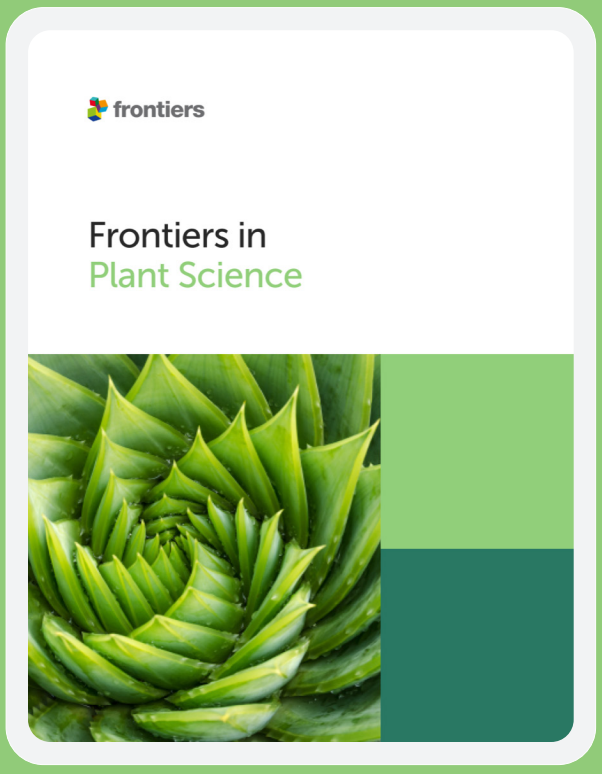


**Frontiers**

Avenue du Tribunal-Fédéral 34
1005 Lausanne, Switzerland
frontiersin.org

**Contact us**

+41 (0)21 510 17 00
frontiersin.org/about/contact